DESIGN, SYNTHESIS AND EVALUATION OF NOVEL TOCOPHEROL BASED CATIONIC LIPIDS & AMINO ACID BASED GEMINI CATIONIC LIPIDS: THEIR APPLICATIONS IN NUCLEIC ACID DELIVERY AND GENE EDITING

A THESIS SUBMITTED TO

NATIONAL INSTITUTE OF TECHNOLOGY
WARANGAL

FOR THE DEGREE OF

DOCTOR OF PHILOSOPHY
IN
CHEMISTRY
BY

RAPAKA HITHAVANI
(Roll No. 701387)

DEPARTMENT OF CHEMISTRY
NATIONAL INSTITUTE OF TECHNOLOGY
WARANGAL-506 004, TELANGANA, INDIA
July-2022

DEDICATED

TO

MY PARENTS

Prof. P. V. Srilakshmi
Professor
Department of Chemistry
National Institute of Technology
Warangal - 506 004
Telangana, India

Email: patrisrilakshmi@nitw.ac.in
Ph. Office: 0091-0870-2462672
Mobile No: 9441965575

CERTIFICATE

This is to certify that the research work presented in this thesis entitled **"Design, Synthesis and Evaluation of Novel Tocopherol Based Cationic Lipids & Amino Acid Based Gemini Cationic Lipids: Their Applications in Nucleic acid Delivery and Gene Editing"** submitted by **Mrs. Rapaka Hithavani** for the degree of Doctor of Philosophy in Chemistry, National Institute of Technology, Warangal (Telangana), under my supervision and that the same has not been submitted elsewhere for a degree.

Date: 29-07-2022

Place: NIT Warangal

p.v. Srilakshmi

Prof. P. V. Srilakshmi

Thesis Supervisor

DECLARATION

I hereby declare that the matter embodied in this thesis entitled **"Design, Synthesis and Evaluation of Novel Tocopherol Based Cationic Lipids & Amino Acid Based Gemini Cationic Lipids: Their Applications in Nucleic acid Delivery and Gene Editing"** is based entirely on the results of the investigations and research work carried out by me under the supervision of **Prof. P. V. Srilakshmi**, Department of Chemistry, National Institute of Technology, Warangal. I declare that this work is original and has not been submitted in part or full, for any degree or diploma to this or any other University.

(Rapaka Hithavani)

ACKNOWLEDGEMENTS

During the long period of my research work, it is my great pleasure to acknowledge the people whose contribution made my academic journey successful. It is a pleasant aspect that now I have the opportunity to extend my heartfelt gratitude and appreciation to each and every one of them.

It is my privilege to express my profound sense of gratitude to my research supervisor ***Prof. P. V. Srilakshmi***, Professor, Department of Chemistry, National Institute of Technology, Warangal for her guidance, constant encouragement and constructive criticism during my doctoral research.

I deeply obliged to ***Prof. N. V. Ramana Rao***, Director, National Institute of Technology, Warangal allowing me to submit my research work in the form of a thesis. I express my gratitude to ***Prof. T. Srinivasa Rao*** and ***Prof. G. R. C. Reddy***, former Directors, National Institute of Technology, Warangal for giving me the opportunity to carry out the research work.

My sincere duty is to express my flawless thanks to ***Dr. Vishnu Shanker*** Head, Department of Chemistry and ***Prof. P. V. Srilakshmi***, ***Prof. K. V. Gobi, Prof. V. Rajeswar Rao***, ***Late Prof. B. Rajitha,*** former Heads, Department of Chemistry, National Institute of Technology, Warangal for their valuable advice, help and support.

I express my sincere thanks to the Doctoral Scrutiny Committee (DSC) members, ***Prof. V. Rajeswar Rao, Prof. K. Laxma Reddy,*** Department of Chemistry and ***Prof. Y. Pydisetty,*** Department of Chemical Engineering for their support and encouragement.

I take this opportunity to express thanks to ***Prof. B. Venkata Appa Rao (Retd)***, ***Prof. G. V. P. Chandramouli (Retd)***, ***Prof. I. Ajit Kumar Reddy (Retd)***, ***Prof. A. Ramachandraiah (Retd)***, ***Prof. K. Laxma Reddy, Prof. P. Nageswara Rao, Dr. Vishnu Shanker***, ***Dr. D. Kashinath***, ***Dr. B. Srinivas, Dr. K. Hari Prasad, Dr. Venkatathri Narayanan***, ***Dr. Raghu Chitta, Dr. S. Nagarajan, Dr. M. Raghasudha, Dr. C. Jugun Prakash, Dr. Ravinder Pawar, Dr. Mukul Pradhan, Dr. Rajeshkhanna Gaddam, Dr. V. Rajeshkumar*** for their suggestions and encouragement.

I gratefully acknowledge the support received from ***Dr. M. Srujan kumar,*** Christian Medical College (CMC), Centre for Stem Cell Research (**CSCR**), Vellore, Tamilnadu,

INDIA for allowing me to carry out part of my research work. I can't thank enough for the support received from lab mates at ***CSCR*** Vellore.

Financial assistance from **SERB**, Department of Science and Technology (**DST**), Government of India, New Delhi from the Government of India and Ministry of Human Resource Development ***(MHRD)*** in the form of fellowship is gratefully acknowledged.

I am very delighted to work with my colleagues and will miss organic research lab. My sincere thanks to ***Dr. G. Mallikarjun, R. Venkatesh and M. Shireesha*** for their support and encouragement through entire my Ph. D and this thesis would not have come to a successful completion, without the help of these members.

It gives me a great pleasure to express my gratitude to my colleagues and friends ***Dr. M. Saikumar, Dr. K. Ramaiah, Dr. Vinay Pogaku, Dr. N. V. Bharat, Dr. S. Nagaraju, Dr. B. Paplal, N. Satyanarayana, Dr. B. Rajitha, Dr. M. Nooka Raju, Dr, A. Rajini, Dr. M. Satyanarayana, Dr. Chaithanya kumar, Dr. M. Narsimha Reddy, Dr. P. Sreenu, Dr. K. Koteshwara Reddy, Dr. T. Ramesh, Dr. G. Srinivasa Rao, Dr. R. Rajkumar, Dr. T. Surendar, Dr. B. Thirupaiah, Dr. B. Janardhan, Dr. G. Ramesh, Dr. V. Krishnaiah, Dr. V. Ravi Babu, Dr. L. Suresh, Dr. P. Sagar Vijay Kumar, Dr. K. Sujatha, Dr. Manjula Reddy, Dr. A. Varun, Dr. Ch. Suman, Dr. J. Paramehswara chary, Dr. M. Srikanth, Dr. P. Babji, Dr. K. Satish, Dr. V. Sunil Kumar, Dr. A. Bhargava Sai, K. Vijendar reddy, Ramesh ajmera, R. Venkatesh, Dr. K. Shekar, Dr. G. Ambedhkar, G. Sivaparwathi, G. Srinath, G. Sripal Reddy, K. Sampath, T. Shirisha, B. Sravanthi, P. Venkatesham, B. Prashanth, R. Varaprasad, R. Arun, B. Anjaiah, Akansha Sangolkar, B. Srikanth, Pooja, Anindya Roy, Khushboo Agarwala, Tohira Banoo, M. Sasi Sree, Akash Kumar, Avinash Sharma, B. Apurba, M. Subir, M. Faizan, M. Arokiaraj, M. Vijayand and all the research scholars of various Departments*** for their good compensation and creating a nice atmosphere in and outside the laboratory and their encouragement and help during my research period.

Also, my sincere thanks to ***K. Narasimha, K. Venkanna*** (NMR instrument operators) *and* ***B. Srinivas*** (Mass Spectrometer operator) for their support to characterize the synthesized compounds. My special thanks to non-teaching and technical supporting staff of Chemistry Department ***P. Heeralal, Kishore kumar, B. Sadanandam, T. Kiran, Md. Shaheen begum, G. Santhosh, J. Praveen, K. Sreenivas, K. Keshavulu, A. Rajini, V. Bhavani and K. Kavya*** for their help in every time needed.

Dr. Abdul Kalam states that “One best book is equal to hundred good friends, but one good friend is equal to a library.” I am really fortunate enough to get many good friends in NITW like ***Dr. S. Manasa, Dr. B. Mayuri, Dr. Kayalvizhi, Mrs. P. Sowmya, Dr. S. Suresh, Dr. K. Vimal Kumar, Mr. T. Dhanunjay Rao,*** all many others during my Ph.D. days. I always enjoy their company, and they are my strength for many things. I would like to express my gratitude and all the support and love for making many memories in good and bad times.

This acknowledgment would not be complete without mentioning the pain staking efforts of my families for making this dream come true. No words are adequate to express my indebtedness to my parents, sisters, in-laws, husband, kids and other family members. I owe this thesis to my loving and supportive parents (***Sri. Narasimha Rao, Smt. Rama Laxmi***) who stood by me in every single step of my life. I am grateful for the continuous support and encouragement received from my elder sister, brother-in-law and kids (***Hima Bindu, Praveen Kumar, Lakshmi Manya Sri & Shanmukha Vachaspathi***) in pushing me towards my goal. I am truly thankful to my younger sister (***R. Himaja***) for always being there for me in my difficult times and for her endless patience, unconditional love and continuous support during my Ph.D. tenure.

I express my deep sense of gratitude to my husband ***Dr. J. Pavan Kumar***, for his love, understanding, tremendous moral support and help he extended to me all the time. I am thankful for the support received from my in-laws and brothers-in-law throughout this journey (***Sri. Narasimha Rao, Smt. Sunitha, Murali Krishna & Venkata Ramana***). Last and the best, I am thankful to the Almighty for making my journey more memorable and special by blessing us with a beautiful daughter in and out (***J. Lakshmi Janvika***) and the other little human being that is being formed in my womb.

Lastly, I express my hearty thanks to those whom I might have missed to mention by name, who helped directly or indirectly and co-operated me a lot in completion of my research work.

(Rapaka Hithavani)

ABBREVIATIONS

AAVS1	:	Adeno-Associated Virus Integration Site 1
Boc	:	Di-tert-butyl-dicarbonate
BSA	:	Bovine serum albumin
Cas	:	CRISPR associated genes
CDCl3	:	Deuterated chloroform
CH3CN	:	Acetonitrile
CHCl3	:	Chloroform
Chol	:	Cholesterol
CRISPR	:	Clustered regulartary interspaced palintromic repeats
crRNA	:	CRISPR RNA
CuSO4	:	Copper (II) sulfate
DAPI	:	4',6-diamidino-2-phenylindole
dCAS9	:	Nuclease - deficient Cas9
DCC	:	Dicyclohexyl carbodiimide
DCM	:	Dichloromethane
DIPEA	:	N, N-Di-isopropyl ethylamine
DLS	:	Dynamic light scattering
DMAP	:	4-N, N-Dimethyl aminopyridine
DMC	:	Dimethyl carbonate
DMEM	:	Dulbecco's modified eagle's medium
DMF	:	N, N-Dimethyl formamide
DMSO	:	Dimethyl sulfoxide
DMSO-d6	:	Deuterated dimethyl sulfoxide
DNA	:	Deoxyribonucleic acid
DOPE	:	1,2-dioleoyl-sn-glycerol-3-phosphoethanolamine
DPBS	:	Dulbecco's phosphate buffered saline
DSB	:	Double stranded break
EDCI. HCl	:	1-ethyl-3-(3-dimethylaminopropyl) carbodiimide Hydrochloride
EDTA	:	Ethylendiaminetetra acetic acid

ESI-MS	:	Electron Spray Ionization Mass Spectrometry
Et3N	:	Triethylamine (TEA)
EtOH	:	Ethanol
FACS	:	Fluorescence assisted cell sorter
FBS	:	Fetal bovine serum albumin
FITC	:	Fluorescein isothiocyanate
gRNA	:	guide RNA
H2SO4	:	Sulfuric Acid
HCl	:	Hydrochloric acid
HDR	:	Homology-Directed Repair
HEK	:	Human embryonic Kidney cells
HOBt	:	1-Hydroxybenztrazole
HPLC	:	High performance liquid chromatography
HRMS	:	High Resolution Mass Spectrum
Indel	:	insertion and/or deletion
LB agar	:	Luria britani agar
LB broth	:	Luria britani broth
mg	:	Milligram
min	:	Minutes
mL	:	Millilitre
mmol	:	Milli mole
mol	:	Mole
MTT	:	3-(4,5-Dimethylthiazol-2-yl)-2,5-Diphenyltetrazolium Bromide
Na2SO4	:	Sodium sulfate
NaCl	:	Sodium chlorite
NaHCO3	:	Sodium bicarbonate
NaN3	:	Sodium azide
NaNO2	:	Sodium nitrite
NaOH	:	Sodium hydroxide
NHEJ	:	Non-Homologous End Joining
NMR	:	Nuclear Magnetic Resonance
NPs	:	Nanoparticles

PAM	:	Protospacer-Adjacent Modif
PBS	:	Phosphate buffer saline
PPh3	:	Triphenylphosphine
ppm	:	Parts per million
RIPA	:	Radioimmunoprecipitation assay
RNA	:	Ribonucleic acid
RPMI	:	Roswell Park Memorial Institute medium
rt	:	Room temperature
s	:	Singlet
SDS	:	Sodium dodecyl sulphate
SDS-PAGE	:	Sodium dodecyl sulfate polyacrylamide gel Electrophoresis
sgRNA	:	single guide RNA
siRNA	:	Short interfering RNA
t	:	Triplet
TALEN	:	Transcription activator effector nuclease
TBS	:	Tris buffered saline
tBu	:	Tertiary butyl
t-BuOH	:	tert-Butyl alcohol
TFA	:	Trifluoroacetic acid
THF	:	Tetrahydrofuran
TLC	:	Thin layer chromatography
tracrRNA	:	trans-activating crRNA
Tris-HCl	:	Tris (hydroxymethyl) aminomethane hydrochloride
ZFN	:	Zinc-Finger Nuclease
δ	:	Chemical shift scale
µL	:	Micro litre
µM	:	Micro molar
µmol	:	Micromoles

Table of Contents

Chapter No.	Information	Page No.
I	**Introduction**	1-33
	1.1 Introduction	2
	1.2 Brief History & Progress	3
	1.3 Methods of Gene Delivery	5
	1.4 Lipofection Pathway	11
	1.5 Genome Editing	14
	1.6 Present Thesis	20
	1.7 References	27
II	**Influence of hydrophobicity in hydrophilic region of cationic lipids on enhancing nucleic acid delivery and gene editing**	34-73
	2.1. Introduction	35
	2.2. Results and Discussion	38
	2.3. Gene Editing	50
	2.4. Conclusions	53
	2.5. Experimental Section	54
	2.6. References	64
	2.7. Spectral Data	67
III	**Effect of Methylation in the Hydrophilic Domain of Tocopheryl Ammonium Based Lipids on their Gene Delivery Properties**	74-100
	3.1. Introduction	75
	3.2. Results and Discussion	77
	3.3. Conclusions	85
	3.4. Experimental Section	86
	3.5. References	92
	3.6. Spectral Data	94
IV	**Influence of hydrophobic tail on Amino acid based dipeptide cationic lipids for efficient Gene delivery**	101-125
	4.1. Introduction	102

	4.2. Results and Discussion	103
	4.3. Conclusions	112
	4.4. Experimental Section	112
	4.5. References	119
	4.6. Spectral Data	123
V	**Proline head group based gemini like cationic lipids: The effect of spacer length on transfection properties**	126-148
	5.1. Introduction	127
	5.2. Results and Discussion	129
	5.3. Conclusions	134
	5.4. Experimental Section	135
	5.5. References	141
	5.6. Spectral Data	144
VI	**Summary and Conclusions**	149
	Appendices	i-ii
	List of Publications	i
	Biography of The Author	ii

CHAPTER I

INTRODUCTION

1.1. Introduction

For the treatment of genetic illnesses, cationic lipid-guided nucleic acid delivery has considerable potential in gene therapy and genome-editing applications. A number of prevalent human diseases have been directly related to gene regulation, are carried down to the next generation, and are the result of mutations. During the time from the late 1960s to the early 1970s, the idea of gene manipulation by employing a corrected copy of the gene sequence as "gene therapy" was presented in an effort to treat these disorders at their genetic source[1]. The search for novel alternate ways has made gene therapy an appealing concept to treat both hereditary and acquired disorders, as many pharmaceutical treatments are failing to effectively cure numerous diseases. This has increased interest in gene therapy and helped to progress future developments in the domains of medicine, biochemistry, and biotechnology, among others. When gene therapy first began, its main objective was to treat inherited diseases by replacing defective genes with functional copies of the gene sequence, but it has now expanded to treat acquired illnesses as well, such as cancer, and to deliver genetic vaccines to trigger both cell-mediated and humoral immune responses[2]. Gene therapy has several applications, including the introduction of new cellular bio-functions and the replacement of damaged or missing genes. Despite being a versatile approach, gene therapy has not yet made the therapeutic progress anticipated.

The objectives and principles of gene therapy rely mainly on two key factors, namely (i) the development of appropriate oligo nucleic acid strands that can carry out the necessary tasks in the targeted cells[3], and (ii) their effective intracellular delivery into predetermined cells.[4] There are various genes that can express the necessary functionalities, and it is now possible to create genetically modified material that expresses a therapeutic phenotype in large enough numbers for clinical trials. Gene therapy's clinical success is seriously hampered by the methods used to deliver drug mimics to the locations where their expression is required. Vector-mediated gene delivery is at the forefront of the diverse spectrum of oligonucleotide delivery techniques that have been developed so far[5], and it requires additional development for optimal delivery.

Biomolecules like pDNA, micro-RNA, mRNA, sgRNA encoded pDNA, CRISPR/Cas9, etc. are now delivered using gene delivery. The application of gene delivery for investigating as well as

influencing cellular processes has expanded as a result of recent biological discoveries, such as CRISPR associated Cas9 mediated gene editing. The insertion, deletion, or replacement of nucleic acid at a specific site in the genome of an organism or cell is the foundation of gene editing. Using designed nucleases like CRISPR-Cas9, ZFNs, or TALENs, the genome can be edited. Cas has been frequently used to alter genes in model systems, such as human cells and animal zygotes, and it holds great promise for both fundamental research and clinical applications. The Cas9 protein and guide RNA (gRNA), which present in the CRISPR/Cas9 RNA-endonuclease complex, are structured as per the streptococcus pyogenes SF370 adaptive immune system. It may be trained to detect almost any gene by manipulating gRNA sequences and targets genomic regions that are complementary to the gRNA and include the trinucleotide protospacer adjacent motif (PAM). The Double Strand Breaks (DSBs) produced by Cas9 binding and subsequence target site cleavage are repaired by either NHEJ or HDR, producing indels or precise repair, respectively. The CRISPR/Cas9 system's simplicity, speed, and effectiveness have made it suitable for a wide range of uses, including genome editing, research into the functions of genes, and gene therapy in both animal and human cells.

1.2 Brief History & Progress:

The notion of gene therapy that has been the subject of decades of research was to bring this treatment to clinic, but only a small number of patients have significantly benefited from its use. Only 1843 clinical trials were performed, are currently being conducted, or have been received approval from 1960s i.e, from the time the concept of gene therapy was first proposed in the 1960s[6]. A functional gene was introduced into murine bone marrow[7], 3T3 cells[8], or a human HPRTB-lymphoblast cell line[9] in 1983 using a retroviral vector. The first human gene therapy experiment was performed on a four-year-old child with ADA deficiency on September 14, 1990. Her immunodeficiency was successfully treated with experimental therapy (with the right copy of the gene composition) by Dr. W. French Anderson and Michael Blaese[10], demonstrating the concept's preliminary viability. The community's spirits were raised in the year 2000 by the successful treatment of kids with SCID-X1[11]. The prepared liposomes using cationic lipid DC-Chol and co-lipid DOPE were complexed with pDNA containing CFTR cDNA under the

transcriptional controller of SV40[12] and through single nasal delivery RSV 3'LTR promoters were evaluated for their safety and effectiveness in the first non-viral clinical trials[13]. An interest in non-viral vector based nucleic acid delivery, in particular lipid nanoparticle mediated nucleic acid delivery[22], was sparked by the successful presentation of liposomal siRNA medication, GIVOSIRAN, and recent lipid enabled mRNA-based vaccinations for COVID19.

The substantial development made possible by gene therapy in relation to the cause of the disease has been illustrated as follows.

Immune deficiencies: Gene delivery is used to treat various inherited immunological disorders. Ex vivo experimental therapy was performed, which entails transducing blood stem cells with a virus and DNA complex outside the body of the patient before administering the cells back inside the patient by restoring the corrected functions. With SCID treatments, some trials[14] had leukaemia signs that were activated, but with ADA treatments, the majority of patients didn't need any additional ADA enzyme injections, and none of them got leukemia[15].

1.2.1 Hereditary blindness: Gene therapy is a relatively new form of treatment for inherited blindness, but it has the potential to restore eyesight, as shown by some encouraging outcomes in animal models. Retina being crucial component of the eye, which is simple to access, and partially immune system protected. As a result, the virus/DNA complex can easily enter and cannot spread to other organs. One of the degenerative types of blindness, Leber Congenital Amaurosis (LCA), has been effectively treated with AAV based gene delivery[16]. In another investigation, a virus was used to deliver a functional REP1 gene was improved the vision of 6 out of 9 individuals with the degenerative condition choroideremia[17].

1.2.2 Hemophilia: Most severe disorders caused by internal blood loss or blood loss due to small cut are caused by a lack of the clotting protein Factor IX. The Factor IX gene was successfully delivered to liver cells using an adeno-associated viral vector, and as a result, the majority of patients produced at least some Factor IX and experienced minimal bleeding incidents[18].

1.2.3 Blood disease: Red blood cells have a role in -thalassemia disease because they develop from defective globin genes, which produce red blood cells with an oxygen-carrying protein. Due to shortage of red blood cells, individuals frequently require blood transfusions[19]. In 2007,

a patient with severe Thalassemia undergone ex vivo experimental gene therapy, in which blood stem cells were extracted from the patient's bone marrow and treated with retrovirus [20]. His body received the altered stem cells, which generated healthy red blood cells. Even after seven years of treatment, the patient didn't need any blood transfusions. For the treatment of sickle cell disease patients, a similar strategy could be applied.

1.2.4 Fat metabolism disorder: A gene called Lipoprotein lipase (LPL) produces a protein that aids in the breakdown of blood fats to keep their concentrations from reaching dangerously high levels. The working copy of the LPL gene was successfully delivered to muscle cells via an adeno-associated virus in Glybera, the first viral gene therapy medication to receive European approval in 2012[21].

1.2.5 Cancer: One of the hazardous diseases, cancer, is accountable for the majority of recent global human mortality in various forms. Various gene therapy techniques are in development to treat cancer[27]. T-VEC is an effective remedy for melanoma (a skin cancer) [28]. The virus is directly injected into the tumour of the patient, where it multiplies till the cancer cells get burst, thereby releasing more viruses which impacts additional cancer cells other than healthy cells.

1.2.6 Parkinson's disease: It is a brain ailment that occurs over time as a result of loss of brain cells that produce the signalling molecule dopamine. Patients experience a loss of control on their movements as the condition worsens. Three genes were implanted into the brain cells of few patients with advanced Parkinson's disease using a retroviral vector[30]. These three newly added genes enable the cells to produce dopamine because they lack the ability to do so naturally. Thus, all of the patients showed improved muscular control following the therapy.

The discovery of delivery devices that can transmit nucleic acids from extracellular to intracellular is crucial for the success of gene therapy. To advance the gene delivery strategy toward success, a wide variety of vectors are being used and developed.

1.3 Methods of Gene Delivery:

In numerous earlier studies, significant attempts were made to demonstrate the successful delivery of genes into specific cells by utilising a variety of tactics and potent tools. Based on the

tools utilised for gene delivery, all of these strategies were primarily divided into three separate methodologies. These methodologies are described below

1.3.1 Naked DNA delivery:

One of the major categories of ways of delivering nucleic acids into cells is naked DNA delivery. This is the physical or technical transfer of simple DNA into the tissues nearby or into the bloodstream. Different varieties are generated based on the tools and physical methods utilised for gene delivery, as shown in the list below.

a. Electroporation: In this method, DNA molecules can pass through temporary gaps in the cell membrane. This is done in order to provide the high voltage electric brief pulses that are necessary for pore formation in cell culture. Even in challenging cell types, transfection can be carried out with this technique. The high incidence of cell death associated with this application, limits its use in clinical trials[31].

b. Gene Gun: Another physical technique for DNA transfection is the use of a gene gun or particle bombardment. This method involves coating DNA with gold particles and loading it into a machine that forces to allow the DNA/gold to enter the cells. This method is quick, easy, and secure, making it successful for delivering nucleic acids to both cultured cells and cells in vivo, particularly for gene transfer to skin[32] and shallow wounds.

c. Sonoporation: Ultrasonic frequencies are used in sonoporation to introduce DNA into cells. It is believed that sonic cavitations cause the cell membrane to rupture, allowing DNA to enter cells.

d. Magnetofection: This technique involves complexing DNA with magnetic particles, which are then brought into touch with a cell monolayer by placing a magnet underneath the tissue culture plate.

e. Microinjection: Using a tiny glass needle and a microscope, the DNA is directly injected into the nuclei of target cells in this procedure. Even though the procedure is straightforward, clinical application is highly challenging. Though this method of gene transfer is almost completely effective, it is time-consuming and difficult, often allowing only a few numbers of cells (for example, 500 or less) to be transfected per experiment[33].

Limitations inspired the notion of enclosing the DNA in a specific substance and enabling delivery to the greatest number of cells. Viral-mediated gene delivery refers to the viruses being the first

materials that were used to pack DNA followed by delivery.

1.3.2 Virus mediated DNA delivery:

Researchers typically use viral vectors to deliver functional genetic material into cells. Monkey kidney cells which were kept in cell culture were infected by Paul Berg using modified SV40 virus that contained plasmid from the bacteriophage lambda[34]. Various viral vector types have been applied so far are listed below.

I. Retrovirus: Many clinical trials for gene therapy employ retroviruses as their vectors. Due to their restricted DNA payload capabilities, they have a reverse transcriptase that enables integration into the host genome[35]. The main disadvantage of utilising retroviruses is that transduction takes place only in actively dividing cells. It is suspected that insertional mutagenesis brought on by integration into the host genome would result in leukaemia or cancer.

II. Lentivirus: The genomes of both dividing and non-dividing cells may accommodate this kind of virus[36]. When a virus infects a cell, it reverse-transcribes the viral genome into DNA, which the viral integrate enzyme subsequently inserts into the genome at a random location. Lentivirus vectors, as compared to gamma-retroviral vectors, have been found in studies to have a decreased propensity to integrate into areas that may cause cancer[37].

III. Adenovirus: Adenoviruses contain double-stranded DNA that is about 36 kb in size and is used to carry the genetic material[38]. These viruses cause eye, gastrointestinal, and respiratory infections as well as a quick immunological reaction that could have negative effects.

IV. Adeno-associated virus: These are tiny viruses with a single stranded DNA genome of around 4.7 kb that is encased in a protein coat[39]. The wild type AAV can almost always successfully insert genetic material at a specific location on chromosome 19. Nevertheless, there are certain drawbacks associated with using AAV. Carrying and delivering even a small amount of DNA is difficult and challenging using AAV.

V. Herpes simplex virus: The neurological system is the main area of investigation for these viruses[40].

Although viruses are the most effective means of gene transfer till date, their extensive clinical effectiveness has been hampered by a number of significant limitations linked to their usage.

These significant limitations are listed below:

- Immunogenicity
- Insertional mutagenesis
- Limited gene loading capacities

As a result of these issues, viral vectors have come under intense scrutiny, which has made it crucial to look for safer alternatives.

1.3.3 Non-Viral mediated DNA delivery:

Compared to viral methods, non-viral methods have some advantages, such as simple large-scale production, no restriction on gene loading, and little host immunogenicity. Recent advancements in vector technology have led to the creation of compounds and procedures with transfection efficiencies comparable to viruses.

i. **Polymeric Vectors:** Successful delivery relying on endocytosis could be achieved using these carriers, coupled to the targeted gene or other biological molecules[42]. Therefore, a wide range of polymers, including chitosan, PEI, polylysine, polyamino ester, and others, have been studied for gene delivery[43].

ii. **Dendrimer-Based Vectors:** A class of macromolecules known as dendrimers has highly branching, spherical forms that are easily soluble in water and have a distinctive surface covered in primary amino groups[44]. When comparing dendrimers to several other types of polymers recently investigated[45], they can be distributed uniformly[46]. Due to their distinctive qualities, including their restricted molecular dispersion, excellent molecular homogeneity, highly functionalized terminal surface, and specified size and shape, PAMAM dendrimers have been widely investigated as non-viral gene carriers[47].

iii. **Nano particles:**

Quantum Dots: When exposed to light and electricity, quantum dots, which are nanoscale materials, can emit fluorescence, which is very useful for tagging and monitoring proteins inside cells [50]. Compared to organic fluorophores, quantum dots have a longer fluorescence lifetime [51].

Gold nano particles: Due to their benefits, such as their ability to be fabricated in a scalable manner with low size dispersion, AuNPs are the appealing materials for DNA delivery applications[54, 55].

iv. Cationic lipids: When cationic lipids are disseminated in aqueous solution, they can form bilayer membrane-type vesicles of the surfactant type. These lipid bilayer-based vesicles that have been created artificially are termed as liposomes. These imitators of biological membranes are easily able to diffuse across cell plasma membranes and enter the cell cytosol. Due to their structure, chemical structure, and colloidal size, liposomes display a number of characteristics that may be beneficial in a variety of applications. The most crucial characteristics include colloidal size, which refers to relatively homogenous particle size distributions between 20 nm and 10 m, as well as unique membrane and surface properties. These include the way the bilayer phase behaves, its permeability and mechanical properties, the density of the charge, the presence of surface-bound or grafted polymers, and the attachment of ligands. Furthermore, due to their amphiphilic character, liposomes are efficient solubilizing systems for a variety of chemicals. In addition to these physical qualities, liposomes also display a wide range of unique biological properties, such as particular interactions with various cell types and biological membranes[57].

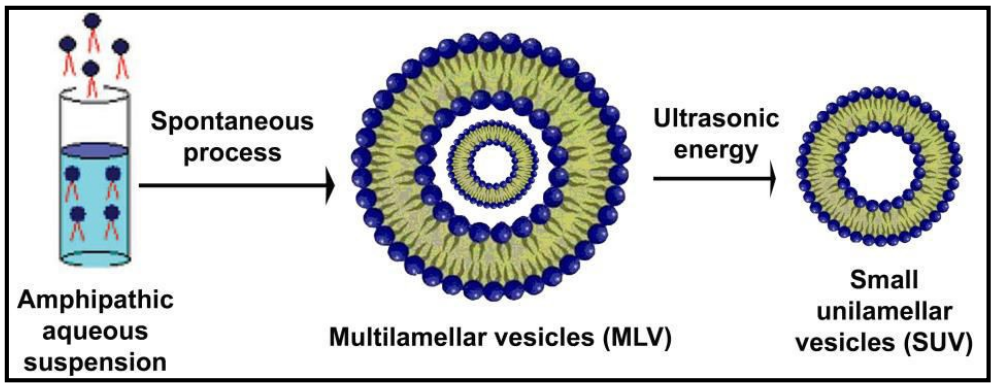

Figure 1. Liposome Formation

Liposomes can carry both hydrophobic and hydrophilic molecules by dissolving hydrophobic compounds into the membrane. The lipid bilayer can combine with another bilayer, such as the cell membrane, to carry the molecules to sites of action. This releases the liposomal contents.

MLV (Multi Lamellar Vesicles), SUV (Small Unilamellar Vesicles), and LUV are three different forms of liposomes. Bio molecules can be delivered using liposomes. Cationic liposomes could also accomplish targeted distribution by covalently attaching receptor-specific ligands to the liposomal surface. Due to the plasmid size and a substandard transfection technique, it can be technically difficult to encapsulate DNA into conventional liposomes. On the basis of this, cationic lipid-based alternative technology was established in the late 1980s[58]. The goal was to capture plasmids more effectively and transfer DNA to the cells by offsetting negatively charged plasmids using lipids' positive charge. This process requires adding the cationic lipids to the cells after combining them with the DNA. As a result, aggregates made of DNA and cationic lipids are formed.

Felgner et al. synthesised the cationic lipid DOTMA, which was used to describe non-viral cationic lipid mediated gene transfer for the first time. This lipid, alone or in conjunction with other neutral lipids, spontaneously forms multilamellar vesicles. Small unilamellar vesicles can then be created by sonicating these vesicles. To create lipoplexes, nucleic acids spontaneously bind with DOTMA. The positively charged head group of DOTMA and the negatively charged phosphate groups of DNA are assumed to interact ionically to create complexes. For transfection of various cell lines commercialized DOTMA (Lipofectin, Gibco-BRL, Gaithersburg, MD) with DOPE are mixed at similar ratio and have been successfully used[59]. Numerous metabolizable quaternary ammonium salts have been developed in an effort to reduce the cytotoxicity of DOTMA, and when combined with DOPE[60], their efficiency is comparable to Lipofectin's.

1.4 Lipofection Pathway

When a desired functional material, such as an active nucleotide, is injected into cells using liposomal membrane vesicles across the cell membrane, the process is known as lipofection. It entails a number of steps, including (a) the formation of a lipid-DNA complex (lipoplex), (b) adhesion of the lipoplex to the cell's surface, (c) internalisation of the lipoplex, (d) endosomal escape, (e) transport of released nucleic acid from the endosomal compartment to the nucleus followed by gene expression (Figure 2). The efficiency of the entire process is impacted by the hurdles that are encountered at each stage of the lipofection pathway.

(a) ***Formation of a Lipoplex*****:** A supramolecular aggregate known as lipoplex is created when negatively charged plasmid DNA ends are electrostatically attracted to positively charged lipid vesicles. The primary assumption was that a large number of liposomes may team up with a single plasmid molecule in order to regulate its charge and compact the DNA into a tiny, dense lipoplex[80a]. However, electron microscopy studies have obtained images of lipoplexes with a range of sizes of 100-200 nm macromolecular structures[80b–80d]. The DNA complexation or condensation that results in elongated, "spaghetti-shaped" lipoplexes is what causes their modest size80e. Also seen are large aggregations, or "meatball" lipoplexes, which are thought to contain a large number of lipid and DNA molecules. Uncertainty exists regarding which of them represents the greatest transfection-efficient fraction.

(b) ***Cellular internalization of lipid-DNA complex*****:** Initially, it was believed that specific types of exposed cell membrane components caused cationic amphiphile-DNA complexes to enter cells by absorbing net positive charge onto the negatively charged cell surface[58]. The bilayered plasma membrane, which is usually referred to as endocytosis, was found to be engulfing nonviral vector produced lipoplexes in studies on cell entrance and intracellular trafficking[81]. Few endocytotic pathways, including those mediated by clathrin via coated pits, adsorptive via proteoglycon fusion[82a], and caveolae via caveolae vesicles, as well as phagocytosis and macropinocytosis[82c], have been characterised and extensively reported.

As shown in Figure 2, lipoplex can be absorbed by either one of the aforementioned mechanisms or numerous pathways. The lipoplex is driven into the early endosome stage, when

the internal pH is greater than five, by each of the endocytotic mechanisms, which are engaged with various types of unique proteins. Numerous molecular biology research has been successful in identifying inhibitors that can restrict the production of certain proteins, hence preventing the activity of the associated pathway. While methyl-β-cyclodextrin (m-β-CD) or filipin-III inhibit caveolae-mediated endocytosis[82c], chlorpromazine (CPZ) inhibits clathrin-mediated endocytosis[82a,82b].

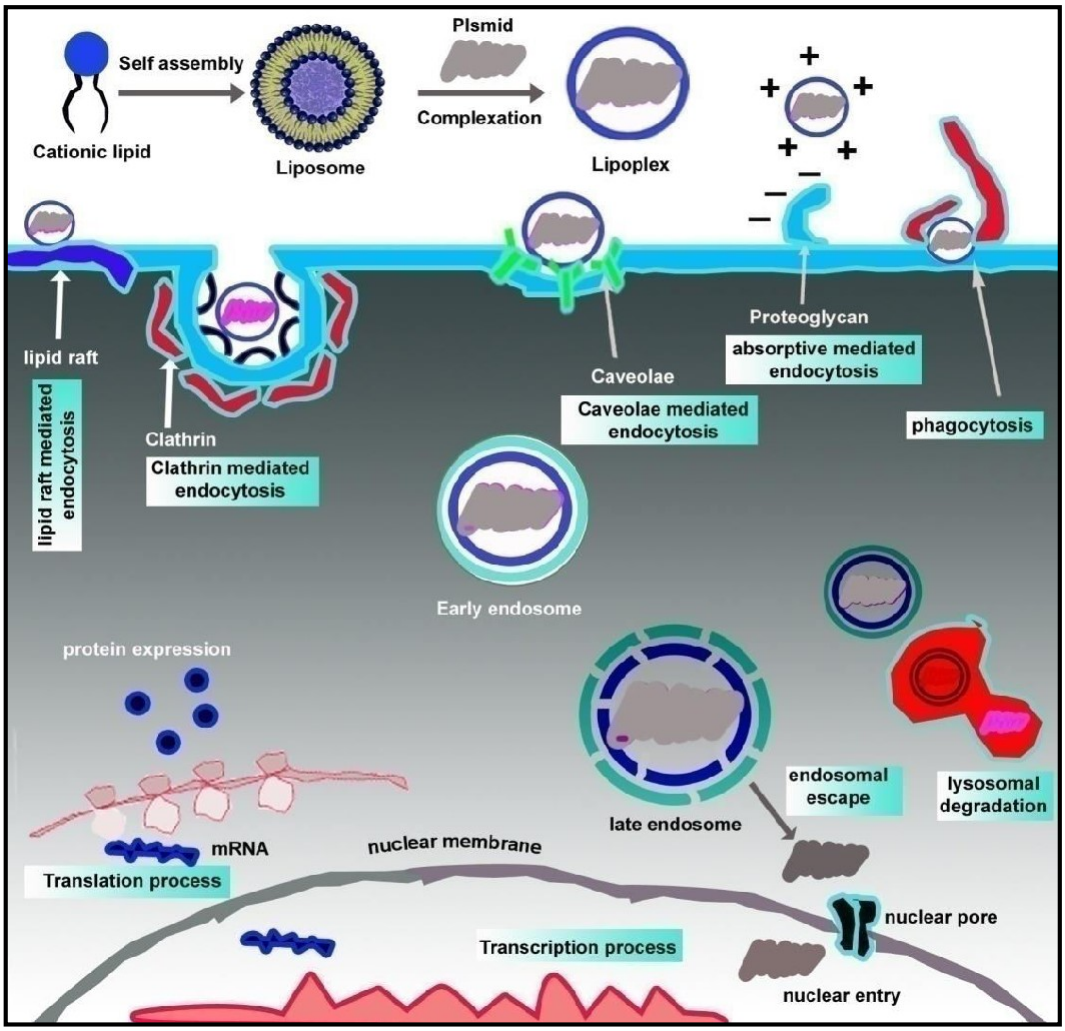

Figure 2. Lipofection Pathway

By influencing membrane ruffling and actin polymerization, cytochalasin D prevents macropinocytosis[82d]. Vesicle trafficking is aided by wortmannin, a PI 3-kinase inhibitor that

promotes vesicle fusion[82e]. Nocodazole is known to limit complex buildup in endosomes by blocking the transport of complexes from endosomes to lysosomes[82f]. The vacuolar ATPase enzyme is responsible for preserving the lysosomes' acidic pH[82g], and bafilomycin A1 is an inhibitor of this enzyme. Nystatin was utilised to sequester cholesterol, which was then used to determine the route of internalisation[82b]

(c)*Endosomal Escape:* In order to release the packed DNA material into the cytoplasm for lysosomal degradation, endosome rupture or unfolding is one of the crucial steps in determining transfection efficiency. There have been a number of hypotheses put forth to explain the mechanistic insight, despite the fact that the release of DNA from this endosome state to the cytosol is not fully known. By using a flip-flop mechanism, this can cause the endosome membrane to become unstable, which in turn leads to the DNA becoming decomplexed. Additionally, non-cationic helper lipids like neutral DOPE can speed up the breakdown of endosomal membranes [84a-84c] and assist membrane fusion. It is true that DOPE tends to produce an inverted hexagonal phase, which is frequently seen when membranes are fused.

(d) ***Nuclear entry of DNA:*** After endosome escape, the nucleic acid must navigate the cytoplasm and reach the nucleus while avoiding obstacles such as DNA destruction caused by cytoplasmic nucleases and very poor cytoplasmic mobility. The nuclear pore complex and mixing of the cytoplasm after the loss of the nuclear membrane during mitosis[86a] are two plausible ideas for how the cytoplasmic pDNA can enter the nucleus[86b]. It has repeatedly been demonstrated that mitotic activity for the lipoplexes significantly increases gene transfer in cultured cells. As a result of their frequent mitosis, tumour cells are more specifically targeted, whereas non-dividing cells—like healthy brain cells—rarely get transfection. Nuclear localization sequences (NLS), which can be integrated into DNA complexes, can be used to transfer the plasmid into the nucleus in non-dividing cells. NLS are short peptide sequences (5–25 amino acids) that are both required and sufficient for a protein's nuclear localization[86b]. These sequences can be directly connected to the plasmid[86d] or included in complexes with cationic lipids[86c]. Nevertheless, 5% and 80% of non-dividing endothelium cells transfected with and without a NLS showed good results[86c].

1.5 GENOME EDITING

The term "genome" refers to an organism's entire DNA sequence. The deliberate alteration of a living cell's DNA sequence is known as genome editing. In this, a DNA strand is broken at a specific point, and the broken DNA strands are then repaired by cellular repair processes that occur naturally. When the DNA is cut, new DNA sequences can be supplied and used as templates to create a changed sequence.

1.5.1 CRISPR/Cas9 system:

Ability to precisely alter the genomes of eukaryotic cells has greatly enhanced as a result of recent developments in genome editing technologies. Programmable nucleases, primarily the CRISPR/Cas system, are already altering the ability to examine how the genome functions and may be applied clinically to target or introduce genetic changes to cure diseases that are resistant to conventional treatments.

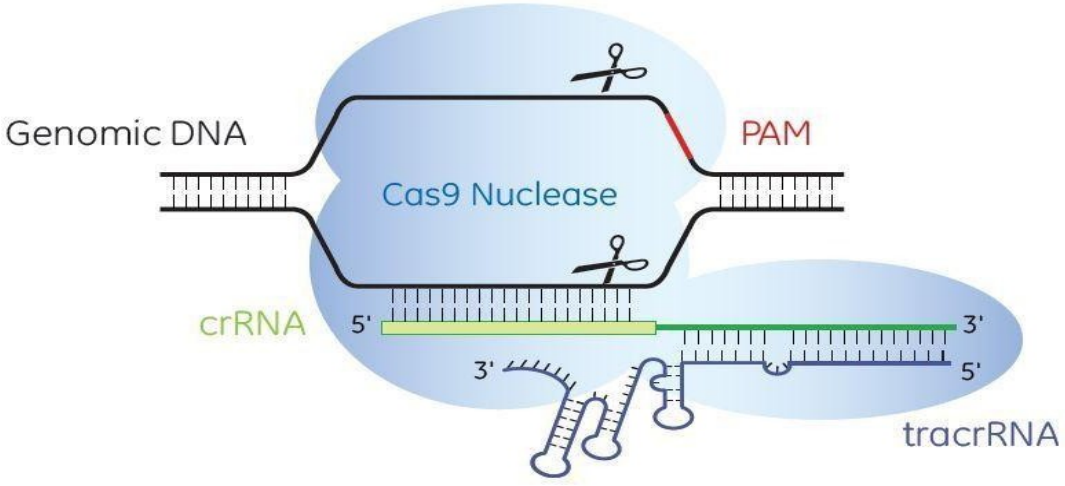

Figure 3: Schematic representation of CRISPR/Cas9 structure

A significant structural change between apo-Cas9 unbound to nucleic acid and Cas9 in a composite with crRNA and tracrRNA, establishing a central channel to accommodate the RNA-DNA heteroduplex, was disclosed by Streptococcus pyogenes Cas9 (SpCas9). Three forms of the type II CRISPR locus are further differentiated based on the diversity of linked Cas genes (IIA–IIC). The RuvC and HNH hallmark nuclease domains of the Cas9 protein

family were each given their respective names based on their structural similarity to other known nuclease domains. Numerous groups have thoroughly investigated the Streptococcus pyogenes Cas9 selectivity employing mismatched guideRNA libraries for in vitro selection and reporter studies. Cas9's structural and functional diversity makes it a distinctive type II gene and is only connected to the type II CRISPR locus. The Cas9, Cas1 and Cas2 genes, as well as a CRISPR array and tracrRNA, are the main components of type II CRISPR loci. Only these few Cas genes are present in type IIC CRISPR systems, but type IIA and type IIB systems each feature an extra signature Cas2 or Cas4 gene.

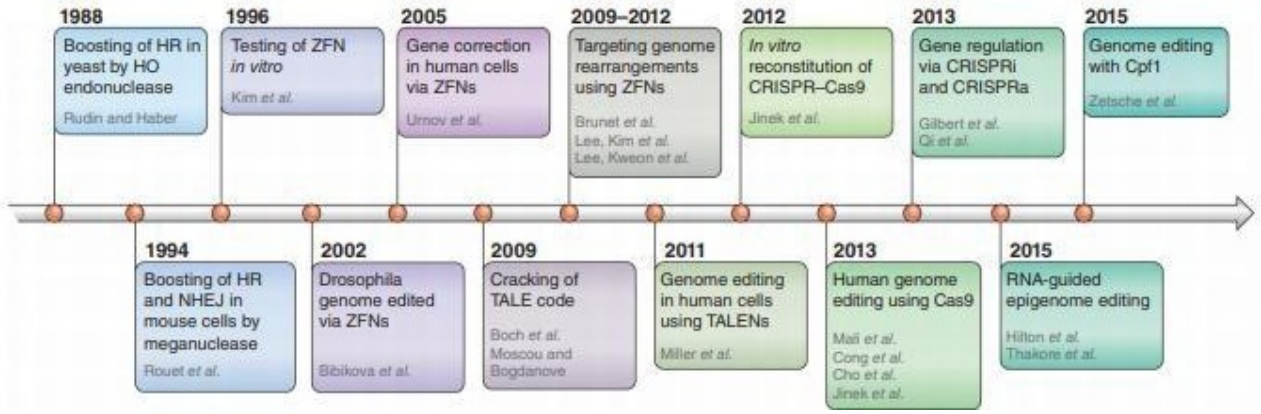

Figure 4: CRISPR/Cas9 systems' development and discovery

1.5.2 Role and Mechanisms of CRISPR/Cas9

CRISPR/Cas9 is RNA mediated adaptive immune system present in bacteria and archaea (prokaryotes) to shelter from phage and plasmid. In addition, it requires many groups of Cas gene to react against the foreign DNA sequentially and their role is participating in three different phases. First it requires a locus or array that contains spacer area where the defending host acquire from phage or plasmid and it is positioned in host genome. First phase is acquisition of target DNA where it is recognized, captured and consequently integrated as spacer between two flanking repeat sequence in a CRISPR locus. The spacer resulting from plasmid or phage is called as protospacer. Purine and pyrimidine base adjacent to protospacer are termed as Protospacer Adjacent Motif (PAM) which plays an important part in acquisition phase of DNA. Before this process occurs CRISPR/Cas is

activated by Cas1 and Cas2 which is unanimously present in all genome and generates CRISPR to function. Second phase is RNA processing that transcribes the CRISPR locus which produces a pre CRISPR RNA (prcrRNA) and the endonuclease cleaves the pre CRISPR RNA (prcrRNA) into the active state of CRISPR RNA (crRNA). The third and last phase is immunity and interference phase, that produces crRNA which forms a multiple protein complex that will identify through base pairs with great specificity in the region of incoming foreign DNA and degrades, then it maintains the phage immunity. If the base pairs and PAM are not well formed, the bacteria lose its resistance against the invading particles and it gets infected.

CRISPR is further categorized into three types by their function. Multi domain CASCADE (Cas6e/Cas6f) is involved in performing unity with processed crRNA in Type I to form ribonucleoprotein through seed sequencing and base pair activation. An essential Cas9 signature protein system is participated in Type II which contains two active domains such as RUV-C and NHN domains that are essential to endonuclease activity. Cas9 forms a large multifunctional protein complex with single guide RNA (crRNA and tracrRNA) that degrades foreign DNA. Type III needed RAMP protein, Cas9 and Cas10 and they work together to cleave the target DNA. A uniqueness of this type of protein is that, it is capable of destroying the target DNA without using PAM sequence. The double strand breaks are repaired by DNA repair mechanisms, which are done either by homologous directed repair or by NHEJ. Both the mechanisms are used to prevent the cell viability and genomic integrity.

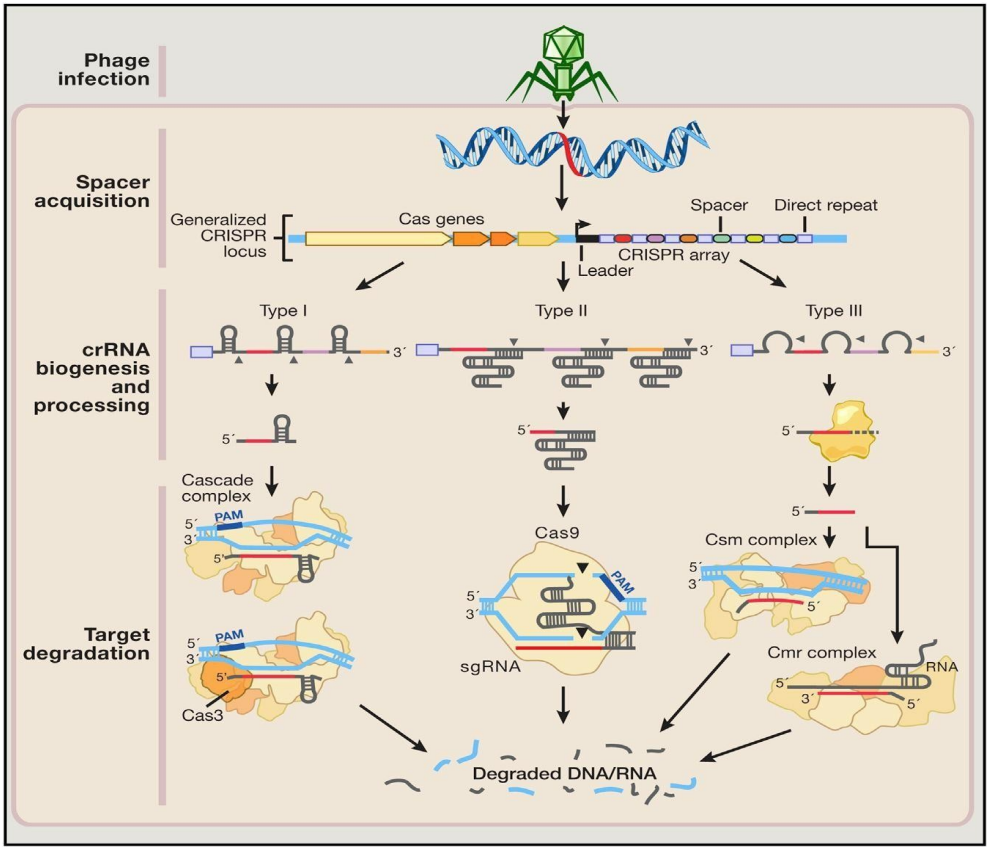

Figure 5: Natural Mechanisms of Microbial CRISPR Systems in Adaptive Immunity

1.5.3 Genome editing tools comparison

PROPERTY	**CRISPR**	**TALEN**	**ZFN**
Recognition	RNA-DNA	Protein-DNA	Protein-DNA
Methylation sensitivity	No	Sensitive	Sensitive
Off target effect	Higher potential for off target effects due to DNA wobbling	Protein sequence specific to binding anucleotide sequence linkedto nuclease such as Fok	Zinc finger sequence specificity recognizing3bp sequence linked to Fok1

Mechanism of action	Induce double strand break, outcome may be NHEJ or HDR, depends on toll design		
Identified form	Adaptive immunesystem of bacteria and archaea	Plant pathogenic bacterial species Xanthomonas	Eukaryotic gene expression regulators
Number of nucleases for an experiment	One or more sgRNA and only one Cas9 nuclease	A pair of TALEN for one target site	A pair of ZFN for one target site
Success rate	High (~99%)	High (>99%)	Low (~24%)
Specific length oftarget size	20-22bp	30-40bp	18-36bp
Size	4.2kb of Cas9 + 0.1kb of sgRNA	~3kb * 2	~1kb * 2

Table 1: Genome editing tools comparison

1.5.4 Role of CRISPR/Cas9 in treating monogenic disease

Cas9 has a wide application in research which has an immense place in world science. The multiplexing abilities of Cas9 provide a promising method for researching widespread polygenic human disorders such as diabetes, heart disease, schizophrenia, and autism. Cas9 has previously been employed extensively in research. The advancement of Cas9 as a therapeutic

technique for treating genetic abnormalities is an interesting future outlook[24]. In cells with dystrophin mutations that cause Duchenne muscular dystrophy, the CRISPR/Cas9 system is utilised to restore the expression of the dystrophin gene (DMD). As a result, dystrophin expression is reestablished in vitro in myoblasts from DMD patients. After transplanting genetically repaired patient cells into immune-deficient mice, human dystrophin is also found in vivo. Importantly, the CRISPR/Cas9 system's exclusive ability to edit genes in multiple ways at once makes it possible to make vast deletion that can fix up to 62% of DMD mutations.

1.5.5 Cas9 delivery methods

Technologies based on CRISPR/Cas9 are being developed quickly for gene correction and disease modelling. Recent improvements in Cas9/guide RNA (gRNA) delivery are based on both viral and non-viral vectors.

When delivering a gene of interest in vivo or into cell types like immune cells that are resistant to conventional transfection techniques, viral vectors like AAV or lentivirus are often used.

AAV is a non-enveloped, tiny (20 nm), single-stranded DNA parvovirus with a 4.7 kb genome. More than 200 other molecularly manufactured or naturally occurring versions of AAV exist as well. The first AAV-based gene therapy medicine, Glybera, was licenced in Europe in 2012 for the treatment of patients with lipoprotein lipase deficiency, demonstrating the immense potential of AAV for gene therapy. The plasmid-based CRISPR Cas9 system uses the same AAV used for gene therapy. The packing restriction of AAV creates an obstacle for CRISPR-Cas9 distribution via AAV (approximately 4.5 kb).

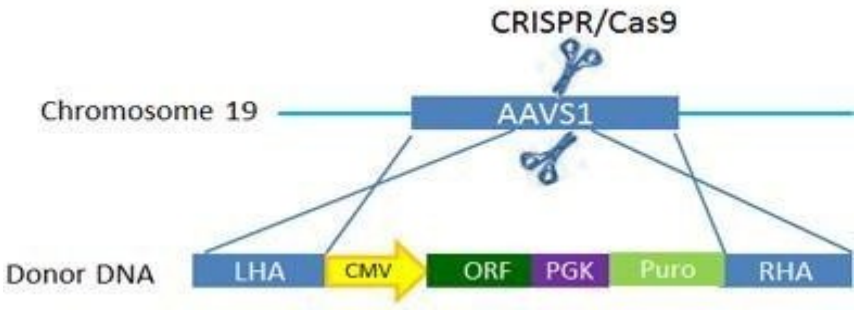

Figure 6: CRISPR Cas9 AAVS1 locus

1.6 Present Thesis

Any synthetic cationic lipid, in general, is made up of three fundamental components: a positively charged hydrophilic portion, which is typically derived from nitrogen, phosphorus, and arsenic atoms; a hydrophobic portion, which is typically derived from simple aliphatic long alkyl chains; a steroidal skeleton, such as cholesterol and a vitamin structure, such as tocopherol. These two distinct components are joined using a covalent bond directly or by using a functional moiety indirectly such as an ester, ether, sulphide, or carbamate. Each lipid component's unique characteristics, such as fluidity, orientation, cleavage sensitivity of the linker, and hydration potential, among others, could affect the ability of the lipid to deliver genes.

To advance non-viral gene therapy toward the clinic, it is required to develop alternative vectors with various structural kinds and produce more effective transfection vectors. Recent studies that established effective transfection agents utilising alpha-tocopherol as the basis used the structure-activity connection shown in Figure 7 to show how these reagents work. A single alpha-tocopherol serves as the aliphatic backbone of lipids 1a–e, which are coupled to quaternary ammonium cations that contain a variety of head group substitutions. The same backbone was utilised in other remarkable research that found that the same functional lipid units had a small orientation variation. Lipids 2a and 2b were created, and their possible effects on DNA delivery potentials in relation to their physicochemical characteristics were evaluated. For better transfection results, pH-sensitive groups like 1H-imidazole have been added to cationic head groups in the majority of recent findings in favour of endosomolysis. To illustrate the ability of the histidine and tocopherol groups to resist endosomolysis and serum sensitivity, the lipids 3a-b and 4a-b were developed. Again, the usage of tocopherol in a number of gemini lipids, including Lipid 5a-c for siRNA delivery, demonstrates its compatibility with serum. Tocopherol was used as a lipid backbone in all of the tests for the current thesis based on these favourable findings.

Due to its closeness to the negative polarity of nucleic acid and its important role in the self-assembly of bilayered membranes, head group, one of the potential lipid counter components, has gotten a lot of attention in several recent research studies. Conjugating

hydrophobic amino acid moieties to cationic lipids play a vital role in enhancing transfection efficacy by endosomal escape. As a result, four cationic lipids were formed using the head groups of several aromatic/hydrophobic amino acids, including glycine (G), proline (P), phenylalanine (F), and tryptophan (W), which were then attached to an anchoring backbone, alpha-tocopherol, using a triazole linker. These lipids' synthesis, characterization, and transfection potentials were covered in chapter 2. Regarding their physicochemical characteristics, thorough structure activity research of these lipids on transfection potentials was explained. The efficacy of these lipids in *in vitro* nucleic acid delivery by using various nucleic acids were discussed. Further, the efficacy of these cationic lipids mainly TTW as a toolset in nano-carrier system's for delivering genome-editing were also discussed.

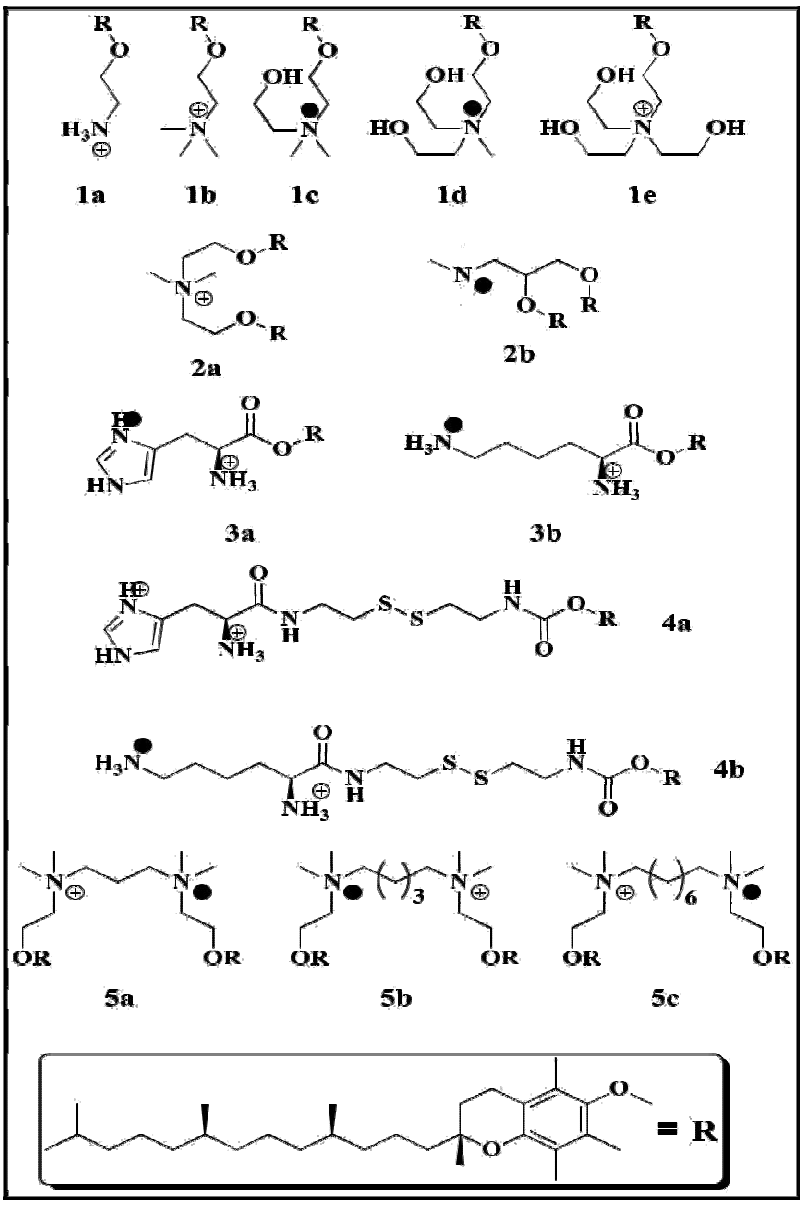

Figure 7. Tocopherol based cationic lipids reported in literature.

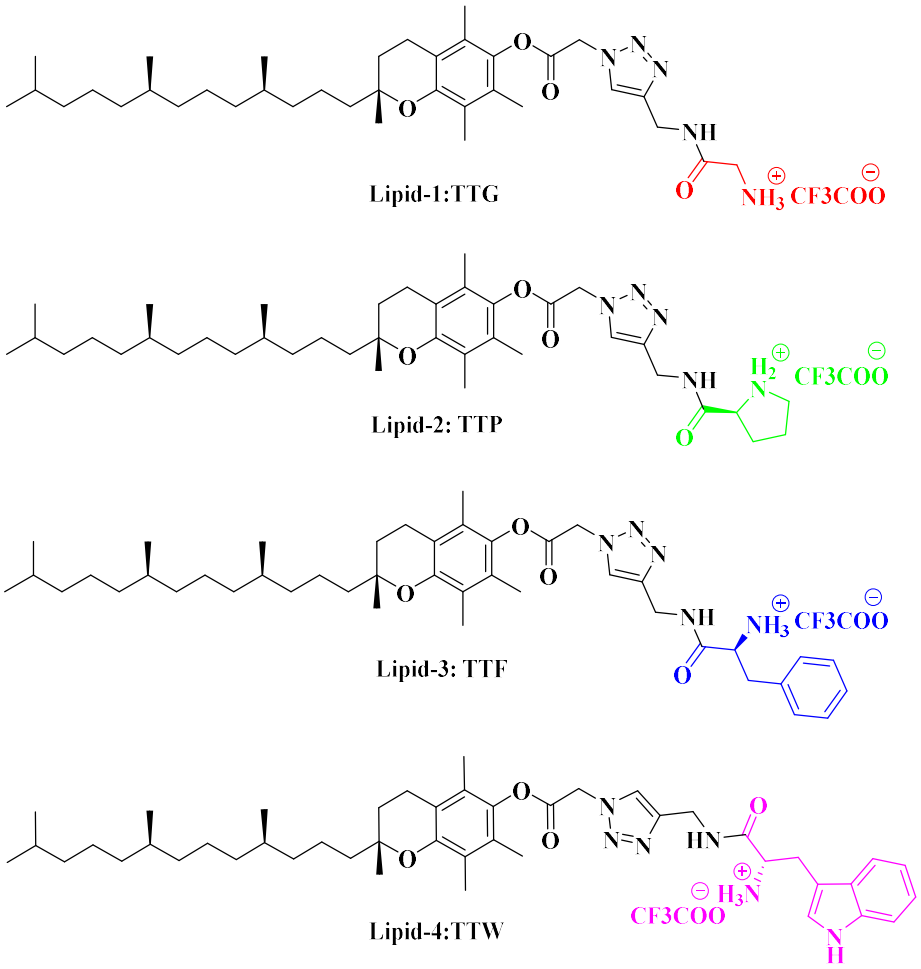

Figure 8. Molecular structures of amino acid based tocopherol derived cationic lipids

Lipid enabled nucleic acid delivery garnered tremendous attention in the recent times. DC-Chol with a head group of dimethyl ammonium and cholesterol as hydrophobic moiety is found to be one of the most successful lipids and being used in clinical trials. However, limited efficacy is a major limitation for its broader therapeutic application. In our prior studies, we demonstrated that Tocopherol as a potential alternative hydrophobic moiety with an addition antioxidant property to develop efficient and safer liposomal formulations. In our constant attempt to develop effective cationic lipids for non-viral gene delivery, **chapter 3** describes the structure activity investigation

of tocopherol (Vitamin E) based cationic lipids by varying in the degree of methylation. herein, reported the design, synthesis of four alpha-tocopherol based cationic derivatives, varying the degree of methylation, AC-Toc (no methylation), MC-Toc (mono methylation derivative), DC-Toc (di methylation derivative), and TC-Toc (tri methylation derivative) and backbone through a carbamate bond as linker. The cellular internalization studies in presence of different endocytosis blockers, consistent experimental results and analytical data were used to describe these designed lipids and compare their transfection profiles.

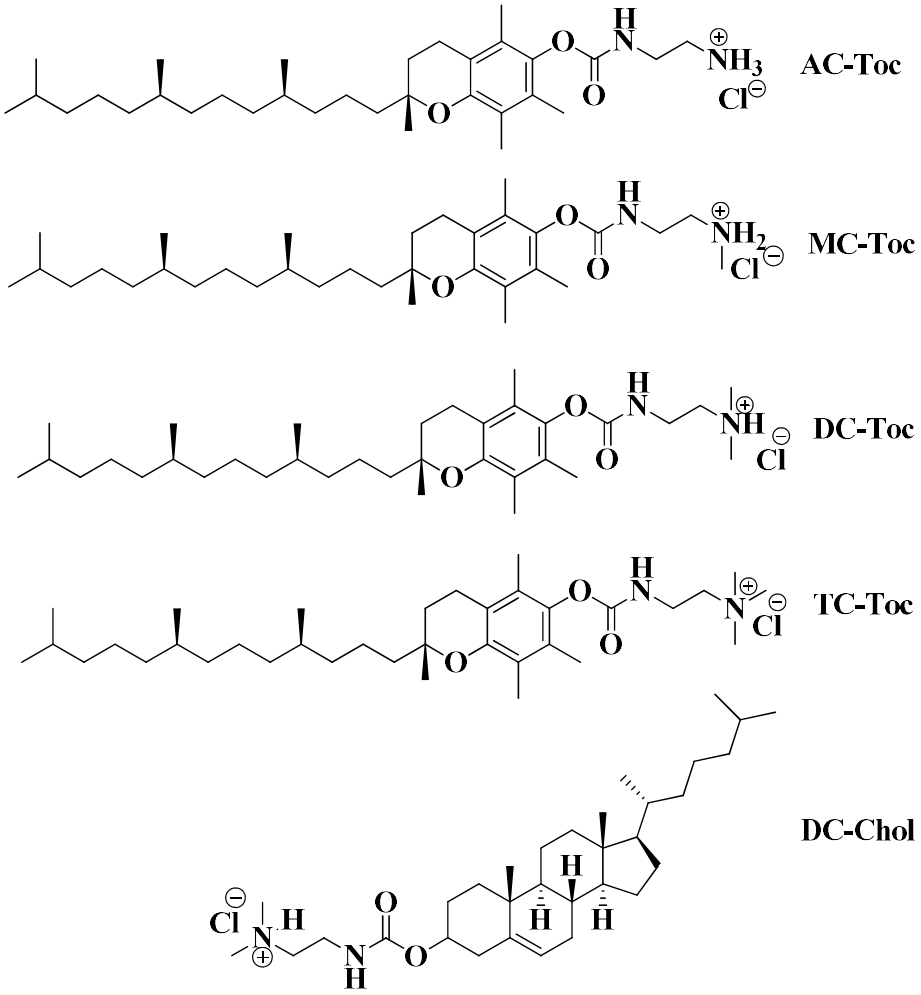

Figure 9. The structures of the synthesized and control cationic lipids.

Peptide-based cationic lipids gained a lot of interest among these non-viral vectors, because sequences are far more permeable. Adding peptide groups to cationic

amphiphiles has been shown to increase their targeting and increase their half-life *in vivo*. As a result, peptide-based lipids have outperformed other cationic lipids in terms of biocompatibility, biodegradability, and cell targeting ability, as well as prospective applications in increasing gene therapy delivery. Towards this direction, in Chapter 4, we developed two new di-peptide cationic lipids for gene delivery. Glycine and lysine amino acids choose for the di-peptide synthesis, influenced by corresponding amino-acids incredible role earlier in gene delivery studies. With varying the hydrophobic moieties, are alpha-tocopherol and cholesterol. Tocopherol-gly-lys (TGK) and cholesterol-gly-lys (CGK) are two di-peptide cationic amphiphiles that have been researched for their effectiveness in efficient gene transfer employing a variety of physicochemical investigations and transfection supporting experimental data. The overall structure activity research was described, along with the synthesis and characterisation of cationic lipids.

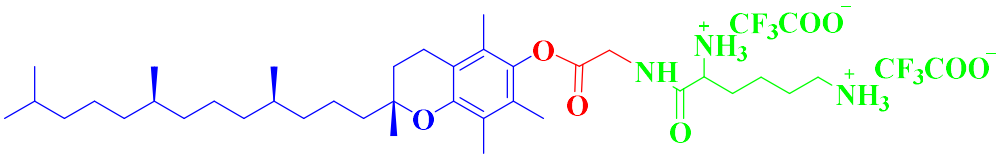

Lipid 1: TGK

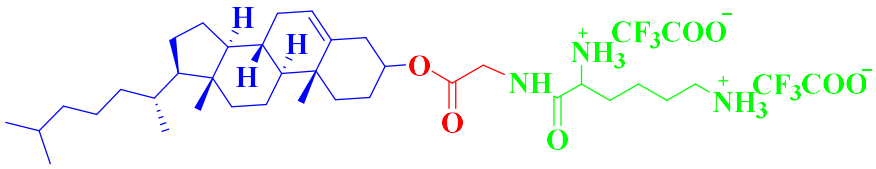

Lipid 2: CGK

Figure 10: Molecular structure of cationic lipids.

Gemini cationic lipids are among major classes of non-viral neuclic acid delivery vectors to enhance transfection. Satisfactory performance of gemini cationic lipids better than a simple cationic lipid in delivering a plasmid with reduced toxicities raising a remarkable interest to synthesize novel cationic gemini lipids. A gemini lipid is a simple cationic lipid dimer with a spacer between the two head groups. Spacer is a connecting

molecular unit directly affects the aggregation of lipid in self-assembly subsequently transfection efficiency. Natural cationic head groups are provided by amino acids, and the carboxylic acid terminals of amino acids can be utilised to conjugate to hydrophobic moieties. We have developed proline head group based gemini cationic lipids by taking into account these noteworthy characteristics. Changing spacer lengths may have an affect on DNA binding, which may have an impact on transfection. Six novel gemini cationic lipids were thoroughly synthesised, characterised, and their ability to be transfected was examined in **Chapter 5** using physicochemical and lipid/DNA interaction tests.

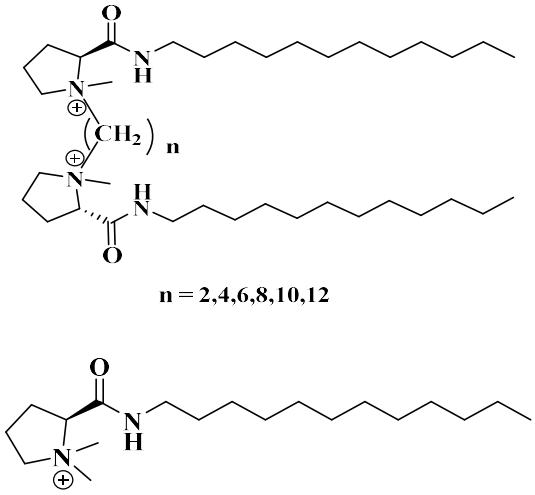

Figure 11. Structures of Control lipids and Gemeni lipids

1.7 References

1. (a) Tatum, E. L. Perspect Biol Med. 1966, 10(1), 19. (b) Sinsheimer, R. L. Am Sci. 1969, 57(1),134. (c) Davis, B. D. Science. 1970, 170, 1279. (d) Friedmann, T.; Roblin, R. Science. 1972, 175, 949. (e) Morrow, J. F. Science. 1976, 265, 13.
2. (a) Ledley, F. D., Pharm Res., 1996, 13, 1595. (b) Garmory, H. S.; Brown, K. A.; Titball, R. W. Genet Vaccines Ther. 2003, 1, 2.
3. Vacik, J.; Dean, B. S.; Zimmer, W. E.; Dean, D. A., Gene Ther. 1999, 6, 106.
4. Schaffer, D. V.; Lauffenburger, D. A., J. Biol. Chem. 1998, 273, 28004.
5. (a) Mintzer, M. A.; Simanek, E. E., Chem Rev. 2008, 2, 259. (b) Morille, M.; Passirani, C.; Vonarbourg, A.; Clavreul, A.; Benoit, J. P., Biomaterials, 2008, 24, 3477.
6. Ginn, S. L.; Alexander, I. E.; Edelstein, M. L.; Abedi, M. R.; Wixon, J., J Gene Med. 2013, 2, 65.
7. Joyner, A.; Keller, G.; Phillips, R. A.; Bernstein, A. Nature. 1983, 305, 556.
8. Miller, A. D.; Jolly, D. J.; Friedmann, T.; Verma, I. M. Proc. Natl. Acad. Sci. U.S.A. 1983, 80, 4709.
9. Willis, R. C.; Jolly, D. J.; Miller, A. D. J. Biol. Chem. 1984, 259, 7842.
10. Blaese, R. M.; Culver, K. W.; Miller, A. D.; Carter, C. S.; Fleisher, T. Science. 1995, 270, 475.
11. Cavazzana-Calvo, M.; Hacein-Bey, S.; de Saint Basile, G. Science. 2000, 288,669.
12. Caplen, N. J. Nat. Med. 1995, 1, 39.
13. 13. Gill, D. R. Gene. Ther. 1997, 4, 199.
14. Hacein-Bey-Abina, S.; Garrigue, A.; Wang, G. P.; Soulier, J.; Lim, A.; Morillon, E.; Clappier, E.; Caccavelli, L.; Delabesse, E.; Beldjord, K.; Asnafi, V., J Clin Invest. 2008, 9, 3132.
15. (a) Aiuti, A.; Slavin, S.; Aker, M.; Ficara, F.; Deola, S.; Mortellaro, A.; Morecki, S.; Andolfi, G.; Tabucchi, A.; Carlucci, F.; Marinello, E., Science, 2002, 5577, 2410. (b) Aiuti, A.; Cattaneo, F.; Galimberti, S.; Benninghoff, U.; Cassani, B.; Callegaro, L.; Scaramuzza, S.; Andolfi, G.; Mirolo, M.; Brigida, I.; Tabucchi, A., N Engl J Med. 2009, 5, 447.
16. Cideciyan, A. V.; Jacobson, S. G.; Beltran, W. A.; Sumaroka, A.; Swider, M.; Iwabe, S.; Roman, A. J.; Olivares, M. B.; Schwartz, S. B.; Komáromy, A. M.; Hauswirth, W. W., Proc. Natl. Acad. Sci. U.S.A. 2013, 6, 517.

17. MacLaren, R. E.; Groppe, M.; Barnard, A. R.; Cottriall, C. L.; Tolmachova, T.; Seymour, L.; Clark, K. R.; During, M. J.; Cremers, F. P.; Black, G. C.; Lotery, A. J., The Lancet, 2014, 9923, 1129.
18. (a) LoDuca, P. A.; Hoffman, B. E.; Herzog, R. W., Curr. Gene Ther. 2009, 2, 104. (b) Nathwani, A. C.; Tuddenham, E. G.; Rangarajan, S.; Rosales, C.; McIntosh, J.; Linch, D. C.; Chowdary, P.; Riddell, A.; Pie, A. J.; Harrington, C.; O'beirne, J., N Engl J Med. 2011, 365, 2357.
19. Niemeyer, G. P.; Herzog, R. W.; Mount, J.; Arruda, V. R.; Tillson, D. M.; Hathcock, J.; van Ginkel, F. W.; High, K. A.; Lothrop, C. D., Blood, 2009, 4, 797.
20. (a) Nienhuis, A. W. and Persons, D. A., Cold Spring Harb Perspect Med. 2012,11, a011833. (b) Persons, D. A. Nature, 2010, 7313, 277
21. Ylä-Herttuala, S. MolTher. 2012, 10, 1831.
22. L. Schoenmaker, D. Witzigmann, J. A. Kulkarni, R. Verbeke, G. Kersten, W. Jiskoot and D. J. A. Crommelin, *Int. J. Pharm.*, 2021, 601.
23. M. K. K. Azhagiri, P. Babu, V. Venkatesan and S. Thangavel, Stem Cell Res. Ther., 2021, 12.
24. H. Frangoul, D. Altshuler, M. D. Cappellini, Y.-S. Chen, J. Domm, B. K. Eustace, J. Foell, J. de la Fuente, S. Grupp, R. Handgretinger, T. W. Ho, A. Kattamis, A. Kernytsky, J. Lekstrom-Himes, A. M. Li, F. Locatelli, M. Y. Mapara, M. de Montalembert, D. Rondelli, A. Sharma, S. Sheth, S. Soni, M. H. Steinberg, D. Wall, A. Yen and S. Corbacioglu, *N. Engl. J. Med.*, DOI:10.1056/nejmoa2031054.
25. Szent-Györgyi A. Cell division and cancer. Science. 1965;149:34-7.
26. Martin TA, Ye L, Sanders AJ, Lane J, Jiang WG. *Landes Bioscience*; 2013.
27. Amer, M. H. *Mol Cell Ther*. 2014, 1, 27.
28. Johnson, D. B.; Puzanov, I.; Kelley, M. C. Immunotherapy, 2015, 6, 611.
29. Palfi, S.; Gurruchaga, J. M.; Ralph, G. S.; Lepetit, H.; Lavisse, S.; Buttery, P. C.; Watts, C.; Miskin, J.; Kelleher, M.; Deeley, S.; Iwamuro, H., The Lancet, 2014, 9923, 1138.
30. (a) Heller, R. FEBS Lett. 1996, 389, 225. (b) Heller, L. Gene Ther. 2000, 7, 826.(c) Dujardin, N. Pharm. Res. 2001, 18, 61.
31. Benn, S. I. J. Clin. Invest. 1996, 98, 2894.
32. Hengge, U. Nat. Genet. 1995, 10, 161.
33. Goff, S. P.; Berg, P. Cell. 1976, 9, 695.

34. Dachs GU, Dougherty GJ, Stratford IJ, Chaplin DJ. *Oncology Research Featuring Preclinical and Clinical Cancer Therapeutics.* 1997;9:313-25.

35. Miller, A. D. *Methods. Enzymol*. 1993, 217, 581.

36. Zufferey, R. *Nat. Biotech*. 1998, 15, 871.

37. Cattoglio, C.; Facchini, G.; Sartori, D. *Blood*. 2007, 110, 1770.

38. Schneider, G. *Nat. Genet*. 1998, 18, 180.

39. Xiao, W. J. *Virol*. 1999, 73, 3994.

40. Neve, R. L.; Geller, A. I. *Clin. Neurosci.* 1995, 3, 262.

41. Zhang, S.; Xu, Y.; Wang, B.; Qiao, W.; Liu, D.; Li, Z. J. Control. Release. 2004, 100, 165.

42. (a) Zhang, B.; Ma, X. P.; Murdoch, W.; Radosz, M.; Shen, Y. Q., Biotechnol Bioeng. 2013, 110, 990. (b) Schaffert, D.; Troiber, C.; Wagner, E., Bioconjugate Chem. 2012, 6, 1157.

43. (a) Pfeifer, B. A.; Burdick, J. A.; Little, S. R.; Langer, R., Int J Pharm. 2005, 304,210. (b) Anderson, D. G.; Akinc, A.; Hossain, N.; Langer, R., Mol Ther. 2005, 3, 426. (c) Hwang, S. J.; Bellocq, N. C.; Davis, M, E., Bioconjugate Chem. 2001, 2,280. (d) Kean, T.; Roth, S.; Thanou, M., J Control Release. 2005, 3, 643. (e) Thanou, M.; Florea, B. I.; Geldof, M.; Junginger, H. E.; Borchard, G., Biomaterials, 2002, 1, 153.

44. (a) Navarro, G.; de Ilarduya, C. T., Nanomedicine, 2009, 3, 287. (b) Wen, Y. T.; Guo, Z. H.; Du, Z.; Fang, R.; Wu, H. M.; Zeng, X.; Wang, C.; Feng, M.; Pan, S. R., Biomaterials, 2012, 32, 8111. (c) Yin, Z.; Liu, N.; Ma, M. S.; Wang, L.; Hao, Y. L.; Zhang, X. N., Int J Nanomedicine, 2012, 7, 4625

45. (a) Yang, J.; Zhang, Q.; Chang, H.; Cheng, Y., Chem Rev.2015, 6, 5274. (b) Hu, J.; Hu, K.; Cheng, Y., Actabiomaterialia, 2016, 35, 1.

46. (a) Han, M. H.; Chen, J.; Wang, J.; Chen, S. L.; Wang, X. T., J Biomed Nanotechnol, 2013, 9, 1736. (b) Cao, D.; Qin, L.; Huang, H.; Feng, M.; Pan, S.; Chen, J., Mol Biosyst. 2013, 9, 3175.

47. Daneshvar, N.; Abdullah, R.; Shamsabadi, F. T.; How, C. W.; MH, M. A.; Mehrbod, P., Cell Biol Int. 2013, 37, 415.

48. Gupta, B.; Levchenko, T. S.; Torchilin, V. P., Adv. Drug Delivery Rev. 2005, 57, 637.

49. Haralambidis, J.; Duncan, L.; Tregear, G. W., Tetrahedron Lett. 1987, 28, 5199.

50. Park, J.; Lee, J.; Kwag, J.; Baek, Y.; Kim, B.; Yoon, C. J.; Bok, S.; Cho, S. H.; Kim, K. H.; Ahn, G. O.; Kim, S., ACS nano, 2015, 9, 6511.

51. Alivisatos, A. P.; Gu, W.; Larabell, C. Ann. Rev. Biomed. Eng. 2005, 7, 55.

52. Clapp, A. R.; Medintz, I. L.; Mauro, J. M.; Fisher, B. R.; Bawendi, M. G.; Mattoussi, H. J. Am. Chem. Soc. 2004, 126, 301.

53. Srinivasan, C.; Lee, J.; Papadimitrakopoulos, F.; Silbart, L. K.; Zhao, M.; Burgess, D. J. Mol. Ther. 2006, 14, 192.

54. (a) Ghosh, P.; Han, G.; De, M.; Kim, C. K.; Rotello, V. M. Adv Drug Deliv Rev. 2008, 60, 1307. (b) Rana, S.; Bajaj, A.; Mout, R.; Rotello, V. M. Adv Drug Deliv Rev. 2012, 64, 200. (c) Jewell, C. M.; Jung, J. M.; Atukorale, P. U.; Carney, R. P.; Stellacci, F.; Irvine, D. J., Angew Chem Int Ed Engl. 2011, 50, 12312.

55. (a) Boisselier, E.; Astruc, D. Chem Soc Rev. 2009, 38, 1759. (b) Gindy, M. E.; Prud'homme, R. K. Expert Opin Drug Deliv. 2009, 6, 865. (c) Panyala, N. R.; Pena-Mendez, E. M.; Josef, H. J Appl Biomed. 2009, 7, 75. (d) Park, K.; Lee, S.; Kang, E.; Kim, K.; Choi, K.; Kwon, I. C. Adv Funct Mater. 2009, 19, 1553. (e) Beaux, M. F.; McIlroy, D. N.; Gustin, K. E. Expert Opin Drug Deliv. 2008, 5, 725. (f) Roca, M.; Haes, A. J., Nanomedicine (Lond), 2008, 3, 555.

56. (a) Daniel, M. C.; Astruc, D. Chem Rev. 2004, 104, 293. (b) Sun, Y.; Xia, Y. Science, 2002, 298, 2176. (c) Zhu, Z. J.; Carboni, R.; Quercio, M. J.; Yan, B.; Miranda, O. R.; Anderton, D. L. Small, 2010, 6, 2261. (d) De Jong, W. H.; Hagens, W. I.; Krystek, P.; Burger, M. C.; Sips, A. J.; Geertsma, R. E. Biomaterials, 2008, 29, 1912. (e) Wang, B.; He, X.; Zhang, Z.; Zhao, Y.; Feng, W. Acc Chem Res, 2013, 46, 761.

57. Lasic, D. D. Am. Sci. 1992, 80, 20.

58. Felgner, P. L.; Gadek, T. R.; Holm, M.; Roman, R.; Chan, H. W.; Wenz, M.; Northrop, J. P.; Ringold, G. M.; Danielsen, M. Proc. Natl. Acad. Sci. U.S.A. 1987, 84, 7413.

59. (a) Brigham, K. L.; Meyrick, B.; Christmann, B.; Berry, L. C.; King, G. Am J Resp Cell Mol. 1989, 1, 95. (b) Innes, C. L.; Smith, P. B.; Langenbach, R.; Tindall, K. R.; Boone, L. R. J. Virol. 1990, 64, 957. (c) Brant, M.; Nachmansson, N.; Norrman, K.; Regnell, A.; Bredberg, A. DNA Cell Biol. 1991, 10, 75. (d) Li,A. P.; Myers, C. A.; Kaminski, D. L. *In Vitro* Cell Dev Biol Anim. 1992, 28, 373.

60. Leventis, R.; Silvius, J. R. (BBA) Biomembranes. 1990, 1023, 124.

61. Van Der Woude, I.; Wagenaar, A.; Meekel, A. A.; TerBeest, M. B.; Ruiters, M. H.; Engberts, J. B.; Hoekstra, D. Proc. Natl. Acad. Sci. U.S.A. 1997, 94, 1160.
62. Pinnaduwage, P.; Schmitt, L.; Huang, L. (BBA) Biomembranes. 1989, 985, 33.
63. Byk, G.; Dubertret, C.; Escriou, V. J. Med. Chem. 1998, 41, 224
64. Hofland, H. E.; Shephard, L.; Sullivan, S. M., Proc. Natl. Acad. Sci. 1996, 93, 730
65. Aissaoui, A.; Martin, B.; Kan, E.; Oudrhiri, N.; Hauchecorne, M.; Vigneron, J. P.; Lehn, J. M.; Lehn, P. J Med Chem. 2004, 47, 5210.
66. Gao, H.; Hui, K. M., Gene Ther. 2001, 8, 855.
67. Misra, S. K.; Muñoz-Úbeda, M.; Datta, S.; Barrán-Berdón, A. L.; Aicart-Ramos, C.; Castro-Hartmann, P.; Kondaiah, P.; Junquera, E.; Bhattacharya, S.; Aicart, E., Biomacromolecules, 2013, 14, 3951.
68. Heyes, J. A.; Niculescu-Duvaz, D.; Cooper, R. G.; Springer, C. J. J Med Chem.2002, 45, 99.
69. Gao, X.; Huang, L. Biochem Biophys Res Commun. 1991, 179, 280.
70. Aberle, A. M.; Tablin, F.; Zhu, J. Biochemistry. 1998, 37, 6533.
71. Duvaz-N, D.; Heyes, J.; Springer, C. J. Curr. Med. Chem. 2003, 10, 1233.
72. (a) Miller, A. D. Angew. Chem. Int. Ed. 1998, 37, 1768. (b) Kumar, V. V.; Singh,R. S.; Chaudhuri, A. Curr. Med. Chem. 2003, 10, 1297.
73. (a) Kedika, B.; Patri, S. V. J Med Chem, 2010, 54, 548. (b) Kumar, K.; Maiti, B.; Kondaiah, P.; Bhattacharya, S. Org Biomol chem, 2015, 13, 2444. (c) Zheng, L. T.; Yi, W. J.; Su, R. C.; Liu, Q.; Zhao, Z. G. ChemPlusChem, 2016, 81, 125. (d) Kedika, B.; Patri, S. V.; Bioconjug Chem, 2011, 22, 2581.
74. Menger, F. M.; Keiper, J. S., Angew Chem Int Ed, 2000, 39, 1906.
75. (a) Bajaj, A.; Paul, B.; Kondaiah, P.; Bhattacharya, S. Bioconjugate Chem, 2008, 19, 1283. (b) Misra, S. K.; Naz, S.; Kondaiah, P.; Bhattacharya, S. Biomaterials, 2014, 35, 1334. (c) Kumar, K.; Maiti, B.; Kondaiah, P.; Bhattacharya, S. Mol Pharm, 2014, 12, 351. (d) Kedika, B.; Patri, S. V., Mol Pharm, 2012, 9, 1146.
76. Kumar, K.; Barrán-Berdón, A. L.; Datta, S.; Muñoz-Úbeda, M.; Aicart-Ramos, C.; Kondaiah, P.; Junquera, E.; Bhattacharya, S.; Aicart, E., J Mater Chem B, 2015, 3, 1495.
77. Fuhrhop, J. H.; Wang, T., Chem Rev, 2004, 104, 2901.
78. Blume, A.; Drescher, S.; Graf, G.; Köhler, K.; Meister, A., Adv. Colloid Interface Sci. 2014, 208, 264.

79. (a) Jain, N.; Arntz, Y.; Goldschmidt, V.; Duportail, G.; Mély, Y.; Klymchenko, A. S., Bioconjug Chem. 2010, 21, 2110. (b) Khan, M.; Ang, C. Y.; Wiradharma, N.; Yong, L. K.; Liu, S.; Liu, L.; Gao, S.; Yang, Y. Y. Biomaterials, 2012, 33, 4673. (c) Patil, S. P.; Kim, S. H.; Jadhav, J. R.; Lee, J. H.; Jeon, E. M.; Kim, K. T.; Kim,B. H.; Bioconjug Chem. 2014, 25, 1517.

80. (a) Felgner, P. L.; Ringold, G. M. Nature. 1989, 337, 387. (b) Zabner, J. J Biol Chem. 1995, 270, 18997. (c) Sternberg, B.; Sorgi, F. L.; Huang, L. FEBS Lett. 1994, 356, 361. (d) Gershon, H. Biochemistry. 1993, 32, 7143. (e) Safinya, C. R. CurrOpinStructBiol, 2001, 11, 440.

81. Wattiaux, R.; Laurent, N.; Wattiaux-De Coninck, S.; Jadot, M. Adv Drug Deliv Rev, 2000, 41, 201.

82. (a) Perumal, O. P.; Inapagolla, R.; Kannan, S.; Kannan, R. M. Biomaterials, 2008, 29, 3469. (b) Khalil, I. A.; Kogure, K.; Akita, A.; Harashima, H. Pharmacol Rev. 2006, 58, 32. (c) Parton, R. G.; Richards, A. A. Traffic, 2003, 4, 724. (d) Boleti, B.; Benmerah, A.; Ojcius, D. M.; Cerf-Bensussan, N.; Dautry-Varsat, A. J Cell Sci. 1999, 112, 1487. (e) Martys, J. L.; Wjasow, C.; Gangi, D. M.; Kielian, M. C.; McGraw, T. E.; Backer, J. M. J Biol Chem. 1996, 271, 10953. (f) Li, D.; Li, P.; Li, G.; Wang, J.; Wang, E. Biomaterials, 2009, 30, 1382. (g) Yamamoto, A.; Tagawa, Y.; Yoshimori, T.; Moriyama, Y.; Masaki, R.; Tashiro, Y. Cell Struct Funct, 1998, 23, 33.

83. (a) Xu, Y.; Szoka, Jr, F. C. Biochemistry, 1996, 35, 5616. (b) Zelphati, O.; Szoka, Jr, F. C. Proc Natl Acad Sci U S A, 1996, 93, 11493.

84. (a) Hafez, I. M.; Maurer, N.; Cullis, P. R. Gene Ther, 2001, 15, 1188. (b) Ellens, H.; Bentz, J.; Szoka, F. C. Biochemistry, 1986, 2, 285. (c) Gao, X.; Huang, L. Gene Ther, 1995, 10, 710.

85. (a) Escriou, V.; Carriere, M.; Bussone, F.; Wils, P.; Scherman, D. J Gene Med, 2001, 2, 179. (b) Brunner, S.; Furtbauer, E.; Sauer, T.; Kursa, M.; Wagner, E. Mol Ther, 2002, 1, 80.

86. (a) Tseng, W. C.; Haselton, F. R.; Giorgio, T. D. (BBA)-Gene. 1999, 1445, 53. (b) Jans, D. A.; Chan, C. K.; Huebner, S. Med. Res. Rev. 1998, 18, 189. (c) Subramanian, A.; Ranganathan, P.; Diamond, S. L. Nat. Biotechnol. 1999, 17,873. (d) Sebestyen, M. G.; Ludtke, J. J.; Bassik, M. C.; Zhang, G.; Budker, V. Nat.

Biotechnol. 1998, 16, 80. (b) Zanta, M. A.; Belguise-Valladier, P.; Behr, J. P. Proc. Natl. Acad. Sci. USA. 1999, 96, 91.

87. Szostak JW, Orr-Weaver TL, Rothstein RJ, Stahl FW. 1983 The double-strand-break repair model for recombination. Cell. May. 33. 25-35.

88. J.Miller, A.D.Mclachlan and A.Klug. 1985 Repetitive zinc-binding domains in the protein transcription facor from xenopus oocytes. The EMBO journal vol. 4. 169-1614,

89. AndreaPellagatti, HamidDolatshad, BonHam Yip, Simona Valletta, Jacqueline Boultwood. 2015 Application of genomic editing technologies to the study and treatment of hematological disease. Elsevier. 123-132.

90. Dana Carroll. 20111 Genome engineering with Zinc-Finger Nuclease. Genetics. 773-782.

91. Carroll, D. 2014 Genome engineering with targetable nucleases. Annu. Rev. Biochem. 83, 409–439.

92. Pabo, C.O., Peisach, E. & Grant, R.A. 2000 Design and selection of novel Cys2His2 zinc finger proteins. Annu. Rev. Biochem. 70, 313–340

93. Kim, Y-G., Cha, J. & Chandrasegaran, S. 1996 Hybrid restriction enzymes: zinc finger fusions to FokI cleavage domain. Proc. Natl. Acad. Sci. U. S. A. 93, 1156–1160.

94. Moscou, M.J. & Bogdanove, A.J. 2009. A simple cipher governs DNA recognition by TAL effectors. Science. 326, 1501.

CHAPTER II

Influence of hydrophobicity in hydrophilic region of cationic lipids on enhancing nucleic acid delivery and gene editing

2.1 Introduction

Delivery and expression of therapeutic gene in gene therapy is a major challenge as it includes two barriers, i.e., uptake of gene into cells and endosomal escape[1]. Viral vectors and non-viral vectors are the two types of vectors used for delivering genes *in-vitro* as well as *in-vivo*. Though viral vectors have more efficacy in delivering the gene, due to the problems associated with safety and the immunogenicity limit their application. More importantly, viral vector production is challenging and adds humongous cost to the product. With successful demonstration of liposomal siRNA drug, GIVOSIRAN and recent lipid enabled mRNA-based vaccines for COVID19 generated enthusiasm on non-viral vector based nucleic acid delivery, in particular lipid nanoparticle mediated nucleic acid delivery[2].

In gene therapy, usage of cationic lipids as non-viral vectors is a general practice. These cationic liposomes form complexes with DNA which is highly negative in charge, called lipoplexes[3]. However, their low efficacy compared with viral vectors results in limited therapeutic use. Generally, Cationic lipids contain a head group which is hydrophilic and an anchoring group which is hydrophobic in nature, and are mostly connected through a linker/ spacer group. Their molecular framework plays a key role in influencing transfection[4]. The exact structural features needed for a better transfection is still not clear [5]. Hence, researchers have been focusing on various structure-activity modulations in order to correlate the structure with their efficacy and toxicity[3,5]. This further abridges the complication during transfection process to enhance their efficiency[6]. Several modifications such as variation/asymmetry in the aliphatic chain[4,7-9] and steroid moieties of hydrophobic domain[5,9] have been carried out. Insertion of amines, amino acids, quaternary ammonium, guanidinium groups and heterocyclic molecules in the hydrophilic head group are also published[10,11]. Different type of groups such as ester, ether, carbonate, amide, di sulphide and triazole moieties are widely explored as linker/spacer groups for cationic lipids[3]. A triazole, which is a heterocyclic aromatic ring has been used as linker in designing cationic amphiphiles, due to its unique property of being stable in acidic and basic environments and also in oxidative and reductive conditions[12,14].

In this context, fat soluble tocol family vitamins have been widely explored for multifaceted delivery of therapeutic molecules[15-21]. Tocopherol, is a natural amphiphilic molecule with lipid soluble property and even at high doses it shows non-

toxic nature[18]. Alpha-Tocopherol has been used as hydrophobic moiety in preparing cationic lipids for gene delivery[16,17,19-22]. Therapeutic use of tocopherol has been widely reported as an antioxidant and for a number of disorders[23-25]. In addition, serum stability, biocompatibility and solvent capacity of vitamin E has led to development of nano-medicines for cancer therapy[26]. Use of α-Tocopherol based vector for the nucleic acid delivery in *in vivo* has also been reported[27-31]. Hence, owing to the above features, different cationic lipids were prepared using α-Tocopherol as hydrophobic domain in our study.

The escape of gene from endosomal membrane is one of the major barriers for developing the efficient non-viral gene delivery vector. It is the key limiting step. Chloroquine is a lysosomotropic agent and endosomal disrupting molecule which can be used to increase transfection efficiency in liposome mediated nucleic acid delivery. It can easily penetrate through plasma membrane by mimicking the phospholipid bilayer because of its lipophilic nature in their unprotonated stage. Upon entering into the cells, it can facilitate the escape of the nucleic acid from endosomes by preventing the degradation in endocytosis pathway[40]. The lipid formation can also impact the behavior of chloroquine in the liposome mediated gene delivery. Chloroquine and other endosomal escape agents enhance gene delivery but these are often too toxic to use in preclinical studies.

Conjugating hydrophobic amino acid moieties to cationic lipids play a vital role in enhancing transfection efficacy by endosomal escape. Aromatic hydrophobic R group containing amino acids such as Phenylalanine (F) and Tryptophan (W) forms pore with their hydrophobic R groups to destabilize cellular membranes[32-36]. It has reported that incorporation of F and W enhanced the cellular uptake of cell penetrating peptides[37,38,48-52].

Genome-editing is an emerging technology for treatment of genetic disorders, as it alters the defected gene on site. CRISPR/Cas9 based genome-editing is widely explored[46-47]. CRISPR/Cas9 system is made up of CRISPR- a nucleic acid and sequence-single guided RNA (sgRNA), that is associated with Cas9 nuclease protein. This sgRNA directs Cas9 protein to a targeted genomic site via RNA-DNA base complementary[41]. Therapeutic gene editing can be done either through homology directed repair (HDR) or through non homologous end joining (NHEJ)[39-41]. Cas9 can be delivered in pDNA, mRNA and ribonucleo protein (RNP) form. Delivering cas9 in pDNA form is easy and economical. However sustained expression of nuclease leads

to unwanted off-target effects. Hence, delivering Cas9 in mRNA form for both *in vitro* and *in vivo* gene editing is gaining importance in the recent times[4]. Prior findings successfully demonstrated that liposomes can be ued for delivering cas9 mRNA for efficient gene-editing[42-44].

Taking cues from prior findings, including our own, in this present investigation we developed cationic lipid vector consisting of α- Tocopherol as hydrophobic tail and triazole as a linker for conjugating the head group containing aromatic/hydrophobic amino acids. Here, we used four different aromatic/hydrophobic amino acids such as glycine (G), proline (P), phenylalanine (F) and tryptophan (W) as head groups to study their influence on endosomal escape for the enhanced transfection efficacy (Figure 1). The efficacy of these lipids in *in vitro* nucleic acid delivery by using various nucleic acids are evaluated. Further, expanded the horizon of these cationic lipids mainly TTW as a toolset in nano-carrier system's for delivering genome-editing tools as a toolset.

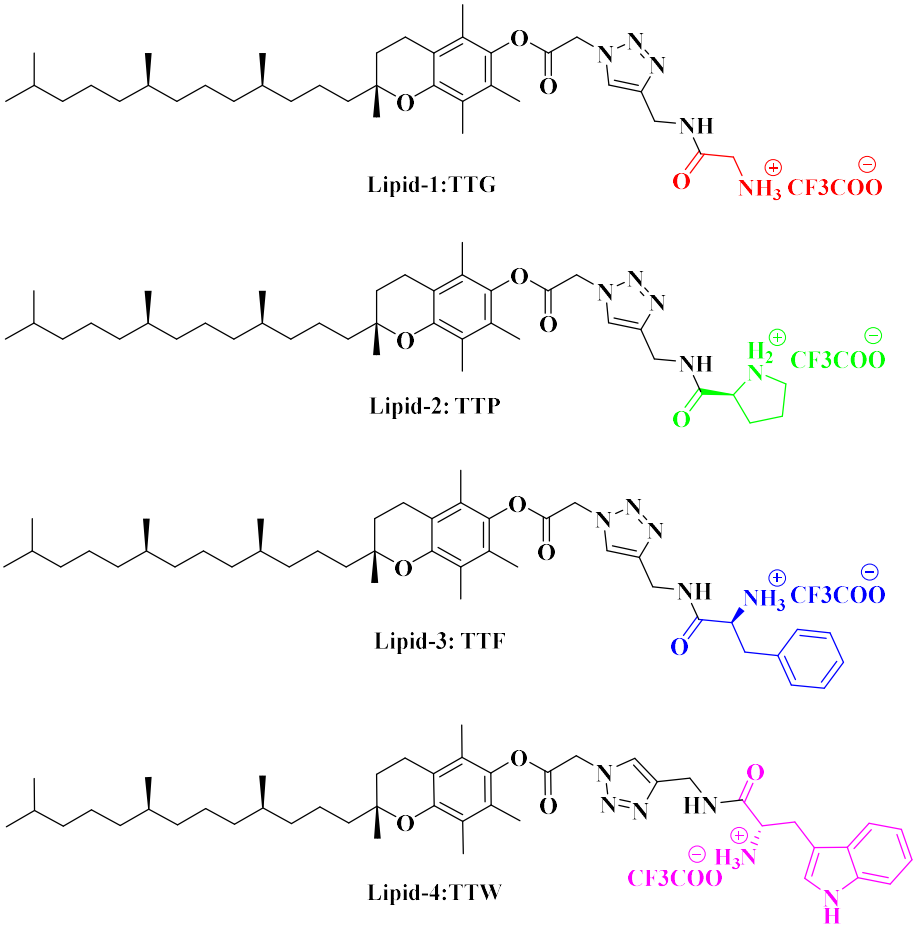

Figure 1: Molecular structure of cationic lipids.

2.2 Results and Discussion:

Herein, reported the synthesis as well as physicochemical characterization of four aromatic/ hydrophobic amino acid based tocopherol lipids TTG, TTP, TTF and TTW. In this study, also reported the transfection efficiencies of lipids TTG, TTP, TTF and TTW on four cell lines viz., (EA.HY926), neural (NEURO-2a), kidney (HEK-293) and ovary (CHO) through the results of *in vitro* transfection experiments carried out. In addition, the potential of TTW in genome editing and nucleic acid delivery with CRISPR/Cas9 are described.

2.2.1 Chemistry: To understand the influence of the hydrophobicity in the head group region of lipids in gene delivery, we have designed and synthesized four *α*-tocopherol based cationic amphiphiles, by incorporating aromatic/hydrophobic amino acids, phenylalanine, proline, tryptophan and glycine (Scheme 1) using triazole as the linker such that the lipids differ only in the hydrophobicity/aromaticity in the head group region. As demonstrated these cationic lipids TTG, TTP, TTF and TTW were synthesized using corresponding boc protected amino acids. These boc protected amino acids were coupled with propargyl amine using EDCI.HCl coupling reagent, to form acetylene derivatives. These acetylene derivatives were further treated with tocopherol azide, followed by developing 1, 2, 3-triazole heterocyclic ring using click chemistry (huisgen 1, 3-dipolar cycloaddition strategy) e. Boc deprotection of these click derived adducts resulted in Lipid 1, 2, 3, 4. (Scheme 1). ^{1}H NMR and high resolution mass spectra were used to confirm the structures of intermediates involved in all the reactions carried out and the final lipids.

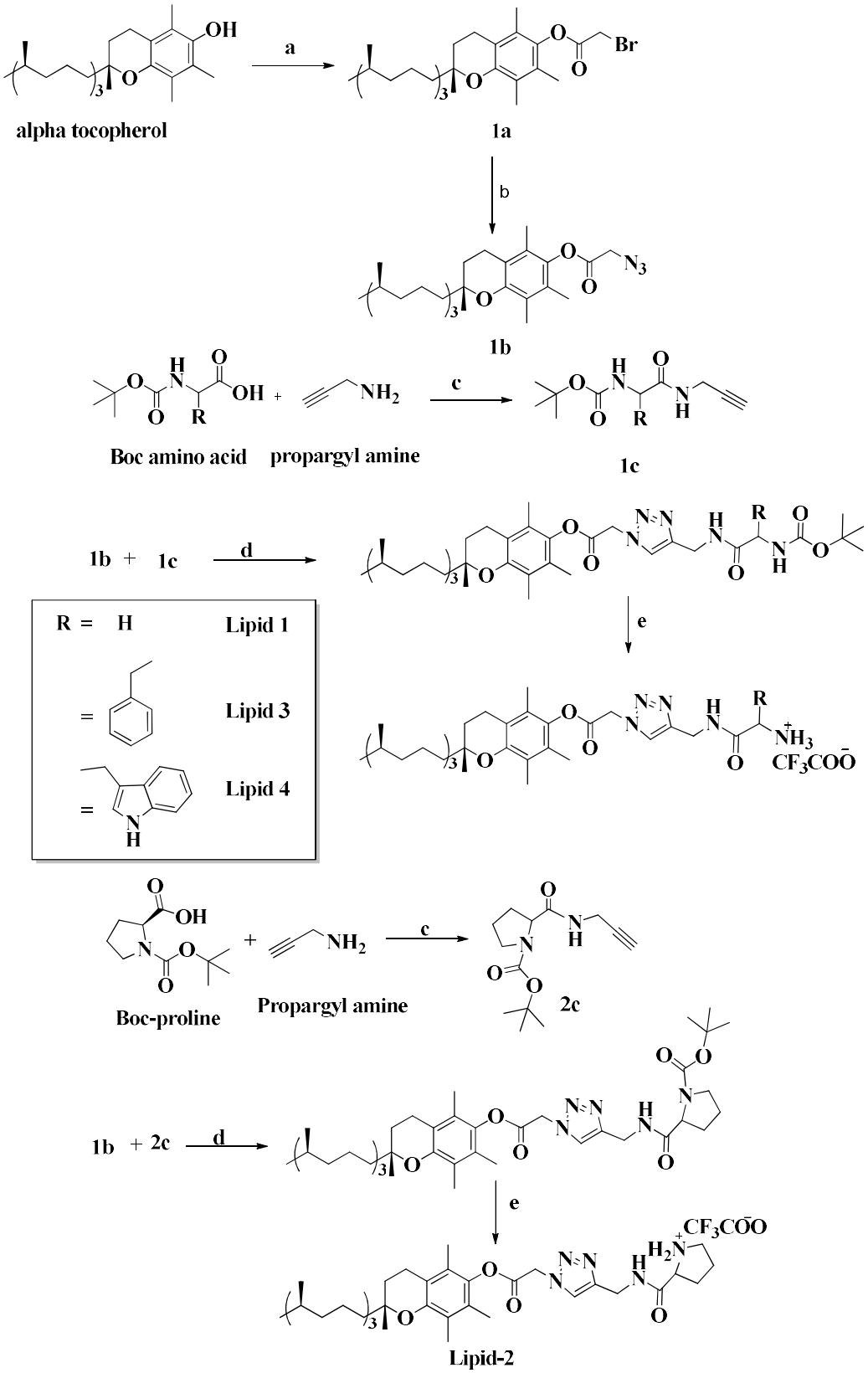

Scheme 1: Synthesis pathway of tocopheral based cationic lipids

Reagents & Conditions: (a) Bromo acetyl bromide, Pyridine, Dry DCM, 0^0C; (b) NaN_3, Acetonitrile, reflux; (c) EDCI.HCI, HOBt, DIPEA, DCM, 0^0C; (d) Na Ascorbate, $CuSO_4.H_2O$, ter-Butanol:H_2O (e) 1:2 Dry DCM, TFA

2.2.2 Physico-chemical properties:

The vesicles prepared by the synthesized lipids were characterized for their particle size and surface charge.

2.2.2.1 Particle size and zeta potentials:

A rational design of the gene delivery vector in *in-vitro* requires various physicochemical characterizations of liposomes/lipoplexes such as charge of liposomes, it's size and lipid–DNA complexes binding stability. We have prepared liposomes as a first step in order to determine the surface charge and size of liposomes. Lipoplexes were prepared by changing the N/P charge ratios (1:1, 2:1, 4:1 and 8:1) with pDNA to determine DNA binding ability using Gel retardation and Heparin-displacement assay.

The liposomal size is a combination of various forces such as hydrophilic–hydrophobic, vander waals and repulsive electrostatic which exists between the lipid molecules. DLS method was used to determine the synthosized liposomes' size and zeta-potential. The size of all the synthesized liposomal formulations as depicted in Figure 2A was nearly <250 nm and all the liposomes were found to be positive. The particle diameter of TTG is found to be 248.8 nm, TTP is 173.8 nm, TTF is 238.7 nm and for TTW is 192.9 nm is as given in Figure 2A. Figure 2B depicts that zeta potentials for TTG, TTP, TTF and TTW were 29.2 mV, 15.3 mV, 12.7 mV and 5.8 mV respectively. The heterocyclic aromatic based lipid TTW zeta potential is much less than that of open chain amino acid, glycine-based lipid TTG, non-aromatic heterocyclic amino acid TTP and moderately less than aromatic lipid TTF. The simple explanation for such variation in the liposomal surface charge of the four lipids is that, because of the cyclic delocalization of π electrons on the flat face of an aromatic ring, the hetero cyclic aromatic amino acid based liposomes (TTW) exhibited less surface zeta potentials than the simple benzene based aromatic amino acid liposomes (TTF) and also much less than the non-aromatic amino acid based liposomes (TTG & TTP).

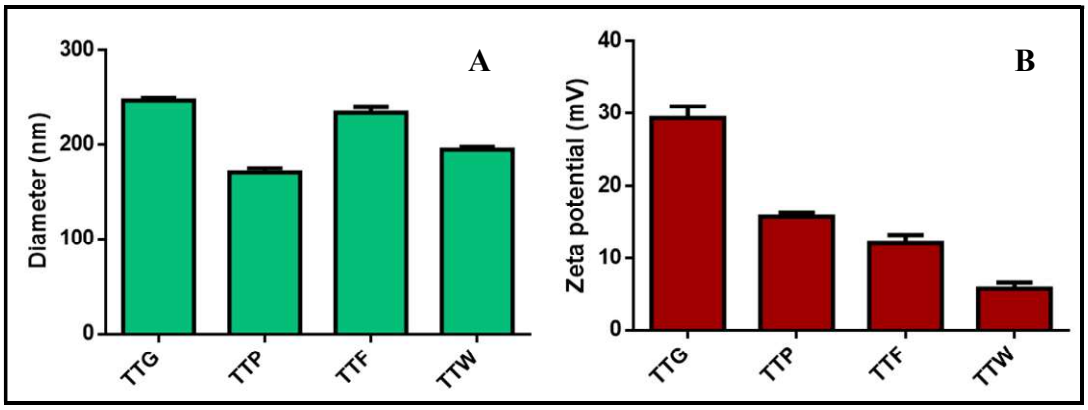

Figure 2. (A) Particle size and (B) Zeta potential values of synthesized liposomes(n=3)

2.2.2.2 DNA binding studies by Gel Electrophoresis and Heparin-displacement assay:

DNA binding capacity with liposomes was studied by conventional agarose gel electrophoresis assay and heparin-displacement assay at different liposomes to DNA charge ratios such as 1:1, 2:1, 4:1 and 8:1. Gel retardation assay was used to understand the level of binding capacity of lipids to DNA using Agarose gel electrophoresis. In this, the amount of unbound pDNA was examined by the extent of migration of different ratios of lipoplexes in reference to free plasmid DNA in agarose gel as shown in Figure 3 (A). It has been found that all TTG, TTP, TTF and TTW have shown strong binding capacity with pDNA except for TTF at 1:1 charge ratio. Though TTW and TTF has less zetapotential than the open and non-aromatic amino acid liposomes (TTG and TTP), they shown optimal binding may be due to the aromatic-aromatic interactions between the amino acid side chain and the nucleic acid base other than electrostatic interactions[49].

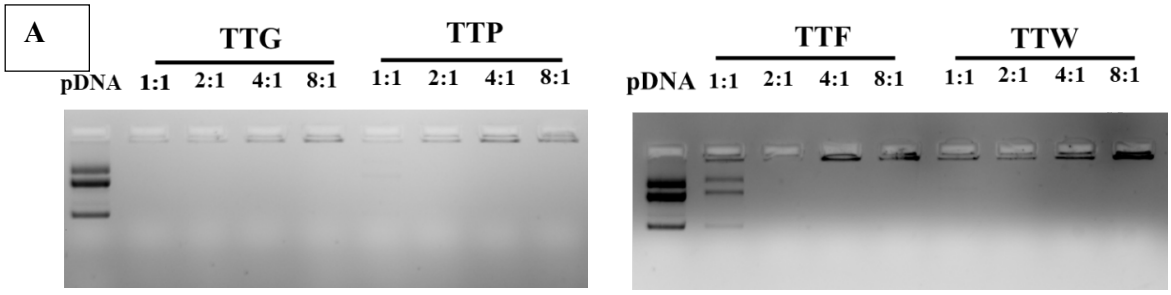

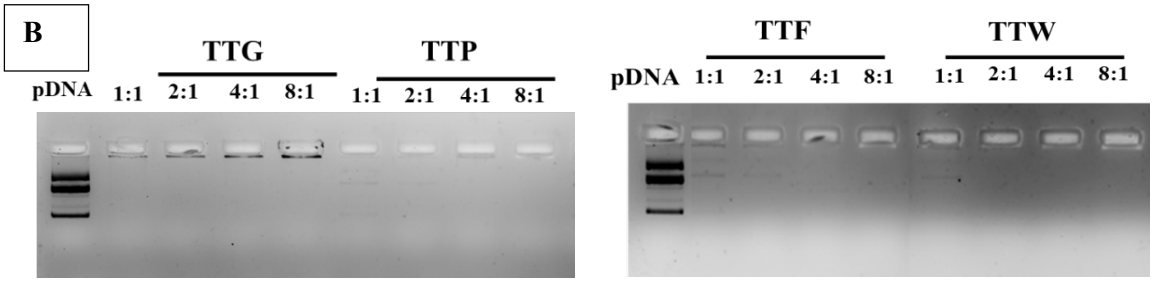

Figure 3. (A) DNA binding patterns of lipoplexes at different ratios of liposomes: pDNA on agarose gel electrophoresis. (B) Heparin-displacement assay of various liposomes associated with pDNA at different charge-ratios.

Further, in order to confirm the binding strength and stability of DNA with the prepared liposomes, heparin displacement assay was performed. In this, lipoplexes with above mentioned charge ratios were treated with heparin, which is a highly polar glycosaminoglycan used as an anticoagulant, that competes with anionic pDNA. The results given in Figure 3 (B) have shown that, there is a retardation of migration in TTG, TTP, TTW at all ratios of lipoplexes and TTF except for 1:1 ratio indicating that, liposome-DNA interactions are strong which are unaffected even in presence of heparin. These results were in accordance with that of gel retardation assay. Therefore, from above analyses it is clearly shown that all the lipids except TTF at low charge ratio (1:1) have excellent binding capability with pDNA, which is important criteria in transfection.

2.2.3 *In vitro* transfection studies:

Various nucleic acids were used to study the effectiveness of transfection of the produced lipoplexes in *in vitro* gene delivery. In current study, we have chosen different cell lines based on tissue specific distribution of tocopherol in *in vivo*. Previous reports revealed that, liver, prostate, whole brain, kidney and ovary have high levels of distribution towards this fat-soluble vitamin. Accordingly, (EA.HY926), neural (NEURO-2a), kidney (HEK-293) & ovary (CHO) cells were selected[10,13].

2.2.3.1 pDNA transfection:

The qualitative and quantitative analysis of prepared liposomes (1:1, 2:1, 4:1 and 8:1 ratios) was carried out using enhanced green fluorescent protein (eGFP) encoded plasmid DNA in all afore mentioned cell lines. It was observed from

fluorescence microscopy as well as flow cytometry that, lipoplexes of all four synthesized lipids showed the highest eGFP expression at 4:1 charge ratio. Hence 4:1 charge ratio is considered for further structure activity studies. The fluorescent microscopic images of eGFP expression in Neuro-2a cell line transfected with the four lipids synthesized is given in Figure 4A. The percentage of eGFP positive cells in CHO, Neuro-2a, EA.HY926 and HEK293 cell lines measured at 4:1 ratio using flow cytometry is depicted in Figures. 4B, 4C, 4D and 4E respectively. Herein, we observed that, lipoplexes of TTF and TTW exhibited better transfection than TTG and TTP in all the cell lines studied.

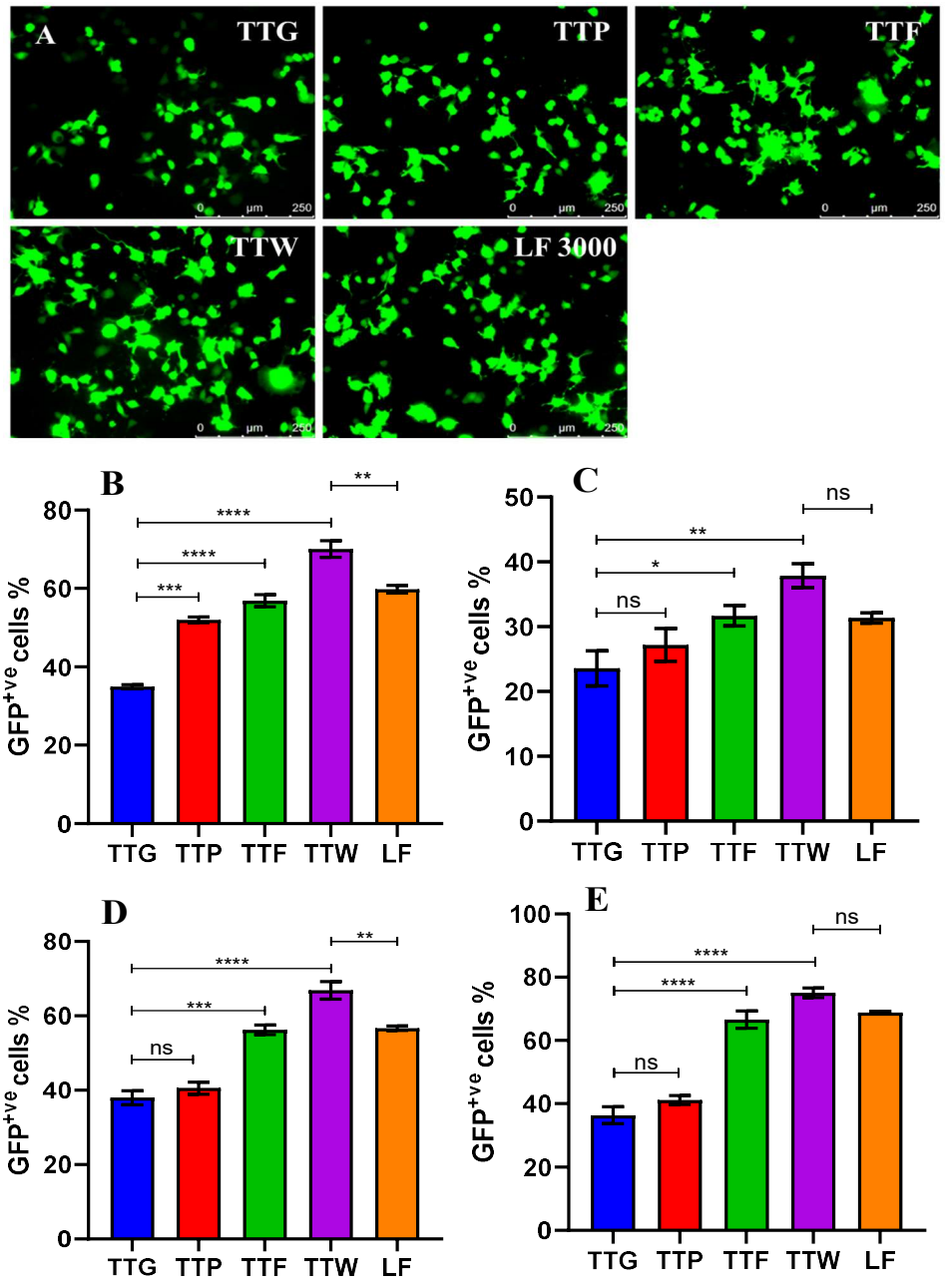

Figure 4. Fluorescent microscopic images and flow cytometry analysis of liposomes with best charge ratio 4:1 in Neuro-2a cell line. (A) Relative *in vitro* pDNA transfection efficiencies in different cell lines at lipid/DNA 4:1 charge ratio using flow cytometry, Graphpad prism was used to perform statistical analysis, CHO (n=2) (**P 0.001, ***P 0.0003, ****p<0.0001). (B) Neuro-2a (n=2). (*P 0.0285, **P 0.0025). (C) EA.HY926 (n=2). (***P 0.0003, ****P < 0.0001, **P 0.0049). (D) HEK293 (n=2). (****P < 0.0001). (E) € and LF 3000 which is a transfection reagent available commercially was used as the positive control.

Moreover, the transfection efficiency of all the lipoplexes except TTG was either comparable or even more than LF 3000 for all the cell lines studied. The transfection potential of TTW is greater than LF 3000, whereas TTF is exhibiting comparable transfection to LF3000 in all the cell lines. This difference in transfection potential may be arising from their efficacy to enhance endosomal escape. Increase in the hydrophobicity of hydrophilic head group in case of TTF and TTW played a key role in endosomal escape, this further enhanced the transfection efficiency. The combining results of size, zeta potential and transfection potentials of these lipids emphasizes that the superior transfection efficiency of TTW is not arising due to the size or zetapotential as it shown lower zeta potential and optimal size. Hence, it may be because of the improved endosomal escape which may favoured the lipid TTW to show high potential transfection efficiency among the four lipids. This is further evidenced with the cellular uptake and co-localization experiments which are discussed in the later sections.

2.2.4 Cellular uptake study and Effect of lysosomotropic agent (Chloroquine) on non-viral gene delivery:

Rhodamine-PE labelled liposomes were used for studying the cellular uptake in CHO cell line. It is observed from the Figure 5 that, there is no considerable difference in uptake (Figure 5A) but significant variation among the four liposomes in the transfection efficiency (Figure 5B). This may be due to endosomal escape which helped in showing higher transfection efficiency. It is well known fact that the critical bottleneck in efficient gene delivery is the cytoplasmic release of the macromolecules by escaping from endosomes in a non-cytotoxic fashion[39-41]. In the current study, to gain further awareness of the endocytic route following internalization of lipoplexes and endosomal disruption ability of the lipids, CHO cells were pre-treated with 100 μM chloroquine for 4 hours prior to transfection using four liposomes at their best charge ratio (4:1). The transfection efficiencies of four lipid nano-carrier systems were determined by FACS analysis as % eGFP positive cells is given in Figure 5B. It is also observed that pre-treatment of cells with the lysosomotropic agent, chloroquine (100 μM) increased the transfection efficiency of lipoplexes of all the lipids studied except TTW. There is almost no change in the transfection efficiency of TTW with and without chloroquine treatment which clearly indicated that endosomal escape played major role for TTW in enhancing the transfection efficiency. It also demonstrates that

by the development of such kind of endosomal disrupting lipids viz., TTW can avoid the usage of endosomal escape or endolytic agents, such as chloroquine which are often too toxic in the macromolecular therapeutics delivery.

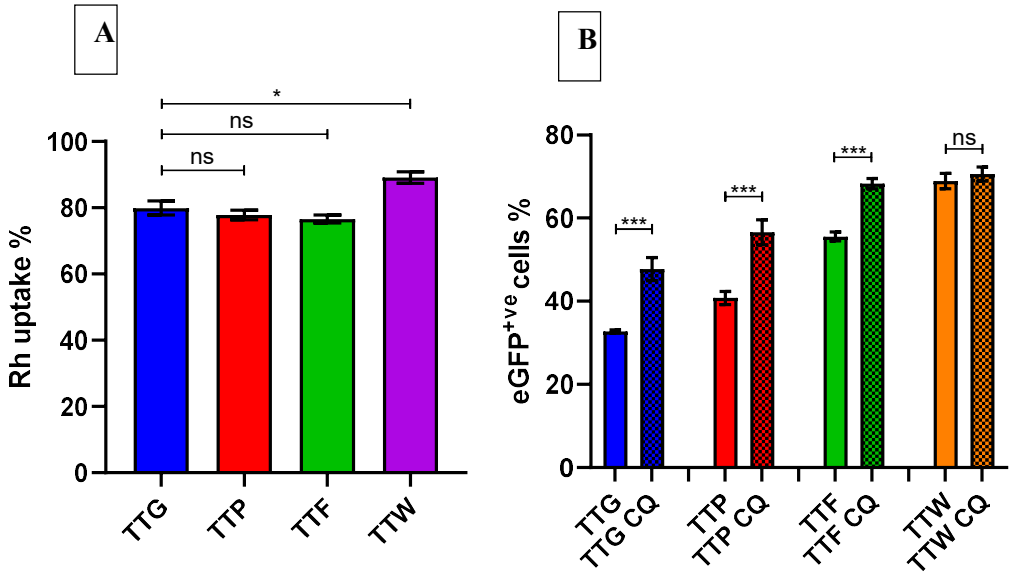

Figure. 5. (A) Cellular membrane uptake of Rhodomine-PE labeled liposomes in CHO cell line (n=2). (*P 0.01). (B) % of eGFP positive cells by flow cytometry in CHO cell line at lipid/DNA 4:1 charge ratio (n=2). (***P < 0.006). Graphpad prism was used to perform Statistical analysis.

2.2.5 Uptake profile and co-localization:

The endosomal escape is one of the major challenges to the development of efficient non-viral gene delivery vectors. Hence, estimation of cellular uptake followed by intracellular co-localization becomes significant. In the current study, internalization of lipoplexes was performed using lipoplexes of Rhodamine-DHPE labelled liposomal formulations of TTG, TTP, TTF and TTW. The microscopic images as given in the Figure 6 from co-localization studies the red fluorescence observed in the left lane of clearly depicts the similar uptake potency of all the four lipids. To gain further insight into the endosomal escape potency of the lipids and an attempt to address the enhanced transfection efficiency of TTW, co-localization studies of lipoplexes of lipids TTG, TTP, TTF and TTW were performed using lysotracker green to label the lysosomal compartments in Neuro-2a cell lines. The lipoplexes with minimal co-localization in lysosomes represents more efficient in endosomal escape. Rhodamine-labeled liposomal formulation co-localization investigations' microscopic

images are shown in Figure 6 (in the form of lipoplexes). The middle lane shows the lysosomal labelling using lysotracker green. A distinct red fluorescence having no co-localization was observed for TTW formulations and minimal co-localization in case of TTF formulations. Whereas, in case of lipoplexes of TTG and TTP formulations translocation in lysosomal compartments was observed. Results are in accordance with the results obtained from transfection studies the more potent transfecting lipoplexes viz., TTW and TTF showed minimal co localization in the lysosomal compartment. These formulations' effective lysosome escape has undoubtedly facilitated the passage of cargo across the endosomal membrane and into the nucleus.

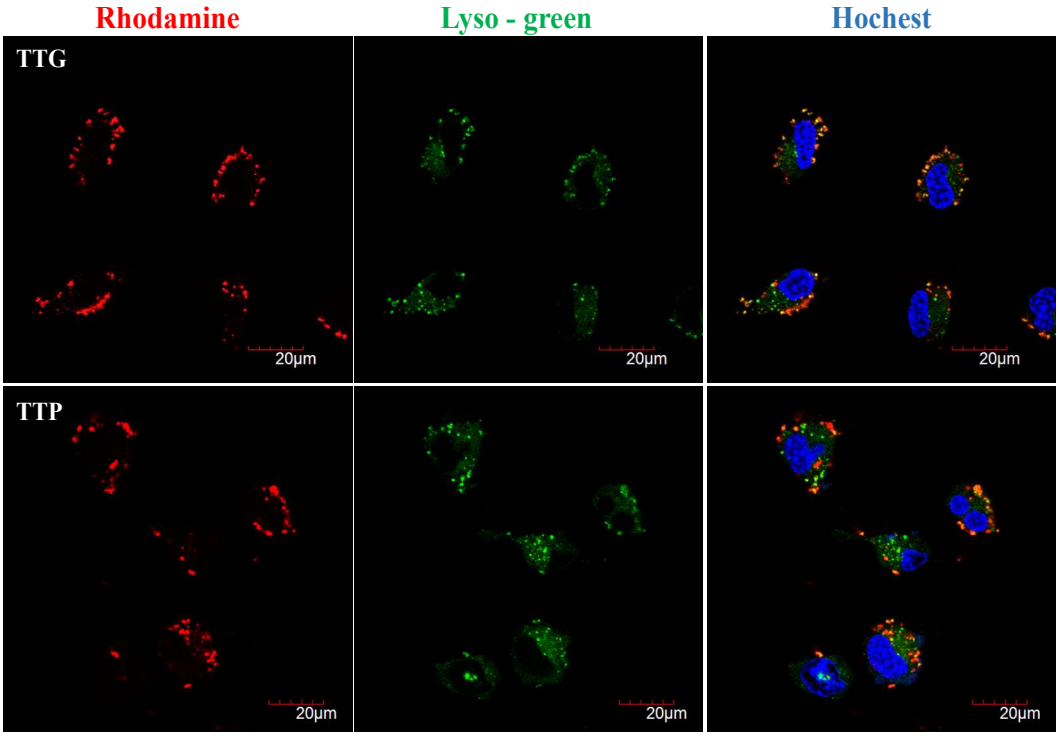

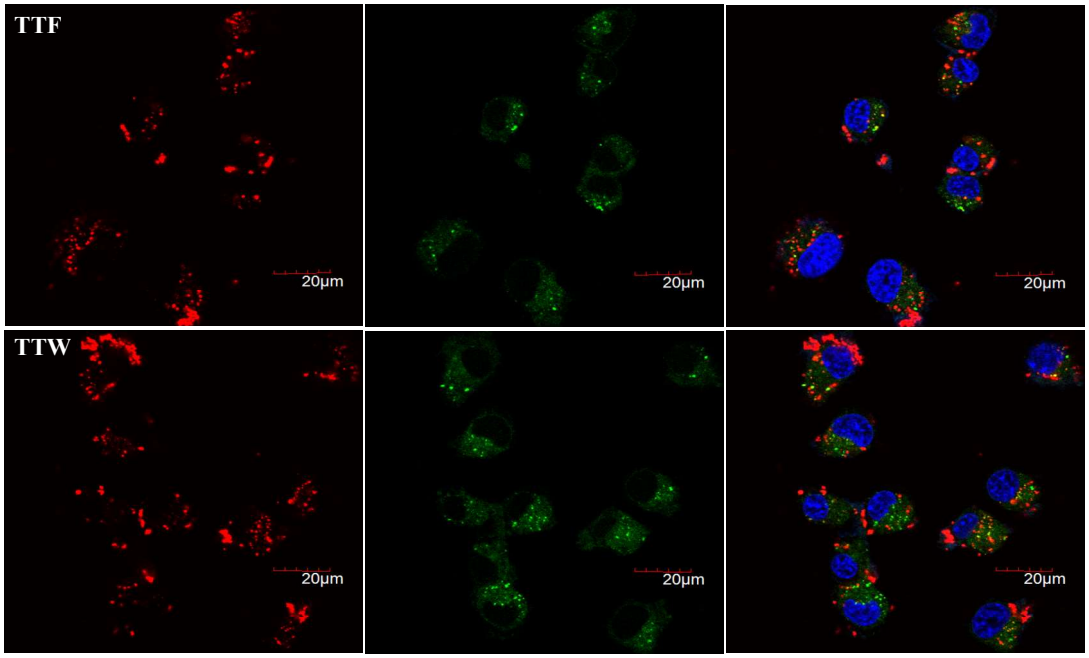

Figure 6. Representative confocal images of lipoplex localization and cell uptake in Neuro-2a cells at 4:1 N/P tagged with rhodamine lipoplexes

2.2.6 mRNA transfection:

After achieving the efficient pDNA transfections, further explored the capability of synthesized lipids in delivering the linear, single stranded mRNA nucleic acid. The transfection efficiencies of four liposomes were evaluated in Hek-293 and CHO cell lines by using GFP encoding mRNA as shown in Figure 7. Respectively. It is observed that the high mRNA transfection efficiency of all the lipid nano-carriers studied is shown at 8:1 charge ratio. The transfection efficiencies at 8:1 is considered for further studies and it is observed that the transfection efficiencies determined by FACS data the liposomal formulations of TTF and TTW shown comparable potential as commercially available LFmMAX control in both the cell lines. Whereas other two liposomal formulations of TTG and TTP are moderately less potential when compared to LFmMAX.

In brief, the two aromatic hydrophobic head group containing lipids TTF & TTW have displayed higher transfection efficiencies for circular pDNA as well as for linear mRNA. The maximum transfection efficiency for pDNA was observed at 4:1 charge ratio, while in case of mRNA it was 8:1. In general, mRNA requires high

charge ratios compared to pDNA because of high net negative charge on linear mRNA over low net negative charge on circular pDNA[53].

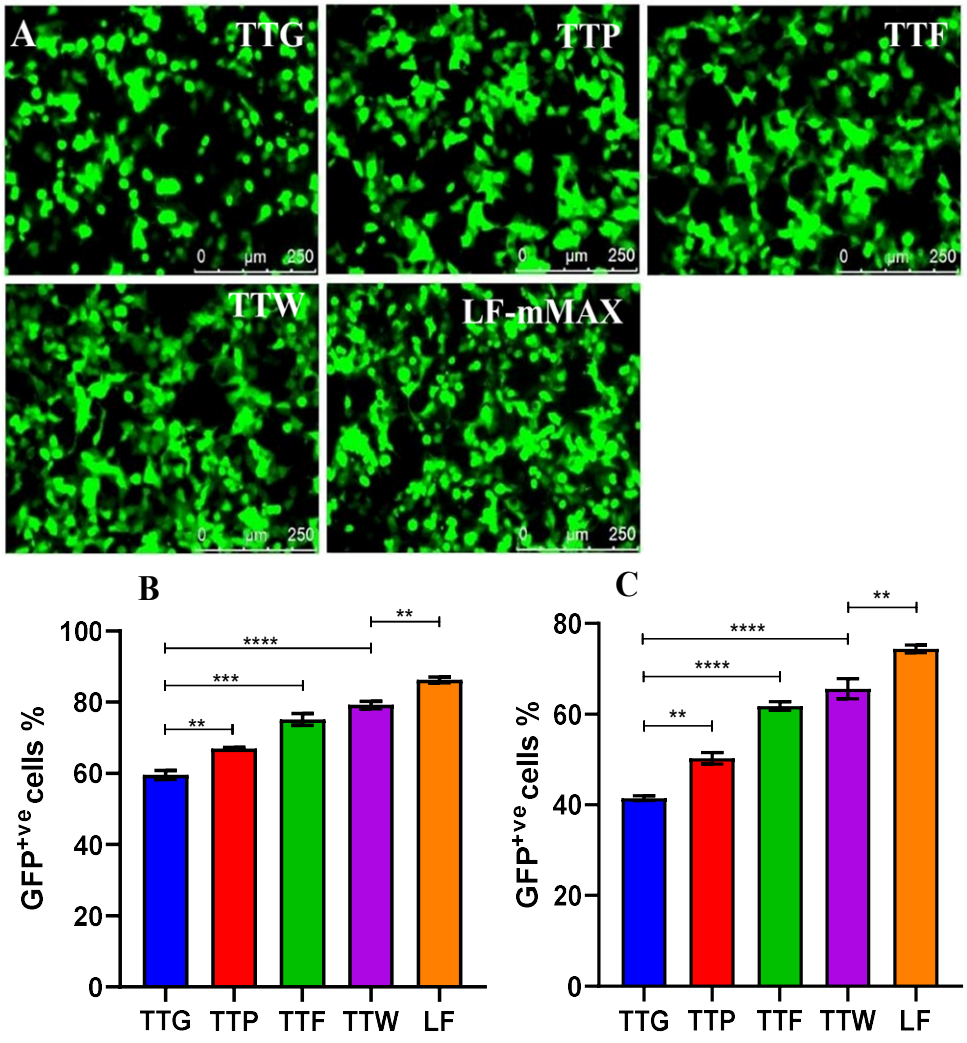

Figure 7. (A) Fluorescent microscopic images of liposomes with best charge ratio 8:1 in Hek-293 cellline. (B) *in vitro* mRNA delivery with cationic lipid carrier systems in Hek 293 (n=2) (**P < 0.0047, ***P 0.0001, ****P < 0.0001). (C) CHO cell lines at lipid/DNA 8:1 charge ratio (n=2) (**P < 0.0033, ****P < 0.0001). GraphPad prism was used to perform statistical analysis.

2.2.7 CRISPR/Cas9 transfection:

Based on the above positive transfection results, further extended the studies to evaluate the efficiency of synthesized lipids in transfecting with the CRISPR tools. Advancement in genome editing and nucleic acid delivery with CRISPR/Cas9 in recent studies has resulted in development of wide variety of nonviral vectors that are

safe and effective. CRISPR plasmid was constructed as pL-CRISPR.EFS.GFP (11.7 kb) that shows Cas9 protein as well as eGFP protein driven as a single unit through the EFS promoter transcript[54]. Delivery of CRISPR/Cas9 encoded pDNA using viral vectors was reported[55-57]. But, there are only a few reports in literature on the use of cationic lipids for delivering CRISPR tools.

The *in vitro* CRISPR/Cas9 pDNA delivery using the four liposomes at best charge ratio (4:1) was carried out in CHO and EA.hy926 cell lines. The four lipid nano-carrier systems' transfection efficiencies in two cell lines determined by FACS analysis is given in Figure 8(A) and (B) respectively. The lipoplexes of TTF and TTW have shown high transfections compared to that of TTG and TTP. Moreover, the transfection efficiency of TTW was comparable with that of commercially available LF 3000 respectively.

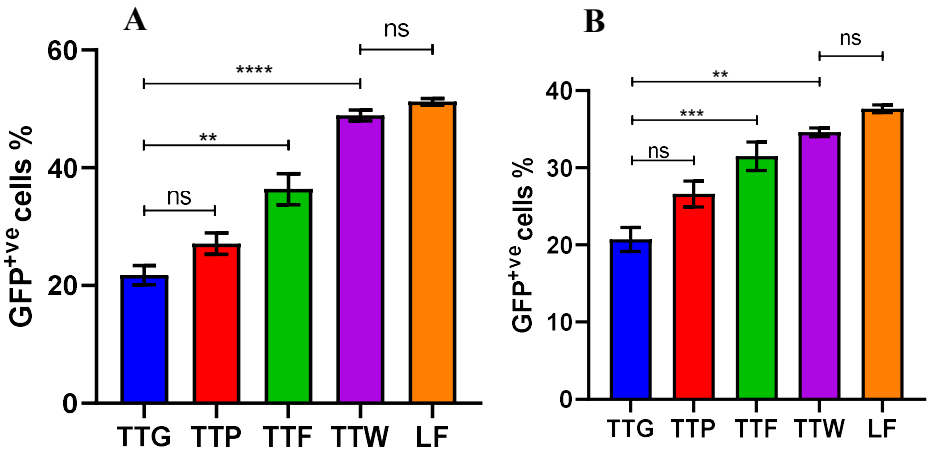

Figure 8. (A) *In vitro* Flow cytometric analysis of CRISPR/Cas 9 pDNA delivery using all the four cationic lipid nanocarrier systems with best charge ratio 4:1 in CHO, (**P 0.001, ****P < 0.0001) and (B) EA.hy926 (**P < 0.0015, ***P < 0.0005) cell lines (n=2). GraphPad prism was used to perform statistical analysis.

2.3 Gene editing:

To further evaluate the utility of TTW lipid in delivering gene-editing reagents compared to LF, we have co-transfected sgRNA targeting AAVS1 locus and Cas9 mRNA in CHO, Neuro-2a, and EA.hy926 cell lines using TTW and LF lipids. After 48hrs, genomic DNA was isolated from three different cell lines to assess the indel rates in the AAVS1 locus. Using the T7 endonuclease I assay, a successful

introduction of indels was observed in the target locus, as measured by the cleaved product at the expected position. Quantitative analysis of cleaved products using ImageJ in CHO cell lines transfected using TTW is 53% (vs 49% in LF). Similarly, NEURO-2A cell lines transfected with TTW showed 62% indels (vs 60% in LF). In EAHY926 cell lines, 56% indels were achieved on transfection using TTW (vs 63% in LF) as depicted in Figure 9. Compared to LF, a modest increase in the indel rates in CHO and NEURO-2A cell lines was achieved by using TTW lipids for transfection. This demonstrates that the in-house synthesized TTW lipid is as efficient as commercially available LF and can be used for delivering CRISPR/Cas9 reagents.

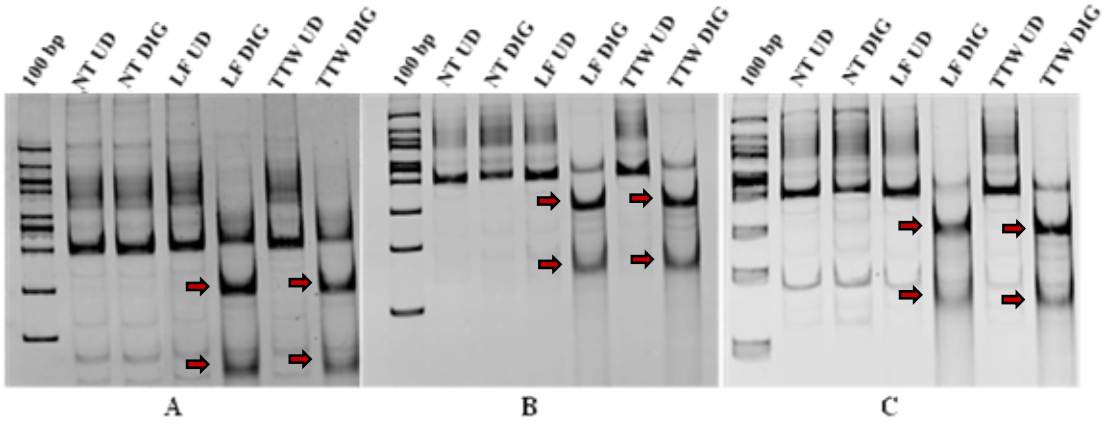

Figure 9. Validation of CRISPR/Cas9 gene-editing using T7E1 assay in (A) CHO, (B) Neuro-2a, (C) EA. Hy926 cell lines. Representative images of T7-endonuclease I (T7E1) assay performed on gDNA from CHO, Neuro-2a, and EA.hy926 cell lines co-transfected with sgRNA targeting AAVS1 locus and Cas9 mRNA. Uncleaved products with an amplicon size of 450bp and T7E1 cleaved products showed bands of 200bp and 300bp in size, highlighted with red arrows. NT UD, Non-treated T7E1 undigested; NT DIG, Non-treated T7E1 digested; LF UD, LF 3000 T7E1 undigested; LF DIG, LF 3000 T7E1 digested; TTW UD, Tocopherol-Triazole-Tryptophan T7E1 undigested; TTW DIG, Tocopherol-Triazole-Tryptophan T7E1 digested.

2.3.1 Cell viability assay:

Another important feature that increases the probability of synthetic gene delivery vector being used in gene therapy is its low cytotoxicity. MTT assay was carried out in Hek 293 and CHO cell lines by using TTG, TTP, TTF and TTW

lipoplexes for 24 hours. Cell viability of all the lipid complexes has been observed to be maximum at 1:1 and 2:1 lipid: pDNA charge ratios. (Hek 293 as given in Figure 10A and CHO in Figure10B). The statistics unambiguously show that, even at greater charge ratios, no formulation is more hazardous than the industry standard LF 3000. Among non-viral gene delivery methods, lipofectamine has traditionally been regarded as the gold standard for transfection. The main drawback of Lipofectamine is its cytotoxicity, though. As a result, when creating gene delivery vectors, transfection without compromising safety must be taken into account. Because of their high transfection properties and low cytotoxicity, the cationic lipids mentioned above are essential for *in vitro* applications.

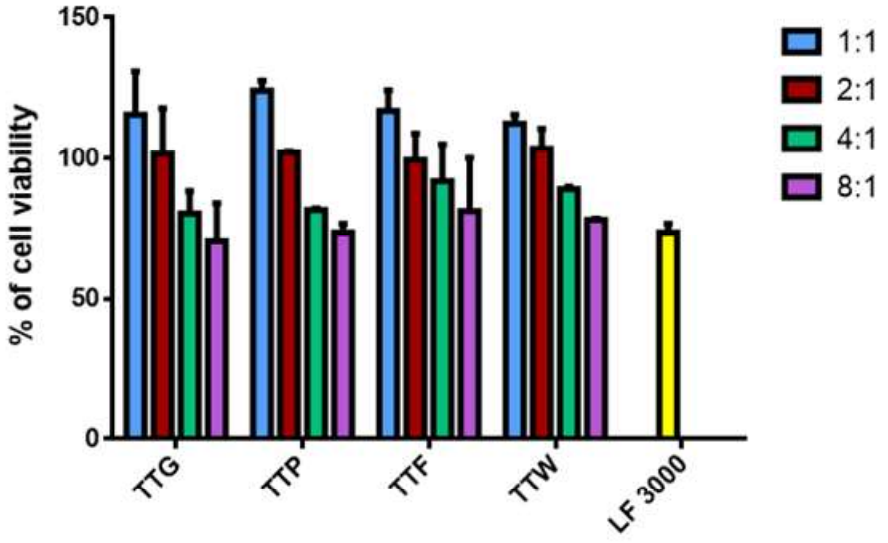

Figure 10A: % cell viability of TTG, TTP, TTF and TTW lipoplexes at different charge ratios in Hek-293 cell line.

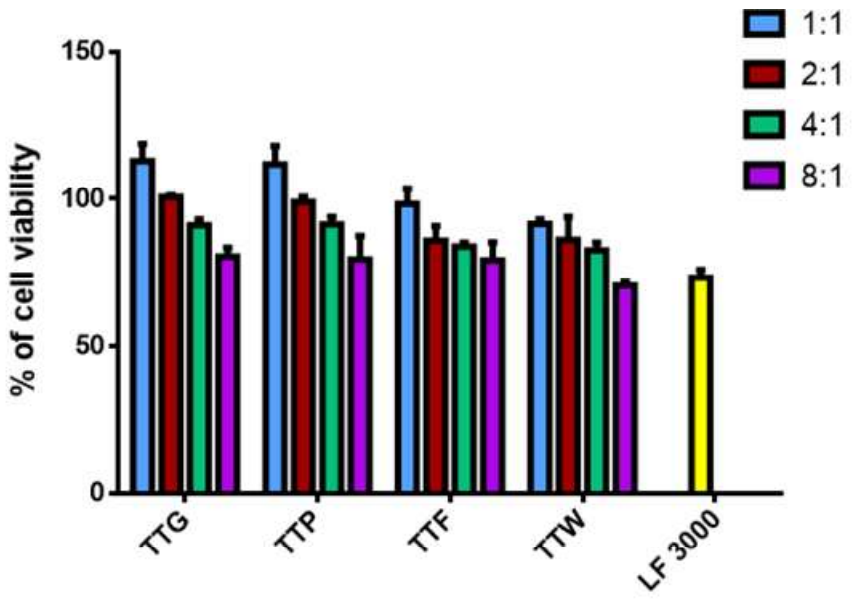

Figure. 10 B: % cell viability of TTG, TTP, TTF and TTW lipoplexes at different charge ratios in CHO cell line.

2.4 Conclusions:

In this study, the lipids TTF, TTW exhibited similarly efficiency of plasmid DNA (pDNA) and mRNA transfection in various cultured cells compared with commercial transfecting reagents, LF 3000 and LFMM respectively. It is also observed that, the cationic lipids containing hydrophobic aromatic R group containing amino acid derivatives could deliver both circular and linear nucleic acids efficiently. In this study, it was further shown that the liposomes delivered genome-editing tools using CRISPR/Cas9 encoded with pDNA effectively and also displayed improved efficiency in genome-editing. The transfection potential of TTW was comparable with that of commercially available LF 3000. These liposomes were also found to be effective in delivering Cas9 mRNA and demonstrated equal efficiency of gene editing AAVS1 locus compared to LF messenger Max in multiple cultured cell lines including CHO, Neuro-2a, EA.hy926 cells. In conclusion, our research shows that the hydrophobic R group in amino-tocopherol has a significant impact on the intracellular delivery of biomolecules and that the cationic lipid nanocarrier system (TTW) may be more efficient, affordable, and secure for applications such as the delivery of nucleic acids and genome editing.

2.5 Experimental Section:

2.5.1 Materials & Methods:

Alpha tocopherol, boc protected amino acids, propargyl amine and coupling reagents hydroxy benzotriazole (HOBT), EDCI.HCl were purchased from Sigma-Aldrich. Chemicals which were used for click chemistry such as sodium azide, sodium ascorbate, copper sulphate ($CuSO_4.5H_2O$) and bromo acetyl bromide, bases diisopropylethylamine (DIPEA), pyridine was procured from Alfa Aesar and Spectrochem Pvt. Ltd. Trifluoroacetic acid, solvents as used for reactions and column (compound purification) were obtained from Finar Limited. We bought silica gel thin-layer chromatography plates (0.25 mm) from Merck to track the development of the reaction. A Varian FT400 MHz NMR spectrometer was used to record the 1H and 13C NMR spectrum data. Using a commercial LCQ ion trap mass spectrometer with an ESI source, mass spectral data were obtained (Thermo Finnigan, SanJose, CA, U.S.). Sigma-Aldrich provided the co-lipid DOPE for the synthesis of liposomes. FBS, PBS, MTT, and trypsin were used in all biological experiments. These items were obtained from Thermo Fischer Scientific and Invitrogen.

2.5.2 Synthesis of alpha-tocopheryl-2-bromoacetate (Toc-Br):

To 1 mmol, 3g of alpha-tocopherol, 2 mmol, 1.68 mL of pyridine and 4 mL of dichloromethane (DCM) were added and kept it for stirring in ice bath at 0 °C then 1.5 mmol of bromo acetyl bromide (0.93 mL) taken in 10 mL of dichlromethane was added to the above solution drop by drop and continued the stirring for 2 hrs. After monitoring the consumption of substrate using TLC, the resultant reaction mixture was dissolved in 150 mL of ethyl acetate, washed three times with 1N HCl, twice with saturated NaHCO3 solution, and then washed once more with brine (50 mL). The solvent was then dried on sodium sulphate before being evaporated using a rotary evaporator. This was further purified by column chromatography using silica gel (60-120 mesh), eluting with 1% (v/v) per ether/ethyl acetate. (R_f = 0.7, 5% PE/EA) Yield:, 4.2 g (7.64 mmol, 93.82%) of pale yellow liquid. 400 MHz ^{1}H NMR (Solvent $CDCl_3$) [δ/ppm] 4.09 (s, 2H), 2.62 (t, J = 6.7 Hz, 2H), 2.13 – 1.93 (m, 9H), 1.80 (dt, J = 20.4, 6.9 Hz, 2H), 1.66 – 1.06 (m, 27H), 0.88 (t, J = 7.8 Hz, 12H). ESI-HRMS *m/z*: calculated:550.3022, found: 551.3087 $[M + H]^+$.

2.5.3 Synthesis of alpha-tocopheryl-2-azidoacetate (Toc-N_3):

1 mmol of Toc-Br (1.9 g) was taken in acetonitrile (10 mL), to this 5 mmol of sodium azide was added. This resulting mixture was refluxed about 24 hrs. After 24 hrs. it was dissolved in 100 mL of ethyl acetate followed by washings with water two times (2 x 50 mL) and once with brine (50 mL). The organic layer was dried on Na_2SO_4 and the solvent was removed by rotary evaporation and the residue was pure enough for proceeding further reaction. 400 MHz ^{1}H NMR (Solvent $CDCl_3$) [δ/ppm] 4.19 (s, 2H), 2.63 (t, J = 6.7 Hz, 2H), 2.20 – 2.01 (m, 9H), 1.81 (ddt, J = 20.0, 13.3, 6.5 Hz, 2H), 1.66 – 1.03 (m, 27H), 0.89 (t, J = 7.7 Hz, 12H). ESI- HRMS *m/z*: calculated: 513.3930, found: 514.4002 $[M + H]^+$.

2.5.4 General procedure of 1c and 2c derivatives:

1 mmol of boc-protected amino acid and 1.5 mmol of diisopropylethylamine (0.13 mL) in 10 mL of DCM were taken in a 100 mL of RB flask and kept it for stirring in ice bath at 0^{o}C. After five minutes of stirring sequentially HOBt (1.5 mmol), EDCI.HCl (1.5 mmol) were added to the stirred reaction mixture. After 10 minutes of stirring at 0^{o}C propargyl amine (1.2 mmol) was added, raised the temperature to RT and stirred continuously overnight. After consumption of substrate, resultant mixture was taken in 100 mL of ethyl acetate followed by washings with water two times (2 x 50 mL). Sodium sulphate was added to the pooled organic layer to dry the moisture and then filtered. The solvent from the filtrate was removed by evaporation under reduced pressure.

Boc-gly-acetylene:

By eluting the crude boc-glycine acetylene with 12% (v/v) pet ether in ethyl acetate, the boc-glycine acetylene was refined using column chromatography (R_f = 0.5, 20% PE/EA). 400 MHz, ^{1}H NMR (Solvent $CDCl_3$) [δ/ppm] 6.88 (s, 1H), 5.47 (s, 1H), 4.05 (s, 2H), 3.82 (s, 2H), 2.23 (s, 1H), 1.45 (s, 9H). ESI- HRMS *m/z*: calculated: 212.1161, found: 235.1068 $[M + Na]^+$.

Boc-pro-acetylene:

By eluting the crude boc-proline acetylene with 13% (v/v) pet ether in ethyl acetate, the boc-proline acetylene was refined using column chromatography (R_f = 0.5, 20% PE/EA). ^{1}H NMR (Solvent $CDCl_3$) [δ/ppm] 6.66 (s, 1H), 4.38 – 4.09 (m, 2H), 3.98 (d, *J* = 16.4 Hz, 2H), 3.47 (s, 2H), 2.25 (s, 2H), 2.09 (s, 1H), 1.88 (s, 2H), 1.47 (s, 9H). ESI-HRMS *m/z*: calculated: 252.1471, found: 275.1385 $[M + Na]^+$.

Boc-pheala-acetylene:

By eluting the crude boc-phenylalanine acetylene with 15% (v/v) pet ether in ethyl acetate, the boc-phenylalanine acetylene was refined using column chromatography (R_f = 0.3, 20% PE/EA). ^{1}H NMR (Solvent $CDCl_3$) [δ/ppm] 7.26 (d, *J* = 8.3 Hz, 2H), 7.20 (t, *J* = 7.0 Hz,3H), 5.34 (s, 1H), 4.43 (s, 1H), 3.96 (s, 2H), 3.06 (dd, *J* = 19.6, 14.2 Hz, 2H), 2.18 (s, 1H), 1.38 (s, 9H). ESI-HRMS *m/z*: calculated: 302.1630, found: 325.1637 $[M + Na]^+$.

Boc-trp-acetylene:

By eluting the crude boc-tryptophan acetylene with 30% (v/v) pet ether in ethyl acetate, the boc-tryptophan acetylene was refined using column chromatography (R_f = 0.6, 40% PE/EA). ^{1}H NMR (Solvent $CDCl_3$) [δ/ppm] 8.36 (s, 1H), 7.62 (d, *J* = 7.8 Hz, 1H), 7.35 (d, *J* = 8.1 Hz, 1H), 7.19 (t, *J* = 7.5 Hz, 1H), 7.11 (t, *J* = 7.4 Hz, 1H), 7.02 (s, 1H), 6.20 (t, *J* = 4.9 Hz, 1H), 5.19 (s, 1H), 4.44 (s, 1H), 3.89 (s, 2H), 3.24 (dd, *J* = 32.8, 8.4 Hz, 2H), 2.14 (s, 1H), 1.41 (s, 9H). ESI-HRMS *m/z*: calculated: 341.1739, found: 342.1832 $[M + H]^+$.

2.5.5 General procedure for click chemistry:

1 mmol of acetylene compound and 2.5 mmol of Toc-N_3 compound were mixed with 4 mL of *tert*-BuOH and 4 mL of H_2O (1:1), kept it for stirring followed by the addition of 0.5 mmol of sodium ascorbate taken in 1 mL of H_2O and continued stirring. After 5 min of stirring added a freshly prepared 0.1 mmol $CuSO_4.5H_2O$ in 1 mL of H_2O solution and stirred the reaction mixture for 24 hrs. After confirming the disappearance of starting materials, an excess of water was added to the reaction mixture and extracted the product using 3 x 30 mL of ethyl acetate. The pooled organic fractions dried over Na_2SO_4 and the solvent is evaporated using rotary evaporator.

Boc-gly-tri-toc:

The glycine compound was further purified using column chromatography by eluting with 35% (v/v) pet ether in ethyl acetate (R_f = 0.4, 40% PE/EA) followed by Boc deprotection. ^{1}H NMR (Solvent $CDCl_3$) [*δ*/ppm] 7.79 (s, 1H), 7.36 (t, *J* = 5.7 Hz, 1H), 5.43 (s, 2H), 4.54 (d, *J* = 5.7 Hz, 2H), 3.79 (d, *J* = 5.1 Hz, 2H), 2.57 (t, *J* = 6.6 Hz, 2H), 2.28 (s, 1H), 2.11 – 1.92 (m, 9H), 1.78 (ddq, *J* = 20.0, 13.2, 6.8 Hz, 2H), 1.63 – 1.00 (m, 34H), 0.86 (dd, *J* = 10.5, 5.2 Hz, 12H). ESI-HRMS *m/z*: calculated: l5.5091, found: 726.5219 $[M + H]^+$.

Boc-pro-tri-toc:

The proline compound was furrther purified using column chromatography by eluting with 35% (v/v) pet ether in ethyl acetate (R_f = 0.4, 40% PE/EA) followed by Boc deprotection. ^{1}H NMR (Solvent $CDCl_3$) [*δ*/ppm] 7.81 (s, 1H), 5.41 (s, 2H), 4.55 (d, *J* = 5.8 Hz, 2H), 4.22 (d, *J* = 32.0 Hz, 1H), 3.43 (m, 1H), 2.57 (t, *J* = 6.2 Hz, 2H), 2.36 – 2.08 (m, 2H), 2.07 – 1.90 (m, 9H), 1.90 – 1.68 (m, 4H), 1.63 – 1.00 (m, 35H), 0.85 (t, *J* = 7.6 Hz, 12H). ESI- HRMS *m/z*: calculated: 765.5404, found 766.5526 $[M + H]^+$.

Boc-pheala-tri-toc:

The phenylalanine compound was further purified using column chromatography by eluting with 2% $CH_3OH/CHCl_3$ (R_f = 0.5, 5% $CH_3OH/CHCl_3$) followed by Boc deprotection. ^{1}H NMR (Solvent $CDCl_3$) [*δ*/ppm] 7.64 (s, 1H), 7.31 (s, 1H), 7.25 – 7.22 (m, 3H), 7.14 (d, *J* = 6.9 Hz, 2H), 6.75 (s, 1H), 5.42 (s, 2H), 4.50 (d, *J* = 5.6 Hz, 2H), 4.12 (m, 1H), 3.06 (d, *J* = 6.9 Hz, 2H), 2.58 (t, *J* = 6.6 Hz, 2H), 2.03 (dd, *J* = 34.6, 15.9 Hz, 9H), 1.85 – 1.73 (m, 2H), 1.45 – 1.22 (m, 37H), 0.91 – 0.83 (m, 12H). ESI-HRMS *m/z*: calculated: 815.5561, found: 816.5684 $[M + H]^+$.

Boc-trp-tri-toc:

The tryptophan compound was further purified using column chromatography by eluting with 3% $CH_3OH/CHCl_3$ (R_f = 0.4, 5% $CH_3OH/CHCl_3$) followed by Boc deprotection. ^{1}H NMR (Solvent $CDCl_3$) [*δ*/ppm] 8.39 (s, 1H), 7.52 (d, *J* = 7.8 Hz, 1H), 7.34 (s, 1H), 7.14 (d, *J* = 8.0 Hz, 1H), 7.06 (t, *J* = 7.4 Hz, 1H), 6.99 (t, *J* = 7.4 Hz, 1H), 6.68 (s, 1H), 5.28 (s, 2H), 5.21 (s, 2H), 4.32 – 4.23 (m, 1H), 3.21 (d, *J* = 12.3 Hz, 1H), 3.02 (dd, *J* = 14.3, 7.6 Hz, 1H), 2.50 (t, *J* = 6.6 Hz, 2H), 2.04 – 1.85 (m, 9H), 1.78 – 1.62 (m, 2H), 1.54 – 0.91 (m, 35H), 0.81 – 0.75 (m, 12H). ESI- HRMS *m/z*: calculated: 854.5670, found: 855.5795 $[M + H]^+$.

2.5.6 Synthesis of final lipids (Boc deprotection):

1 mmol of boc protected compound in dry DCM (8 mL) was taken in a 50 mL RB flask, placed in an ice cooled solution and then added 4 mL of trifluoro acetic acid (TFA) at 0°C followed by the raise in temperature to RT and continued stirring overnight. The solvent and excess TFA were removed under reduced pressure, the obtained residue was dissolved in (30 mL) ethyl acetate and the solvent was evaporated using rotary evaporation followed by further drying under high vacuum for three hours. The compound was pure and 90% yielded.

Lipid-1 TTG:

^{1}H NMR (Solvent $CDCl_3$) [δ/ppm] 8.17 (s, 2H), 7.75 (s, 1H), 5.36 (s, 2H), 4.36 (s, 2H), 3.76 (s, 2H), 2.49 (s, 2H), 2.17 – 1.82 (m, 9H), 1.68 (s, 2H), 1.41 – 0.98 (m, 26H), 0.85 (t, J = 7.3 Hz, 12H). ^{13}C NMR [δ/ppm] (126 MHz, $CDCl_3$) 165.64, 149.80, 139.98, 126.36, 124.77, 123.26, 117.70, 75.24, 50.50, 41.00, 39.38, 37.62, 37.47, 37.44, 37.41, 37.30, 34.23, 32.80, 32.73, 30.97, 30.90, 27.98, 24.82, 24.47, 22.72, 22.62, 21.03, 20.42, 19.74, 19.68, 19.61, 19.58, 19.55, 19.52, 12.59, 11.73, 11.67. ESI-HRMS *m/z*: calculated: 626.4640, found: 626.4682 $[M]^+$.

Lipid-2 TTP:

^{1}H NMR (Solvent $CDCl_3$) [δ/ppm] 9.92 (s, 1H), 7.08 (s, 1H), 5.48 (s, 2H), 4.50 (s, 1H), 4.15 (m, J = 7.1 Hz, 1H), 3.42 (s, 2H), 2.58 (t, J = 5.6 Hz, 2H), 2.42 (s, 1H), 2.15 – 1.89 (m, 13H), 1.87 – 1.71 (m, 2H), 1.65 – 1.02 (m, 28H), 0.87 (dd, J = 10.4, 5.1 Hz, 12H). ^{13}C NMR [δ/ppm] (126 MHz, $CDCl_3$) 165.32, 149.95, 139.94, 126.28, 124.67, 123.37, 117.77, 75.34, 59.96, 50.78, 46.55, 39.37, 37.57, 37.45, 37.40, 37.29, 32.79, 32.71, 30.98, 30.93, 29.81, 29.70, 27.98, 24.81, 24.45, 24.35, 22.72, 22.62, 21.02, 20.53, 19.74, 19.68, 19.62, 19.59, 19.57. ESI-HRMS *m/z*: calculated: 666.4958, found: 666.4993 $[M]^+$.

Lipid-3 TTF:

^{1}H NMR (Solvent $CDCl_3$) [δ/ppm] 8.09 (s, 1H), 7.58 (s, 1H), 7.05 (d, J = 23.9 Hz, 5H), 5.29 (s, 2H), 4.18 (d, J = 59.9 Hz, 2H), 3.02 (d, J = 9.8 Hz, 2H), 2.45 (s, 2H), 1.94 (dd, J = 72.5, 34.8 Hz, 9H), 1.72 – 1.57 (m, 2H), 1.52 – 0.93 (m, 26H), 0.77 (dd, J = 11.0, 4.5 Hz, 12H). ^{13}C NMR [δ/ppm] (126 MHz, $CDCl_3$) 165.38, 149.93, 139.95, 133.76, 129.37, 128.92, 127.71, 126.25, 124.64, 123.40, 117.74, 75.30, 55.10, 50.58, 39.38, 37.57, 37.46, 37.41, 37.29, 32.79, 32.71, 30.90, 29.71, 27.98, 24.81, 24.46,

22.72, 22.63, 21.02, 20.50, 19.75, 19.68, 19.65, 19.62, 19.59, 19.56, 12.79, 11.94, 11.76. ESI-HRMS *m/z*: calculated: 716.5109, found: 716.5149 $[M]^+$.

Lipid-4 TTW:

^{1}H NMR (Solvent $CDCl_3$) [*δ*/ppm] 8.66 (s, 1H), 8.06 (s, 1H), 7.42 (d, *J* = 8.1 Hz, 1H), 7.13 (d, *J* = 8.2 Hz, 1H), 7.04 – 6.99 (m, 1H), 6.98 – 6.91 (m, 1H), 6.80 (s, 1H), 5.28 (s, 2H), 4.17 (d, *J* = 51.9 Hz, 2H), 3.03 (s, 2H), 2.58 – 2.43 (m, 2H), 2.00 (dd, *J* = 50.5, 17.4 Hz, 9H), 1.55 – 1.48 (m, 2H), 1.47 – 0.97 (m, 25H), 0.87 – 0.82 (m, 12H). ^{13}C NMR [*δ*/ppm] (101 MHz, $CDCl_3$) 165.87, 149.88, 139.98, 136.10, 126.83, 126.30, 125.09, 124.71, 123.34, 121.90, 119.43, 118.23, 117.73, 111.57, 106.63, 75.26, 53.42, 50.34, 39.38, 37.60, 37.47, 37.43, 37.41, 37.30, 32.80, 32.72, 31.94, 31.83, 31.64, 30.93, 29.71, 27.98, 27.13, 24.81, 24.46, 22.72, 22.63, 21.03, 20.47, 19.75, 19.69, 19.64, 19.61, 19.58, 19.56, 12.81, 11.95, 11.75. ESI-HRMS *m/z*: calculated: 755.5218, found: 755.5263 $[M]^+$.

2.5.7 Preparation of Liposomes and pDNA:

Liposomes were made using the previous procedure [13,46,58-63]. The final concentrations of TGK with co lipid DOPE and CGK with co lipid DOPE in chloroform were taken at 1:1 molar ratio respectively. 1 mM liposomes were used for *in vitro* studies.

2.5.8 Zeta Potential (ξ) and Global Size Measurements:

To analyse cationic liposomes made from cationic lipid with co-lipid (DOPE) and complexes created from liposomes with DNA particle size and zeta potential, we employed photon correlation spectroscopy and electrophoretic mobility using a zeta sizer 3000HSA (Malvern, UK). The diameters were calculated in DMEM with a refractive index of 1.59 and a viscosity of 0.89. The instrument was calibrated using a polymer of polystyrene with a 200 nm size (Duke Scientific Corps., Palo Alto, CA). The sizes of liposomes and lipoplexes were calculated in automatic mode. The zeta potential was calculated using the following variables: viscosity (0.89 cP), dielectric constant (79), temperature (25°C), F (Ka), 1.50 (Smoluchowski), and maximum current voltage (V). The analysis was calibrated using the Malvern DTS0050 standard, with the average of three repeated measurements of three different values and the zero-field correction size.

2.5.9 DNA-binding assay:

An agarose gel retardation assay was used to test the DNA binding properties of the improved cationic co-liposomal formulations (lipid/DOPE, 1:1). In following experiment, 500 ng of pCMV-gal was complexed with each cationic formulation in 1x PBS (24 µL) at four different N/P (liposome/plasmid) charge ratios of 1:1, 2:1, 4:1 and 8:1. Followed by prepared complexes incubated for 30 minutes. After adding 6x loading dye to the sample, these complexes (12 µL each) were loaded into a freshly prepared 1% agarose gel dyed with EtBr. In a 100 V electrophoresis chamber, electrophoresis was performed for 35 minutes in 1x TAE running buffer[45]. The gel photos were captured in transillumination mode using a gel documentation system.

2.5.10 Heparin Displacement Assay:

The lipoplexes were made as described in the previous section in order to conduct the heparin displacement assay, and they were then incubated for an additional 20 minutes. Following the incubation time, 0.5 µL of 1 mg/mL sodium salt of heparin was added and incubated for an additional 30 minutes. Using a gel documentation equipment, DNA bands were observed.

2.5.11 Cellular uptake study and Effect of lysosomotropic agent (Chloroquine) on non-viral gene delivery:

Cells were planted in a 48-well plate at a density of 25000 cells per well for uptake investigations, typically 12 hours before the treatment. The eGFP plasmid was complexed with rhodamine-PE labelled cationic liposomes using a 1: 1 to 8:1 charge ratio of lipid-DNA complexes (0.4 g of DNA diluted to 20 L with serum free DMEM medium). The cells were given a lipoplex treatment before being incubated at 37°C in a humid environment with 5% CO2. An inverted Leica fluorescence microscope (Leica CTR 6000, Germany) was used to monitor the cells after 4 hours of incubation. The cells were then washed with PBS (200 L) to completely remove the dye from the wells. The cells were then quantified using the FACS BD Celesta Flow system, USA.

Cells were seeded at a density of 25000/well for CHO in a 48-well plate at least 12 hours before the transfection procedures in order to examine the effect of the lysosomotropic drug. Chloroquine (100 M) was used as a pre-treatment for the cells before transfection. The medium was then taken out and replaced with full DMEM (10% FBS and 1% penicillin-streptomycin) after 4 hours of incubation. The cells were

then given the lipoplexes, and they were incubated at 37°C with 5% CO2 after that. After 48 hours, the reporter gene activity was measured by flow cytometric analysis.

2.5.12 Cellular uptake & co-localisation analysis:

Briefly, Neuro-2a cells were harvested at a density of 1×10^4 cells for each confocal dish 24 hours prior to the experiment. Here, rhodamine-DHPE labelled liposomes were used for lipoplex preparation. 40 µL of lipoplexes were added to the seeded cells after attaining 70% confluency at best charge ratio 4:1 for 12 hours. Followed by Lysotracker green DND-26 reagent (100 nM) was also added and incubated for 30 min. After incubation, Hoechst (1 mg per mL) was added to cells and washed twice with PBS. Under a confocal microscope with a 100x oil immersion objective, fluorescence was observed (Leica TCS S52). The emission wavelength for hoechst was set at 361-497 nm, 568–583 nm for lipoplexes labelled with rhodamine-PE, and 504-511 nm for Lysotracker green. The position of the labelled lipoplexes in relation to the lysosomes and nucleus was used to investigate the colocalization of the fluorescent labels for lipids (red) and lysosomal compartments (green).

2.5.13 pDNA Transfection Biology:

Fluorescence microscopy and flow cytometry were used to qualitatively and quantitatively assess the cationic lipoplexes' ability to produce eGFP. At least 12 hours before the transfection studies, cells were seeded in a 48-well plate at a density of 25000/well (for HEK-293, CHO, Neuro-2a, and EA.hy926). In serum-free media with a final volume of 40 µL for 30 minutes, lipoplexes were created using pDNA (0.4 g) and the liposomes of TTG, TTP, TTF, and TTW at a 1:1 to 8:1 lipid/DNA charge ratio. The cells were combined with the prepared lipoplexes. Using a previously described method[67], the reporter gene activity was calculated after 36–48 h of incubation. Following the period of incubation, GFP expression was imaged using a fluorescent microscope (Leica CTR 6000, Germany), and the results were quantified using FACS. The Becton-Dickinson software was used to analyse 10,000 cells per sample, and here, the commercially available transfection reagent LF 3000 served as the positive control.

2.5.14 CRISPR Plasmid Expression Studies:

12–18 hours prior to transfection, 4 104 HEK-293 cells were planted in 24-well plates to analyse the GFP expression in the cells. In serum-free medium, liposomes were produced to bind to pL-CRISPR. EFS.GFP (0.9 g/well) at a 4:1 lipid/DNA charge ratio for 20 minutes. After obtaining the final volumes of complexes to 40 µl, these complexes were added to the cells. GFP expression imaging was carried out

using a fluorescent microscope (Leica CTR 6000, Germany) and quantified in FACS after 36–48 hours of transfections (BD Celesta Flow cytometry, USA).

2.5.15 mRNA Transfection Studies:

Hek 293 and CHO cells were seeded in a 48-well plate at a density of 25000/well for mRNA transfection research at least 12 hours before the experiments. mRNA plexes were made by preparing 0.1 g of GFP-encoding mRNA with different amounts of liposomes (4:1 to 12:1 lipid/mRNA charge ratio) in serum-free DMEM to a final volume of 40 µL for 30 min. According to the manufacturer's instructions, LFmMAX MAX, a commercially available transfection reagent, was utilised for transfection. After introducing the complexes, the cells were cultured for a further 24 hours. After the incubation time, GFP expression imaging was performed using a fluorescent microscope (Leica CTR 6000, Germany), and the results were quantified in FACS (BD Celesta Flow cytometry, USA).

2.5.16 Cell viability assay:

Cytotoxic screening is a necessary step for characterising the tocopherol-based gene delivery vectors that have been made[64]. For this, cells were planted in 96-well plates at a density of 1×104 cells per well. Colorimetric analysis counts the number of feasible cells and compares the intensity of the colour to that number. By incubating Neuro- 2a and HEK-293 cells with the prepared lipoplexes for 20 min at room temperature, followed by treating the cells for 24 h at 37°C in 10% serum-containing DMEM, it was possible to assess the lipid toxicities for lipoplexes made using liposomes and pDNA at varying lipid/DNA charge ratios (1:1–8:1). MTT dye (5 mg/mL) was freshly prepared in serum-free DMEM and 100 µL was added to each well after 24 hours of incubation. The test was then ceased after 3 hours of incubation. After that, 100 µL of DMSO was added after the media had been taken out of each well. The untreated cells were used as controls. Next, the purple dye was dissolved and detected spectroscopically at 540 nm in a multiplate reader. A540 (treated cells)-background/A540 (untreated cells)-background x 100 was used to compute the % viability.

2.5.17 Gene editing:

2.5.17.1 Cell culture and transfection of cells using CRISPR tools:

Neuro-2a, EA.hy926, CHO & HEK-293 cells were cultured in medium supplemented with 10% Fetal Bovine Serum and 1% penicillin−streptomycin. One day before transfection cells were seeded into 24-well plates. Cells were transfected with 15 pmol of sgRNA and 100ng of cas9 mRNA with liposomes at 4:1 lipid/mRNA charge ratio in serum-free DMEM to a final volume of 40 µL for 10 min. The RNP plexes were then added to the cells, and incubated at 37°C and 5% CO_2.

2.5.17.2 Endonuclease assay 1:

The growth media was removed after 48 hours of incubation and the cells were washed with 1X PBS followed by the addition of 0.1% trypsin/EDTA (100 µL). The detached cells were resuspended in 200 µL of growth media. The pooled cells were centrifuged at 1000 rpm 5 minutes after which supernatant was discarded. The cell pellet was washed with 1X PBS and again centrifuged. To the pellet 50 µL of DNA extraction solution was added and the pellet was resuspended. The tubes were kept in thermomixer at 68ºC for 30 minutes. Then the tubes were vortexed for 15 seconds. Again the tubes were kept at theromixer in 98ºC for 15 minutes. Then the tubes were vortexed for 15 seconds. Quantify the DNA sample in nanodrop. Target regions were PCR-amplified for that in the PCR tubes master mix containing buffer, dNTP, AAVS primers and enzyme were added to that 500ng of DNA Template was also added.

PCR products were denatured at 95°C for 1 min, annealed at 60°C per 15 seconds, elongation at 72°C for 7 min. 2% agarose gel was prepared in 1X TAE and 5 µL sample containing 2 µL of 5X loading dye was added to each well along with 5 µL of DNA ladder in one well. Gel was run at 90V. DNA bands were visualized in a Bio-Rad Gel Doc XR + imaging system (Bio-Rad, Hercules, CA, USA).

The hetero complexed PCR product (17 µL) and 2 µL of NE Buffer was incubated at 95°C for 10 min, 85°C for 10 seconds, 25°C for 10 seconds. The Heteroduplex product 19µL and T7 endonuclease enzyme 1 µL was added and kept in the PCR at 37°C for 20 min. T7 endonuclease product was run in 8% native page (30% acrylamide, 10% ammonium per sulphate, 5X TBE, distilled water, TEMED). 20 µL of both undigested and digested samples with 2 µL of 5X loading dye was loaded into each well and allowed to run at 100V. After the electrophoresis, the gel was removed and stained with EtBr solution for 10 min. DNA bands were visualized in a Bio-Rad Gel Doc XR + imaging system (Bio-Rad, Hercules, CA, USA).

2.6 References

1 L. Schoenmaker, D. Witzigmann, J. A. Kulkarni, R. Verbeke, G. Kersten, W. Jiskoot and D. J. A. Crommelin, *Int. J. Pharm.*, 2021, 601.

2 M. K. K. Azhagiri, P. Babu, V. Venkatesan and S. Thangavel, *Stem Cell Res. Ther.*, 2021, 12.

3 H. Frangoul, D. Altshuler, M. D. Cappellini, Y.-S. Chen, J. Domm, B. K. Eustace, J. Foell, J. de la Fuente, S. Grupp, R. Handgretinger, T. W. Ho, A. Kattamis, A. Kernytsky, J. Lekstrom-Himes, A. M. Li, F. Locatelli, M. Y. Mapara, M. de Montalembert, D. Rondelli, A. Sharma, S. Sheth, S. Soni, M. H. Steinberg, D. Wall, A. Yen and S. Corbacioglu, *N. Engl. J. Med.*, , DOI:10.1056/nejmoa2031054.

4 M. A. Mintzer and E. E. Simanek, *Chem. Rev.*, 2009, 109.

5 H. Yin, R. L. Kanasty, A. A. Eltoukhy, A. J. Vegas, J. R. Dorkin and D. G. Anderson, *Nat. Rev. Genet.*, 2014, **15**, 541–555.

6 G. Lin, H. Zhang and L. Huang, *Mol. Pharm.*, 2015, **12**, 314–321.

7 S. Bhattacharya and A. Bajaj, *Chem. Commun.*, 2009.

8 M. A. Maslov, T. O. Kabilova, I. A. Petukhov, N. G. Morozova, G. A. Serebrennikova, V. V. Vlassov and M. A. Zenkova, *J. Control. Release*, 2012, **160**, 182–193.

9 D. Zhi, S. Zhang, S. Cui, Y. Zhao, Y. Wang and D. Zhao, *Bioconjug. Chem.*, 2013, 24.

10 K. Shi, J. Zhou, Q. Zhang, H. Gao, Y. Liu, T. Zong and Q. He, *J. Biomed. Nanotechnol.*, 2015, **11**, 382–391.

11 B. K. G. Theng, 2012, **4**, 319–337.

12 Y. Zhao, S. Zhang, Y. Zhang, S. Cui, H. Chen, D. Zhi, Y. Zhen, S. Zhang and L. Huang, *J. Mater. Chem. B*, 2015, **3**, 119–126.

13 D. Zhi, S. Zhang, B. Wang, Y. Zhao, B. Yang and S. Yu, *Bioconjug. Chem.*, 2010, **21**, 563–577.

14 R. S. Y. Wong and A. K. Radhakrishnan, *Nutr. Rev.*, 2012, **70**, 483–490.

15 N. Duhem, F. Danhier and V. Préat, *J. Control. Release*, 2014, 182, 33–44.

16 Q. Liu, Q. Q. Jiang, W. J. Yi, J. Zhang, X. C. Zhang, M. B. Wu, Y. M. Zhang, W. Zhu and X. Q. Yu, *Bioorganic Med. Chem.*, 2013, **21**, 3105–3113.

17 B. Kedika and S. V. Patri, *J. Med. Chem.*, 2011, **54**, 548–561.

18 B. Kedika and S. V. Patri, *Bioconjug. Chem.*, , DOI:10.1021/bc2004395.

19 V. Muripiti, B. Lohchania, V. Ravula, S. Manturthi, S. Marepally, A. Velidandi and S. V. Patri, *New J. Chem.*, 2021, **45**, 615–627.

20 V. Ravula, V. Muripiti, S. Manthurthi and S. V. Patri, *ChemistrySelect*, 2021, **6**, 13025–13033.

21 S. Patil, Y. G. Gao, X. Lin, Y. Li, K. Dang, Y. Tian, W. J. Zhang, S. F. Jiang, A. Qadir and A. R. Qian, *Int. J. Mol. Sci.*, , DOI:10.3390/ijms20215491.

22 D. A. Medvedeva, M. A. Maslov, R. N. Serikov, N. G. Morozova, G. A. Serebrenikova, D. V. Sheglov, A. V. Latyshev, V. V. Vlassov and M. A. Zenkova, *J. Med. Chem.*, 2009, **52**, 6558–6568.

23 J. C. Rea, R. F. Gibly, A. E. Barron and L. D. Shea, *Acta Biomater.*, 2009, **5**, 903–912.

24 V. Muripiti, B. Lohchania, S. K. Marepally and S. V. Patri, *Medchemcomm*, 2018, **9**, 264–274.

25 M. Jiang, L. Gan, C. Zhu, Y. Dong, J. Liu and Y. Gan, *Biomaterials*, 2012, **33**, 7621–7630.

26 H. M. Aliabadi and A. Lavasanifar, *Expert Opin. Drug Deliv.*, 2006, **3**, 139–162.

27 K. Wang, X. Yan, Y. Cui, Q. He and J. Li, *Bioconjug. Chem.*, 2007, **18**, 1735–1738.

28 M. Westoby, J. Chrostowski, P. De Vilmorin, J. P. Smelko and J. K. Romero, *Biotechnol. Bioeng.*, 2011, **108**, 50–58.

29 C. E. Ashley, E. C. Carnes, K. E. Epler, D. P. Padilla, G. K. Phillips, R. E. Castillo, D. C. Wilkinson, B. S. Wilkinson, C. A. Burgard, R. M. Kalinich, J. L. Townson,

B. Chackerian, C. L. Willman, D. S. Peabody, W. Wharton and C. J. Brinker, *ACS Nano*, 2012, **6**, 2174–2188.

30 M. Rajesh, J. Sen, M. Srujan, K. Mukherjee, B. Sreedhar and A. Chaudhuri, *J. Am. Chem. Soc.*, 2007, **129**, 11408–11420.

31 C. M. Lamanna, H. Lusic, M. Camplo, T. J. Mcintosh, P. Barth and M. W. Grinstaff, .

32 P. Gao, W. Pan, N. Li and B. Tang, *ACS Appl. Mater. Interfaces*, 2019, **11**, 26529–26558.

33 Y. Zhao, T. Zhao, Y. Du, Y. Cao, Y. Xuan, H. Chen, D. Zhi, S. Guo, F. Zhong and S. Zhang, *J. Nanobiotechnology*, 2020, **18**, 1–14.

34 T. HE, L. LF, D. GJ, W. WT, C. SC, K. ML, T. R, L. GS and T. MH, *J. Gene Med.*, 2012, **14**, 44–53.

35 T. Takeuchi, J. Montenegro, A. Hennig and M. Stefan, *Chem. Sci.*, 2011, **2**, 303–307.

36 M. E. Davis, J. E. Zuckerman, C. H. J. Choi, D. Seligson, A. Tolcher, C. A. Alabi, Y. Yen, J. D. Heidel and A. Ribas, *Nature*, 2010, **464**, 1067–1070.

37 D. Zhou, C. Li, Y. Hu, H. Zhou, J. Chen, Z. Zhang and T. Guo, *Chem. Commun.*, 2012, **48**, 4594–4596.

38 C. L. Walsh, J. Nguyen, M. R. Tiffany and F. C. Szoka, *Bioconjug. Chem.*, 2013, **24**, 36–43.

2.7 Spectral data

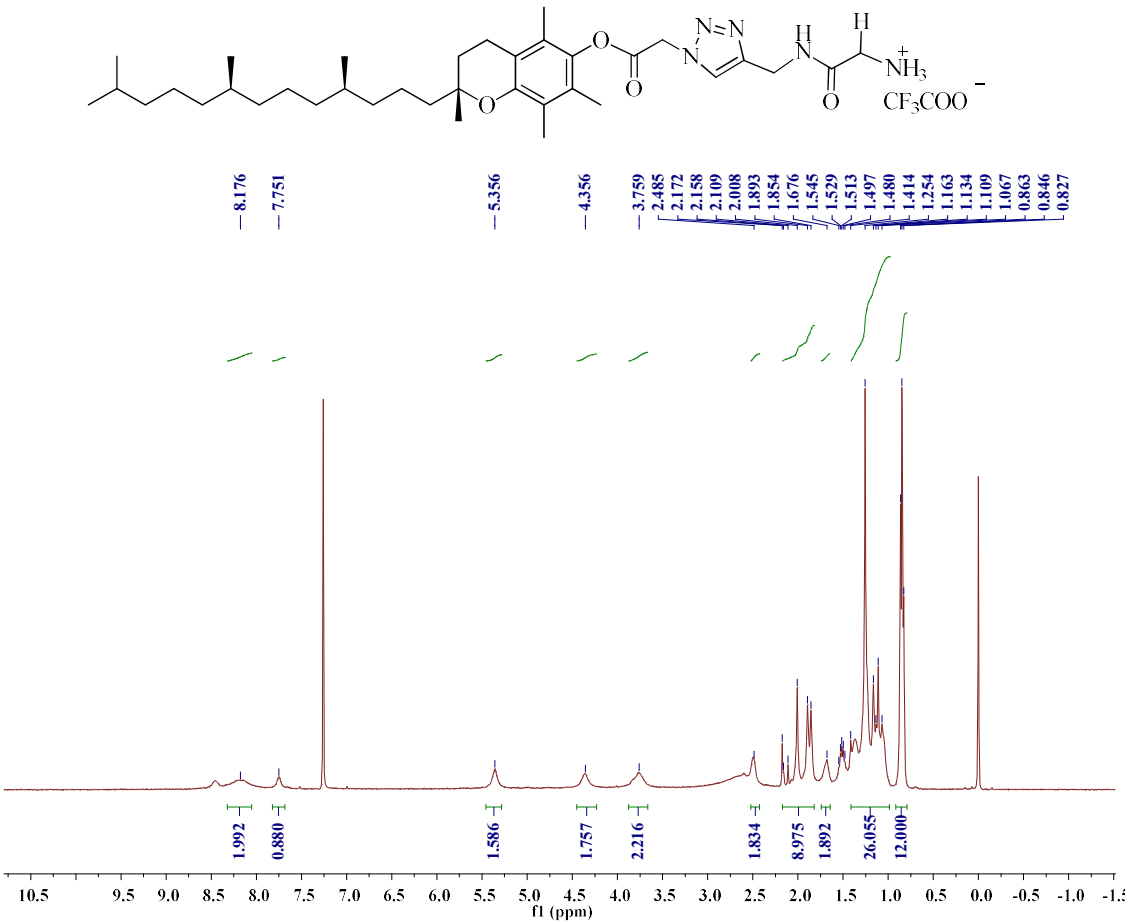

^{1}H NMR Spectrum of **Lipid-1 TTG**

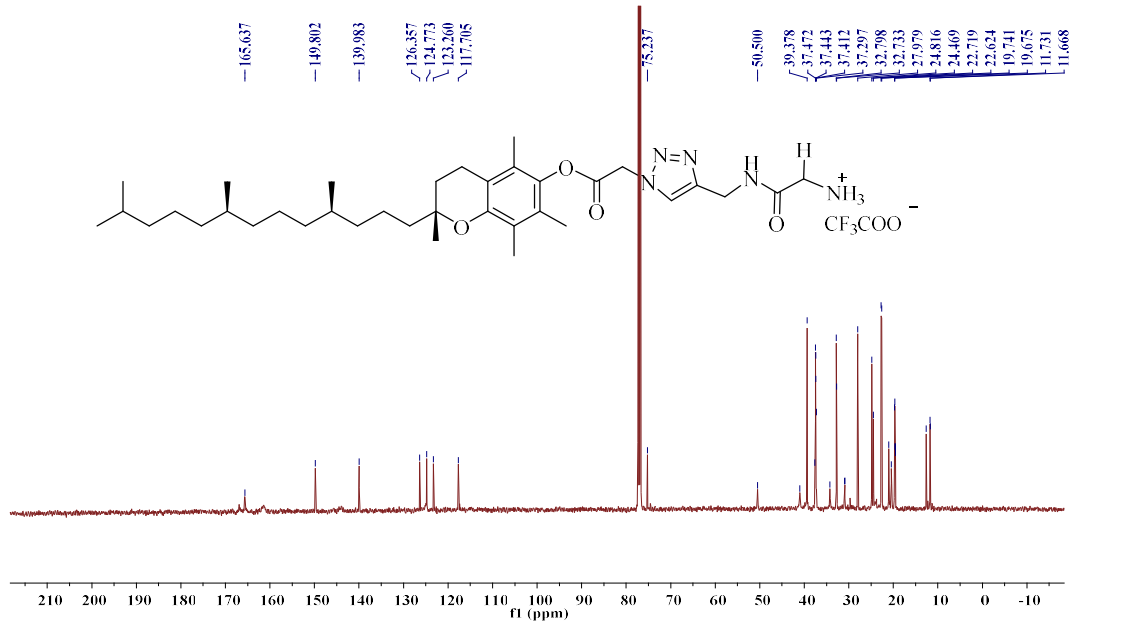

^{13}C NMR Spectrum of **Lipid-1 TTG**

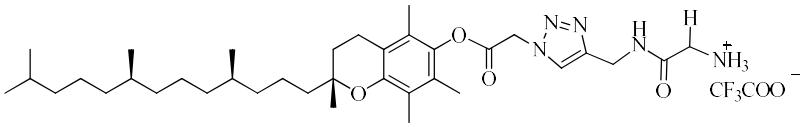

Chemical Formula: $C_{36}H_{60}N_5O_4^+$
Exact Mass: 626.4640

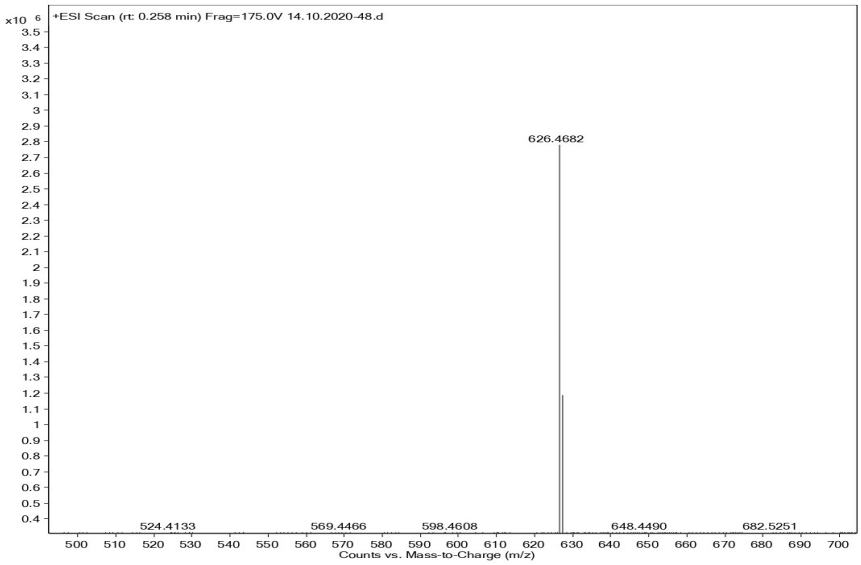

ESI-HRMS Spectrum of **Lipid-1 TTG**

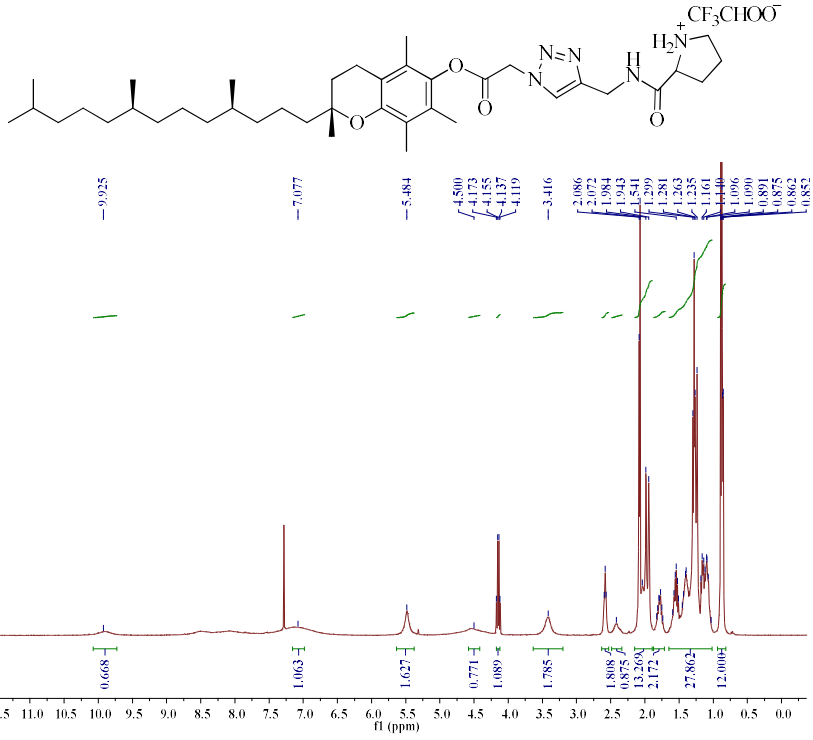

^{1}H NMR Spectrum of **Lipid-2 TTP**

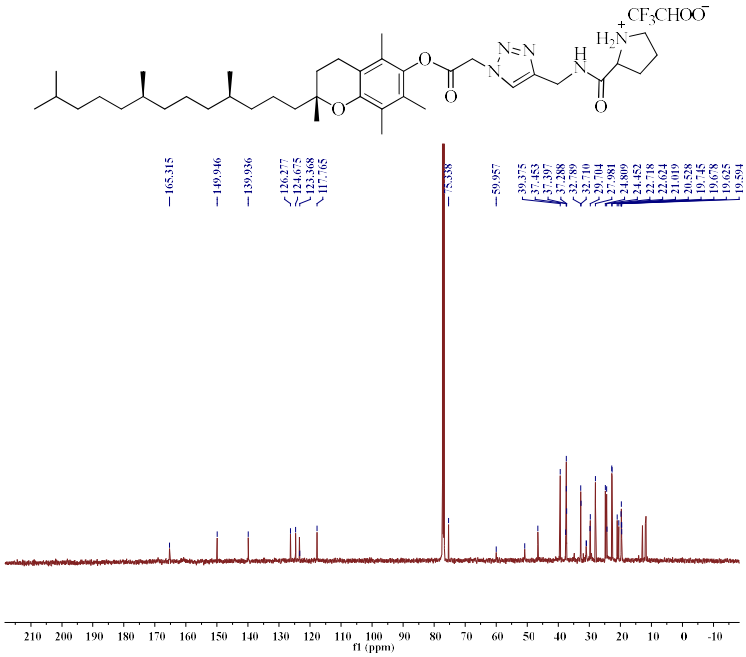

^{13}C NMR Spectrum of **Lipid-2 TTP**

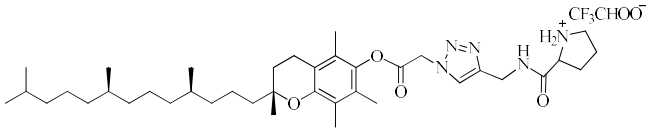

Chemical Formula: $C_{39}H_{71}N_5O_4$
Exact Mass: 666.4958

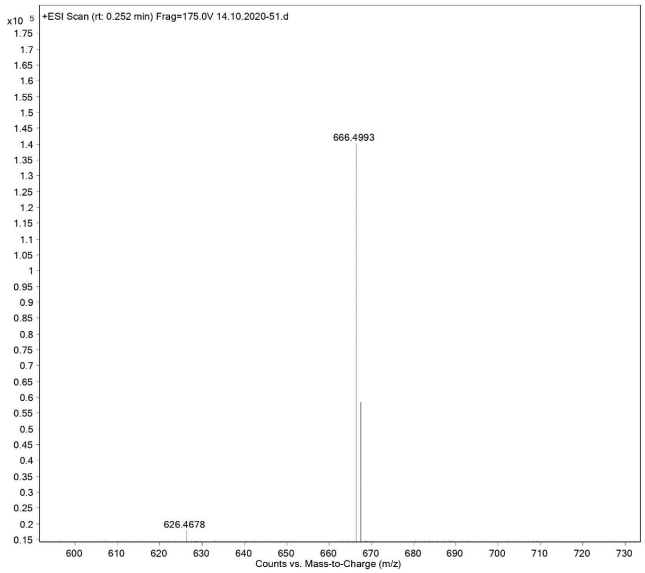

ESI-HRMS Spectrum of **Lipid-2 TTP**

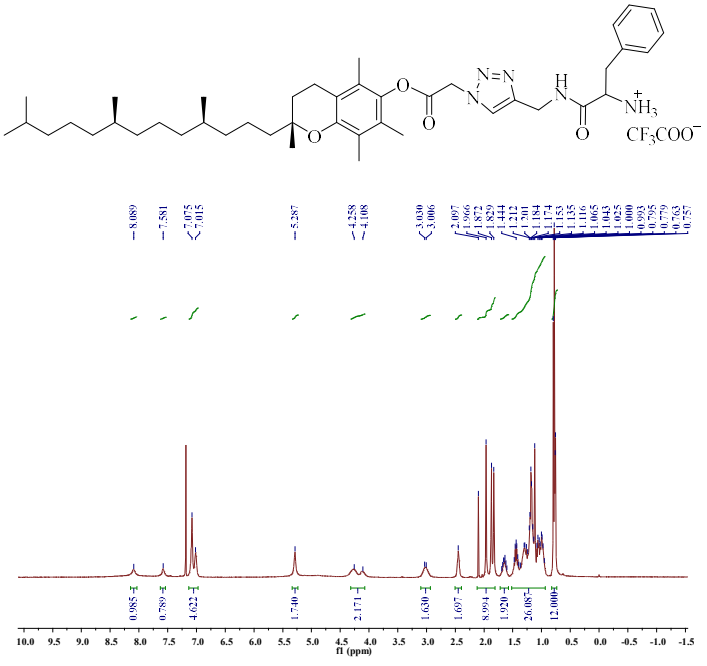

^{1}H NMR Spectrum of **Lipid-3 TTF**

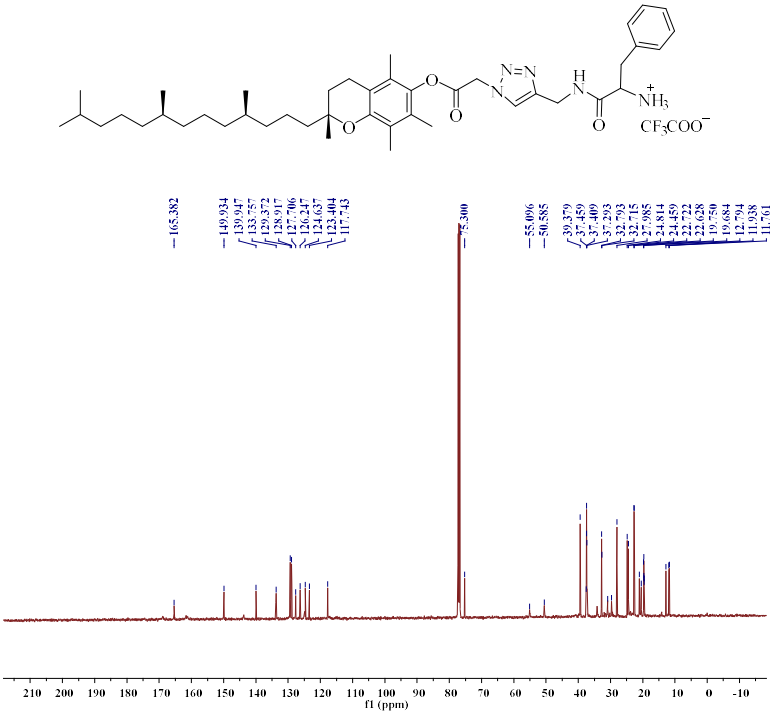

^{13}C NMR Spectrum of **Lipid-3 TTF**

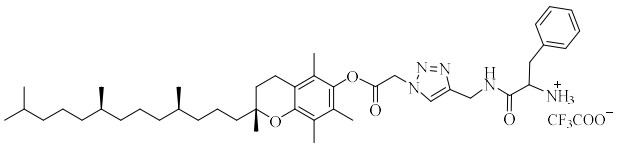

Chemical Formula: $C_{43}H_{66}N_5O_4^+$
Exact Mass: 716.5109

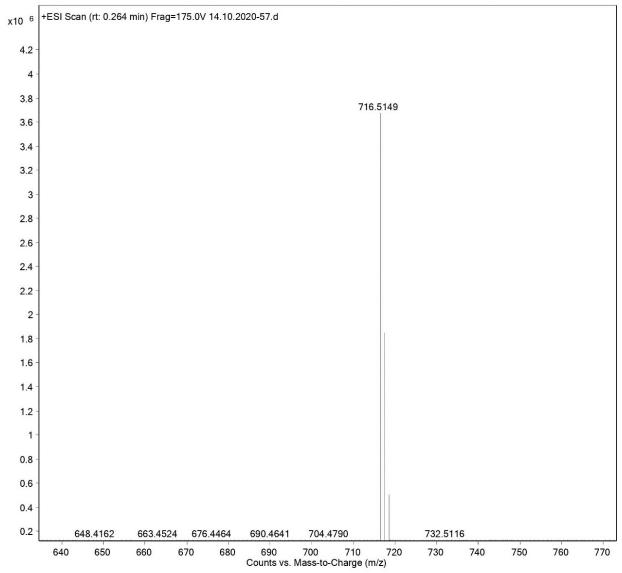

ESI-HRMS Spectrum of **Lipid-3 TTF**

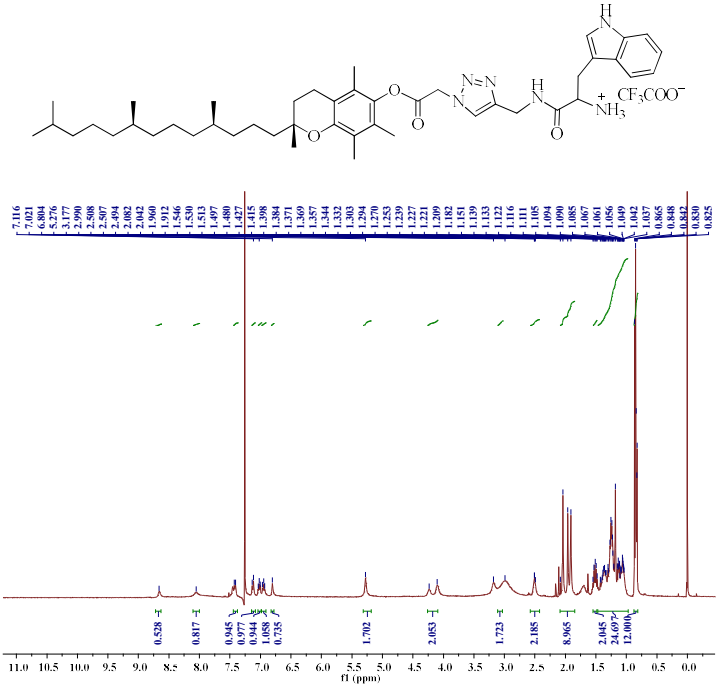

^{1}H NMR Spectrum of **Lipid-4 TTW**

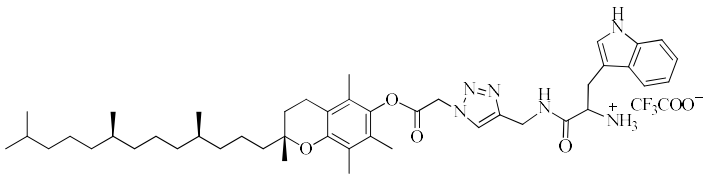

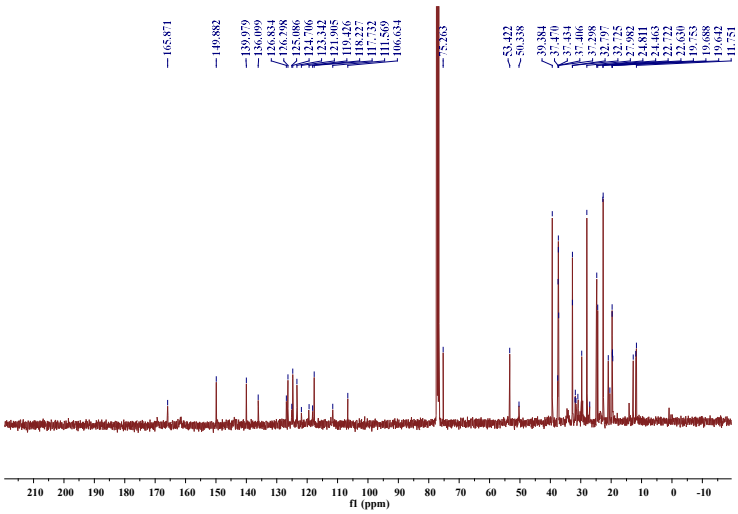

^{13}C NMR Spectrum of **Lipid-4 TTW**

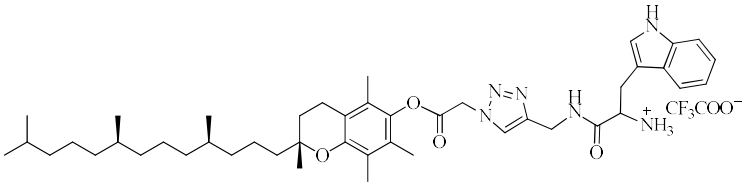

Chemical Formula: $C_{45}H_{67}N_6O_4^+$
Exact Mass: 755.5218

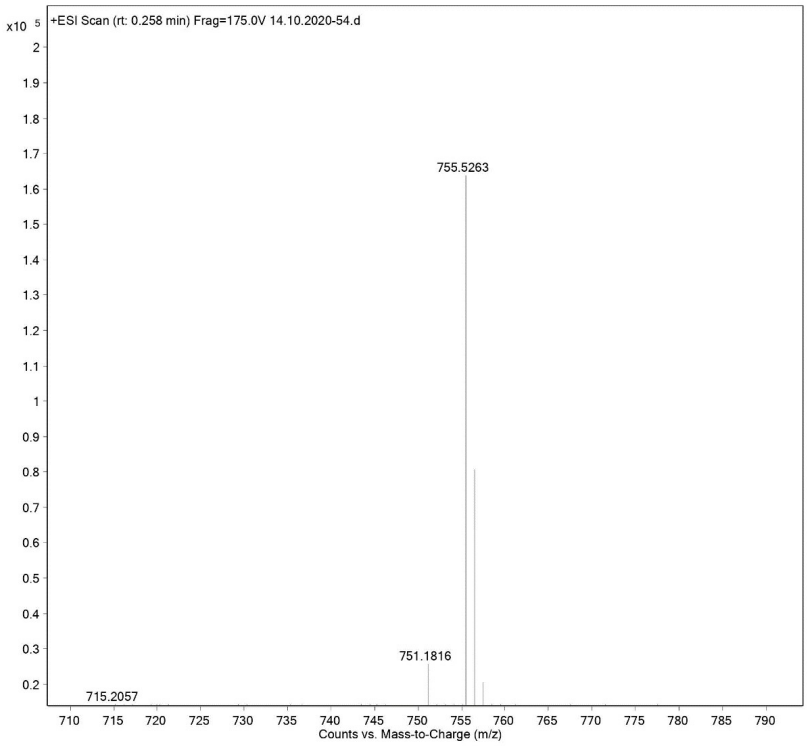

ESI-HRMS Spectrum of **Lipid-4 TTW**

CHAPTER III

Effect of Methylation in the Hydrophilic Domain of Tocopheryl Ammonium Based Lipids on their Gene Delivery Properties

3.1. Introduction

The cationic lipid 3b-[N-(N', N'-dimethylamino-ethane) carbamoyl]-cholesterol hydrochloride, DC, is commercially available. Chol was developed for the first time in 1991 by Gao et al. This is one of cationic lipids in combination with DOPE which is widely used in the liposomal preparation for gene delivery[1,2]. DC-Chol:DOPE has been used to treat cystic fibrosis through nasal application without altering ion transport, bacterial growth or lung function[3]. DC-Chol also enhance significantly the effect of growth inhibition of Antisense oligodeoxynucleotides on tumour cells to inhibit the tumour growth[4]. In terms of the transport of biomolecules, DC-Chol is one of the most effective cationic lipids due to its significant structural characteristics [5].

Generally speaking, cationic lipids have a linkage, a hydrophilic head group, and a hydrophobic backbone [6–8]. In these cationic lipids, the systematic modifications of any of three domains or all can result in the variation of transfection efficiency. Several efforts have been made to generate novel amphiphiles by modifying these domains. However, the appropriate structural domains needed to the stable transfection are still uncertain[9–12]. Therefore, investigations on structure–activity of cationic lipids could reveal the important insights into the correlation between structure, efficiency and toxicity. Hence, the complications involved in the transfection pathway can be simplified. However, in many studies superior cationic lipids have additionally designed by understanding the structure activity correlation and their mechanism. This dictates the formation as well as function of newly developed lipid formulations for clinical application[13–15].

Development of novel gene carriers having less cytotoxicity and efficient gene transfection for effective and safe gene delivery is a major challenge. The efficiency of gene transfection and cytotoxicity, mainly depends on the molecular structure of genetic vectors. Hence, selection of suitable molecular domains and their linkers is very important in gene therapy to construct highly efficient and low toxic gene vectors[5,16,17]. Vitamin E use as antioxidant is widely reported and has therapeutic use for treating multiple disorders. Moreover, because of solvent capacity and biocompatibility, vitamin E based nano medicines in cancer therapy are developed. Furthermore, due to its serum stability, low toxicity and presence of physiological pathways of tocopherol transport to various tissues including brain from blood lead to

several investigations on systemic delivery applications[22,23]. In recent times, reported the efficiency of α-Tocopherol as delivery system in *in vivo* for the delivery of nucleic acids[15,24]. It is reported from previous studies that, α-tocopherol performed similarly as cholesterol in changing liposome, i.e., making the liposomes highly protein-induced disruption resistant and is found that, this inhibition of protein-induced disruption is more effective with tocopherol compared to cholesterol. Therefore, this made tocopherol-based liposomes more efficient vectors for *in vivo* gene delivery[13,25,26]. Together, impressed by DC-Chol applications and the biological importance of tocopherol inspired us to design, synthesize and evaluate four tocopherol-based cationic derivatives, varying the degree of methylation, AC-Toc (3β-[N-(aminoethane)carbamoyl]tocopherol) hydrochloride), MC Toc (3β-[N-(N'-methylaminoethane)carbamoyl]tocopherol hydrochloride), DC-Toc (3β-[N-(N',N'-dimethylaminoethane)carbamoyl]tocopherol hydrochloride) and TC-Toc (3β-[N-(N', N'N'-trimethylaminoethane)carbamoyl]tocopherol hydrochloride) with high purities were synthesized and compared the transfection potentials with commercially available DC-Chol.

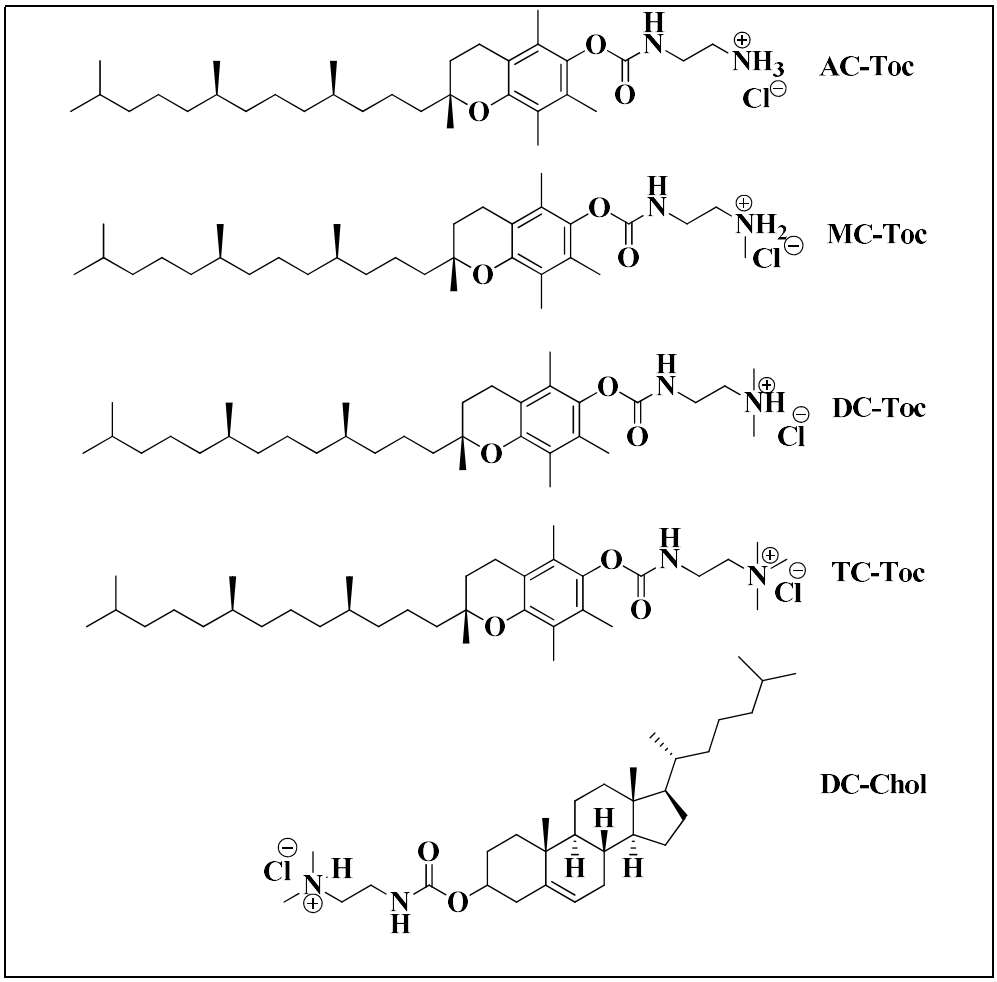

Figure 1. The structures of the synthesized and control cationic lipids.

3.2 Results and Discussion:

In the present study, the four tocopherol-based cationic lipids AC- Toc, MC-Toc, DC-Toc, TC-Toc synthesis and physicochemical characteristics of these lipids viz., size, surface charge and DNA binding abilities were illustrated. Herein, also reported, *in vitro* transfection experiments result of lipoplexes of lipids AC-Toc, MC-Toc, DC-Toc, TC-Toc and DC-Chol performed on four different cell lines viz., hepatic (Hep-G2), neural (NEURO-2a), kidney (HEK-293) and ovary (CHO) cell lines.

3.2.1 Synthesis of lipids:

The molecular structures of the created cationic lipids (AC-Toc, MC-Toc, DC-Toc, TC-Toc) are given in Figure 1. The detailed synthesis process is shown in Scheme 1. As shown in Scheme 1, the alpha-tocopheryl chloroformate was synthesised as previously reported from our laboratory[14]. Alpha-tocopheryl chloroformate was

coupled with ethylenediamine followed by protonation to yield AC-Toc. Alpha-tocopheryl chloroformate was coupled with N-methyl ethylenediamine followed by protonation to yield MC-Toc. Alpha-tocopheryl chloroformate was coupled with N, N-dimethyl ethylenediamine to form an amide derivative. This amide derivative was further treated with HCl to yield DC-Toc and treated with methyl iodide to yield TC-Toc iodide salt. The iodide salts of final lipids were converted to chloride salts by passing repeatedly on to the column containing chloride ion exchange resin, yielded the titled lipid TC-Toc having chloride as counter ion. The structure of the intermediate (I) (Scheme 1) was confirmed by ^{1}H NMR and mass spectra and the final target lipids (Scheme 1) were confirmed by ^{1}H NMR, ^{13}C NMR and ESI-HRMS spectra (supplementary data).

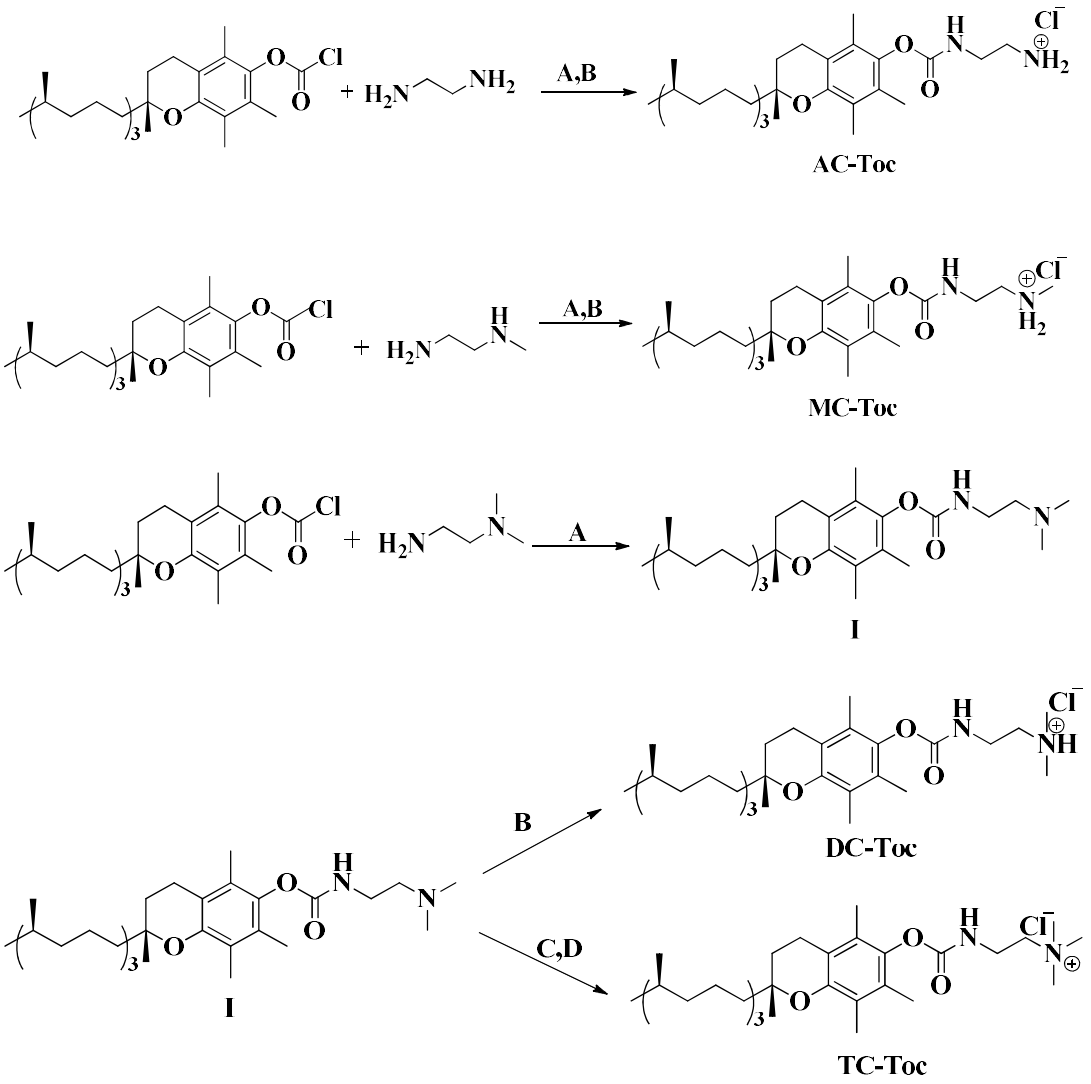

Scheme 1: Synthesis pathway of tocopherol based cationic lipids.

Reagents and conditions: A) Dry DCM, room temp. 24 hrs; B) dry methanol/conc. HCl (1:1), 0°C (1 hrs), 12 hrs room temp; C) methyl iodide, reflex 12 hrs; (D**)** amberlite chloride ion exchange resin.

3.2.2 Preparation of liposomal aggregates:

As mentioned in materials and methods, liposomes can be efficiently made by mixing lipid with DOPE as a co-lipid in a 1:1 molar ratio. DOPE assists in the release of pDNA from the lipoplex by providing the necessary characteristics following endosomal fusion with membranes at low pH[27]. All the liposomes (AC-Toc, MC-Toc, DC-Toc, TC-Toc, and DC-Chol) produced optically transparent and stable water suspensions with no apparent turbidity even after a month of storage at 4°C.

3.2.3 Size and Zeta Potential of the liposomes:

In the approach of physicochemical characterization, a DLS experiment was performed to examine the size and zeta potential of these nano particles suspended in water. This provides the information about their stability, as well as their self-assembly pattern which is used for assessment of transfection potential. The particle diameters (nm) are given in Figure 2A demonstrates of liposomal formulations AC-Toc, MC-Toc, DC-Toc, TC-Toc, and DC-Chol and it was observed that the particle sizes of liposomal formulations were found to be 189 nm, 171.9 nm, 161 nm, 189 nm, and 174 nm, respectively. Hence, all the liposomes had a constant particle size of <200 nm, which aids in the increased entry of lipoplexes into cells through the endocytotic pathway[6]. The zeta potential values of AC-Toc, MC-Toc, DC-Toc, TC-Toc, and DC-Chol liposomal formulations showed moderate to high surface charges, 34.4mV. 36.1mV, 39.3mV, 44.6mV and 49.3mV respectively (Figure 2B).

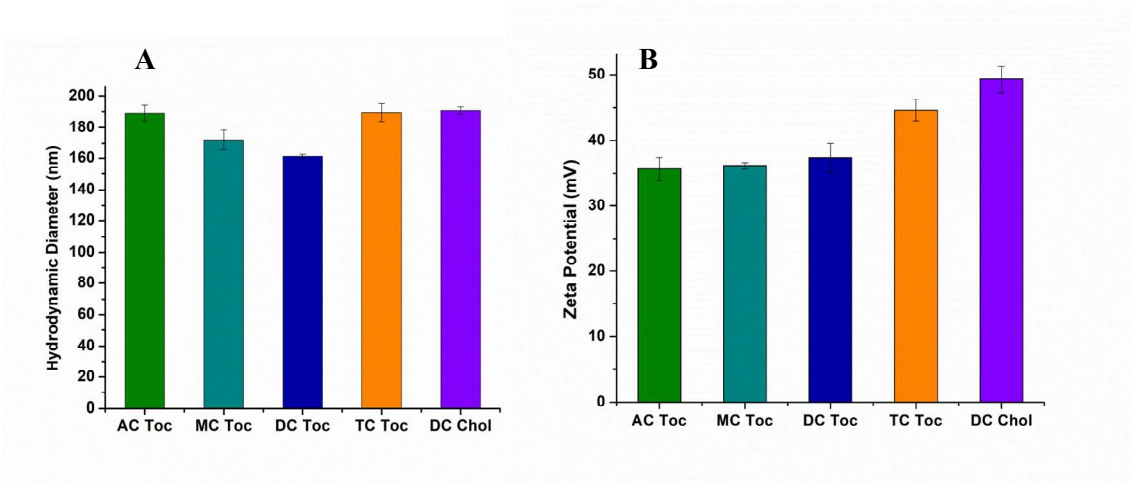

Figure 2. Particle sizes (A) and zeta potential values (B) of different synthesized liposomes

3.2.4 DNA binding assay and Heparin displacement assay:

Effectiveness of gene transfection depends on the electrostatic interactions between liposomes and pDNA[28]. To understand the binding efficiencies of liposomes, gel retardation assay was performed. Using gel retardation electrophoresis experiment, the N/P ratio (1:1, 2:1, 4:1 and 8:1) of lipid/pDNA complex at which the effective binding between lipid and pDNA takes place was determined. It is observed from the Figure 3A that AC-Toc was found to be efficient in binding pDNA even at 1:1 N/P ratio and MC-Toc was found to be efficient in binding pDNA at N/P ratio 2:1. As shown in Figure 3A, TC-Toc, and DC-Chol liposomes were effective at delaying pDNA at a 2:1 N/P ratio for DC-Toc, and at 4:1 and 8:1 N/P ratios, total binding was seen.

To evaluate the above mentioned lipoplexes stability in presence of competing negatively charged molecules, performed the susceptibility of these lipoplexes to heparin displacement. Heparin is one the negatively charged polysaccharides glycosaminoglycans (GAG), which are found in many tissues and also on the cell surface as major components of the extracellular matrix. Monitored the sensitivities of lipoplexes formed with lipids after treatment with heparin displacement indicated the highest stability of lipoplexes formed with lipids. It is observed from the Figure 3B that, the binding efficacies of all the lipoplexes were in coincidence with the gel

retardation assay (Figure 3B). In conclusion, all the lipids were capable of binding to pDNA more reliably.

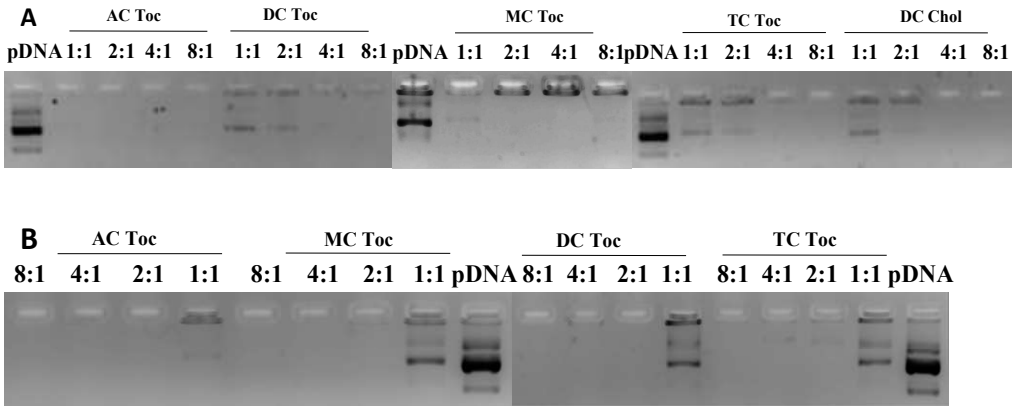

Figure 3. (A) DNA binding patterns of lipoplexes at different N/P ratios of liposome: pDNA on agarose gel electrophoresis. (B) Heparin-displacement assay of various liposomes associated with pDNA at different N/P ratios.

3.2.5 pDNA transfection:

The qualitative and quantitative analysis of prepared liposomes (1:1, 2:1, 4:1 and 8:1 N/P ratios) with eGFP (enhanced green fluorescent protein) encoded plasmid DNA performed in HEK-293, CHO, Neuro-2a and Hep-G2 cell lines. It was observed from fluorescence microscopy as well as flow cytometry that, 2:1 N/P ratio shows high eGFP expression. The percentage of eGFP positive cells in HEK-293, CHO, Neuro-2a and Hep-G2 cell lines measured at 2:1 N/P ratio using flow cytometry is depicted in Figure 4A, 4B, 4C and 4D respectively. Herein, effective mediation of cell transfection was observed for all the liposomes studied. Specifically, AC-Toc liposomes exhibited superior transfection than MC-Toc, DC-Toc, TC-Toc and the control lipid DC-Chol in all the cell lines studied. In addition, DC-Toc showed better transfection than the control DC-Chol in Neuro-2a and Hep-G2 cell lines, whereas TC-Toc showed least transfection in all cell lines. It is interesting to note that specifically in Cancerous cell lines Neuro-2a and Hep-G2, lipid DC-Toc exhibited greater transfection and TC-Toc has shown almost similar transfection efficiency compared to DC-Chol. Thus, AC-Toc may be considered as an alternative to DC-Chol in liposomal transfections.

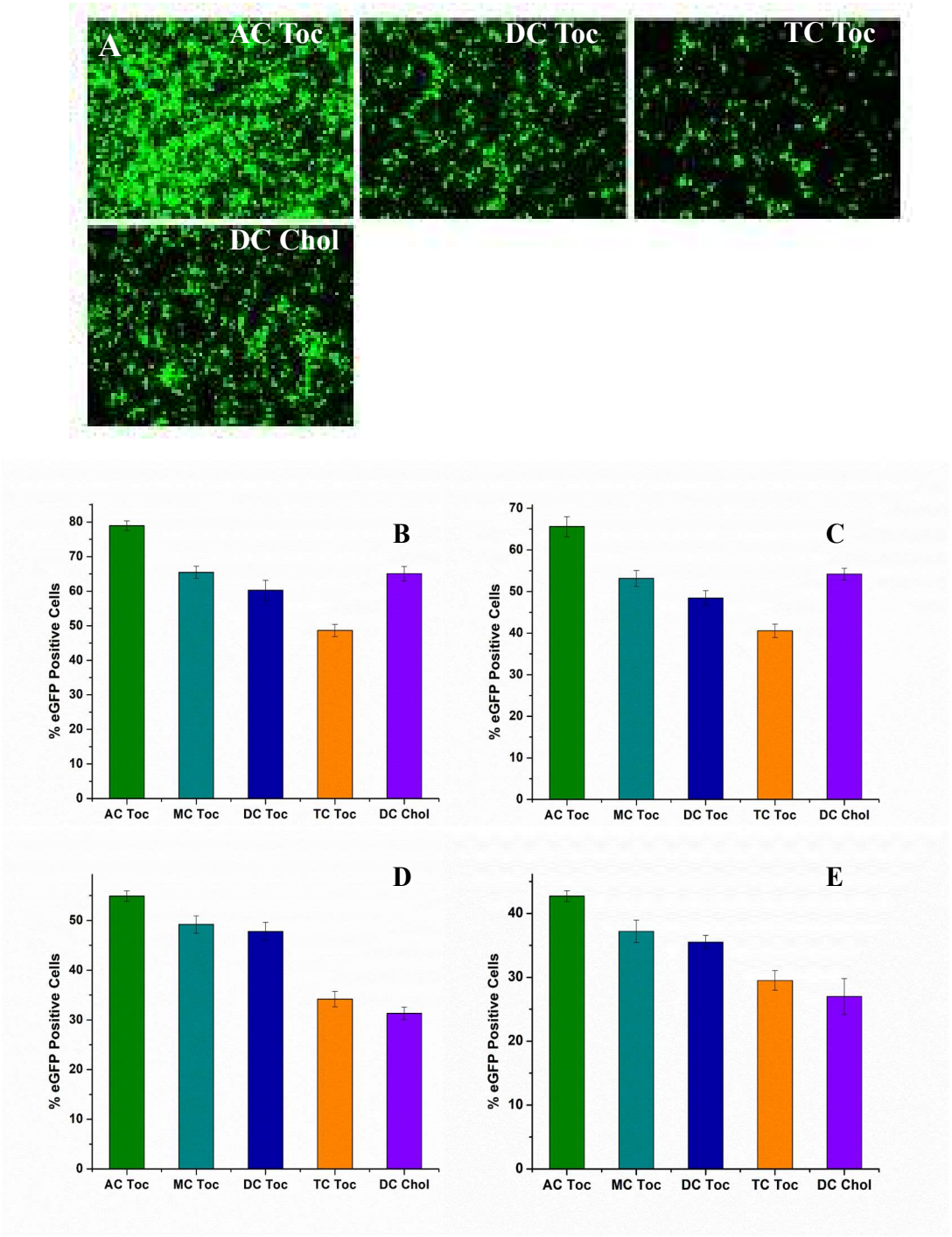

Figure 4. Fluorescent microscopic images and flow cytometry analysis of liposomes with best charge ratio 2:1 in HEK-293 cell line (A). Comparative *in vitro* pDNA transfection efficiencies by flow cytometry in different cell lines at lipid/pDNA 2:1 N/P ratio, HEK-293 (B), CHO (C), Neuro-2a (D), Hep-G2 (E) and cationic lipid DC-Chol was used as positive control.

3.2.6 Determination of the endocytic pathway:

The knowledge of intracellular pathway is important in gene transfection studies[29–31]. The internalization pathway of lipoplexes were studied by using various endocytosis inhibitors at optimised concentrations e.g a clathrin pathway inhibitor, chlorpromazine (CPZ), a caveolae pathway inhibitor Nystatin (NYS), a macropinocytosis pathway inhibitor, amiloride (AML), a caveolae pathway inhibitor, filipin-III (Fil III). The results demonstrated that, for AC-Toc, MC-Toc, DC-Toc and TC-Toc, amiloride inhibitor had less effect on transfection, the macropinocytosis internalization pathway may be ruled out. It is observed that when CPZ inhibitor is used maximum reduction (~70%) of gene expression of these lipoplexes was observed whereas caveolae inhibitors filipin-III, nystatin reduced ~20% of activity, that confirmed that the maximum internalization of these lipoplexes happened at clathrin mediated endocytosis (Figure 5). DC-Chol showed maximum reduction activity by using both chlorpromazine and amiloride which confirms that DC-Chol internalization pathway occurs through both macropinocytosis and clathrin mediated endocytosis. Hence, by changing the hydrophobic moiety can influence the specificity of lipoplexes internalization pathway.

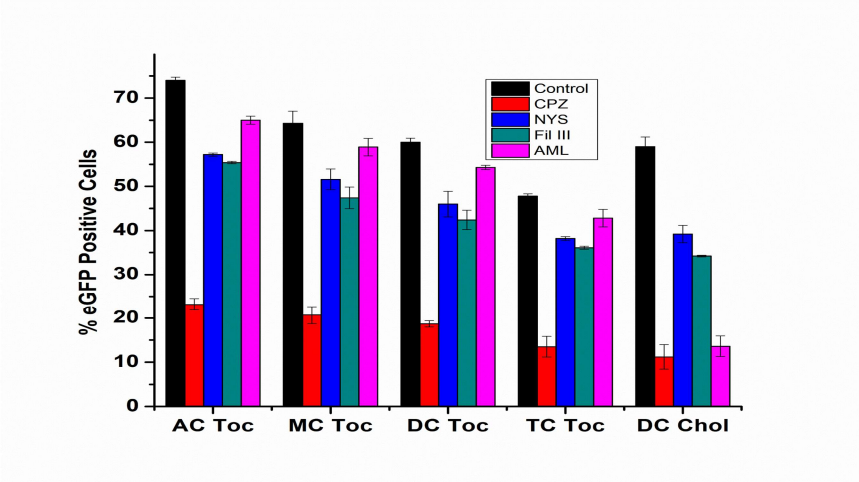

Figure 5. Effect of endocytosis inhibitors on eGFP expression in HEK-293 cell line: % of GFP positive cells were determined using Flow Cytometric analysis after normalization. Cells were pre-treated with the inhibitors (control: black), chlorpromazine (CPZ, red), Nystatin (Nys, blue), Filipin-III (Fil III, dark green) and amiloride (AML, pink) for about 30 min before complex addition.

3.2.7 Anti-oxidant Properties of Lipids:

Reactive oxygen species (ROS) is generated by cells constantly. The generation of ROS leads to oxidative stress in cells, nonspecific protein damage and consequently leading the cell death[32,33]. During transfections, lipid peroxidation and membrane lipid bilayer gets disrupted due to the generation of ROS and leads to cell damage[34]. Hence, to treat the toxicity induced by ROS (reactive oxygen species), development of cationic lipids having antioxidant properties along with transfection potency may be helpful. Previous results demonstrated that α-tocopherol shows better antioxidant properties than cholesterol and it prevents oxidation by two distinct mechanisms such as a free radical scavenging mechanism and a membrane structural mechanism[35,36]. Hence, it is essential to examine the antioxidant potentials of the designed cationic lipids AC-Toc, DC-Toc and TC-Toc. To study the antioxidant potentials of the synthesized lipid through radical scavenger ability, a fluorescence–based assay using DCF-DA was conducted and tested the ability of these lipids in ROS quenching along with DC-Chol as control lipid. N-Acetylcysteine (NAC), a powerful antioxidant was used as a negative control. Hydrogen peroxide (H_2O_2), a ROS inducer was used as a positive control. Results demonstrate that the ROS generation by AC-Toc is lower than DC-Toc, ROS generation by DC-Toc is lower than TC-Toc (Figure 6). However, these three lipids showed less ROS generation than control lipid DC-Chol.

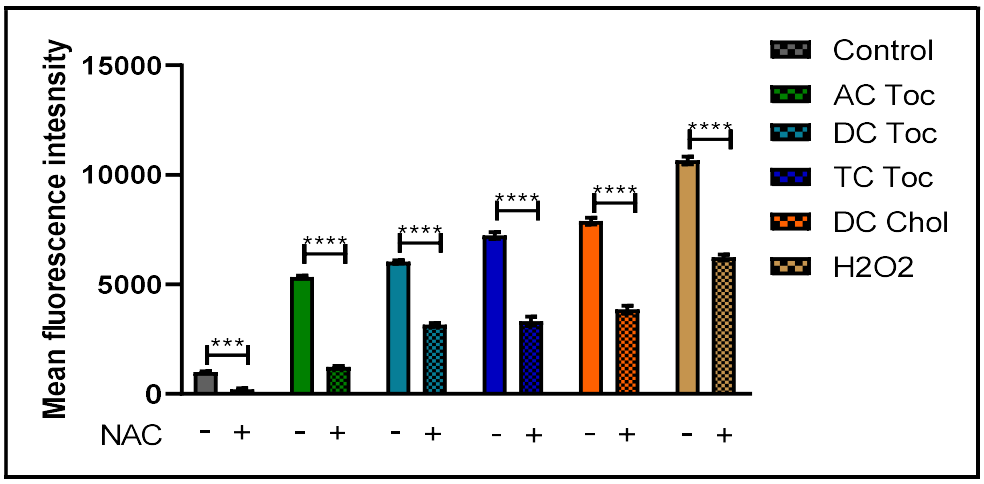

Figure 6. ROS Measurement in HEK-293 cells treated with liposomal formulations. *In vitro assay on* ROS generation was carried out using DCFDA fluorescence dye & measured by flow cytometry.

3.2.8 Cytotoxicity study of lipids:

Another important feature that increases the probability of a synthetic gene delivery vector being used in medical gene therapy is its low cytotoxicity. To determine the safety of the synthetic cationic lipids under evaluation, the MTT assay was used.[37] The viability of AC-Toc, MC-Toc, DC-Toc, TC-Toc and DC-Chol lipid/pDNA complexes in HEK-293T and N2a cell lines was examined (Figure 7) at N/P ratios of 1:1–8:1. Cell viability of all the lipid complexes was observed to be maximum at 1:1 and 2:1 lipid: pDNA N/P ratio and slightly decreased at 4:1 and 8:1 lipid: pDNA N/P ratio (Figure 7). It also observed that the cell viability of all the lipids at the transfection efficient N/P ratio 2:1 was minimal. As a result, the mentioned cationic lipids are potential transfection reagents with minimal cytotoxicity, which is an important feature for *in vitro* applications.

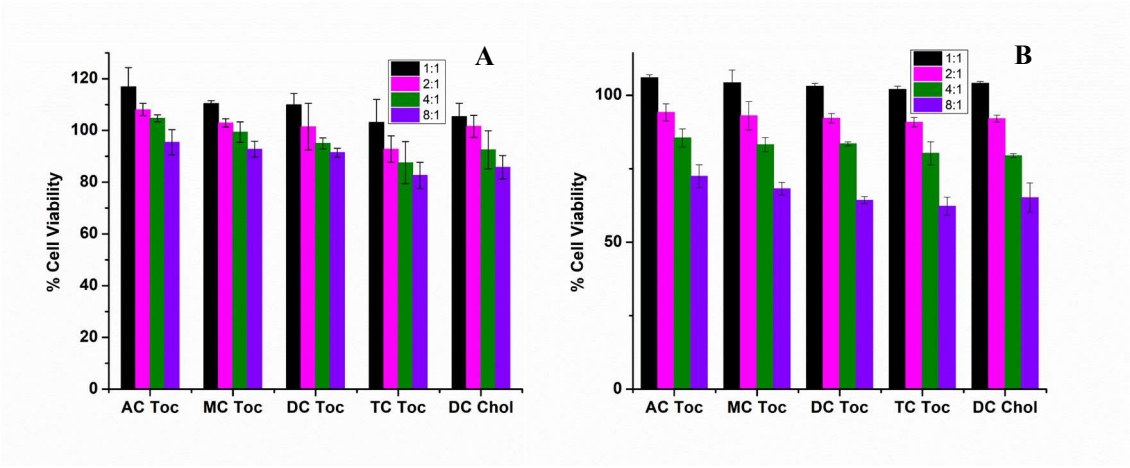

Figure 7. % cell viability of AC-Toc, DC-Toc, TC-Toc and DC-Chol lipoplexes at different N/P ratios in HEK-293 (A), Neuro-2A (B) cell line.

3.3 Conclusions:

The four cationic lipids with tocopherol moieties employed in this present investigation vary with increasing degrees of methylation on their head group. Hence, we observed remarkable differences in performances of these vectors in delivering the gene. The results of this study emphasize that, the cellular interactions of these four cationic lipids varied dramatically, though they have similarities in physicochemical properties and their interaction with pDNA. AC-Toc liposome is promising candidate for pDNA delivery than MC-Toc, DC-Toc, TC-Toc and control DC-Chol in all cell

lines. However, MC-Toc and DC-Toc showed better transfection in cancerous cell lines. The endocytic pathway inhibitor assay proved that the pDNA-derived complexes were involved in clathrin-mediated endocytosis during the internalization process. These novel Toc-lipids have exhibited higher antioxidant property than DC-Chol by generating less ROS, indicating less cytotoxicity. The results from MTT assay proved that, the estimated toxicity of these complexes have low toxicity. In summary, our findings collectively demonstrate that, AC-Toc may be considered as an alternative to DC-Chol in liposomal transfections and these cationic lipids could be more effective, economic, and safer for nucleic acid delivery.

3.4 Experimental Section:

3.4.1 Materials and methods:

Sigma-Aldrich provided high grade alpha tocopherol, ethylenediamine, N-methyl ethylenediamine, N, N- dimethyl ethylenediamine and methyl iodide. Finar Limited provided hydrochloric acid, methanol, DCM (dichloromethane) and solvents for compound purification columns. Avanti polar lipids provided the DC Cholesterol.HCl. Merck's silica gel thin-layer chromatography plates (0.25 mm) were used to track reaction progress. Bruker's AVANCE 400 MHz spectrometer was used to record ^{1}H NMR spectra with $CDCl_3$ as a solvent and TMS as an internal standard. The AVANCE 100 MHz spectrometer from Bruker was used to record ^{13}C NMR spectra. Elemental analyses were carried out utilising an Agilent Q-TOF 6230 and High-Resolution Mass Spectrometry (HRMS). Sigma-Aldrich provided the co-lipid 1,2-dioleoyl-sn-glycerol-3-phosphoethanolamine (DOPE) for liposomal production. The following materials were purchased from Hi-media-India, Thermo Fischer Scientific, and Invitrogen for the biological studies: agarose, 6x loading dye, ethidium bromide, MTT, DMSO, DMEM, PBS, FBS and trypsin-EDTA.

3.4.2 Synthesis of AC-Toc:

A solution of alpha-tocopheryl chloroformate 0.49 g (1 mmol) which is previously prepared by our laboratory in dry DCM (10 mL) was added to ethylenediamine (0.6 g, 10 mmol) in 15 mL of DCM drop wise and stirred for 24 hrs at room temperature. After observing starting materials consumption using TLC, the resulting mixture was transferred to separating funnel using excess DCM and washed with water (2×50 mL) then 50 mL brine. The pooled organic layer was dried by adding

sodium sulphate and the solvent was evaporated on rotary evaporator. The crude product was further purified by column chromatography using 100-200 mesh silica gel, eluting with 3% (v/v) $CH_3OH/CHCl_3$. Subsequently, obtained compound was dissolved in 1 mL of dry methanol and kept in an ice bath for stirring. At 0°C, 1 mL of concentrated HCl was progressively added drop by drop and stirred for 12 hrs. After the starting components were consumed, the solvent was removed by washing three to four times with ethyl acetate and kept it under high vacuum for 3 to 4 hrs**.** Yield: 0.44 g (85 %), (R_f = 0.3, 5% $CH_3OH/CHCl_3$). ^{1}H NMR [*δ*/ppm] (400 MHz, $CDCl_3$) δ 3.48 (s, 2H), 3.10 (s, 2H), 2.50 (s, 2H), 2.13 – 1.97 (m, 9H), 1.71 – 1.65 (m, 2H), 1.55 – 1.06 (m, 24H), 0.86 – 0.83 (m, 12H). ^{13}C NMR [*δ*/ppm] (126 MHz, $CDCl_3$) 156.21, 149.26, 140.48, 127.76, 126.07, 122.87, 117.45, 75.10, 45.57, 40.06, 39.51, 38.88, 37.81, 37.62, 37.60, 37.55, 37.43, 32.93, 32.89, 31.27, 31.20, 29.83, 28.11, 24.95, 24.64, 24.61, 23.44, 22.86, 22.77, 21.18, 20.58, 19.88, 19.81, 19.75, 19.71, 19.70, 19.66, 13.04, 12.21, 11.84. ESI-HRMS *m/z*: calculated: 517.4364, found: 517.4358 $[M]^+$.

3.4.3 Synthesis of MC-Toc:

A solution of alpha-tocopheryl chloroformate 0.49 g (1 mmol) which is previously prepared by our laboratory in dry DCM (10 mL) was added to N-methyl ethylenediamine 0.74 g (10 mmol) in 15 mL of DCM drop wise and was stirred at room temperature for 24 hrs. After observing the starting material consumption using TLC, the resulting mixture was transferred to separating funnel using excess DCM and washed with water (2×50 mL) then 50 mL brine. The collected organic layer was dried on sodium sulphate and the solvent was evaporated on rotary evaporator. Column chromatography (100-200 mesh silica gel) was used to purify the crude product by eluting with 2% (v/v) $CH_3OH/CHCl_3$. Subsequently, obtained compound was dissolved in 1 mL of dry methanol and stirred the mixture at 0 °C by keeping it in an ice bath. At 0 °C, 1 mL of concentrated HCl added drop by drop and stirred for 12 hrs. After the starting components were consumed, the solvent was removed by washing three to four times with ethyl acetate and kept it under high vacuum for 3 to 4 hrs. Yield: 0.41 g (83 %). (R_f = 0.4, 5% $CH_3OH/CHCl_3$) ^{1}H NMR [*δ*/ppm] (400 MHz, $CDCl_3$) δ 3.79 (d, *J* = 12.0 Hz, 2H), 3.37 (s, 5H), 2.54 (t, *J* = 4.0 Hz, 2H), 2.0 (m, 9H), 1.73 (m, 2H), 1.55 – 1.04 (m, 24H), 0.87 – 0.83 (m, 12H). ^{13}C NMR [*δ*/ppm] (101 MHz, $CDCl_3$) δ 155.58, 147.89, 147.01, 127.47, 125.62, 122.67, 117.43, 74.55, 46.16,

39.38, 37.50, 37.43, 37.31, 32.80, 29.70, 27.97, 24.81, 24.49, 22.73, 22.64, 21.05, 19.75, 19.69, 19.59, 13.89, 11.77, 11.59. ESI-HRMS *m/z*: calculated: 531.4526, found: 531.4553 $[M]^+$.

3.4.4 Synthesis of compound I:

To a solution of N, N-dimethyl ethylenediamine (0.88 g, 10 mmol) in dry DCM (15 mL), added dropwise a solution of 1.0 g (2.03 mmol) of alpha-tocopheryl chloroformate in dry DCM (10 mL) and stirred the mixture at room temperature for 24 hrs. After the starting material disappearance on TLC, the reaction mixture was taken into a separating funnel with excess DCM, washed with water (2×50 mL) and 50 mL brine. The organic solvent was dried with sodium sulphate and evaporated with rotary evaporator. Column chromatography (100-200 mesh silica gel) was used to purify the crude product by eluting with 2% (v/v) $CH_3OH/CHCl_3$. Yield: 0.91 g (91 %). (R_f = 0.4, 5% CH_3OH/ $CHCl_3$). ^1H NMR [δ/ppm] (400 MHz, $CDCl_3$) 5.68 (s, 1H), 3.30 (dd, J = 12.0, 8.0 Hz, 2H), 2.50 (t, J = 8.0 Hz, 2H), 2.45 (t, J = 8.0 Hz, 2H), 2.23 (s, 6H), 2.00– 1.90 (m, 9H), 1.73 – 1.66 (m, 2H), 1.46 – 0.97 (m, 24H), 0.80 – 0.76 (m, 12H). ESI-HRMS *m/z*: calculated: 544.4604, found: 545.4706 $[M + H]^+$.

3.4.5 Synthesis of DC-Toc:

A solution of 0.45 g of compound I (0.82 mmol) in methanol (1 mL) was taken in RB flask and kept it for stirring in ice bath. At 0 ^oC, 1 mL of concentrated HCl was added slowly drop by drop and continued stirring for 12 hrs. After consumption of substrate, the solvent was removed by giving 3 to 4 times ethyl acetate washings and kept it for high vacuum about 3 to 4 hrs. Yield: 0.39 g (86 %). ^1H NMR [δ/ppm] (400 MHz, $CDCl_3$) 3.71 (t, J = 4.0 Hz, 2H), 3.33 (s, 2H), 2.91 (s, 6H), 2.56 (s, 2H), 2.06 (s, 9H), 1.74 (s, 2H), 1.53 – 1.07 (m, 24H), 0.85 (t, J = 4.0 Hz, 12H). ^{13}C NMR [δ/ppm] (101 MHz, $CDCl_3$) 155.60, 149.28, 140.31, 127.41, 125.69, 122.87, 117.31, 75.04, 58.30, 57.98, 44.34, 40.20, 40.16, 39.37, 37.57, 37.45, 37.40, 37.28, 36.84, 32.78, 32.72, 31.11, 29.69, 27.97, 24.81, 24.45, 23.83, 22.74, 22.64, 21.04, 20.58, 19.76, 19.69, 19.65, 19.59, 13.11, 12.29, 11.80. ESI-HRMS *m/z*: calculated: 545.4677, found: 545.4682 $[M]^+$.

3.4.6 Synthesis of TC-Toc:

0.45 g (0.82 mmol) of compound (I) taken in methyl iodide was (1 mL) in a sealed tube and stirred for 12 hrs on reflex condition. Monitored TLC to show the consumed starting materials and the obtained final TC-Toc iodide salt was exposed to "repeated chloride ion exchange chromatography" using chloride ion exchange resin (Amberlite A-26) and by eluting with chloroform (approx. 100 mL) as eluent to yield the final product (TC-Toc). Yield: 0.38 g (84 %). ^{1}H NMR [δ/ppm] (400 MHz, $CDCl_3$) δ 4.00 – 3.92 (m, 4H), 3.48 (s, 9H), 2.59 (t, J = 8.0 Hz, 2H), 2.09 – 2.01 (m, 9H), 1.82 – 1.73 (m, 2H), 1.58-1.10 (m, 24H), 0.89-0.86 (m, 12H). ^{13}C NMR [δ/ppm] (126 MHz, $CDCl_3$) δ 156.27, 149.46, 140.03, 127.39, 122.92, 118.17, 75.23, 65.66, 54.79, 39.57, 37.54, 37.24, 36.26, 32.86, 31.26, 29.74, 28.07, 24.86, 24.50, 24.01, 22.70, 21.17, 20.69, 19.82, 13.10, 12.23, 11.94. ESI-HRMS *m/z*: calculated: 559.4833, found: 559.4834 $[M]^+$.

3.4.7 Preparation of Liposomal formulations:

Liposomes were prepared following previous protocol[20]. The final concentrations of TGK with co lipid DOPE and CGK with co lipid DOPE in chloroform were taken at 1:1 molar ratio respectively. 1 mM liposomes were used for *in vitro* studies.

3.4.8 Size Measurements and Zetapotential (ξ):

In order to analyse cationic liposomes made from cationic lipid with co-lipid (DOPE) and complexes created from liposomes with DNA particle size and zeta potential, photon correlation spectroscopy and electrophoretic mobility using a zeta sizer 3000HSA (Malvern, UK) were used. The diameters were calculated in DMEM with a refractive index of 1.59 and a viscosity of 0.89. The instrument was calibrated using a polymer of polystyrene with a 200 nm size (Duke Scientific Corps., Palo Alto, CA). In automatic mode, the sizes of liposomes and lipoplexes were calculated. The zeta potential was calculated using the following variables: viscosity (0.89 cP), dielectric constant (79), temperature (25°C), F (Ka), 1.50 (Smoluchowski), and maximum current voltage (V). The analysis was calibrated using the Malvern DTS0050 standard, with the average of three measurements of three different values and the zero-field correction size.

3.4.9 DNA-binding assay and Heparin displacement assay:

An agarose gel retardation assay was used to test the DNA binding properties of the improved cationic co-liposomal formulations (lipid/DOPE, 1:1). In following experiment, 500 ng of pCMV-gal was complexed with each cationic formulation in 1x PBS (24 µL) at four different N/P (liposome/plasmid) charge ratios of 1:1, 2:1, 4:1 and 8:1. Followed by prepared complexes incubated for 30 minutes. After adding 6x loading dye to the sample, these complexes (12 µL each) were loaded into a freshly prepared 1% agarose gel dyed with EtBr. In a 100 V electrophoresis chamber, electrophoresis was performed for 35 minutes in 1x TAE running buffer. The gel photos were captured in transmillumination mode using a gel documentation system.

The lipoplexes were made as described in the previous section in order to conduct the heparin displacement assay, and they were then incubated for an additional 20 minutes. Following the incubation time, 0.5 µL of 1 mg/mL sodium salt of heparin was added and incubated for an additional 30 minutes. Using a gel documentation equipment, DNA bands were observed.

3.4.10 pDNA Transfection Biology:

Fluorescence microscopy and flow cytometry were used to qualitatively and quantitatively assess the cationic lipoplexes' ability to produce eGFP. In an incubator with 5% CO2 at 37°C, cells were cultured in DMEM with 10% FBS. At least 12 hours before the transfection studies, cells were planted in a 48-well plate at a density of 25000/well (for HEK-293, CHO, N2a, and HepG2). In serum-free media, lipoplexes were created using pDNA (0.4 µg) and the liposomes of AC-Toc, DC-Toc, TC-Toc, and DC-Chol at a final volume of 40 µL and incubated for 30 min at room temperature. After adding the produced lipoplexes to the cells in 10% serum medium, the incubation was carried out for 36–48 hours in a CO2 incubator. The reporter gene activity was then calculated using a previously described procedure[37].

3.4.11 Determination of the endocytic pathway:

HEK-293 and neuro-2a cell lines for seeded on 24 well plate a day before the transfection. For transfection using endocytosis inhibitors, cells were pre-treated with chlorpromazine (10 µg mL^{-1}), Nystatin (80 µM), amiloride (400 µM) and filipin-III (10 µg mL^{-1}) individually for 30 minutes in plain DMEM. After the medium was taken

out, 10% foetal bovine serum and 1% penicillin-streptomycin were added. Consequently, lipoplexes were added to cells, and they were subsequently incubated at 37°C with 5% CO2. The cells were trypsinized and collected in 10% FBS-containing PBS after being incubated with lipoplexes for 36 to 48 hours, and then analysed using FACS.

3.4.12 Evaluation of ROS levels:

The method of 2',7'-dichlorodihydro fluorescein diacetate (DCF-DA) was used to generate intracellular ROS. A day before the transaction, HEK-293 cells were planted into a 24 well plate. Following that, N-Acetylcysteine- and N-Acetylcysteine-free lipoplexes (NAC) were used to transfect the cells. Following a 24-hour treatment period, cells were treated for 15 minutes at 37 °C with 10 M DCF-DA before being subjected to flow cytometric quantitative analysis (BDFACS celesta software – BD biosciences).

3.4.13 Cell viability assay:

The lipoplexes formulations were tested for toxicity using the MTT-based assay, which involves the reduction of MTT by feasible cells to produce purple, insoluble formazan granules. Colorimetric analysis counts the number of feasible cells and compares the intensity of the colour to that number. By incubating Neuro- 2a and HEK-293 cells with the prepared lipoplexes for 20 min at room temperature, followed by treating the cells for 24 h at 37°C in 10% serum-containing DMEM, it was possible to assess the lipid toxicities for lipoplexes made using liposomes and pDNA at varying lipid/DNA charge ratios (1:1−8:1). MTT dye (5 mg/mL) was freshly prepared in serum-free DMEM and 100 L was added to each well after 24 hours of incubation. The test was then stopped after 3 hours of incubation. After that, 100 L of DMSO was added after the media had been taken out of each well. The untreated cells were used as controls. Next, the purple dye was dissolved and detected spectroscopically at 540 nm in a multiplate reader. A540 (treated cells)-background/A540 (untreated cells)-background x 100 was used to compute the % viability.

3.5 References

1 L. Schoenmaker, D. Witzigmann, J. A. Kulkarni, R. Verbeke, G. Kersten, W. Jiskoot and D. J. A. Crommelin, *Int. J. Pharm.*, 2021, 601.

2 M. K. K. Azhagiri, P. Babu, V. Venkatesan and S. Thangavel, *Stem Cell Res. Ther.*, 2021, 12.

3 H. Frangoul, D. Altshuler, M. D. Cappellini, Y.-S. Chen, J. Domm, B. K. Eustace, J. Foell, J. de la Fuente, S. Grupp, R. Handgretinger, T. W. Ho, A. Kattamis, A. Kernytsky, J. Lekstrom-Himes, A. M. Li, F. Locatelli, M. Y. Mapara, M. de Montalembert, D. Rondelli, A. Sharma, S. Sheth, S. Soni, M. H. Steinberg, D. Wall, A. Yen and S. Corbacioglu, *N. Engl. J. Med.*, , DOI:10.1056/nejmoa2031054.

4 M. A. Mintzer and E. E. Simanek, *Chem. Rev.*, 2009, 109.

5 H. Yin, R. L. Kanasty, A. A. Eltoukhy, A. J. Vegas, J. R. Dorkin and D. G. Anderson, *Nat. Rev. Genet.*, 2014, **15**, 541–555.

6 G. Lin, H. Zhang and L. Huang, *Mol. Pharm.*, 2015, **12**, 314–321.

7 S. Bhattacharya and A. Bajaj, *Chem. Commun.*, 2009.

8 M. A. Maslov, T. O. Kabilova, I. A. Petukhov, N. G. Morozova, G. A. Serebrennikova, V. V. Vlassov and M. A. Zenkova, *J. Control. Release*, 2012, **160**, 182–193.

9 D. Zhi, S. Zhang, S. Cui, Y. Zhao, Y. Wang and D. Zhao, *Bioconjug. Chem.*, 2013, 24.

10 K. Shi, J. Zhou, Q. Zhang, H. Gao, Y. Liu, T. Zong and Q. He, *J. Biomed. Nanotechnol.*, 2015, **11**, 382–391.

11 B. K. G. Theng, 2012, **4**, 319–337.

12 Y. Zhao, S. Zhang, Y. Zhang, S. Cui, H. Chen, D. Zhi, Y. Zhen, S. Zhang and L. Huang, *J. Mater. Chem. B*, 2015, **3**, 119–126.

13 D. Zhi, S. Zhang, B. Wang, Y. Zhao, B. Yang and S. Yu, *Bioconjug. Chem.*, 2010, **21**, 563–577.

14 R. S. Y. Wong and A. K. Radhakrishnan, *Nutr. Rev.*, 2012, **70**, 483–490.

15 N. Duhem, F. Danhier and V. Préat, *J. Control. Release*, 2014, 182, 33–44.

16 Q. Liu, Q. Q. Jiang, W. J. Yi, J. Zhang, X. C. Zhang, M. B. Wu, Y. M. Zhang, W. Zhu and X. Q. Yu, *Bioorganic Med. Chem.*, 2013, **21**, 3105–3113.

17 B. Kedika and S. V. Patri, *J. Med. Chem.*, 2011, **54**, 548–561.

18 B. Kedika and S. V. Patri, *Bioconjug. Chem.*, , DOI:10.1021/bc2004395.

19 V. Muripiti, B. Lohchania, V. Ravula, S. Manturthi, S. Marepally, A. Velidandi and S. V. Patri, *New J. Chem.*, 2021, **45**, 615–627.

20 V. Ravula, V. Muripiti, S. Manthurthi and S. V. Patri, *ChemistrySelect*, 2021, **6**, 13025–13033.

21 S. Patil, Y. G. Gao, X. Lin, Y. Li, K. Dang, Y. Tian, W. J. Zhang, S. F. Jiang, A. Qadir and A. R. Qian, *Int. J. Mol. Sci.*, , DOI:10.3390/ijms20215491.

22 D. A. Medvedeva, M. A. Maslov, R. N. Serikov, N. G. Morozova, G. A. Serebrenikova, D. V. Sheglov, A. V. Latyshev, V. V. Vlassov and M. A. Zenkova, *J. Med. Chem.*, 2009, **52**, 6558–6568.

23 J. C. Rea, R. F. Gibly, A. E. Barron and L. D. Shea, *Acta Biomater.*, 2009, **5**, 903–912.

24 V. Muripiti, B. Lohchania, S. K. Marepally and S. V. Patri, *Medchemcomm*, 2018, **9**, 264–274.

25 M. Jiang, L. Gan, C. Zhu, Y. Dong, J. Liu and Y. Gan, *Biomaterials*, 2012, **33**, 7621–7630.

26 H. M. Aliabadi and A. Lavasanifar, *Expert Opin. Drug Deliv.*, 2006, **3**, 139–162.

27 K. Wang, X. Yan, Y. Cui, Q. He and J. Li, *Bioconjug. Chem.*, 2007, **18**, 1735–1738.

28 M. Westoby, J. Chrostowski, P. De Vilmorin, J. P. Smelko and J. K. Romero, *Biotechnol. Bioeng.*, 2011, **108**, 50–58.

29 C. E. Ashley, E. C. Carnes, K. E. Epler, D. P. Padilla, G. K. Phillips, R. E. Castillo, D. C. Wilkinson, B. S. Wilkinson, C. A. Burgard, R. M. Kalinich, J. L. Townson, B. Chackerian, C. L. Willman, D. S. Peabody, W. Wharton and C. J. Brinker, *ACS Nano*, 2012, **6**, 2174–2188.

30 M. Rajesh, J. Sen, M. Srujan, K. Mukherjee, B. Sreedhar and A. Chaudhuri, *J. Am. Chem. Soc.*, 2007, **129**, 11408–11420.

31 C. M. Lamanna, H. Lusic, M. Camplo, T. J. Mcintosh, P. Barth and M. W. Grinstaff, .

32 P. Gao, W. Pan, N. Li and B. Tang, *ACS Appl. Mater. Interfaces*, 2019, **11**, 26529–26558.

33 Y. Zhao, T. Zhao, Y. Du, Y. Cao, Y. Xuan, H. Chen, D. Zhi, S. Guo, F. Zhong and S. Zhang, *J. Nanobiotechnology*, 2020, **18**, 1–14.

34 T. HE, L. LF, D. GJ, W. WT, C. SC, K. ML, T. R, L. GS and T. MH, *J. Gene Med.*, 2012, **14**, 44–53.

35 T. Takeuchi, J. Montenegro, A. Hennig and M. Stefan, *Chem. Sci.*, 2011, **2**, 303–307.

36 M. E. Davis, J. E. Zuckerman, C. H. J. Choi, D. Seligson, A. Tolcher, C. A. Alabi, Y. Yen, J. D. Heidel and A. Ribas, *Nature*, 2010, **464**, 1067–1070.

37 D. Zhou, C. Li, Y. Hu, H. Zhou, J. Chen, Z. Zhang and T. Guo, *Chem. Commun.*, 2012, **48**, 4594–4596.

38 C. L. Walsh, J. Nguyen, M. R. Tiffany and F. C. Szoka, *Bioconjug. Chem.*, 2013, **24**, 36–43.

3.6 Spectral data

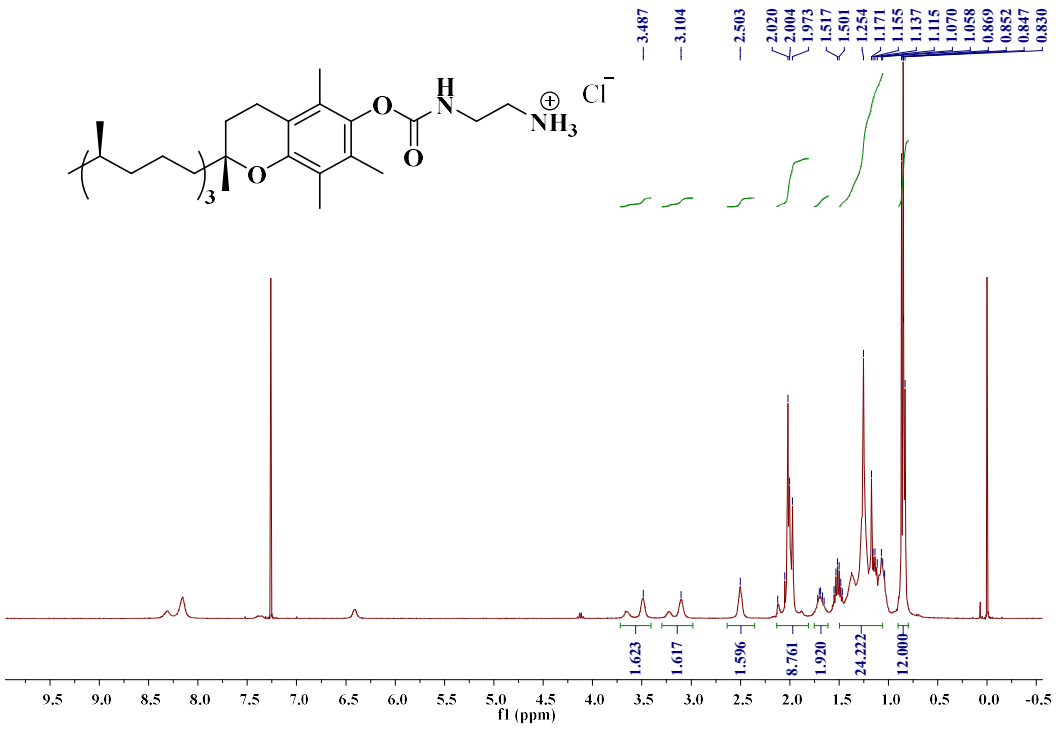

^{1}H NMR Spectrum of **AC-Toc**

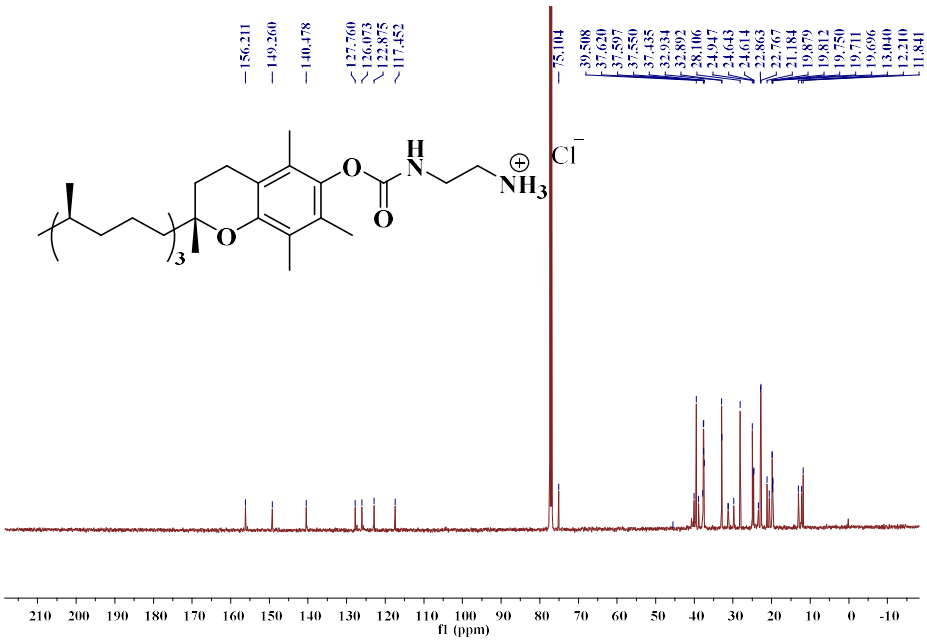

^{13}C NMR Spectrum of **AC-Toc**

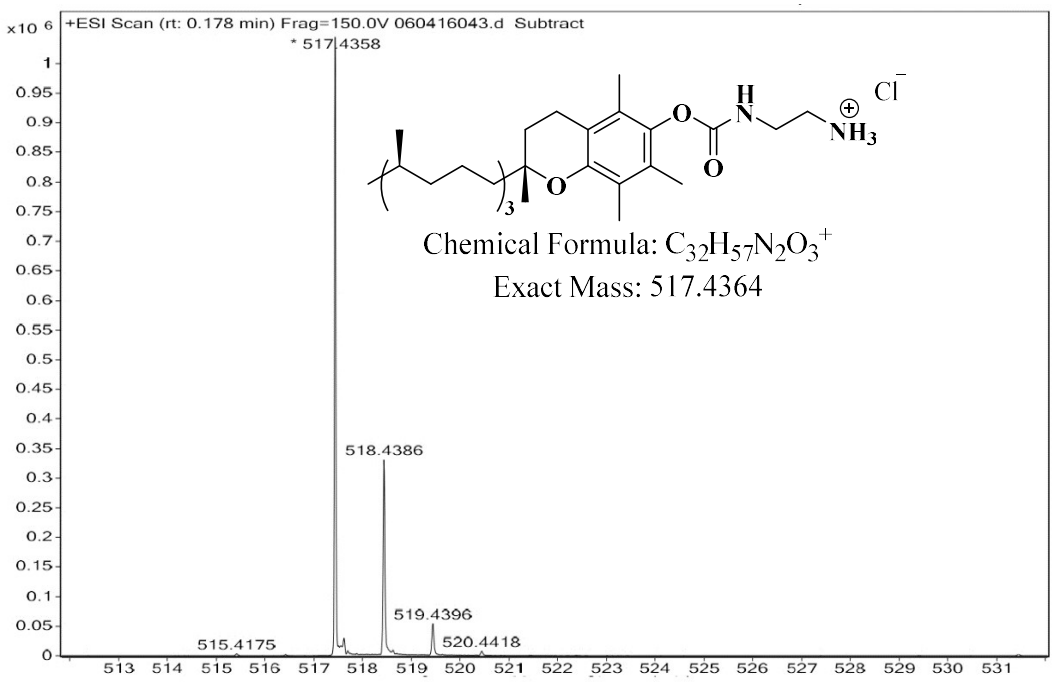

ESI-HRMS Spectrum of **AC-Toc**

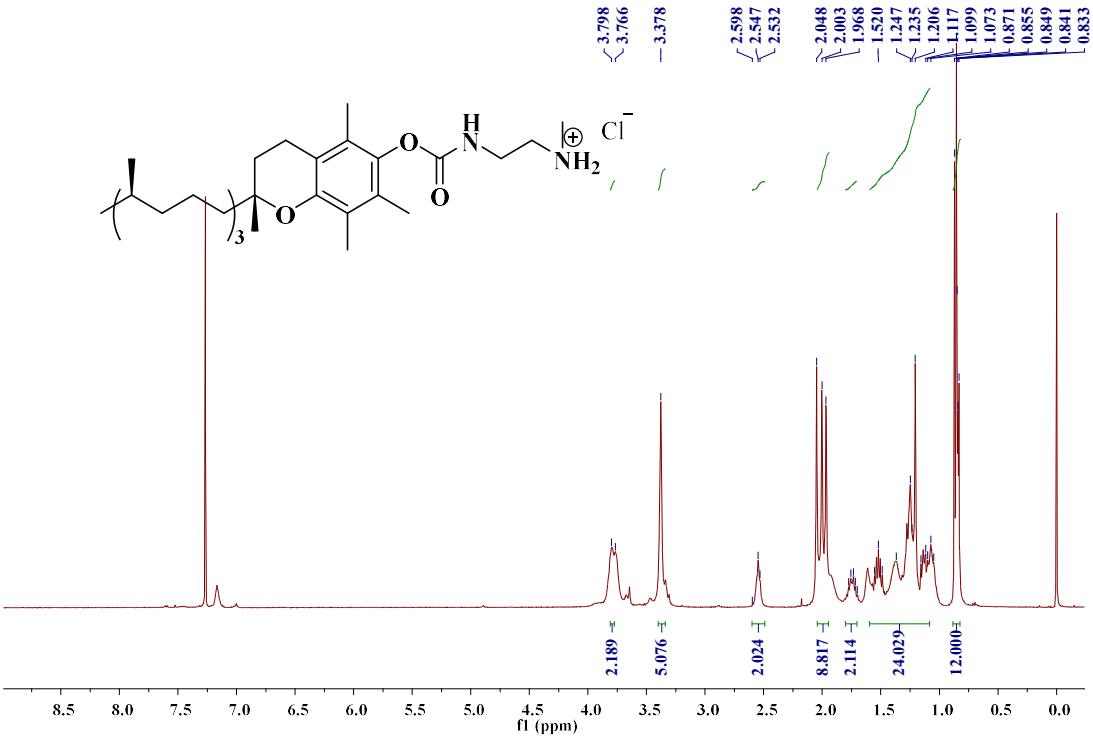

^{1}H NMR Spectrum of **MC-Toc**

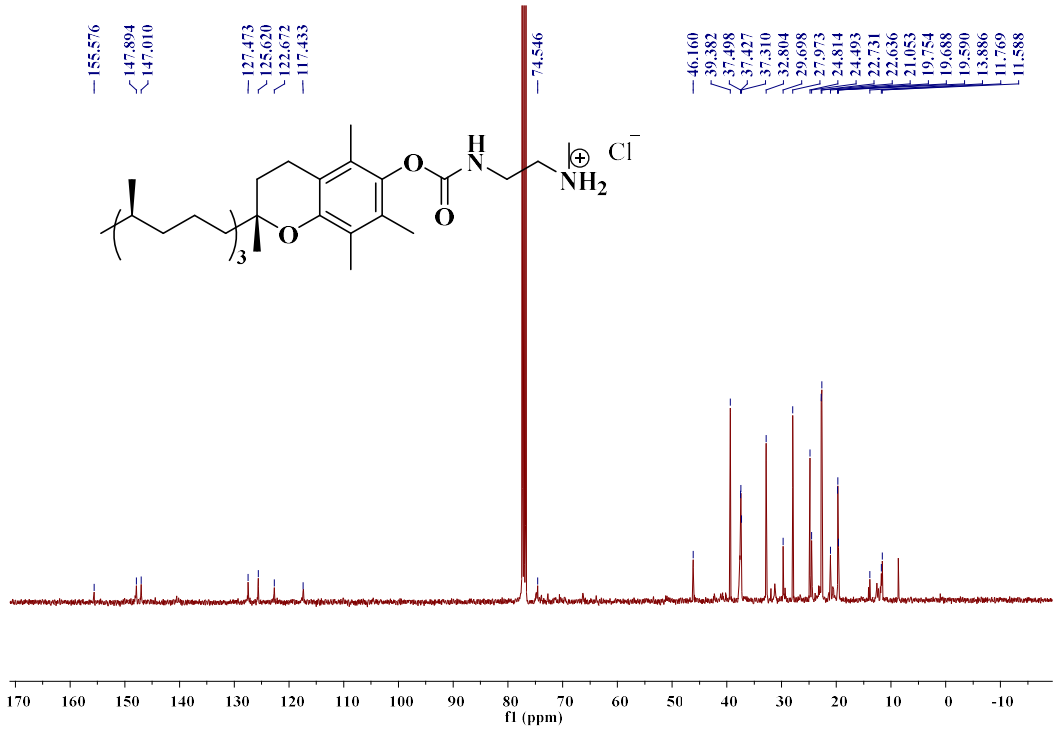

^{13}C NMR Spectrum of **MC-Toc**

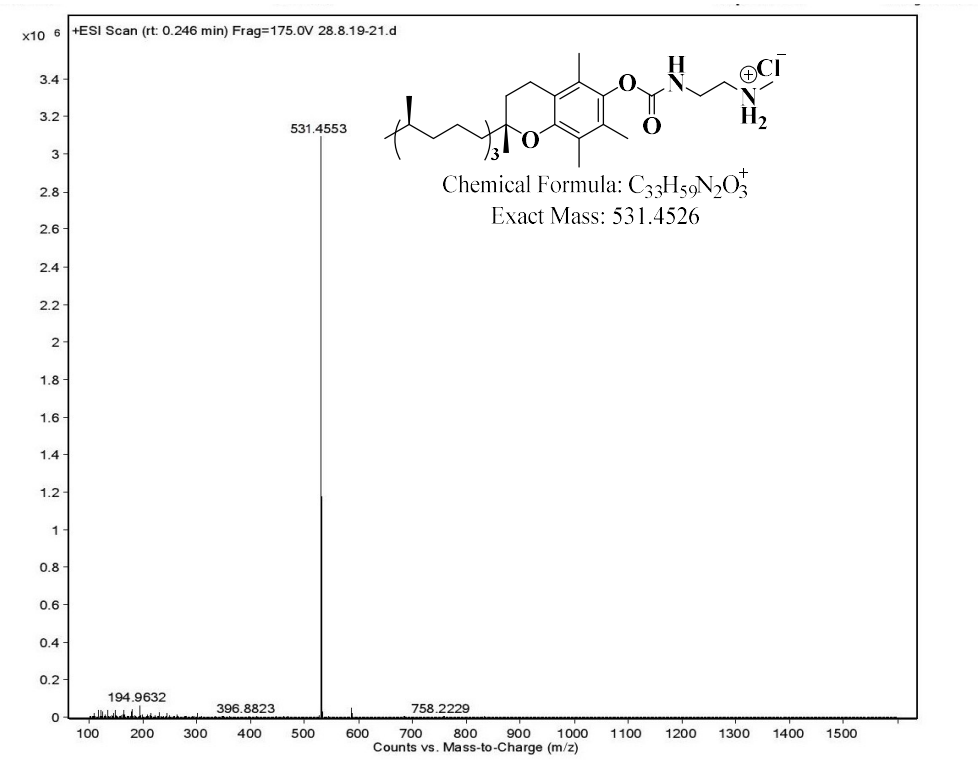

ESI-HRMS Spectrum of **MC-Toc**

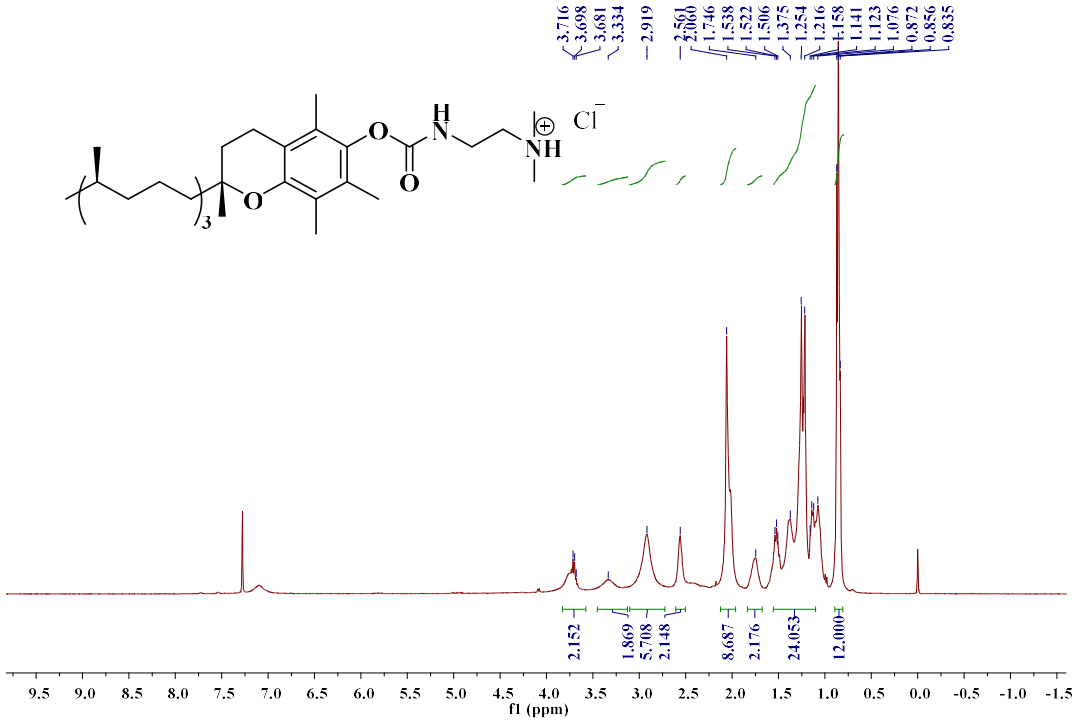

^{1}H NMR Spectrum of **DC-Toc**

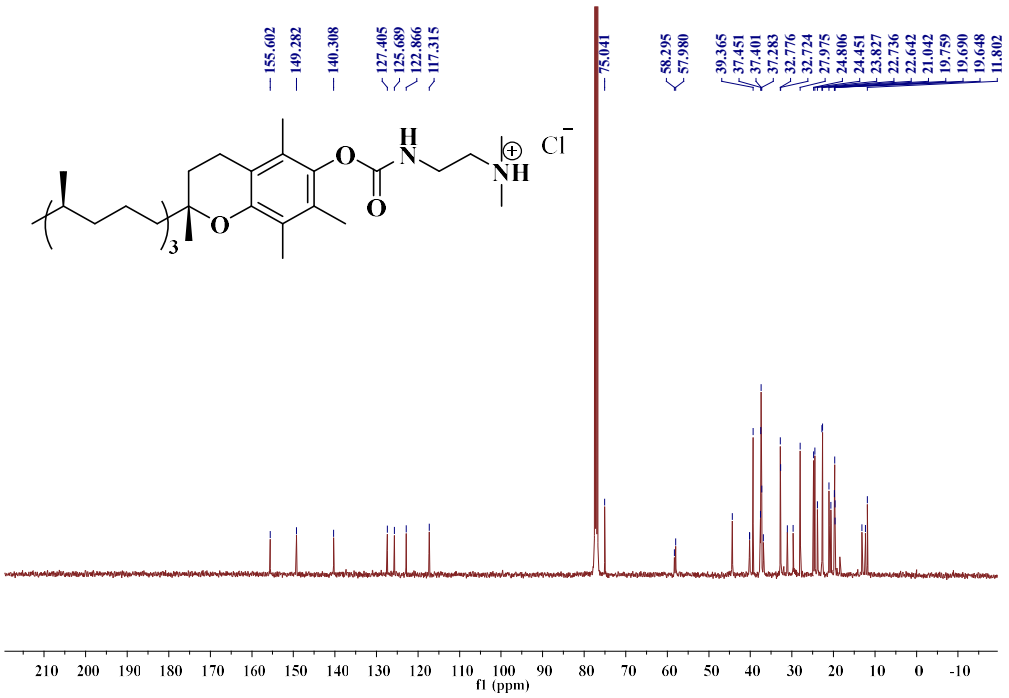

^{13}C NMR Spectrum of **DC-Toc**

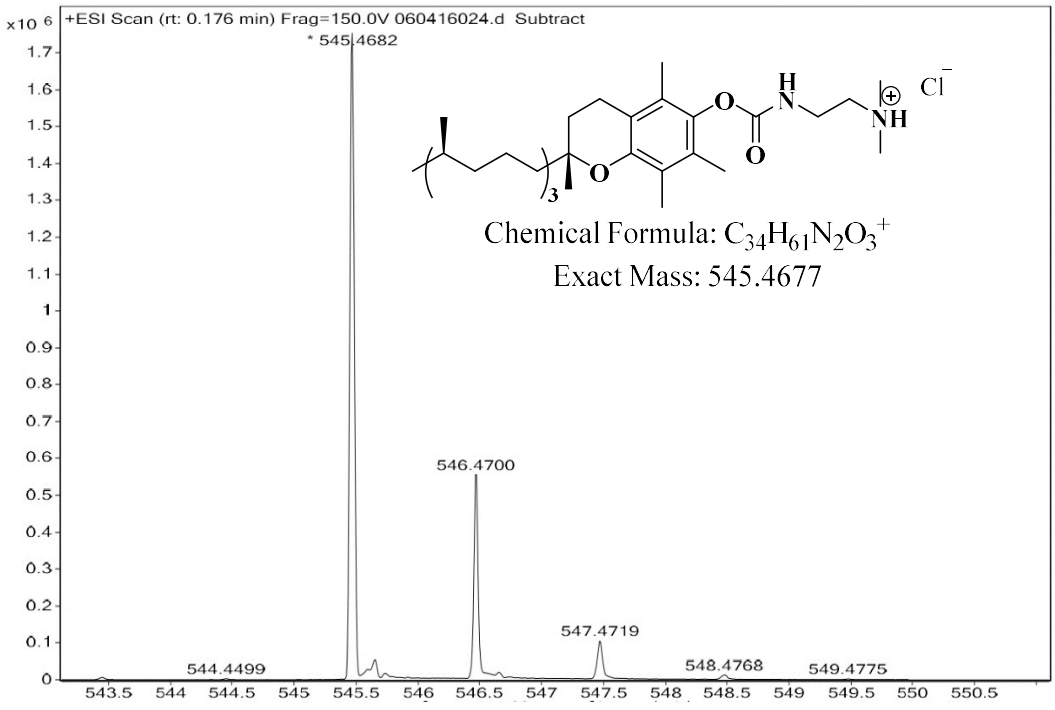

ESI-HRMS Spectrum of **DC-Toc**

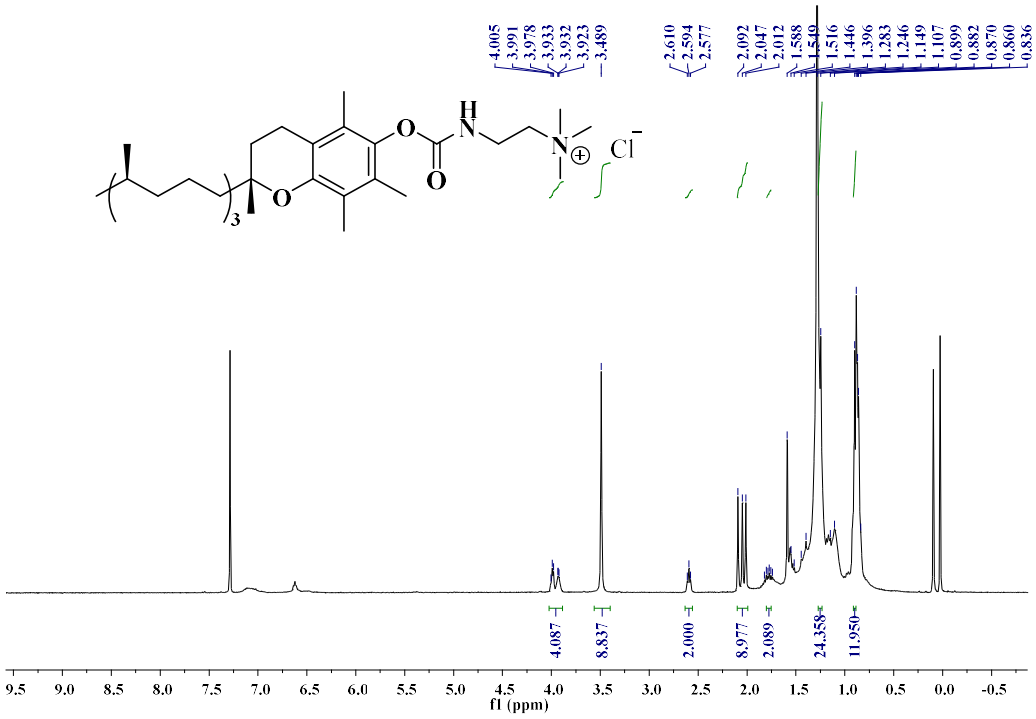

^{1}H NMR Spectrum of **TC-Toc**

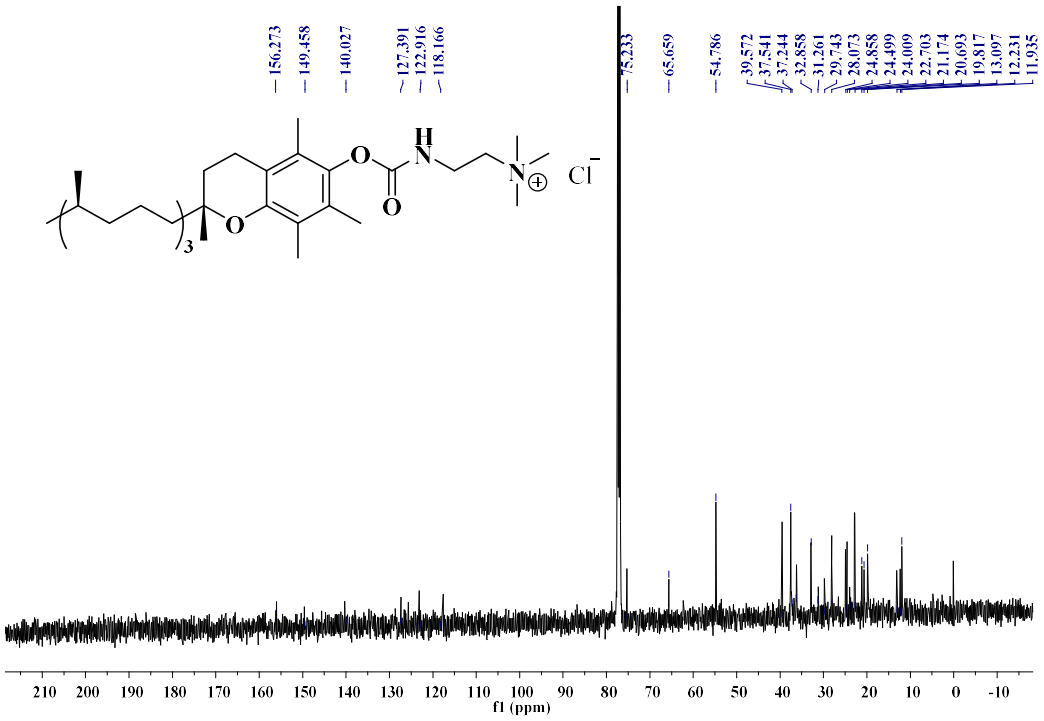

^{13}C NMR Spectrum of **TC-Toc**

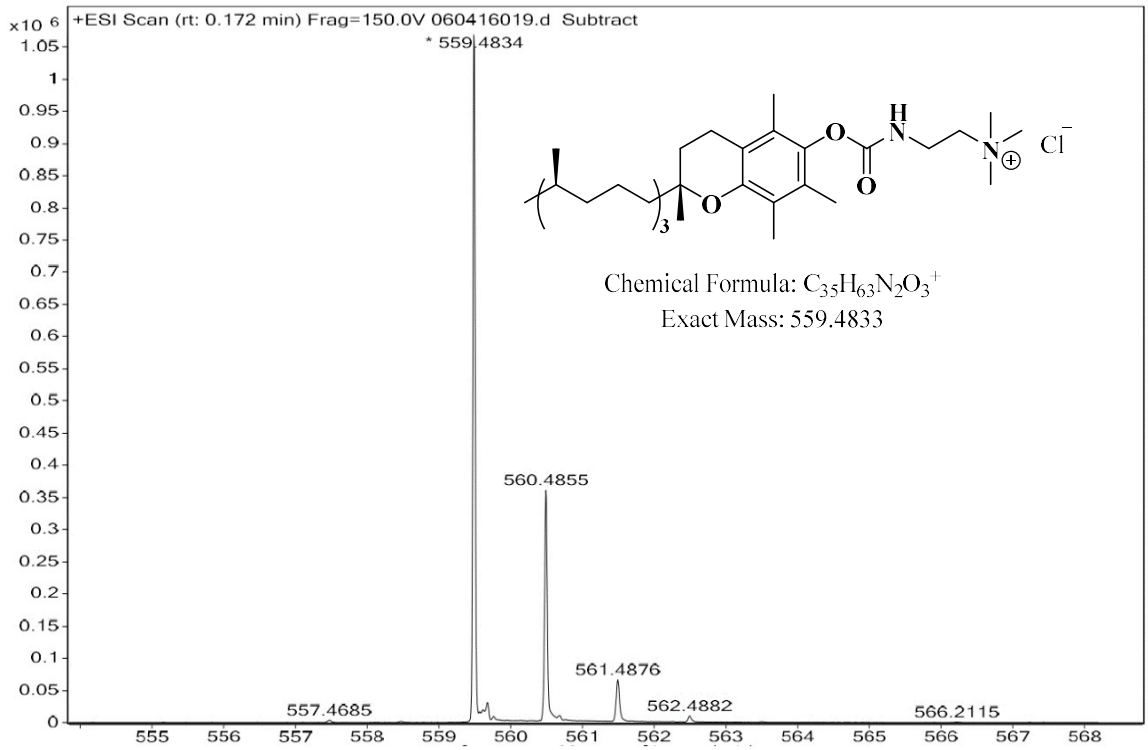

ESI-HRMS Spectrum of **TC-Toc**

CHAPTER IV

Influence of hydrophobic tail on Amino acid based dipeptide cationic lipids for efficient Gene delivery

4.1 Introduction:

Gene therapy has been suggested as a way to treat many different diseases.[4] However, the lack of secure and trustworthy delivery vectors, is one of the biggest challenges to gene delivery.[5] Both viral and non-viral vectors are used for systemic dissemination. More importantly, the synthesis of viral vectors is difficult and expensive. Although viral vectors are much more effective at delivering DNA, their toxicity and hypersensitivity have limited their practical use.[6] Because of this, efficient, less toxic, and biocompatible synthetic vectors are needed for effective and safe nucleic acid delivery. There are constant efforts to create less risky non-viral gene transfer vectors. One of the most promising non-viral vectors for delivering genes via chemical and physical-based non-viral carriers are liposomes.[7] Cationic lipids are amphiphilic chemical compounds with a linker, a hydrophobic backbone, and a hydrophilic head group.[8] Positively charged head-groups are crucial to gene transport because they can combine and attach to nucleic acids using one or more cationic groups.[9] Due to the fact that peptide groups in lipids can lengthen their half-life in vivo and improve targeting[12], the use of biodegradable and biocompatible amino acids or peptides in the head-groups has drawn more attention.[10,11] The hydrophobic backbone is a non-polar component that can form bilayer complexes and interact with biological membranes and may take the shape of a lengthy hydrophobic chain or a steroid. [13] The creation of innovative lipid systems with various structural types is necessary for the integration of enhanced biosynthetic vectors for gene delivery. A well-known antioxidant and a crucial component of human nutrition is tocopherol (Vitamin E). [14] Furthermore, a variety of gene delivery techniques have been developed as a result of the physico-chemical and biological properties of vitamin E derivatives. [15] As a biocompatible hydrophobic tail, tocopherol has traditionally been chemically connected to hydrophilic components. However, recent research by our team and others has shown the potential of novel tocopherol-based cationic lipids for gene transfer. [16,17,18,19,20] Due to its less harmful effect, the cholesterol has also been chosen as the primary hydrophobic domain in cationic lipid gene delivery. [21,22]

Peptide-based cationic lipids gained a lot of interest among these non-viral vectors, because sequences are far more permeable[12,23,24,25]. Peptides and related analogues have been utilized to prohibit cancer cells from migrating, treat acute renal failure, and promote skin regeneration, etc. However, *in vivo*, enzymes efficiently destroy the isolated tiny peptides, and they might be eliminated rapidly.[26,27] Researchers

discovered that adding peptide groups to cationic lipids can extend their half-life *in vivo* and improve their targeting.[28] As a result, peptide-based lipids have outperformed other cationic lipids in terms of biocompatibility, biodegradability, and cell targeting ability, as well as prospective applications in increasing gene therapy delivery.[29,30,31] The flexibility to condense genetic material, preserve it from degradation, and transport it into the cytoplasm with efficacy and accuracy are the essential prerequisites for a successful peptide lipid vector. Furthermore, the liposome/pDNA complex must adhere to the cell membrane, enters into cells by adsorption-mediated endocytosis[32,33,34]. However, there are certain drawbacks to the present peptide-based cationic lipids[35,36]. In this regard, we have designed and synthesized two new di-peptide cationic lipids to make peptide-based lipids easier to apply for gene transfer. Influenced by the earlier studies, Glycine and lysine amino acids were used in di-peptide synthesis[37,38]. Biological importance of tocopherol and cholesterol inspired us to design, synthesize and evaluate two di-peptide cationic derivatives, varying hydrophobic moieties such as tocopherol and cholesterol namely TGK (tocopherol-gly-lys), CGK (cholesterol-gly-lys) and compared the transfection potentials with commercially available reagents.

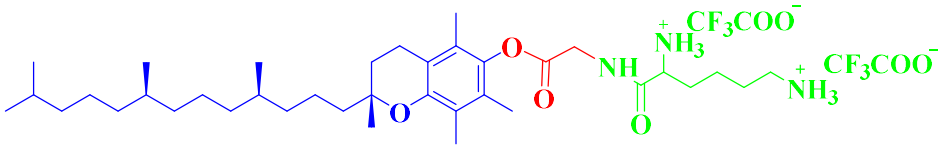

Lipid 1: TGK

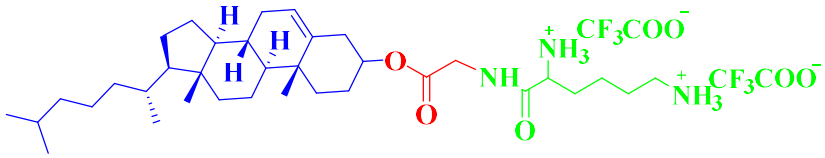

Lipid 2: CGK

Figure 1. Molecular structure of cationic lipids.

4.2 Results and Discussion:

Herein, reported the synthesis as well as physicochemical characterization of two amino acid based tocopherol and cholesterol lipids TGK, CGK. In this study, also reported the transfection efficiencies of these lipids on four cell lines viz., hepatic (Hep-G2), neural (NEURO-2a), kidney (HEK-293) and ovary (CHO) through the results of *in*

vitro transfection experiments carried out. In addition, the potential of these lipids using nucleic acid delivery with CRISPR/Cas9 are described.

4.2.1 Chemistry:

The synthesized cationic lipids with their molecular structures (TGK, CGK) are given in Figure 1**.** The detailed synthesis process is shown in Scheme 1. As shown in Scheme 1, we have designed and synthesized two novel amino acid based cationic lipids by varying hydrophobic moiety (such as α-tocopherol and cholesterol) via biodegradable ester bond linkage were prepared. As demonstrated these cationic lipids TGK and CGK were synthesized using corresponding boc protected amino acids. These boc protected amino acids were coupled with synthesized α-tocopherol and cholesterol amines followed by boc deprotection resulted in Lipid 1, 2. (Scheme 1). ^{1}H NMR and high-resolution mass spectra were used to confirm the structures of intermediates involved in all the reactions carried out and the final lipids.

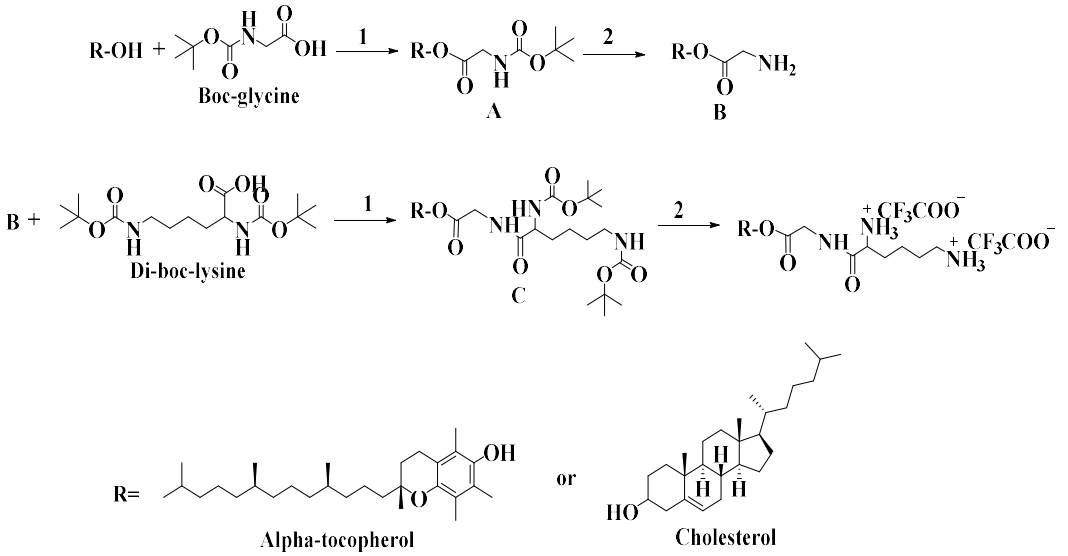

Scheme 1. *Synthesis pathway of Amino acid-based dipeptide cationic lipids*

Reagents & Conditions: (1) EDCI.HCl, HOBt, DIPEA, DCM, 0^{0}C; (2) 1:2 Dry DCM, TFA

4.2.2 Preparation of liposomal aggregates:

As mentioned in materials and methods, liposomes can be efficiently made by mixing lipid with DOPE as a co-lipid in a 1:1 molar ratio. DOPE assists in the release of pDNA from the lipoplex by providing the necessary characteristics following endosomal

fusion with membranes at low pH.[36] The prepared liposomes (TGK and CGK) produced optically transparent and stable water suspensions with no apparent turbidity even after a month of storage at 4°C.

4.2.3 Particle size and zeta potentials:

A rational design of the gene delivery vector in *in-vitro* requires various physicochemical characterizations of liposomes/lipoplexes such as charge of liposomes, it's size and lipid–DNA complexes binding stability. We have prepared liposomes as a first step in order to determine the surface charge and size of liposomes. Lipoplexes were prepared by changing the N/P charge ratios (1:1, 2:1, 4:1 and 8:1) with pDNA to determine DNA binding ability using Gel retardation assay.

The size and zeta-potential of the liposomes were determined by dynamic light scattering (DLS). The size of all the synthesized liposomal formulations as depicted in Figure 2A was nearly <200 nm and all the liposomes were found to be positive. The particle diameter of TGK is found to be 123.48 nm, CGK is 137.2 nm, is as given in Figure 2A. Figure 2B depicts that zeta potentials for TGK and CGK were 25.3 mV and 18.8 mV respectively.

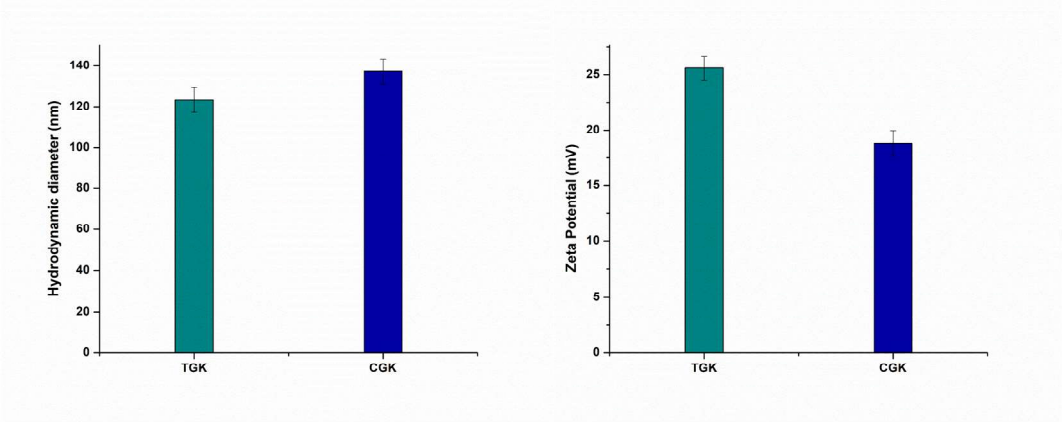

Figure 2. (A) Particle size and (B) Zeta potential values of synthesized liposomes (n=3)

4.2.4 DNA binding studies by Gel Electrophoresis:

DNA binding capacity with liposomes was studied by conventional agarose gel electrophoresis assay at different liposomes to pDNA charge ratios such as 1:1, 2:1, 4:1 and 8:1. Gel retardation assay was used to understand the level of binding capacity of lipids to DNA using Agarose gel electrophoresis. In this, the amount of unbound pDNA was examined by the extent of migration of different ratios of lipoplexes in reference to

free plasmid DNA in agarose gel as shown in Figure 3. It has been observed from Figure 3 that, both TGK and CGK were found to be efficient in binding pDNA at N/P ratio 2:1.

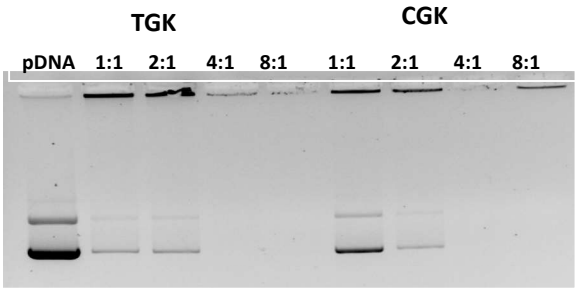

Figure 3. DNA binding patterns of lipoplexes at different ratios of liposomes: pDNA on agarose gel electrophoresis.

4.2.5 pDNA transfection:

The qualitative and quantitative analysis of prepared liposomes (1:1, 2:1, 4:1 and 8:1 ratios) was carried out using enhanced green fluorescent protein (eGFP) encoded plasmid DNA in all afore mentioned cell lines. It was observed from fluorescence microscopy as well as flow cytometry that, lipoplexes exhibited their highest eGFP expression at 2:1 charge ratio. Hence 2:1 charge ratio is considered for further structure activity studies. The fluorescent microscopic images of eGFP expression in Hek 293 cell line transfected with the two lipids synthesized is given in Figure 4A. The percentage of eGFP positive cells in HEK293, CHO, Neuro-2a and Hep G2 cell lines measured at 2:1 ratio using flow cytometry is depicted in Figure. 4B respectively. Herein, we observed that, TGK lipoplex exhibited better transfection than CGK in all the cell lines studied. The transfection potential of TGK is greater than LF 3000, whereas CGK is exhibiting comparable transfection to LF3000 in all the cell lines.

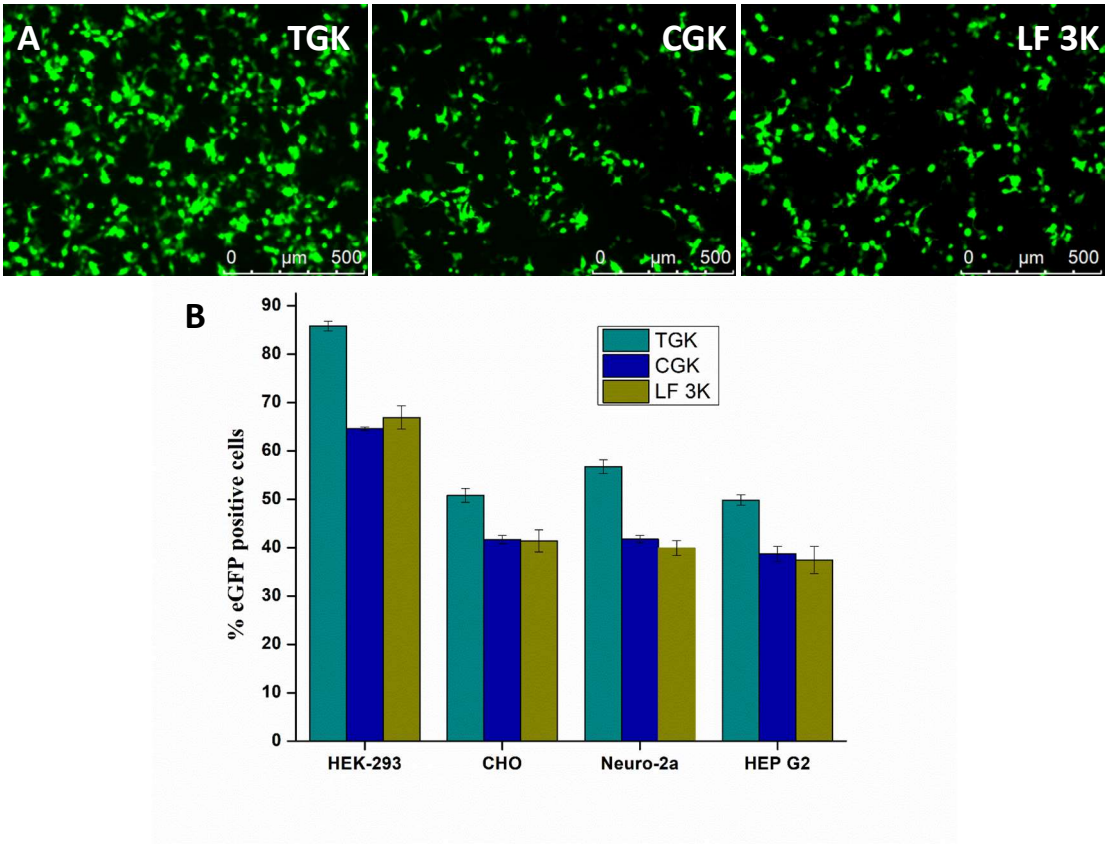

Figure 4. Fluorescent microscopic images and flow cytometry analysis of liposomes with best charge ratio 2:1 in Hek 293 cell line. (A) Comparative *in vitro* pDNA transfection efficiencies by flow cytometry in different cell lines at lipid/DNA 2:1 charge ratio (n=2).

4.2.6 Uptake profile and co-localization:

The escape of gene from endosomal membrane is one of the major barrier for developing the efficient non-viral gene delivery vectors. Hence, estimation of cellular uptake followed by intracellular localization becomes significant. In the current study, internalization of lipoplexes was performed using lipoplexes of Rhodamine-DHPE labelled liposomal formulations of TGK and CGK. The microscopic images as given in Figure 5 from co-localization studies the red fluorescence observed in the left lane of clearly depicts the uptake potency of these lipids. To gain further insight into the endosomal escape potency of the lipids, co-localization studies of lipoplexes of lipids TGK and CGK were performed using lysotracker green to label the lysosomal compartments in Neuro-2a cell lines. The lipoplexes with minimal co-localization in lysosomes represents more efficient in endosomal escape. Rhodamine-labeled liposomal

formulation co-localization investigations' microscopic images are shown in Figure 5 (in the form of lipoplexes). The middle lane shows the lysosomal labelling using lysotracker green. A distinct red fluorescence having no co-localization was observed for TGK formulations and minimal co-localization in case of CGK formulations. Results are in accordance with the results obtained from transfection studies. This suggests that these two lipoplexes may have managed to escape from the endosomes while escaping the lysosomes. These formulations' successful escape from endosomes may have made it easier for the cargo to pass through the endosomal membrane and be transported into the nucleus for final transcription.

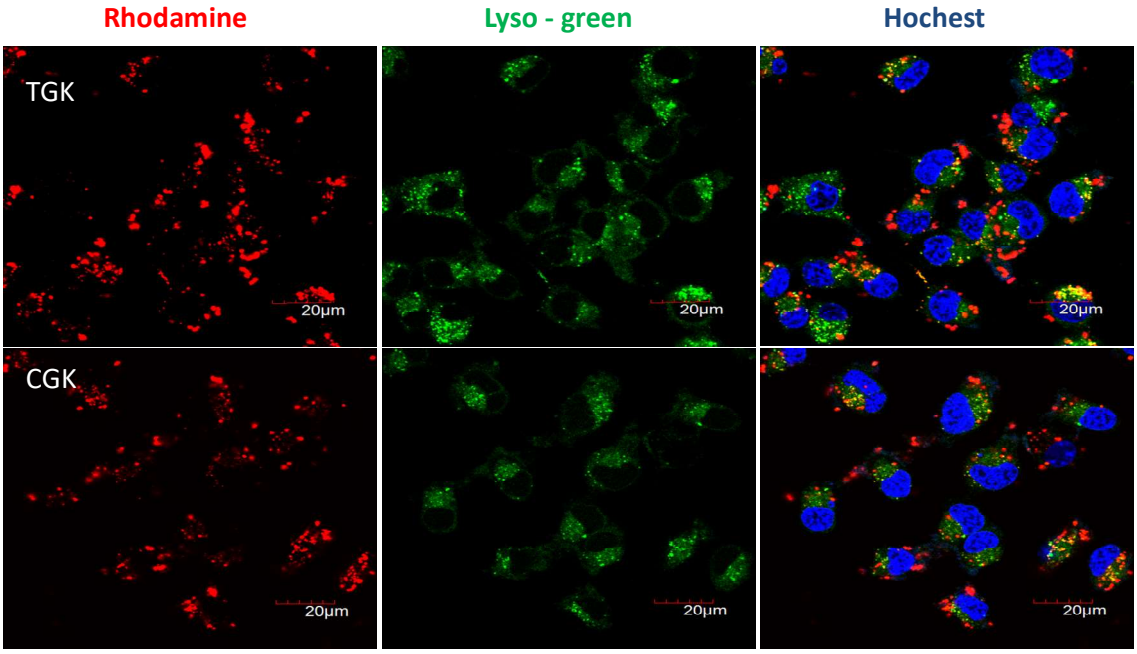

Figure 5. Representative confocal images of cell uptake and localization of lipoplexes at 2:1 N/P in Neuro-2a cells.

4.2.7 Determination of the endocytic pathway:

The knowledge of intracellular pathway is important in gene transfection studies.[37–39] The internalization pathway of lipoplexes were studied by using various endocytosis inhibitors at optimised concentrations e.g a clathrin pathway inhibitor, chlorpromazine (CPZ), a caveolae pathway inhibitor Nystatin (NYS), a macropinocytosis pathway inhibitor, amiloride (AML), a caveolae pathway inhibitor, filipin-III (Fil III). The results demonstrated that, for lipoplexes TGK and CGK amiloride inhibitor had less effect on transfection, the macropinocytosis internalization pathway may be ruled out. It

is observed that when CPZ inhibitor is used maximum reduction (~70%) of gene expression of these lipoplexes was observed whereas caveolae inhibitors filipin-III, nystatin reduced ~20% of activity, that confirmed that, these lipoplexes maximum internalization depends on clathrin coated pits mediated endocytosis (**Figure 6**).

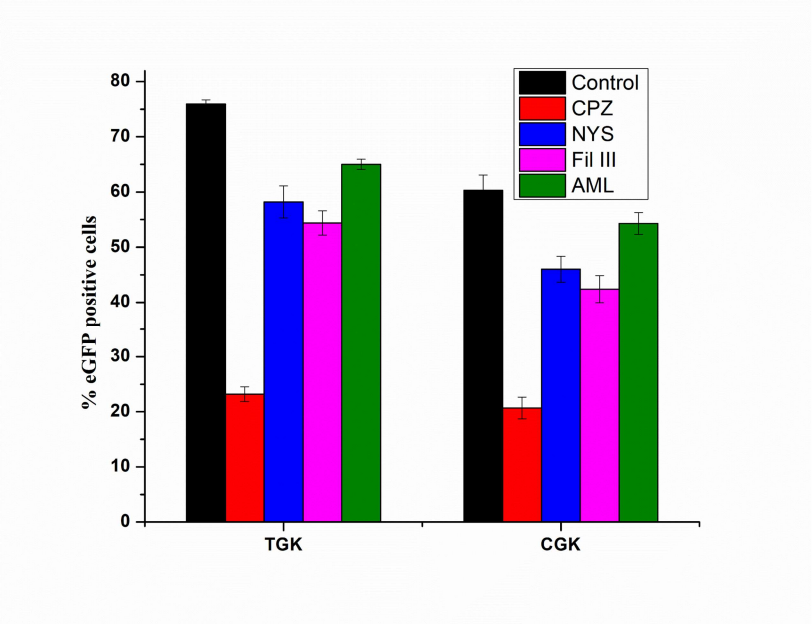

Figure 6. Effect of endocytosis inhibitors on eGFP expression in HEK-293 cell line: % of GFP positive cells were determined using Flow Cytometric analysis after normalization. Cells were pre-treated with the inhibitors (control: black), chlorpromazine (CPZ, red), Nystatin (Nys, blue), Filipin-III (Fil III, pink) and amiloride (AML, dark green) for about 30 min before complex addition.

4.2.8 mRNA transfection:

After achieving the efficient pDNA transfections, further explored the capability of synthesized lipids in delivering the linear, single stranded mRNA nucleic acid. The transfection efficiency of two liposomes was evaluated in Hek-293 cell line by using GFP encoding mRNA. Fluorescent microscopic images of eGFP expression in Hek 293 cell line transfected with the two lipids synthesized is given in Figure 7A. The percentage of eGFP positive cells Hek-293 cell lines measured at 8:1 ratio using flow cytometry is depicted in Figure. 4B. It is observed that the high mRNA transfection efficiency of all the lipid nano-carriers studied is shown at 8:1 charge ratio. The liposomal formulations of

TGK showed comparable potential as commercially available LFmMAX control. Whereas CGK showed moderately less potential when compared to LFmMAX.

In brief, the TGK lipid displayed higher transfection efficiencies for circular pDNA as well as for linear mRNA. The maximum transfection efficiency for pDNA was observed at 2:1 charge ratio, whereas for mRNA it is 8:1. In general, mRNA requires high charge ratios compared to pDNA because of high net negative charge on linear mRNA over low net negative charge on circular pDNA[40].

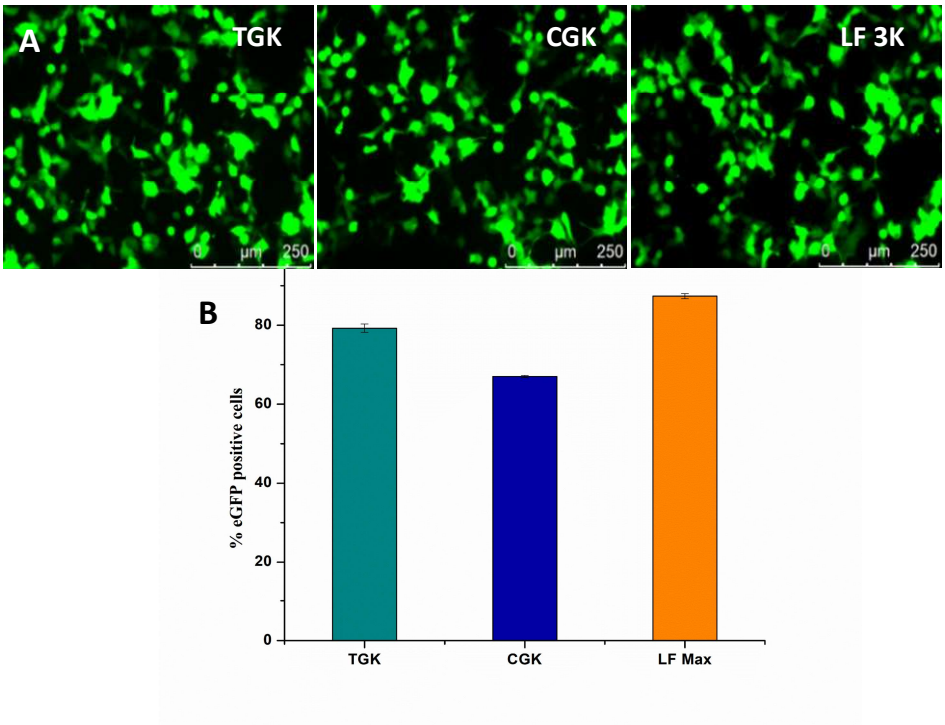

Figure 7. (A) Fluorescent microscopic images of liposomes with best charge ratio 8:1 in Hek-293 cellline. (B) *in vitro* mRNA delivery with cationic lipid carrier systems in Hek 293 (n=2)

4.2.9 CRISPR/Cas9 transfection:

Based on the above positive transfection results, further extended the studies to evaluate the efficiency of synthesized lipids in transfecting with the CRISPR tools. In recent studies, CRISPR/Cas9-encoded pDNA delivery has resulted in development of wide variety of safe and efficient nonviral vectors for gene delivery. CRISPR plasmid was constructed as pL-CRISPR.EFS.GFP (11.7 kb) that expresses both Cas9 protein as well as eGFP protein driven through EFS promoter as a single transcript[41]. Delivery of CRISPR/Cas9 encoded pDNA using viral vectors was reported[42-44]. But there are only a few reports in literature on the use of cationic lipids for delivering CRISPR tools.

The *in vitro* CRISPR/Cas9 pDNA delivery using these liposomes at best charge ratio (2:1) was carried out in Hek-293 cell line. The transfection efficiencies of the two lipid nano-carrier systems in Hek-293 cell line determined by FACS analysis is given in Figure 8. The TGK lipoplex has shown high transfection compared to that of CGK and commercially available LF 3000 control. Moreover, the transfection efficiency of CGK was comparable with that of commercially available LF 3000 respectively.

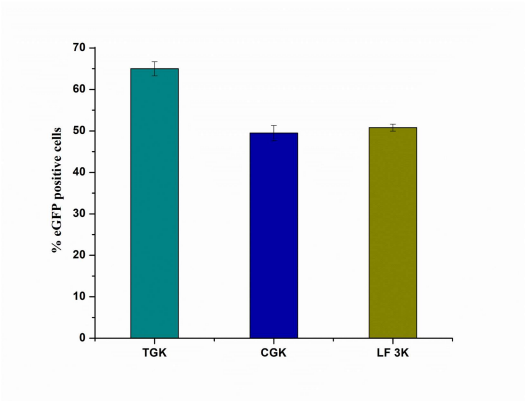

Figure 8. *In vitro* Flow cytometric analysis of CRISPR/Cas 9 pDNA delivery using all the four cationic lipid nanocarrier systems with best charge ratio 4:1 in Hek- 293 cell line.

4.2.10 Cytotoxicity study of lipids:

Another important feature that increases the probability of a synthetic gene delivery vector being used in medical gene therapy is its low cytotoxicity. To determine the safety of the synthetic cationic lipids under evaluation, the MTT assay was used.[45] The viability of TGK and CGK lipid/pDNA complexes in HEK-293 and Neuro-2a cell lines was examined (Figure 9A and Figure 9B respectively) at N/P ratios of 1:1–8:1. Cell viability of all the lipid complexes was observed to be maximum at 1:1 and 2:1 lipid:pDNA N/P ratio and slightly decreased at 4:1 and 8:1 lipid:pDNA N/P ratio . It also observed that the cell viability of all the lipids at the transfection efficient N/P ratio 2:1 was minimal. As a result, the mentioned cationic lipids are potential transfection reagents with minimal cytotoxicity, which is an important feature for *in vitro* applications.

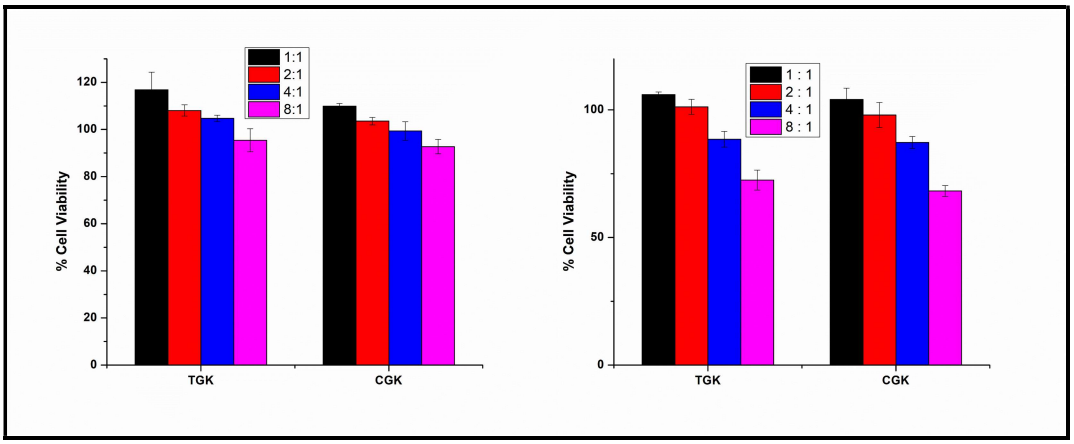

Figure 9. % Cell viability of AC-Toc, DC-Toc, TC-Toc and DC-Chol lipoplexes at different N/P ratios in HEK-293 (A), Neuro-2A (B) cell line

4.3 Conclusions:

The study highlights the delivery of plasmid DNA efficiently using new lipid motifs creates the interest towards development of new synthetic lipid vectors. Co-liposomes with a desirable size and surface charge for transfection were produced by combining cationic lipid formulations with the fusogenic helper lipid DOPE. In comparison to the commercial transfecting reagent, LF 3000, the lipids TGK and CGK had higher and similar transfection efficiencies with plasmid DNA (pDNA) in several cultured cells, respectively. TGK exhibited similar transfection with mRNA in Hek-293 cell line compared with commercial transfecting reagent LFMM. In this study, further demonstrated that the liposomes effectively delivered genome-editing tools having CRISPR/Cas9 encoded with pDNA and showed enhanced efficiency in genome-editing as well. The endocytic pathway inhibitor assay proved that, synthesized lipids were involved in specifically clathrin-mediated endocytosis during the internalization process. In summary, our findings collectively demonstrate that, the designed TGK cationic lipid could be safer, effective and economic for gene delivery and genome-editing tools.

4.4 Experimental Section:

4.4.1 Materials & Methods:

Alpha tocopherol, cholesterol, boc protected amino acids and coupling reagents hydroxy benzotriazole (HOBT), EDCI.HCl were purchased from Sigma-Aldrich. DCC and DMAP were procured from Alfa Aesar and Spectrochem Pvt. Ltd. Trifluoroacetic

acid, solvents as used for reactions and column (compound purification) were obtained from Finar Limited. We bought silica gel thin-layer chromatography plates (0.25 mm) from Merck to track the development of the reaction. A Varian FT400 MHz NMR spectrometer was used to record the ^{1}H and ^{13}C NMR spectrum data. Using a commercial LCQ ion trap mass spectrometer with an ESI source, mass spectral data were obtained (Thermo Finnigan, SanJose, CA, U.S.). Sigma-Aldrich provided the co-lipid 1,2-dioleoyl-sn-glycerol-3-phosphoethanolamine (DOPE) for the synthesis of liposomes. The FBS, PBS, MTT, and trypsin are the ingredients that are employed in all biological experiments. These items were obtained from Thermo Fischer Scientific and Invitrogen.

4.4.2 General procedure of compound A derivatives:

Cholesterol or alpha-tocopherol (2 mmol), N-(tertbutoxycarbonyl) glycine (Boc-glycine, 2 mmol), and DMAP (0.02 mmol) were dissolved in a solution of N,N' -Dicyclohexylcarbodiimide (2.2 mmol) in 10 mL of dichloro methane (DCM). The insoluble precipitate was filtered off and the solvent was removed after being mixed at room temperature for 12 hours to produce a Boc-protected intermediate.

Toc-Boc-Glycine:

The crude Toc-Boc-glycine was further purified by using column chromatography with 100-200 mesh silica gel (Rf = 0.4, 5% CH3OH/CHCl3). 1H NMR (400 MHz, CDCl3) δ 4.00 (s, 2H), 2.53 (t, J = 6.4 Hz, 2H), 2.09 – 1.80 (m, 9H), 1.69 (m, 2H), 1.60 – 0.84 (m, 33H), 0.85 (m, 12H). MS m/z: calculated: 587, found: 610 [M+Na]+.

Chol-Boc-Glycine:

The crude Chol-Boc-glycine was further purified by using column chromatography with 100-200 mesh silica gel (Rf = 0.3, 5% CH3OH/CHCl3). ^{1}H NMR (400 MHz, $CDCl_3$) δ 5.38 (d, *J* = 4.6 Hz, 1H), 4.73 – 4.62 (m, 1H), 3.88 (d, *J* = 5.2 Hz, 2H), 2.33 (d, *J* = 7.6 Hz, 2H), 2.04 – 1.93 (m, 2H), 1.91 – 1.80 (m, 3H), 1.66 – 0.81 (m, 52H), 0.68 (s, 3H). MS *m/z*: calculated: 543, found: 566 $[M+Na]^{+}$.

4.4.3 General procedure of compound B derivatives:

Compound A (0.4 g, 0.65 mmol) was dissolved in 8 mL of dry DCM and cooled the solution to 0 ºC, 4 mL of Triflouroacetic acid was added to the cooled reaction mixture while stirring the solution, continued the stirring for five hours at room temperature. After

complete disappearance of starting material, the solvent was evaporated under reduced pressure and kept under high vacuum for two hours, dissolved the residue in 25 mL of DCM and 25 mL of saturated aqueous $NaHCO_3$ stirred the resulting bilayered mixture for two hours and then separated the two phases of mixture. The organic layer was washed two times with water and one time with brine solution and the solvent was dried on sodium sulphate and concentrated under reduced pressure to obtain primary amine. Which was pure enough for further reactions.

Toc-Glycine:

^{1}H NMR (400 MHz, $CDCl_3$) δ 3.99 (s, 2H), 2.53 (t, *J* = 5.8 Hz, 2H), 1.97 (m, 9H), 1.79 – 1.67 (m, 2H), 1.66 – 0.86 (m, 24H), 0.85 (m, 12H).MS *m/z*: calculated: 487, found: 510 $[M+Na]^+$.

Chol-Glycine:

^{1}H NMR (400 MHz, $CDCl_3$) δ 5.37 (d, *J* = 4.0 Hz, 1H), 4.69 – 4.61 (m, 1H), 3.79 (s, 2H), 2.41 – 2.26 (m, 2H), 2.06 – 1.79 (m, 6H), 1.74 – 0.81 (m, 41H), 0.68 (s, 3H). MS *m/z*: calculated: 443, found: 466 $[M+Na]^+$.

4.4.4 General procedure of compound C derivatives:

1 mmol (0.145 g) of DiBoc Lysine, and 1.5 mmol of Diisopropylethylamine (0.1 mL) in 10 mL of DCM were taken in a 100mL RB flask and kept it for stirring in ice bath at 0 °C. After five minutes of stirring sequentially HOBT (0.096 g, 1.5 mmol), EDCI.HCl (0.12 g, 1.5 mmol) were added to the stirred reaction mixture. After 10 minutes of stirring at 0 °C primary amine intermediate (B) (1.2 mmol) was added, raised the temperature to rt and continued the stirring overnight. The organic layer was dried on sodium sulphate and evaporated the solvent under reduced pressure.

Toc-Gly-Boc-Lysine:

The crude Toc-Gly-Boc-Lysine was further purified by using column chromatography with 100-200 mesh silica gel, eluting with 7% (v/v) Hexane in ethyl acetate (Rf = 0.2, 10% Hexane in ethyl acetate).^{1}H NMR (400 MHz, $CDCl_3$) δ 6.82 (s, 1H), 4.60 (m, 1H), 4.33 (d, *J* = 5.4 Hz, 2H), 4.15 (s, 1H), 3.14 – 3.06 (m, 2H), 2.58 (t, *J* = 6.7 Hz, 2H), 2.10 – 1.95 (m, 9H), 1.78 (m, 2H), 1.66 (s, 6H), 1.56 – 1.03 (m, 48H), 0.88 – 0.83 (m, 12H). MS *m/z*: calculated: 815, found: 838 $[M+Na]^+$.

Chol-Gly-Boc-Lysine:

The crude Toc-Gly-Boc-Lysine was further purified by using column chromatography with 100-200 mesh silica gel, eluting with 5% (v/v) Hexane in ethyl acetate (Rf = 0.5, 10% Hexane in ethyl acetate). ^{1}H NMR (400 MHz, $CDCl_3$) δ 5.44 – 5.41 (m, 1H), 5.39 – 5.31 (m, 2H), 4.80 (m, 1H), 3.57 – 3.48 (m, 2H), 3.46 – 3.35 (m, 1H), 2.43 (dd, *J* = 5.2, 3.2 Hz, 2H), 2.27 – 2.23 (m, 2H), 1.99 (s, 2H), 1.82 (d, *J* = 7.4 Hz, 3H), 1.41 – 0.93 (m, 66H), 0.68 (s, 3H). MS *m/z*: calculated: 771, found: 772 $[M+H]^+$.

4.4.5 Synthesis of title lipids (Boc deprotection):

1 mmol of Boc protected compound was taken into 8 mL of dry DCM in a 50 mL RB flask, placed in an ice cooled solution and 4 mL of TFA was added at 0 °C then temperature was raised to RT and continued the stirring overnight. The solvent and excess TFA were evaporated under reduced pressure and the obtained residue was dissolved in (30 mL) ethyl acetate and the solvent evaporated by rotary evaporation then kept it under high vacuum for three hrs. The compound was pure and 90% yielded.

Lipid-1 TGK:

^{1}H NMR (400 MHz, $CDCl_3$) δ 7.14 (s, 1H), 4.29 (d, *J* = 18.2 Hz, 2H), 4.08 (d, *J* = 16.6 Hz, 1H), 3.09 (s, 2H), 2.54 (t, *J* = 6.2 Hz, 2H), 2.08 – 1.88 (m, 9H), 1.77 – 1.66 (m, 2H), 1.60 – 1.00 (m, 27H), 0.88 – 0.82 (m, 12H). ^{13}C NMR (126 MHz, $CDCl_3$) δ 170.37, 169.77, 141.30, 140.41, 127.71, 127.10, 127.07, 118.51, 82.07, 50.60, 39.90, 39.83, 39.40, 37.58, 37.47, 37.41, 37.31, 32.81, 32.72, 31.57, 31.52, 29.73, 28.10, 28.00, 24.83, 24.47, 23.81, 22.75, 22.65, 21.07, 20.78, 20.62, 19.78, 19.71, 19.68, 19.62, 12.98, 12.24, 11.84, 11.80, 11.30. ESI-HRMS *m/z*: calculated: 617.5121, found: 616.5059 $[M]^+$.

Lipid-2 CGK:

^{1}H NMR (400 MHz, $CDCl_3$) δ 5.42 (m, 1H), 5.35 (m, 2H), 4.80 (m, 2H), 3.53 (m, 2H), 3.46 – 3.32 (m, 1H), 2.45 – 2.38 (m, 2H), 2.29 – 2.25 (m, 2H), 1.99 (s, 4H), 1.85 (d, *J* = 8.5 Hz, 3H), 1.40 – 1.06 (m, 41H), 0.68 (s, 3H). ^{13}C NMR (101 MHz, $CDCl_3$) δ 157.16, 156.75, 140.71, 121.76, 71.87, 56.78, 56.66, 56.18, 56.15, 50.15, 49.97, 42.32, 42.24, 39.80, 39.69, 39.53, 37.45, 37.26, 36.73, 36.52, 36.20, 35.79, 31.92, 31.81, 31.60, 29.71, 28.24, 28.22, 28.02, 27.26, 24.30, 24.27, 23.84, 22.81, 22.56, 21.10, 21.04, 19.39, 19.23, 18.72, 14.11, 11.86. ESI-HRMS *m/z*: calculated: 573.4858, found: 572.4791 $[M]^+$.

4.4.6 Preparation of Liposomes:

TGK and CGK liposomes were prepared following previous protocol[50]. The final concentrations of TGK with co lipid DOPE and CGK with co lipid DOPE in chloroform were taken at 1:1 molar ratio respectively. 1 mM liposomes were used for *in vitro* studies.

4.4.7 Zeta potential (ξ) and size measurements:

Hydrodynamic diameter and the surface charges (zeta potentials) of the nano-formulations were measured on a Lite SizerTM500Particle Analyzer, manufactured by Anton Paar. For stability, the sizes were tested in 10% FBS and deionized water, respectively. Utilizing the 200 nm + 5 nm polystyrene polymer, the system was calibrated (Duke Scientific Corps., Palo Alto, CA). The following factors were used to calculate the zeta potential: viscosity (0.89 cP), dielectric constant (79), temperature (25 °C), F(Ka), 1.50 (Smoluchowski), and maximum current voltage (V). Ten measurements with the zero-field adjustment were made. The Smoluchowskiapproximation was used to compute the potentials.

4.4.8 DNA-binding assay:

An agarose gel retardation assay was used to test the DNA binding properties of the improved cationic co-liposomal formulations (lipid/DOPE, 1:1). In following experiment, 500 ng of pCMV-gal was complexed with each cationic formulation in 1x PBS (24 µL) at four different N/P (liposome/plasmid) charge ratios of 1:1, 2:1, 4:1 and 8:1. Followed by prepared complexes incubated for 30 minutes. After adding 6x loading dye to the sample, these complexes (12 µL each) were loaded into a freshly prepared 1% agarose gel dyed with EtBr. In a 100 V electrophoresis chamber, electrophoresis was performed for 35 minutes in 1x TAE running buffer. The gel photos were captured in transillumination mode using a gel documentation system.

4.4.9 pDNA Transfection Biology:

Fluorescence microscopy and flow cytometry were used to evaluate the produced cationic lipoplexes' ability to express eGFP both qualitatively and quantitatively. At least 12 hours before the transfection studies, cells were placed in a 48-well plate at a density of 25000/well (for HEK-293, CHO, Neuro-2a, and Hep G2). In serum-free media with a final volume of 40 µL for 30 minutes, lipoplexes were created by utilising pDNA (0.4 µg) and the liposomes of TGK and CGK at a 1:1 to 8:1

lipid/DNA charge ratio. The cells were added to the prepared lipoplexes. The reporter gene activity was calculated using a previously described procedure[46] after 36–48 h of incubation. Following the period of incubation, GFP expression was imaged using a fluorescent microscope (Leica CTR 6000, Germany), and the results were quantified using FACS. Here, the transfection reagent LF 3000, which is available commercially, acted as a positive control.

4.4.10 Cellular uptake & co-localisation analysis:

Briefly, Neuro-2a cells were harvested at a density of 1×10^4 cells for each confocal dish 24 hours prior to the experiment. Here, rhodamine-DHPE labelled liposomes were used for lipoplex preparation. 40 µL of lipoplexes were added to the seeded cells after attaining 70% confluency at best charge ratio 4:1 for 12 hours. Followed by Lysotracker green DND-26 reagent (100 nM) was also added and incubated for 30 min. After incubation, Hoechst (1 mg per mL) was added to cells and washed twice with PBS. Fluorescence was visualized under a confocal microscope equipped with 100x oil immersion objective (Leica TCS S52). For Lysotracker green the emission wavelength was set at 504-511 nm, 568–583 nm wavelength was for Rhodamine-PE labelled lipoplexes and 361-497 nm for hoechst. Colocalisation of the fluorescent labels lipids (red) and lysosomal compartments (green) was analyzed using the location of labelled lipoplexes with respect to the lysosomes as well as nucleus.

4.4.11 Determination of the endocytic pathway:

HEK-293 and neuro-2a cell lines for seeded on 24 well plate a day before the transfection. For transfection using endocytosis inhibitors, cells were pre-treated with chlorpromazine (10 µg mL^{-1}), Nystatin (80 µM), amiloride (400 µM) and filipin-III (10 µg mL^{-1}) individually for 30 minutes in plain DMEM. The medium was removed and then replaced with 10% fetal bovine serum and 1% penicillin-streptomycin. Consequently, the lipoplexes were then added to the cells and incubated at 37 °C and 5% CO_2. After 36 to 48 hrs of incubation with lipoplexes, the cells were trypsinized and collected in 10% FBS containing PBS, followed by analysis using FACS.

4.4.12 mRNA Transfection Studies:

At least 12 hours before the experiments, Hek 293 and CHO cells were placed in a 48-well plate at a density of 25000/well for mRNA transfection research. mRNA plexes were created by using 0.1µg of GFP-encoding mRNA with different amounts of liposomes (4:1 to 12:1 lipid/mRNA charge ratio) in serum-free DMEM to a final

volume of 40 µL for 30 min. According to the manufacturer's instructions, LFmMAX MAX, a commercially available transfection reagent, was utilised for transfection. After introducing the complexes, the cells were cultured for a further 24 hours. After the incubation time, GFP expression imaging was performed using a fluorescent microscope (Leica CTR 6000, Germany), and the results were quantified in FACS (BD Celesta Flow cytometry, USA).

4.4.13 CRISPR Plasmid Expression Studies:

12–18 hours prior to transfection, 4 × 104 HEK-293 cells were placed in 24-well plates to analyse the GFP expression in the cells. In serum-free medium for 20 min, TGK and CGK liposomes were produced to bind with pL-CRISPR.EFS.GFP (0.9 µg/well) at a 2:1 lipid/DNA charge ratio. After obtaining final volumes of complexes to 40 µl, these complexes were added to the cells. GFP expression imaging was carried out using a fluorescent microscope (Leica CTR 6000, Germany) and quantified using FACS after 36–48 hours of transfections (BD Celesta Flow cytometry, USA).

4.4.14 Cell viability assay:

An essential procedure for characterization of the produced gene delivery vectors is cytotoxic screening[47,48]. For this, cells were planted in 96-well plates at a density of 1×104 cells per well. Lipid toxicities for lipoplexes prepared using liposomes and pDNA at varying lipid/DNA charge ratios (8:11:1) were assessed using an MTT-based colorimetric reduction assay by incubating for 20 min at room temperature, followed by treating Neuro- 2a & HEK-293 cells with the prepared lipoplexes for 24 h at 37 °C in 10% serum-containing DMEM. MTT [3-(4, 5-imethylthiazole-2-yl)-2, 5-diphenyltetrazolium bromide] was added post incubation to determine the cell viability assay as previously described[49].

4.5 References

1 M. A. Mintzer and E. E. Simanek, *Chem. Rev.*, 2009, 109.

2 H. Yin, R. L. Kanasty, A. A. Eltoukhy, A. J. Vegas, J. R. Dorkin and D. G. Anderson, *Nat. Rev. Genet.*, 2014, **15**, 541–555.

3 G. Lin, H. Zhang and L. Huang, *Mol. Pharm.*, 2015, **12**, 314–321.

4 S. Bhattacharya and A. Bajaj, *Chem. Commun.*, 2009.

5 M. A. Maslov, T. O. Kabilova, I. A. Petukhov, N. G. Morozova, G. A. Serebrennikova, V. V. Vlassov and M. A. Zenkova, *J. Control. Release*, 2012, **160**, 182–193.

6 D. Zhi, S. Zhang, S. Cui, Y. Zhao, Y. Wang and D. Zhao, *Bioconjug. Chem.*, 2013, 24.

7 K. Shi, J. Zhou, Q. Zhang, H. Gao, Y. Liu, T. Zong and Q. He, *J. Biomed. Nanotechnol.*, 2015, **11**, 382–391.

8 B. K. G. Theng, 2012, **4**, 319–337.

9 Y. Zhao, S. Zhang, Y. Zhang, S. Cui, H. Chen, D. Zhi, Y. Zhen, S. Zhang and L. Huang, *J. Mater. Chem. B*, 2015, **3**, 119–126.

10 D. Zhi, S. Zhang, B. Wang, Y. Zhao, B. Yang and S. Yu, *Bioconjug. Chem.*, 2010, **21**, 563–577.

11 R. S. Y. Wong and A. K. Radhakrishnan, *Nutr. Rev.*, 2012, **70**, 483–490.

12 N. Duhem, F. Danhier and V. Préat, *J. Control. Release*, 2014, 182, 33–44.

13 Q. Liu, Q. Q. Jiang, W. J. Yi, J. Zhang, X. C. Zhang, M. B. Wu, Y. M. Zhang, W. Zhu and X. Q. Yu, *Bioorganic Med. Chem.*, 2013, **21**, 3105–3113.

14 B. Kedika and S. V. Patri, *J. Med. Chem.*, 2011, **54**, 548–561.

15 B. Kedika and S. V. Patri, *Bioconjug. Chem.*, , DOI:10.1021/bc2004395.

16 V. Muripiti, B. Lohchania, V. Ravula, S. Manturthi, S. Marepally, A. Velidandi and S. V. Patri, *New J. Chem.*, 2021, **45**, 615–627.

17 V. Ravula, V. Muripiti, S. Manthurthi and S. V. Patri, *ChemistrySelect*, 2021, **6**, 13025–13033.

18 S. Patil, Y. G. Gao, X. Lin, Y. Li, K. Dang, Y. Tian, W. J. Zhang, S. F. Jiang, A. Qadir and A. R. Qian, *Int. J. Mol. Sci.*, , DOI:10.3390/ijms20215491.

19 D. A. Medvedeva, M. A. Maslov, R. N. Serikov, N. G. Morozova, G. A. Serebrenikova, D. V. Sheglov, A. V. Latyshev, V. V. Vlassov and M. A. Zenkova, *J. Med. Chem.*, 2009, **52**, 6558–6568.

20 J. C. Rea, R. F. Gibly, A. E. Barron and L. D. Shea, *Acta Biomater.*, 2009, **5**, 903–912.

21 V. Muripiti, B. Lohchania, S. K. Marepally and S. V. Patri, *Medchemcomm*, 2018, **9**, 264–274.

22 M. Jiang, L. Gan, C. Zhu, Y. Dong, J. Liu and Y. Gan, *Biomaterials*, 2012, **33**, 7621–7630.

23 H. M. Aliabadi and A. Lavasanifar, *Expert Opin. Drug Deliv.*, 2006, **3**, 139–162.

24 K. Wang, X. Yan, Y. Cui, Q. He and J. Li, *Bioconjug. Chem.*, 2007, **18**, 1735–1738.

25 M. Westoby, J. Chrostowski, P. De Vilmorin, J. P. Smelko and J. K. Romero, *Biotechnol. Bioeng.*, 2011, **108**, 50–58.

26 C. E. Ashley, E. C. Carnes, K. E. Epler, D. P. Padilla, G. K. Phillips, R. E. Castillo, D. C. Wilkinson, B. S. Wilkinson, C. A. Burgard, R. M. Kalinich, J. L. Townson, B. Chackerian, C. L. Willman, D. S. Peabody, W. Wharton and C. J. Brinker, *ACS Nano*, 2012, **6**, 2174–2188.

27 M. Rajesh, J. Sen, M. Srujan, K. Mukherjee, B. Sreedhar and A. Chaudhuri, *J. Am. Chem. Soc.*, 2007, **129**, 11408–11420.

28 C. M. Lamanna, H. Lusic, M. Camplo, T. J. Mcintosh, P. Barth and M. W. Grinstaff, .

29 P. Gao, W. Pan, N. Li and B. Tang, *ACS Appl. Mater. Interfaces*, 2019, **11**, 26529–26558.

30 Y. Zhao, T. Zhao, Y. Du, Y. Cao, Y. Xuan, H. Chen, D. Zhi, S. Guo, F. Zhong and S. Zhang, *J. Nanobiotechnology*, 2020, **18**, 1–14.

31 T. HE, L. LF, D. GJ, W. WT, C. SC, K. ML, T. R, L. GS and T. MH, *J. Gene Med.*, 2012, **14**, 44–53.

32 T. Takeuchi, J. Montenegro, A. Hennig and M. Stefan, *Chem. Sci.*, 2011, **2**, 303–307.

33 M. E. Davis, J. E. Zuckerman, C. H. J. Choi, D. Seligson, A. Tolcher, C. A. Alabi, Y. Yen, J. D. Heidel and A. Ribas, *Nature*, 2010, **464**, 1067–1070.

34 D. Zhou, C. Li, Y. Hu, H. Zhou, J. Chen, Z. Zhang and T. Guo, *Chem. Commun.*, 2012, **48**, 4594–4596.

35 C. L. Walsh, J. Nguyen, M. R. Tiffany and F. C. Szoka, *Bioconjug. Chem.*, 2013, **24**, 36–43.

36 Du, Z.; Munye, M. M.; Tagalakis, A. D.; Manunta, M. D. I.; Hart, S. L. *Scientific*

Reports **2014**, *4*. https://doi.org/10.1038/srep07107.

37 Durymanov, M.; Reineke, J. *Frontiers in Pharmacology*. Frontiers Media S.A. August 21, 2018. https://doi.org/10.3389/fphar.2018.00971.

38 Medina-Kauwe, L. K.; Xie, J.; Hamm-Alvarez, S. *Gene Therapy* **2005**, *12* (24), 1734–1751. https://doi.org/10.1038/sj.gt.3302592.

39 Maiti, B.; Kamra, M.; Karande, A. A.; Bhattacharya, S. *Organic and Biomolecular Chemistry* **2018**, *16* (11), 1983–1993. https://doi.org/10.1039/c7ob02835k.

40 Lönn, P.; Dowdy, S. F. *Expert Opinion on Drug Delivery* **2015**, *12* (10), 1627–1636. https://doi.org/10.1517/17425247.2015.1046431.

41 Gump, J. M.; June, R. K.; Dowdy, S. F. *Journal of Biological Chemistry* **2010**, *285* (2), 1500–1507. https://doi.org/10.1074/jbc.M109.021964.

42 Muñoz-Úbeda, M.; Misra, S. K.; Barrán-Berdón, A. L.; Aicart-Ramos, C.; Sierra, M. B.; Biswas, J.; Kondaiah, P.; Junquera, E.; Bhattacharya, S.; Aicart, E. *Journal of the American Chemical Society* **2011**, *133* (45), 18014–18017. https://doi.org/10.1021/ja204693f.

43 Heckl, D.; Kowalczyk, M. S.; Yudovich, D.; Belizaire, R.; Puram, R. V.; McConkey, M. E.; Thielke, A.; Aster, J. C.; Regev, A.; Ebert, B. L. *Nature Biotechnology* **2014**, *32* (9), 941–946. https://doi.org/10.1038/nbt.2951.

44 Yu, X.; Liang, X.; Xie, H.; Kumar, S.; Ravinder, N.; Potter, J.; de Mollerat du Jeu, X.; Chesnut, J. D. *Biotechnology Letters* **2016**, *38* (6), 919–929. https://doi.org/10.1007/s10529-016-2064-9.

45 Gosangi, M.; Rapaka, H.; Ravula, V.; Patri, S. v. *Bioconjugate Chemistry* **2017**, *28* (7). https://doi.org/10.1021/acs.bioconjchem.7b00283

46 Gosangi, M.; Rapaka, H.; Mujahid, T. Y.; Patri, S. v. *MedChemComm* **2017**, *8* (5), 989-999. https://doi.org/10.1039/c6md00699j.

47 Srujan, M.; Chandrashekhar, V.; Reddy, R. C.; Prabhakar, R.; Sreedhar, B.; Chaudhuri, A. *Biomaterials* **2011**, *32* (22), 5231-5240. https://doi.org/10.1016/j.biomaterials.2011.03.059.

48 Chandrashekhar, V.; Srujan, M.; Prabhakar, R.; Reddy, R. C.; Sreedhar, B.; Rentam, K. K. R.; Kanjilal, S.; Chaudhuri, A. *Bioconjugate Chemistry* **2011**, *22* (3), 497-509. https://doi.org/10.1021/bc100537r.

49 Karmali, P. P.; Kumar, V. v.; Chaudhuri, A. *Journal of Medicinal Chemistry* **2004**, *47* (8), 2123-2132. https://doi.org/10.1021/jm030541+.

50 A. Ahmad, S.K. Mondal, D. Mukhopadhyay, R. Banerjee, K.M. Alkharfy, *Molecular pharmaceutics* 13(3) (2016) 1081-1088.

4.6 Spectral data

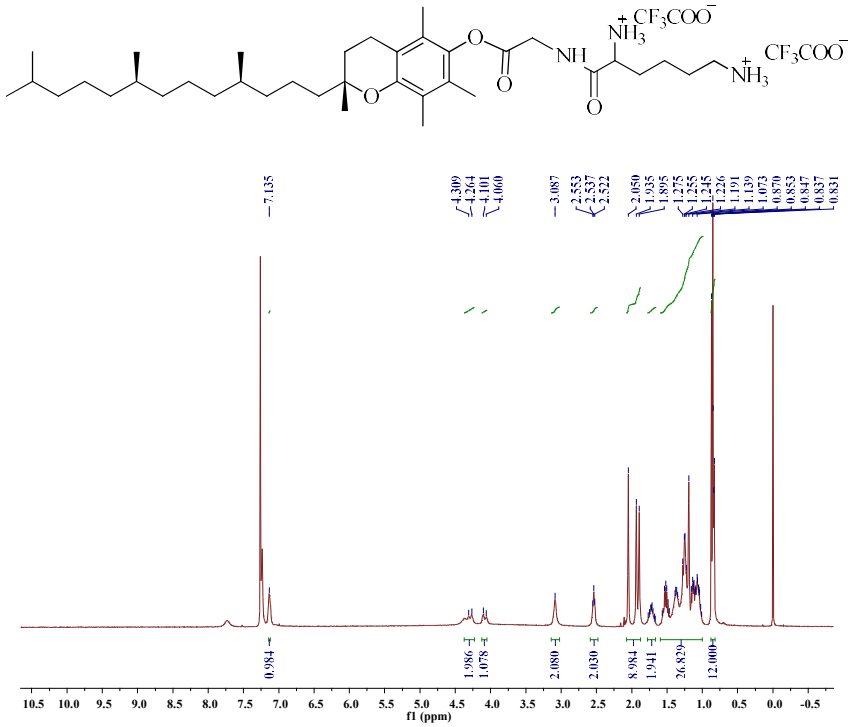

^{1}H NMR Spectrum of **Lipid-1 TGK**

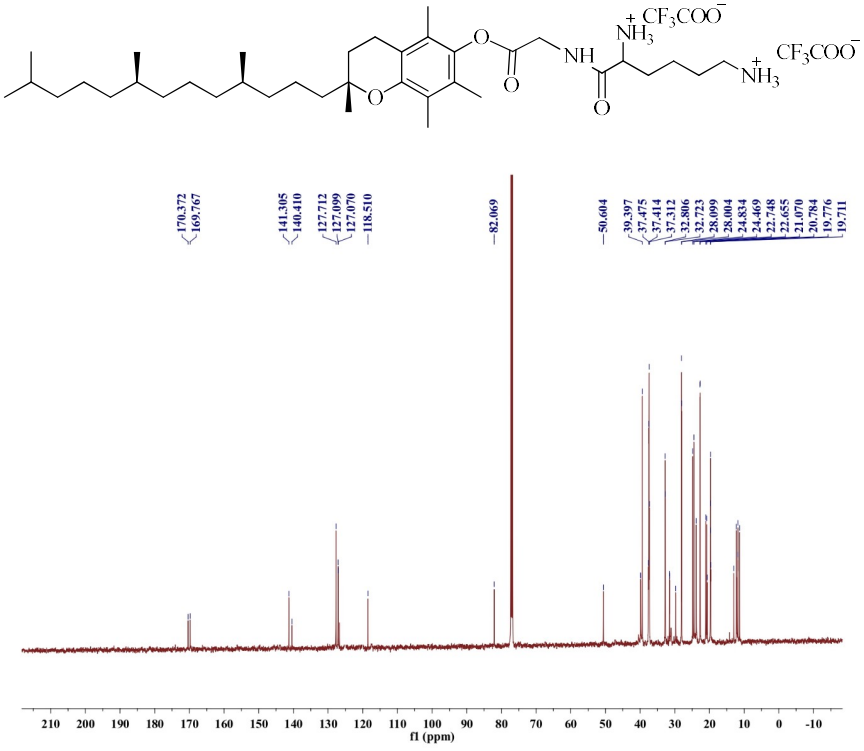

^{13}C NMR Spectrum of **Lipid-1 TGK**

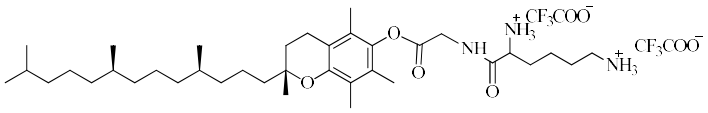

Chemical Formula: $C_{37}H_{67}N_3O_4^{2+}$
Exact Mass: 617.5121

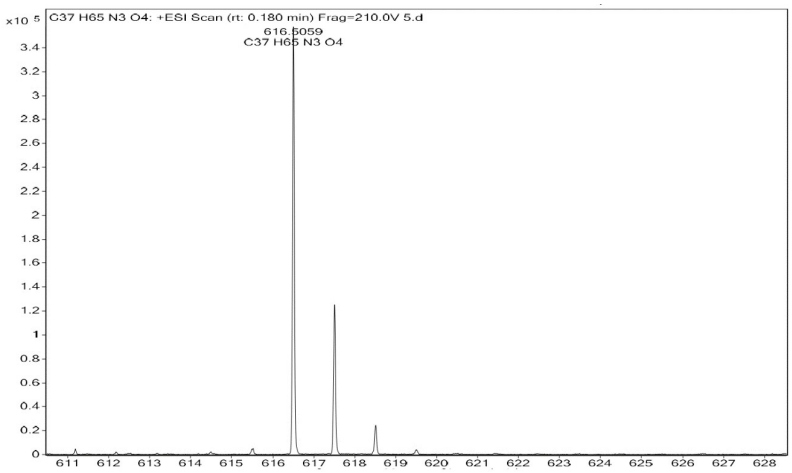

ESI-HRMS Spectrum of **Lipid-1 TGK**

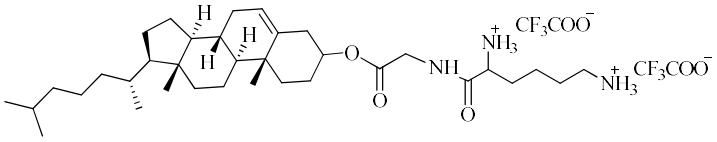

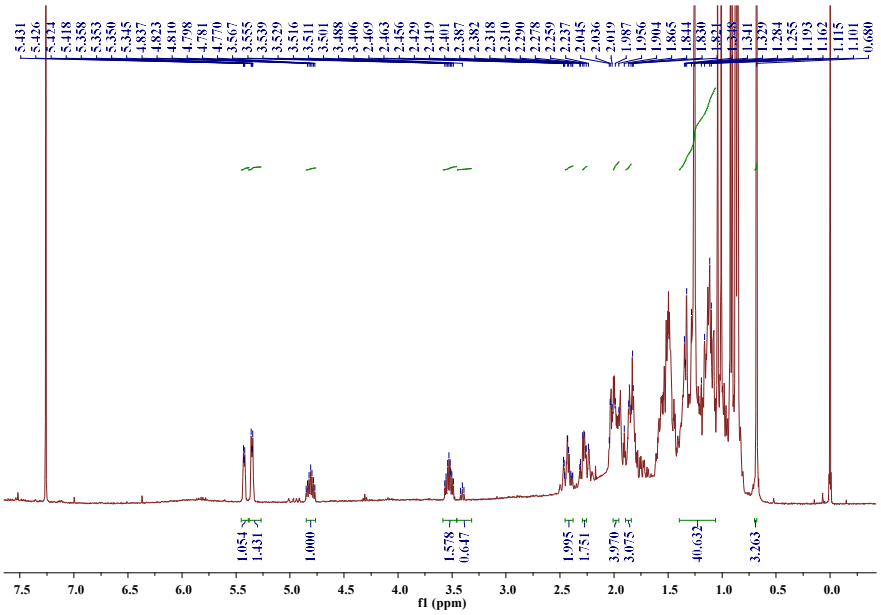

^{1}H NMR Spectrum of **Lipid-2 CGK**

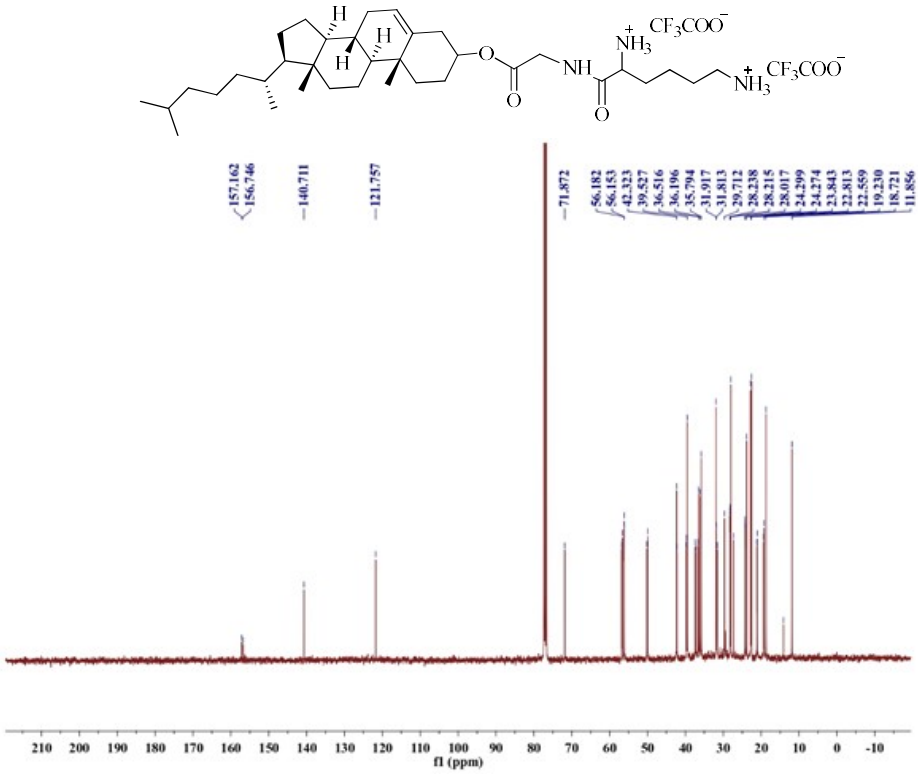

^{13}C NMR Spectrum of **Lipid-2 CGK**

Chemical Formula: $C_{35}H_{63}N_3O_3^{2+}$

Exact Mass: 573.4858

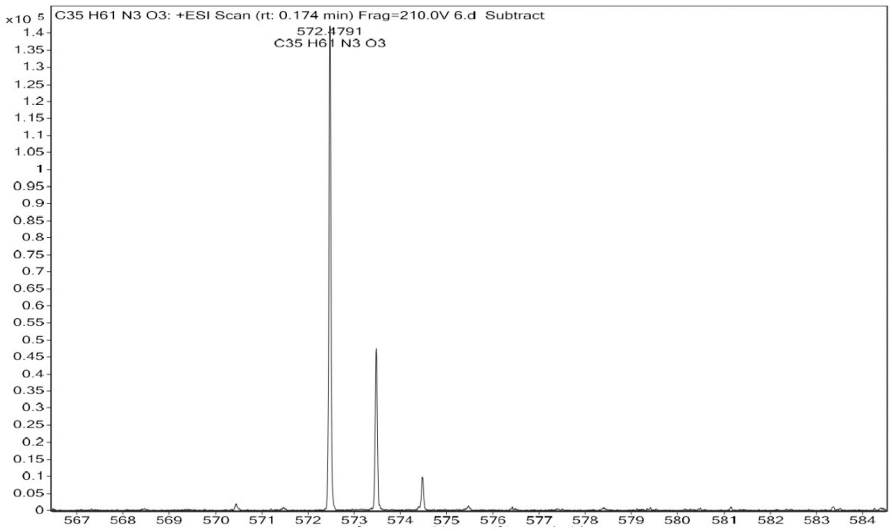

ESI-HRMS Spectrum of **Lipid-2 CGK**

CHAPTER V

Proline head group based gemini like cationic lipids: The effect of spacer length on transfection properties

5.1. Introduction

Because of its rising success rate in clinical studies over the past two decades[1,2], gene therapy has captured the attention of researchers. The idea has not yet achieved its highest therapeutic potential in a clinical setting, nevertheless. Furthermore, the successful transmission of the therapeutic material to the target cell is a significant barrier to gene therapy. The most effective carrier, which can be either viral or non-viral-based carrying reagents, has been created using cutting-edge technology. [3,4]. Because viral delivering reagents are related to non-compiling characteristics of viruses, including immunological pathogenicity, expensive handling procedures, and low-scale production, they are chosen over non-viral delivering reagents. [5,6]. In fact, various types of nano-vectorizations, including cationic vectors (DOTMA, DOSPA), polymeric vectors (PLL, PEI), dendrimer vectors (PAMAM, PPI), polypeptide-based vectors (TAT, MPG peptides), and nanoparticles (quantum dots, gold nanoparticles, carbon nanotubes)[5, 7] are non-viral in nature. These nano-vectorizations were developed to improve oligonucleotide sequence transfection in a variety of cell lines with varying ancestries. Cationic lipids have received a lot of attention among the investigated non-viral carrying systems because they are simple to make, less harmful, and extremely productive. [8-10].

Much emphasis has been placed on creating novel patterns to get beyond these obstacles, despite the fact that synthetic compounds are poisonous and have reduced transfection. Generally speaking, cationic lipids have the ability to self-assemble to form nano-aggregates known as "liposomes"[11]. As part of a process known as "co-liposomal formulation," cationic lipids were converted into liposomes in an aqueous solution either by mixing them with one or more helper lipids such as cholesterol, DOPE, or DOPC, or by doing so alone.[12,13]. The majority of the related work has been on the development of novel formulations and the modification of diverse cationic lipid backbones to obtain superior performance.[14]

Due to their excellent potentials for transfection and least harmful composition, Gemini cationic lipids are occupying a significant area among the broad range of multi-modular cationic lipid systems[15]. The Gemini lipids, a well-known type of cationic lipid that has recently undergone significant development in this non-viral lipid system, have been reported by numerous laboratories to be effective cytofectins[16–30].

Two hydrophobic tails and two polar head groups connected by a flexible or rigid

spacer are the typical characteristics of these gemini lipids. We present here a novel family of gemini lipids with an aliphatic hydrophobic backbone for the development of synthetic cationic lipid formulations for increasing efficacy levels without circling constraints.

Importantly, spacers such as simple alkyl chains of various lengths[31], disulfide bonds[32], and oligo-oxyethylene[33] that are employed to join the cationic head groups of lipids together through a moiety play a role in the effective transfection. In fact, the functional characteristics, chain lengths, and alignment with the head group[34] of spacers are highly sensitive to even small variations in the transfection profiles of cationic amphiphiles.

Finding an appropriate co-lipid that helps to increase the transfection potential of cationic lipids is another important influencing factor with regard to cationic lipid-mediated transfection[35]. Despite the fact that there are many different helper lipids in use, DOPE has consistently emerged as the most helpful co-lipid in earlier studies because of its important characteristics, such as the development of non-bilayer structures and fusogenicity[36–38].

The efficacy of some alkyl surfactants as chemical permeation enhancers for various drugs have been studied and reported in the literature[39-43]. Studies have focused on the influence of the alkyl chain length on the efficiency of the surfactants to act as chemical permeation enhancers. It has been reported that, the alkyl chain having C12 alkyl groups showed the highest enhancer activity[44].

Proline is the only amino acid with a cyclic structure containing a secondary α-amino group and this structural feature gives unique stereochemical and biological properties to the peptides containing proline residue[45]. Previous results suggest that Proline rich peptides represent a new class of naturally occurring cell-permeant peptides that are soluble in aqueous solutions[46]. Furthermore, antimicrobial peptides may represent a rich source of templates for designing novel cell-permeant peptides[46]. Water soluble proline rich peptides have been reported as naturally occurring cell permeant peptides, which are able to break the cell membrane and deliver the attached carriers into the cells without causing lethal membrane disruption.

In present investigation, considering the importance of proline's cell permeation characteristics and the dodecyl alkyl chain's superior permeation enhancer activity. Six distinct gemini cationic lipids based on proline head groups that differ in the length of the

spacer were devised and developed. The two hydrophilic head groups will gradually drift apart as the spacer length rises. This may then have an impact on the transfection profiles, DNA interaction, and aggregation. DOPE was combined with these lipids to create transparent aqueous suspensions. The efficacy of these lipids in *in vitro* nucleic acid delivery was evaluated.

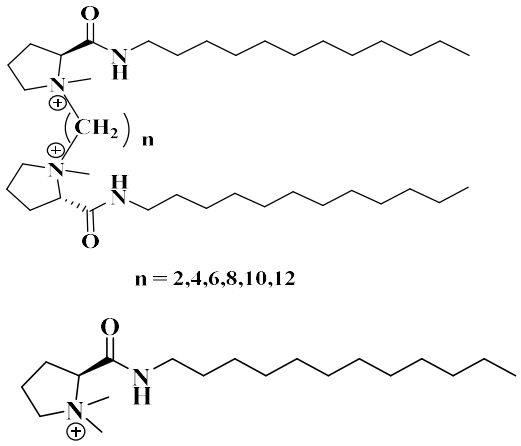

Figure 1. Molecular structures of Dimeric lipids and control lipid

5.2 Results and Discussion

Synthesis: A series of six proline head group based cationic lipids containing spacers with different chain lengths were synthesized by following the steps presented in Scheme 1. Initially, boc proline was coupled with dodecyl amine followed by boc deprotection to yield an amide intermediate, it has been identified and is employed as a common intermediary for all dimeric lipids. This amide intermediate was further treated with methyl iodide quaternization to produce iodide salt as control lipid. To obtain pure labelled lipids, corresponding dibromo alkanes were treated individually using an amide intermediate, followed by quaternization using methyl iodide. Utilizing the spectroscopic information produced by ^{1}H-NMR, ^{13}C-NMR, and LC-MS, the structures of lipids and intermediates were examined.

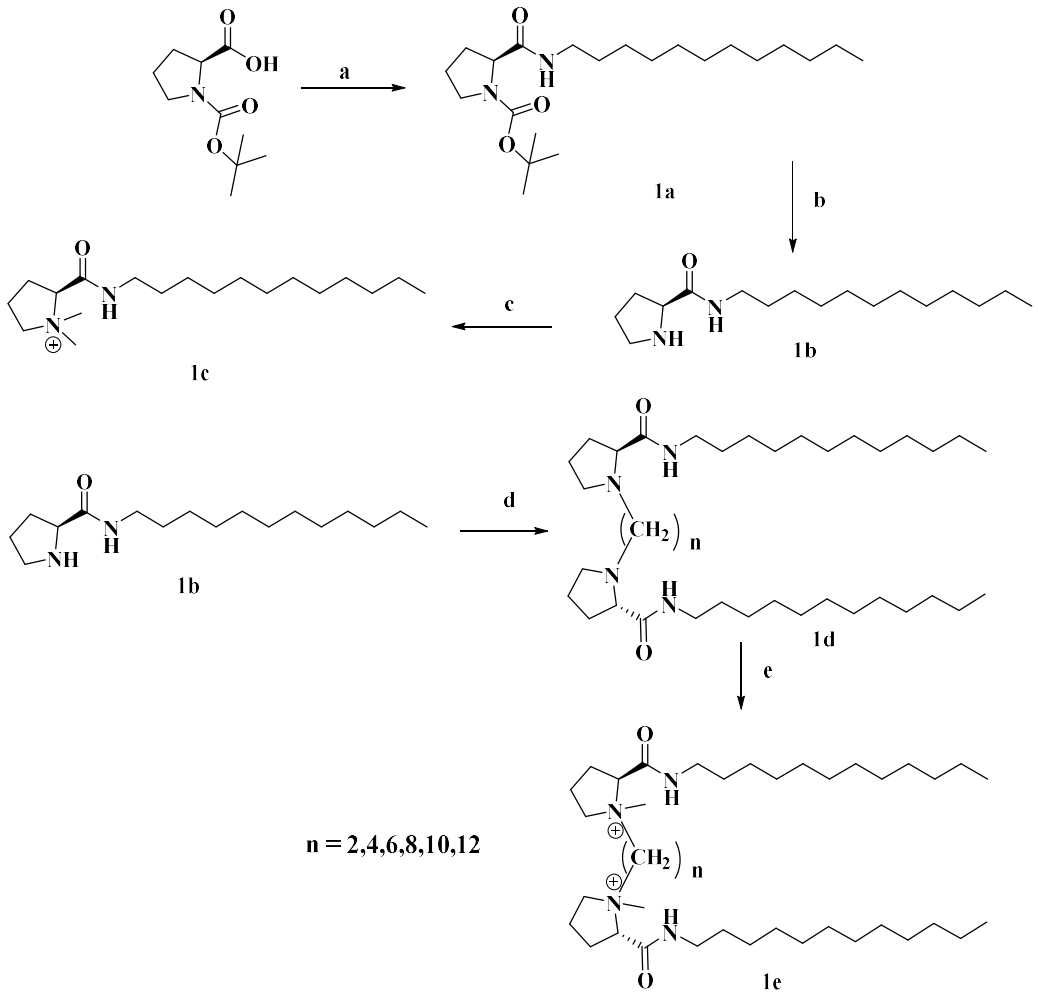

Reagents and conditions: (a) $C_{12}H_{25}NH_2$, EDCI. HCl, HOBt, DIPEA, Dichloromethane, 0 °C; (b) 1:2 TFA: DCM, 0 °C and aq Na_2CO_3: DCM (1:1) ;(c) CH_3I, Acetonitrile, sealed tube, 80 °C, 24 h; (d)dibromoalkane, acetonitrile, K_2CO_3, 80 °C, 16 h; (e) Methyl iodide, acetonitrile, sealed tube, 80 °C, 32 h.

5.2.1 Preparation of liposomal aggregates:

By employing the novel dimeric lipid and DOPE and adhering to the methodology described in other reports[47,48], mixed liposomal suspensions were created. After being vortexed to create multilamellar aggregates, all of the rehydrated lipid thin films were sonicated to create transparent aqueous suspensions that can be stored at 4 °C until usage.

5.2.2 Particle size and zeta potentials:

A rational design of the gene delivery vector in *in vitro* requires various physicochemical characterizations of liposomes/lipoplexes such as charge of liposomes,

it's size and lipid–DNA complexes binding stability. We have prepared liposomes as a first step in order to determine the surface charge and size of liposomes. Lipoplexes were prepared by changing the N/P charge ratios (1:1, 2:1, 4:1 and 8:1) with pDNA to determine DNA binding ability using Gel retardation assay.

The size and zeta-potential of the liposomes were determined using dynamic light scattering (DLS). The results depicted through Figure 2A revealed that, the size of all the synthesized gemini liposomal formulations was nearly ≤ 200 nm and all the liposomes showed positive zeta potential (Figure 2B). The particle diameter of Pro-Cl is found to be 166.58 nm, Pro-1,2 is 169.20 nm, Pro-1,4 is 159.20 nm, Pro-1,6 is 169.90 nm, Pro-1,8 is 206.00 nm, Pro-1,10 is 152.27 nm and Pro-1,12 is 195.71nm is as given in Figure 2A. Figure 2B depicts that, from the zeta potentials of liposomes, it is observed that as the spacer length increases from 2 to 8 zetapotential is decreasing and on further increase of spacer length zeta potential also increasing respectively. The zetapotials of the liposomes observed are as follows Pro-Cl is 6.0 mV, Pro-1,2 is 28.9 mV, Pro-1,4 is 12.9, Pro-1,6 is 12.7 mV, Pro 1,8-is 9.1 mV, Pro-1,10 is 15.8 mV and Pro-1,12 is 37.1 mV respectively.

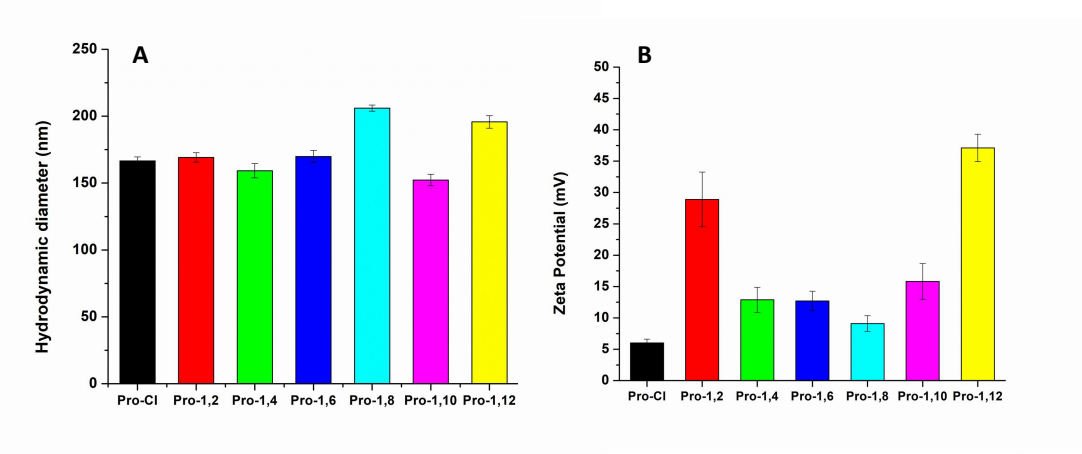

Figure 2. (A) Particle size and (B) Zeta potential values of synthesized liposomes (n=3)

5.2.3 DNA binding studies by Gel Electrophoresis:

DNA binding capacity with liposomes was studied by conventional agarose gel electrophoresis assay at different liposomes to pDNA charge ratios such as 1:1, 2:1, 4:1 and 8:1. Gel retardation assay was used to understand the level of binding capacity of lipids to DNA using agarose gel electrophoresis. In this, the amount of unbound pDNA was examined by the extent of migration of lipoplexes at different charge ratios in

reference to free plasmid DNA in agarose gel as shown in Figure 3. Pro-Cl, Pro-1,2 and pro-1,12 among the current lipid series were exhibiting maximum binding by entirely delaying plasmid at a ratio of 1:1, while other lipids began delaying pDNA with a ratio of 2:1 or greater charge ratio.

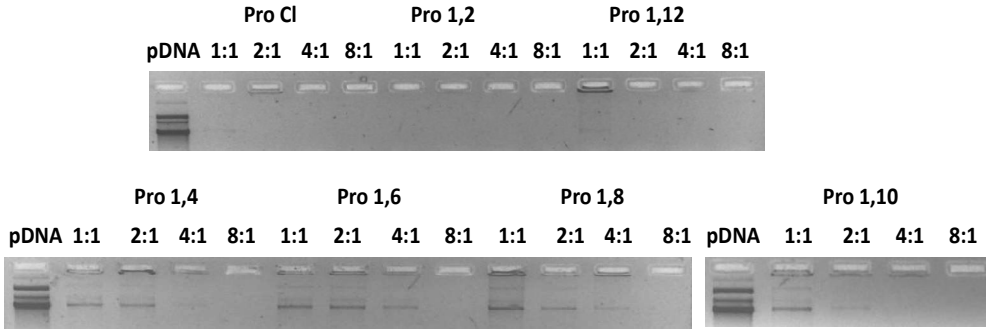

Figure 3. DNA binding patterns of lipoplexes at different ratios of liposomes: pDNA on agarose gel electrophoresis.

5.2.4 pDNA transfection:

The qualitative and quantitative analyses of prepared liposomes (1:1, 2:1, 4:1 and 8:1 ratios) for their transfection potentials were carried out using enhanced green fluorescent protein (eGFP) encoded plasmid DNA in three different cell lines (HEK293, Neuro-2a and HepG2). It was observed from the fluorescence microscopy as well as flow cytometry studies that, lipoplexes exhibited their highest eGFP expression at 1:1 charge ratio. The percentage of eGFP positive cells in HEK293, CHO and Neuro-2a cell lines measured at 1:1 ratio using flow cytometry is depicted in Figure. 4 respectively. Herein, it is observed that there is a significant increase in the transfection efficiency from monomeric lipid, Pro-Cl to the Gemini lipid, Pro- 1,2. Further it is observed that there is a decrease in the transfection efficiency with the spacer length from 2 to 6 and on further increase in the spacer length to 12, the transfection efficiency is increasing, in all the cell lines studied. The lipids Pro-1,2 and Pro-1,12 at 1:1 charge ratio exhibiting comparable transfection to LF3000 in all the cell lines studied. It has been reported that, the optimized transfection efficiency of pDNA was higher for lipoplexes containing gemini cationic lipids with a longer or shorter spacer[49,50]. High transfection efficiency observed at Pro-1,2 was probably due to the distance between two cationic head groups on gemini cationic lipids. As the cationic head groups are moving away from each other the complexation abilities were going down. But complexation abilities were regained at Pro-1,12 and showed high transfection efficiency maybe because of flexibility between two cationic head groups. In

summary, the gemini lipid Pro-1,2 is highly transfection potential when compared to the monomeric lipid and also the spacer length played a major role in tuning the transfection efficiencies of the gemini lipids, the shorter and the longer spacers observed to be improving the transfection potentials of the gemini lipids significantly.

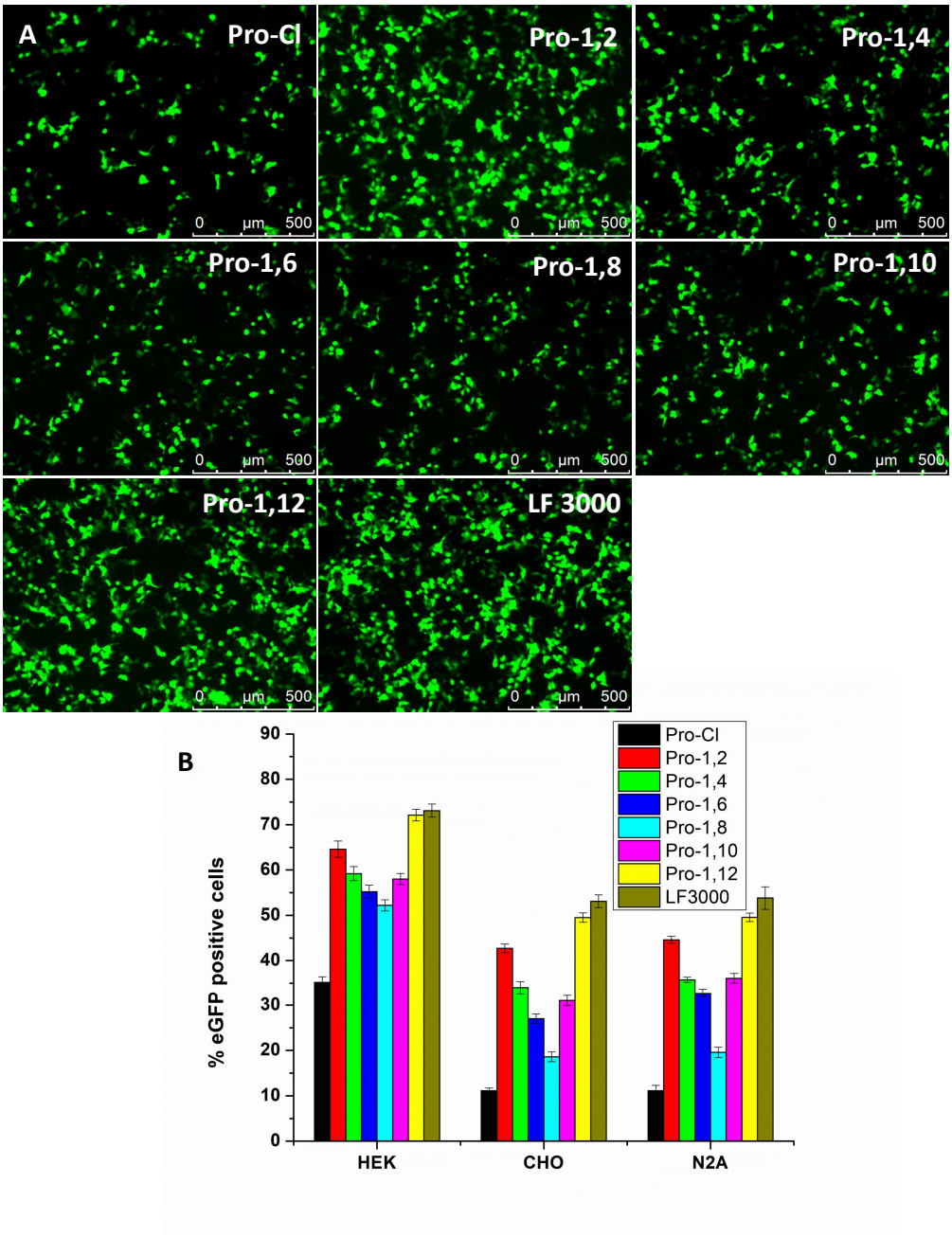

Figure 4. (A) Fluorescent microscopic images and flow cytometry analysis of liposomes with best charge ratio 1:1 in Hek 293 cell line. (B) Comparative *in vitro* pDNA transfection efficiencies by flow cytometry in different cell lines at lipid/DNA 2:1 charge ratio (n=2)

5.2.5 Cytotoxicity study of lipids:

Another important feature that increases the probability of a synthetic gene delivery vector being used in medical gene therapy is its low cytotoxicity. To determine the safety of the synthesized cationic lipids under evaluation, the MTT assay was used[51]. The viability of all synthesized gemini lipid/pDNA complexes in HEK-293 and Neuro-2a cell lines was examined (Figure 5A and Figure 5B respectively) at N/P ratios of 1:1–8:1. Cell viability of all the lipid complexes was observed to be maximum at 1:1 and 2:1 lipid:pDNA N/P ratio and slightly decreased at 4:1 and 8:1 lipid:pDNA N/P ratio . As a result, the mentioned cationic lipids are potential transfection reagents with minimal cytotoxicity, which is an important feature for *in vitro* applications.

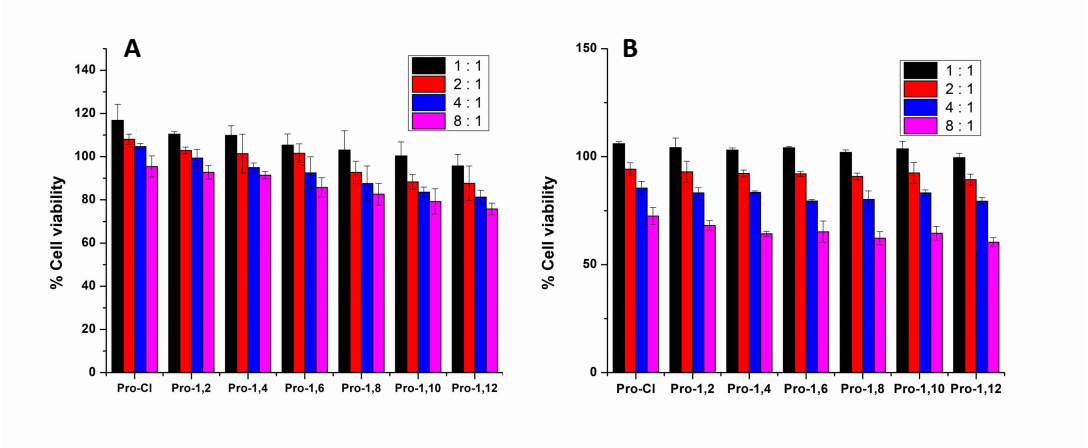

Figure 5. % Cell viability of Pro-Cl, Pro-1,2, Pro-1,4, Pro-1,6, Pro-1,8, Pro-1,10 and Pro-1,12 lipoplexes at different N/P ratios in HEK-293 (A), Neuro-2A (B) cell line

5.3 Conclusions:

When combined with the helper lipid DOPE, the recently synthesised proline gemini cationic lipids were able to form tiny unilamellar vesicles, and the ideal molar ratio was optimised. Using a gel electrophoresis experiment, the DNA binding potentials of various lipid formulations were carefully examined. The resulted data suggests that, spacer chain length is the major determining factor to condense the DNA which has led to affect the transfection further. The results derived from transfection of eGFP pDNA in multiple cell lines demonstrate that the transfection efficiencies of the present series of lipids greatly dependent on the spacer chain length. All the experimental results support that the two and twelve methylene aliphatic spacer

containing gemini lipids (Pro-1,2 and Pro-1,12) has shown the maximum potential among the series of lipids studied in delivering plasmid DNA. The superior activity, DNA compaction potentials and least toxicity of these present dimeric lipids can be further explored in *in-vivo* systemic applications.

5.4 Experimental Section:

5.4.1 Materials & Methods:

In this work, all of the reactions and experiments were conducted using reagents and solvents that were purchased at the highest purity from Sigma, Spectrochem, and Alfa Aeser and used without additional purification. We bought silica gel thin-layer chromatography plates (0.25 mm) from Merck to track the development of the reaction. A Varian FT400 MHz NMR spectrometer was used to record the ^{1}H and ^{13}C NMR spectrum data. Using a commercial LCQ ion trap mass spectrometer with an ESI source, mass spectral data were obtained (Thermo Finnigan, SanJose, CA, U.S.). Sigma-Aldrich provided the co-lipid DOPE for the synthesis of liposomes. The FBS, PBS, MTT, and trypsin are the ingredients that are employed in all biological experiments. These items were obtained from Thermo Fischer Scientific and Invitrogen.

5.4.2 Synthesis of Boc Proline:

To a 100 mL of RB flask a solution of 4.4 g (1.1 mol) of sodium hydroxide in 11 mL of water and 1.151 g (1 mol) of L-proline were added while stirring. The mixture is then diluted with 7.5 mL of tert-butyl alcohol . To the well-stirred, clear solution 2.23 g (1 mol) of di- tert -butyl dicarbonate was added slowly dropwise. A white precipitate appears during addition of the di- tert -butyl dicarbonate and stirred the resulting solution at RT about overnight. At this time, the clear solution will have reached a pH of 7.5–8.5. The reaction mixture was extracted two times with 100 mL of hexane, and the organic phase was washed three times with 100 mL of saturated aqueous sodium bicarbonate solution. The combined aqueous layers are acidified to pH 1–1.5 by careful addition of a solution of 2.24 g (1.65 mol) of potassium hydrogen sulfate in water. The turbid reaction mixture is then extracted with 100 mL of hexane. The combined organic layers are washed two times with 200 mL of water, dried over anhydrous sodium sulfate. The solvent is removed under reduced pressure using a rotary evaporator. The yellowish oil that remains is treated with 1.5 mL of hexane and allowed to stand

overnight. Within 1 day the following portions of hexane are added with stirring to the partially crystallized product: 2 ×0.5 mL, 4 × 1 mL, and 1 × 2 mL. The solution is placed in a refrigerator overnight; the white precipitate is collected and washed with cold hexane.

5.4.3 Synthesis of compound 1b:

1mmol (0.15 g) of Boc-Proline and 1.5 mmol of Diisopropylethylamine (0.145 mL) in 10 mL of DCM were taken in a 100mL of RB flask and kept it for stirring in ice bath at 0°C. After five minutes of stirring sequentially HOBT (0.13 g, 1.5 mmol), EDCI.HCl (0.16 g, 1.5 mmol) were added to the stirred reaction mixture. After 10 minutes of stirring at 0 °C dodecylamine (0.13 mL, 1.2 mmol) was added, raised the temperature to rt and continued the stirring overnight. After consumption of starting materials, the resulting reaction mixture was transferred to separating funnel using excess DCM and gave 2 times water washing then 1 time brine washing respectively. The solvent was dried on sodium sulphate and the solvent was evaporated on rotary evaporator. The crude was purified by using column chromatography with 100-200 mesh silica gel, eluting with 15% (v/v) Hexane in ethyl acetate (Rf = 0.4, 20% Hexane in ethyl acetate).

5.4.4 Synthesis of compound 1c:

1mmol of Boc protected compound was taken into 8 mL of dry DCM in a 50 mL RB flask. The flask was placed in an ice cooled solution and 4 mL of TFA was added at 0°C and the temperature was raised to RT and continued the stirring overnight. The solvent and excess TFA were evaporated under reduced pressure and the obtained residue was dissolved in ethyl acetate and the solvent was evaporated by rotary evaporation. The resulting compound was dissolved in dichloromethane and gave washings with aqueous sodium carbonate to get free amine. The compound was pure and 99% yielded.

5.4.5 Synthesis of compound 1d:

The chemical 1c and a magnetic stir bar were added to 3 mL of dry acetonitrile to fill a 30 mL screw-top pressure tube. The proper amount of methyl iodide was added, and the mixture was then set up for a 24-hour reflux at 80 °C. Cooling of the reaction mixture and vacuum-assisted solvent evaporation. After several rounds of washing with the CHCl3: EtOAC mixture, the crude reaction mixture produced a pure product with an 80% yield. The Rf was 0.3 in a 9:1 CHCl3/MeOH solution.

5.4.6 Synthesis of compound 1e:

2eq of compound 1c, 1eq of dibromo alkane and excess amount of oven dried K_2CO_3 were taken in a 50 mL RB flask to that 5mL of acetonitrile was added then placed for the reflux at 80 °C for about 24 hrs. Reaction mixture was cooled and solvent was evaporated under the vacuum. After the initial components were consumed, the reaction mixture that resulted was transferred to a separating funnel using extra DCM and subjected to two rounds of water washing and one round of brine washing, respectively. On sodium sulphate, the solvent was dried, and then it was evaporated on a rotary evaporator. By utilising column chromatography and silica gel of 100–200 mesh to purify the crude, it was eluted with 1–2% (v/v) CH3OH/CHCl3. (Rf = 0.2 to 0.4, 5% CH_3OH/ $CHCl_3$).

5.4.7 General procedure of 1f derivatives:

The component 1d derivatives and a magnetic stir bar were added to 3 mL of dry acetonitrile to fill a 30 mL screw-top pressure tube. Methyl iodide was added in the proper quantity, and the mixture was then set up for a 72-hour reflux at 80 °C. Under a vacuum, the solvent was evaporated while the reaction mixture was cooled. After several rounds of washing with the CHCl3: EtOAC mixture, the crude reaction mixture produced a pure product with an 80% yield. In a 9:1 CHCl3/MeOH solution, the Rf varied from 0.3 to 0.6.

Control Lipid Pro-Cl:

^{1}H NMR (400 MHz, $CDCl_3$) δ 9.12 (s, 1H), 4.93 (s, 1H), 3.86 – 3.56 (m, 3H), 3.32 (s, 3H), 3.15 (d, *J* = 27.5 Hz, 4H), 2.76 – 1.86 (m, 4H), 1.43 (d, *J* = 6.2 Hz, 2H), 0.95 (d, *J* = 142.9 Hz, 18H), 0.75 (dd, *J* = 9.1, 4.1 Hz, 3H). ^{13}C NMR (101 MHz, $CDCl_3$) δ 165.41, 73.96, 65.91, 52.66, 48.40, 48.35, 39.88, 31.80, 29.53, 29.24, 29.15, 28.94, 26.97, 25.51, 22.55, 20.87, 14.02. HRMS-m/z: 311.3057, found: 311.3062

Lipid-1 Pro-1,2:

^{1}H NMR (400 MHz, $CDCl_3$) [*δ*/ppm] 9.12 (d, *J* = 49.2 Hz, 2H), 4.79 (d, *J* = 104.7 Hz, 2H), 4.33 (d, *J* = 34.0 Hz, 3H), 4.21 – 3.96 (m, 4H), 3.96 – 3.76 (m, 2H), 3.28 (dd, *J* = 48.7, 15.2 Hz, 10H), 2.66 – 2.53 (m, 2H), 2.29 (dd, *J* = 25.6, 17.7 Hz, 6H), 2.07 (dd, *J* = 25.1, 12.8 Hz, 2H), 1.54 (s, 5H), 1.34 – 1.06 (m, 34H), 0.86 (t, *J* = 6.7 Hz, 6H). ^{13}C NMR

(101 MHz, $CDCl_3$) δ 164.62, 164.27, 74.07, 57.51, 56.46, 45.59, 43.34, 41.21, 40.28, 40.20, 31.91, 29.65, 29.36, 29.26, 28.97, 27.09, 22.69, 14.13.

Lipid-2 Pro-1,4:

^{1}H NMR (400 MHz, $CDCl_3$) [*δ*/ppm] 9.43 (s, 2H), 5.23 (d, *J* = 73.2 Hz, 2H), 3.91 – 3.65 (m, 3H), 3.59 (s, 3H), 3.09 (t, *J* = 41.2 Hz, 12H), 2.52 (s, 2H), 2.27 (dd, *J* = 23.6, 9.6 Hz, 6H), 1.94 – 1.58 (m, 4H), 1.52 (s, 4H), 1.19 (s, 52H), 0.82 (t, *J* = 6.8 Hz, 6H). ^{13}C NMR (101 MHz, $CDCl_3$) δ 166.41, 165.27, 74.29, 74.03, 63.90, 63.54, 63.46, 63.02, 61.01, 49.07, 44.36, 39.98, 39.84, 31.87, 29.61, 29.55, 29.31, 29.24, 29.22, 28.96, 28.92, 28.86, 28.82, 28.79, 28.74, 28.61, 27.06, 26.41, 26.34, 26.18, 26.10, 26.02, 25.83, 25.35, 24.06, 23.56, 22.64, 20.98, 20.31, 14.09.

Lipid-3 Pro-1,6:

^{1}H NMR (400 MHz, $CDCl_3$) δ 9.20 (d, *J* = 32.9 Hz, 2H), 4.87 (s, 2H), 3.89 (s, 7H), 3.56 – 3.41 (m, 3H), 3.16 (d, *J* = 44.0 Hz, 10H), 2.49 (s, 2H), 2.23 (d, *J* = 12.2 Hz, 5H), 2.03 – 1.83 (m, 4H), 1.24 (d, *J* = 57.7 Hz, 42H), 0.82 – 0.78 (m, 6H). ^{13}C NMR (101 MHz, $CDCl_3$) δ 166.76, 165.53, 73.53, 73.29, 73.14, 72.71, 64.90, 64.63, 64.06, 64.05, 63.88, 63.65, 60.83, 49.48, 49.36, 44.82, 44.55, 39.91, 39.69, 31.85, 29.58, 29.30, 29.26, 29.22, 29.12, 28.98, 28.94, 27.03, 14.07, 14.07, 14.06.

Lipid-4 Pro-1,8:

^{1}H NMR (400 MHz, $CDCl_3$) δ 9.21 (t, *J* = 21.4 Hz, 2H), 5.13 – 4.76 (m, 2H), 3.73 (s, 7H), 3.56 (d, *J* = 12.3 Hz, 3H), 3.28 – 3.03 (m, 9H), 2.48 (s, 2H), 2.17 (d, *J* = 68.4 Hz, 6H), 1.80 (s, 4H), 1.53 – 0.99 (m, 46H), 0.86 – 0.71 (m, 6H). ^{13}C NMR (101 MHz, $CDCl_3$) δ 166.76, 165.53, 73.53, 73.29, 73.14, 72.71, 64.90, 64.63, 64.06, 64.05, 63.88, 63.65, 60.83, 49.48, 49.36, 44.82, 44.55, 39.91, 39.69, 31.85, 29.58, 29.30, 29.26, 29.22, 29.12, 28.98, 28.94, 27.03, 14.07, 14.07, 14.06.

Lipid-4 Pro-1,10:

^{1}H NMR (400 MHz, $CDCl_3$) δ 9.20 (s, 2H), 5.16 (d, *J* = 64.8 Hz, 2H), 3.93 – 3.55 (m, 6H), 3.22 (d, *J* = 33.0 Hz, 14H), 2.43 (d, *J* = 97.0 Hz, 7H), 2.11 – 1.83 (m, 3H), 1.82 – 1.17 (m, 52H), 0.91 – 0.84 (m, 6H). ^{13}C NMR (101 MHz, $CDCl_3$) δ 166.43, 165.21, 73.97, 73.86, 73.70, 73.62, 64.07, 64.03, 63.40, 63.33, 61.04, 60.99, 49.12, 44.61, 44.52, 39.91, 39.73, 31.83, 29.56, 29.52, 29.27, 29.18, 28.96, 28.91, 28.45, 28.32, 28.28, 28.22,

28.15, 28.05, 27.01, 26.17, 25.98, 25.89, 25.84, 25.49, 23.92, 23.83, 23.37, 23.29, 22.61, 20.88, 20.34, 20.31, 14.06. HRMS-m/z:732.7209, found: 732.7244

Lipid-1 Pro-1,12:

^{1}H NMR (400 MHz, $CDCl_3$) δ 9.43 (s, 2H), 5.23 (d, *J* = 73.2 Hz, 2H), 3.91 – 3.65 (m, 3H), 3.59 (s, 3H), 3.09 (t, *J* = 41.2 Hz, 12H), 2.52 (s, 2H), 2.27 (dd, *J* = 23.6, 9.6 Hz, 6H), 1.94 – 1.58 (m, 4H), 1.52 (s, 4H), 1.19 (s, 52H), 0.82 (t, *J* = 6.8 Hz, 6H). ^{13}C NMR (101 MHz, $CDCl_3$) δ 166.41, 165.27, 74.29, 74.03, 63.90, 63.54, 63.46, 63.02, 61.01, 49.07, 44.36, 39.98, 39.84, 31.87, 29.61, 29.55, 29.31, 29.24, 29.22, 28.96, 28.92, 28.86, 28.82, 28.79, 28.74, 28.61, 27.06, 26.41, 26.34, 26.18, 26.10, 26.02, 25.83, 25.35, 24.06, 23.56, 22.64, 20.98, 20.31, 14.09. HRMS-m/z:760.7522, found: 760.7540

5.4.8 Preparation of Liposomes:

Liposomes were prepared following previous protocol[52]. The final concentrations of TGK with co lipid DOPE and CGK with co lipid DOPE in chloroform were taken at 1:1 molar ratio respectively. 1 mM liposomes were used for *in vitro* studies.

5.4.9 Zeta potential (ξ) and size measurements:

On an Anton Paar Lite SizerTM500Particle Analyzer, the hydrodynamic diameter and surface charges (zeta potentials) of the nano-formulations were examined. For stability, the sizes were tested in 10% FBS and deionized water, respectively. Utilizing the 200 nm + 5 nm polystyrene polymer, the system was calibrated (Duke Scientific Corps., Palo Alto, CA). The following factors were used to calculate the zeta potential: viscosity (0.89 cP), dielectric constant (79), temperature (25 °C), F(Ka), 1.50 (Smoluchowski), and maximum current voltage (V). Ten measurements with the zero-field adjustment were made. The Smoluchowskiapproximation was used to compute the potentials.

5.4.10 DNA-binding assay:

An agarose gel retardation assay was used to test the DNA binding properties of the improved cationic co-liposomal formulations (lipid/DOPE, 1:1). In following experiment, 500 ng of pCMV-gal was complexed with each cationic formulation in 1x PBS (24 µL) at four different N/P (liposome/plasmid) charge ratios of 1:1, 2:1, 4:1 and 8:1. Followed by prepared complexes incubated for 30 minutes. After adding 6x loading dye to the sample, these complexes (12 µL each) were loaded into a freshly prepared 1%

agarose gel dyed with EtBr. In a 100 V electrophoresis chamber, electrophoresis was performed for 35 minutes in 1x TAE running buffer. The gel photos were captured in transillumination mode using a gel documentation system.

5.4.11 pDNA Transfection Biology:

Fluorescence microscopy and flow cytometry were used, respectively, to analyse the qualitative and quantitative aspects of the cationic lipoplexes' ability to express eGFP. At least 12 hours before the transfection studies, cells were planted in a 48-well plate at a density of 25000/well (for HEK-293, CHO, and Neuro-2a). In serum-free media with a final volume of 40 µL for 30 minutes, lipoplexes were created by utilising pDNA (0.4 µg) and the liposomes of TGK and CGK at a 1:1 to 8:1 lipid/DNA charge ratio. The cells were added to the prepared lipoplexes. Using a previously described method[53], the reporter gene activity was calculated after 36–48 h of incubation. Following the period of incubation, GFP expression was imaged using a fluorescent microscope (Leica CTR 6000, Germany), and the results were quantified using FACS. Here, the transfection reagent LF 3000, which is available commercially, acted as a positive control.

5.4.12 Cell viability assay:

The lipoplexes formulations were tested for toxicity using the MTT-based assay, which involves the reduction of MTT by feasible cells to produce purple, insoluble formazan granules. Colorimetric analysis counts the number of feasible cells and compares the intensity of the colour to that number. Lipid toxicities for lipoplexes prepared using liposomes and pDNA at varying lipid/DNA charge ratios (1:18:1) were assessed using an MTT-based colorimetric reduction assay by incubating for 20 min at room temperature, followed by treating Neuro- 2a and HEK-293 cells with the prepared lipoplexes for 24 h at 37 °C in 10% serum-containing DMEM. MTT dye (5 mg/mL) was freshly prepared in serum-free DMEM and 100 µL was added to each well after 24 hours of incubation. The test was then stopped after 3 hours of incubation. After that, 100 µL of DMSO was added after the media had been taken out of each well. The untreated cells were used as controls. Next, the purple dye was dissolved and detected spectroscopically at 540 nm in a multiplate reader. A540 (treated cells)-background/A540 (untreated cells)-background x 100 was used to compute the % viability.

5.5 References

1. Naldini, L., *Nature*. **2015**, *526*, 351.
2. Ginn, S.L.; Alexander, I. E.; Edelstein, M. L.; Abedi, M. R.; Wixon, J. *J GeneMed.* **2013**, *15*, 65.
3. Jin, L.; Zeng, X.; Liu, M.; Deng, Y.; He, N. *Theranostics*. **2014**, *4*, 240.
4. Nayerossadat, N.; Maedeh, T.; Ali, P. A. *Adv Biomed Res.* **2012**, *1*, 27.
5. Yin, H.; Kanasty, R. L.; Eltoukhy, A. A.; Vegas, A. J.; Dorkin, J. R.; Anderson, D. G. *Nat Rev Genet.* **2014**, *15*, 541.
6. Thomas, C. E.; Ehrhardt, A.; Kay, M. A. *Nature Rev Genet.* **2003**, *4*, 346.
7. Mintzer, M. A.; Simanek, E. E. *Chem Rev.* **2008**, *109*, 259.
8. Felgner, P. L.; Gadek, T. R.; Holm, M.; Roman, R.; Chan, H. W.; Wenz, M.; Northrop, J. P.; Ringold, G. M.; Danielsen, M. *Proc. Natl. Acad. Sci. U.S.A.* **1987**, *84*,7413.
9. Srinivas, R.; Samanta, S.; Chaudhuri, A. *Chem Soc Rev.* **2009**, *38*, 3326.
10. Karmali, P. P.; Chaudhuri, A. *Med Res Rev.* **2007**, *27*, 696.
11. Balazs, D. A.; Godbey, W. T. *J Drug Deliv.* **2010**, *2011*.
12. Du, Z.; Munye, M. M.; Tagalakis, A. D.; Manunta, M. D.; Hart, S. L. *Sci. Rep.* **2014**, *4*, 7107.
13. Fasbender, A.; Marshall, J.; Moninger, T. O.; Grunst, T.; Cheng, S.; Welsh. M.J. *Gene Ther.* **1997**, *4*, 716.
14. Bhattacharya, S.; Bajaj, A. *Chem. Commun.* **2009**, *31*, 4632.
15. Karmali, P. P.; Chaudhuri, A. *Med Res Rev*, **2007**, *27*, 696.
16. Bajaj, A.; Kondaiah, P. and Bhattacharya, S. *Biomacromolecules*, **2008**, *9*, 991.
17. Bajaj, A.; Kondiah, P. and Bhattacharya, S. *J. Med. Chem.* **2007**, *50*, 2432.
18. Biswas, J.; Mishra, S. K.; Kondaiah, P. and Bhattacharya, S. *Org. Biomol. Chem.* **2011**, *9*, 4600.
19. Munoz-ubeda, M.; Misra, S. K.; Barran-Berdon, A. L.; Aicart-Ramos, C.; Sierra, M. B.; Biswas, J.; Kondaiah, P.; Junquera, E.; Bhattacharya, S. and Aicart, E.; *J. Am. Chem. Soc.*, **2011**, *133*, 18014.

20. Misra, S. K.; Naz, S.; Kondaiah, P. and Bhattacharya, S. *Biomaterials*, **2014**, *35*, 1334.

21. Bombelli, C.; Faggioli, F.; Luciani, P.; Mancini, G. and Sacco, M. G. *J. Med. Chem.*, **2005**, *48*, 5378.

22. Rosenzweig, H. S.; Rakhmanova, V. A. and MacDonald, R. C. *Bioconjugate Chem.*,**2001**, *12*, 258.

23. Chien, P. Y.; Wang, J.; Carbonaro, D.; Lei, S.; Miller, B.; Sheikh, S.; Ali, S. M.; Ahmad, M. U. and Ahmad, I. *Cancer Gene Ther.*, **2005**, *12*, 321.

24. Damen, M.; Aarbiou, J.; van Dongen, S. F.; Buijs- Offerman, R. M.; Spijkers, P. P.; van den Heuvel, M.; Kvashnina, K.; Nolte, R. J.; Scholte, B. J. and Feiters, M. C. *J. Controlled Release*, **2010**, *145*, 33.

25. Zhao, Y. N.; Qureshi, F.; Zhang, S. B.; Cui, S. H.; Wang, B.; Chen, H. Y.; Lv, H. T.; Zhang, S.-F. and Huang, L. *J. Mater. Chem. B*, **2014**, *2*, 2920.

26. Sharma, V. D.; Aifuwa, E. O.; Heiney, P. A. and Ilies, M. A. *Biomaterials*, **2013**, *34*, 6906.

27. Wettig, S. D.; Verrall, R. E. and Foldvari, M. *Curr. Gene Ther.,* **2008**, *8*, 9.

28. Wettig, S. D.; Badea, I.; Donkuru, M.; Verrall, R. E. and Foldvari, M. *J. Gene Med.*, **2007**, *9*, 649.

29. Badea, I.; Verrall, R.; Baca-Estrada, M.; Tikoo, S.; Rosenberg, A.; Kumar, P. andFoldvari, M. *J. Gene Med.*, **2005**, *7*, 1200.

30. Donkuru, M.; Wettig, S. D.; Verrall, R. E.; Badea, I. and Foldvari, M. *J. Mater.Chem.*, **2012**, *22*, 6232

31. Kumar, K.; Maiti, B.; Kondaiah, P. Bhattacharya, S. *Mol Pharm*, **2014**, *12*, 351.

32. Kedika, B.; Patri, S. V. *Mol Pharm*, **2012**, *9*, 1146.

33. Bajaj, A.; Kondaiah, P.; Bhattacharya, S. *Bioconjugate Chem*, **2007**, *18*, 1537.

34. Bajaj, A.; Kondaiah, P.; Bhattacharya, S. *J Med Chem*, **2008**, *51*, 2533.

35. Fasbender, A.; Marshall, J.; Moninger, T. O.; Grunst, T.; Cheng, S.; Welsh, M. J.*Gene Ther*, **1997**, *4.*

36. Du, Z.; Munye, M. M.; Tagalakis, A. D.; Manunta, M. D.; Hart, S. L.; *Sci Rep*, **2014**,*4*.

37. Mochizuki, S.; Kanegae, N.; Nishina, K.; Kamikawa, Y.; Koiwai, K.; Masunaga, H.;Sakurai, K. *(BBA)-Biomembranes*, **2013**, *1828*, 412.
38. Cheng, X.; Lee, R. J. *Adv Drug Deliv Rev*, **2016**, *99*, 129.
39. Walters, KA.; Bialik, W.; Brain, KR.; Int J Cosmet Sci, 1993, 15(6), 260-71.
40. Tan, EL.; Lid, JC.; Chien, YW.; Drug Dev Ind Pharm, 1993, 19(6), 685-99.
41. Babu. R,; Mandip, S.; Narayanasamy, K.; 2nd ed. Informa Healthcare, 2005, p.17-33.
42. Ashton, P.; Walters, KA.; Brain, KR.; Hadgraft, J.; Int J Pharm, 1992, 87(1-3): 261-4.
43. Kitagawa, S.; Kasamaki, M.; Ikarashi, A.; Chem Pharm Bull, 2000; 48:1698-701.
44. Lopez, A.; Llinares, F.; Cortell, C.; Herraez, M.; Int J Phram 2000; 202(1-2); 133-40.
45. Isabel Calaza, M.; Cativiela, C.; Eur.J.Org.Chem 2008;3427-3448.
46. Hernandez, TJ.; Padilla Silvia., Adrio Javier.; Carretero, JC.; Angew.Chem.Int.Ed. 2012;51, 1-6.
47. Dua, J. S.; Rana, A. C.; Bhandari, A. K. *Int J Pharm Stud Res*, **2012**, *3*, 14.
48. Chandrashekhar, V.; Srujan, M.; Prabhakar, R.; Rakesh Reddy, C.; Sreedhar, B.;Kiran, R.; Sanjit, K.; Chaudhuri, A. *Bioconjug Chem,* **2011***, 22*, 497.
49. Munoz-Ubeda, M.; Misra, SK.; Barran-Berdon, L.; Data, S.; Aicart-Ramos, C.; Castro-Hartmann, P.; Kondaiah, P.; Junquera, E., Bhattacharya, S.; Aicart, E.; Biomacromolecules 2012; 13, 3926-3937.
50. Ana L.Barran-Berdon; Santosh K. Misra; Sougata Datta; Monica Munoz-Ubeda; Paturu Kondaiah; Elena Junquera; Santanu Bhattacharya; Emilio Aicart; J.Mater.Chem.B 2014;2, 4640.
51. Gosangi, M.; Rapaka, H.; Ravula, V.; Patri, S. v; *Bioconjugate Chemistry* **2017**, *28* (7). https://doi.org/10.1021/acs.bioconjchem.7b00283
52. A. Ahmad, S.K. Mondal, D. Mukhopadhyay, R. Banerjee, K.M. Alkharfy; Molecular pharmaceutics 13(3) (2016) 1081-1088.
53. Gosangi, M.; Rapaka, H.; Mujahid, T. Y.; Patri, S. v; *MedChemComm* **2017**, *8* (5), 989-999. https://doi.org/10.1039/c6md00699j.

5.6 Spectral Data

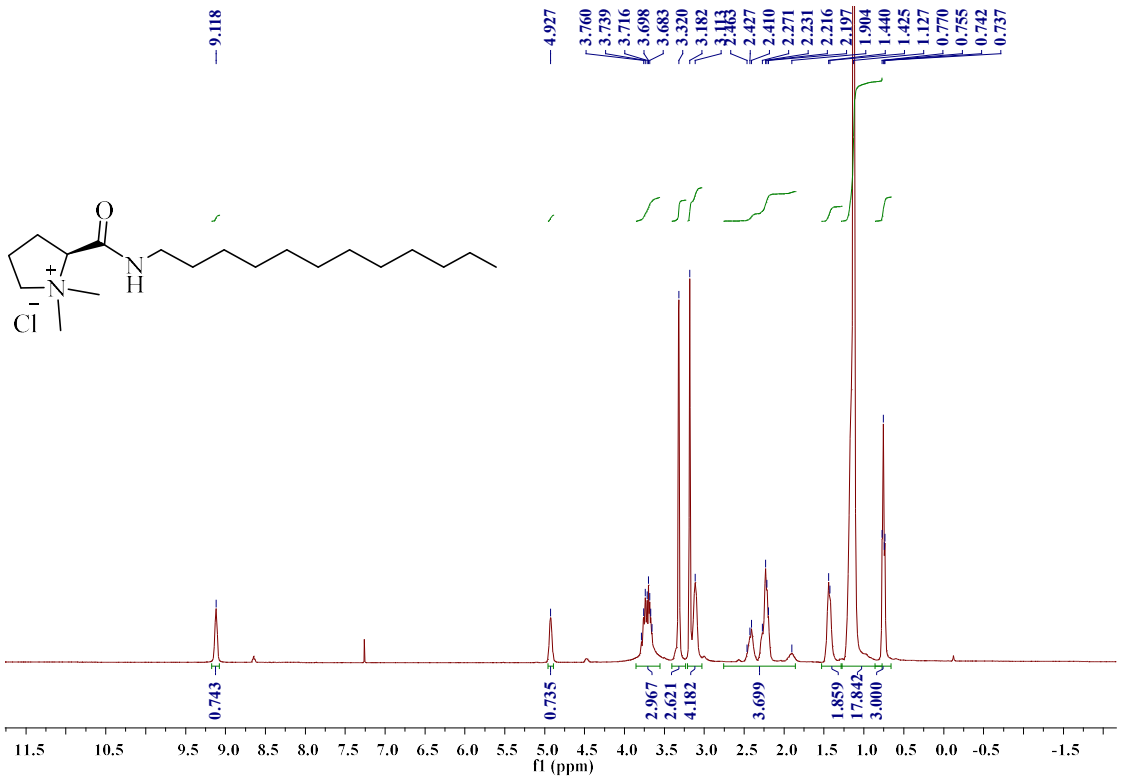

^{1}H NMR Spectrum of **Lipid Pro-Cl**

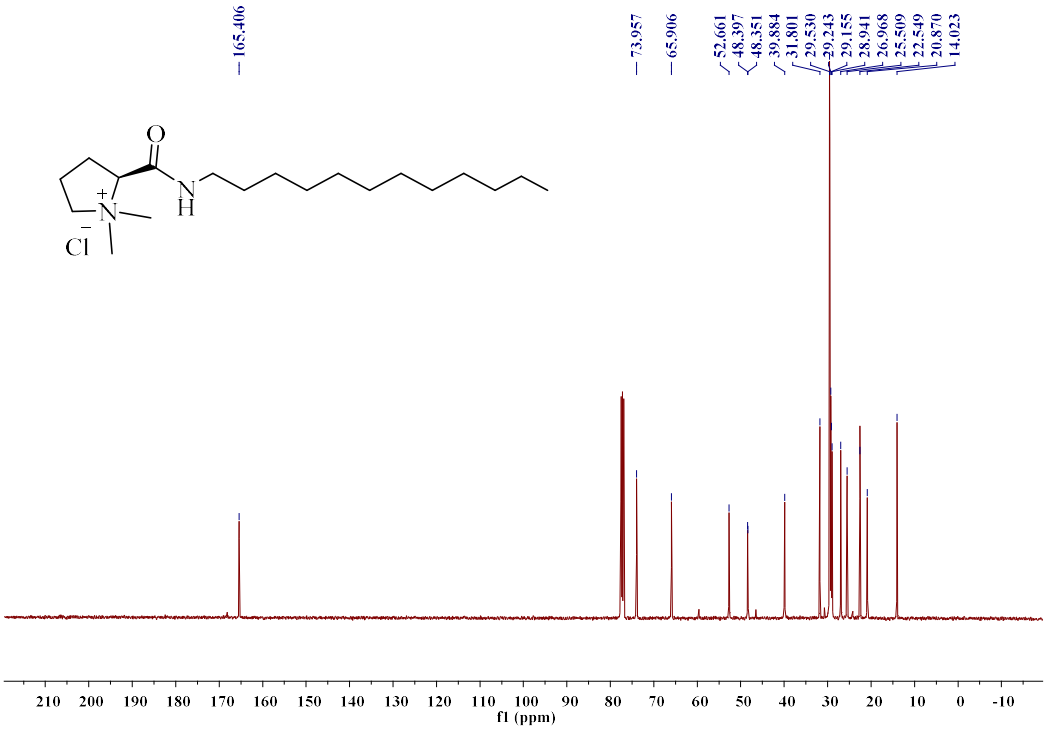

^{13}C NMR Spectrum of **Lipid Pro-Cl**

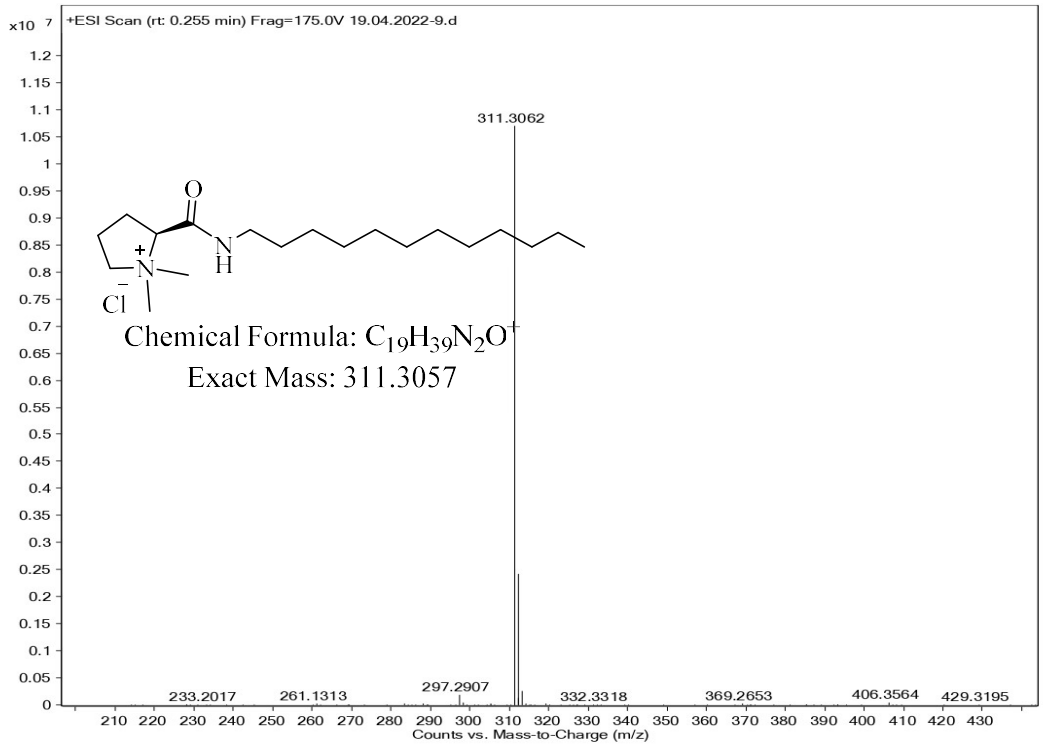

ESI-HRMS Spectrum of **Lipid Pro-Cl**

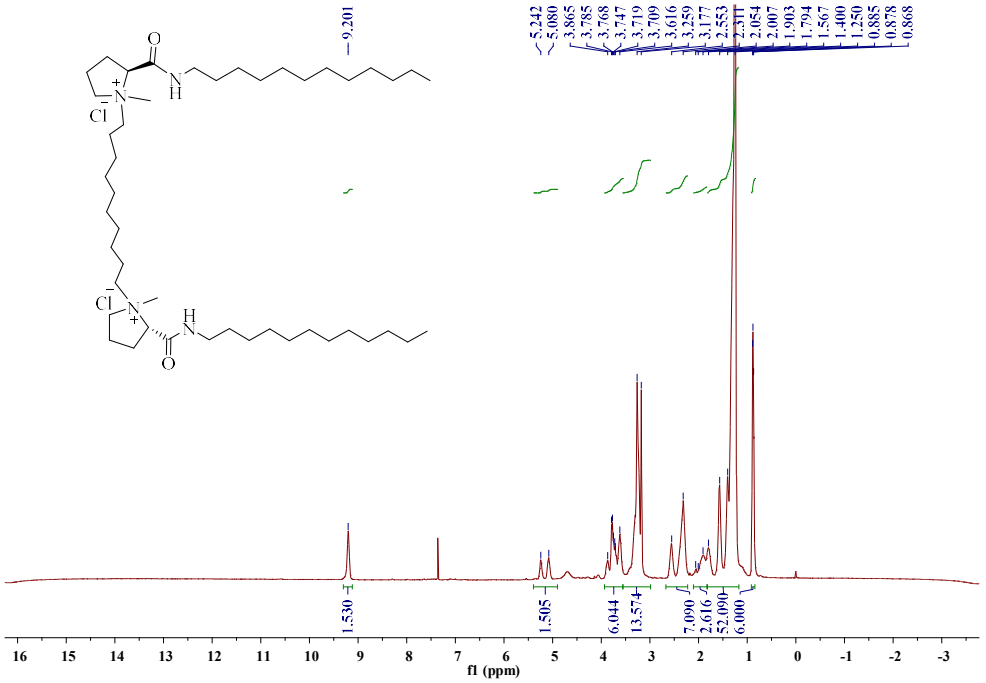

^{1}H NMR Spectrum of **Lipid Pro-1,10**

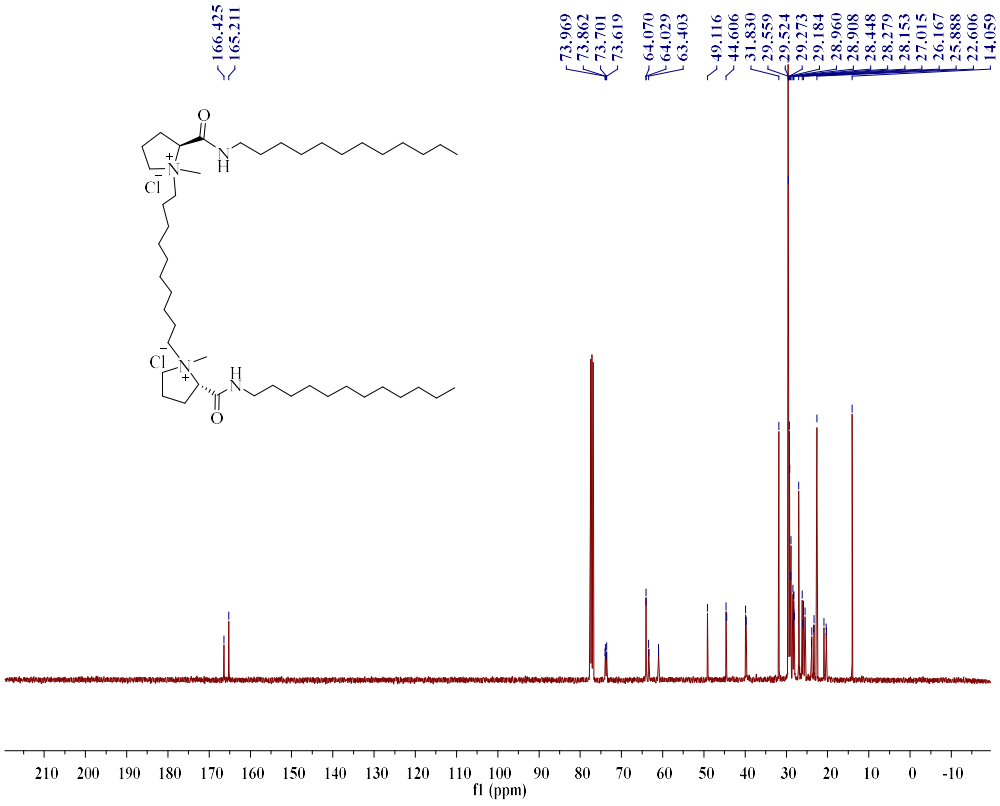

^{13}C NMR Spectrum of **Lipid Pro-1,10**

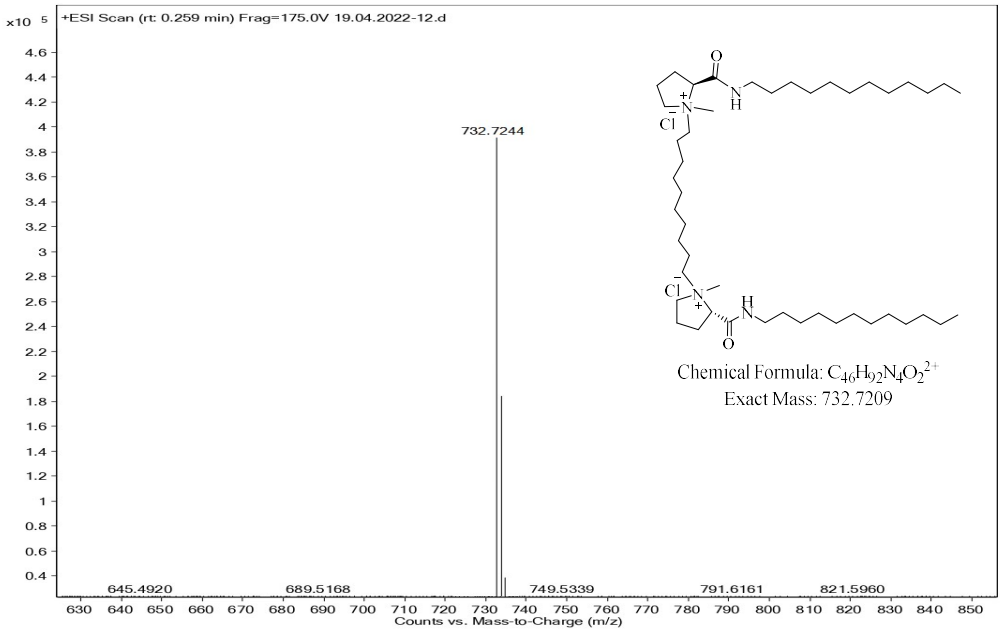

ESI-HRMS Spectrum of **Lipid Pro-1,10**

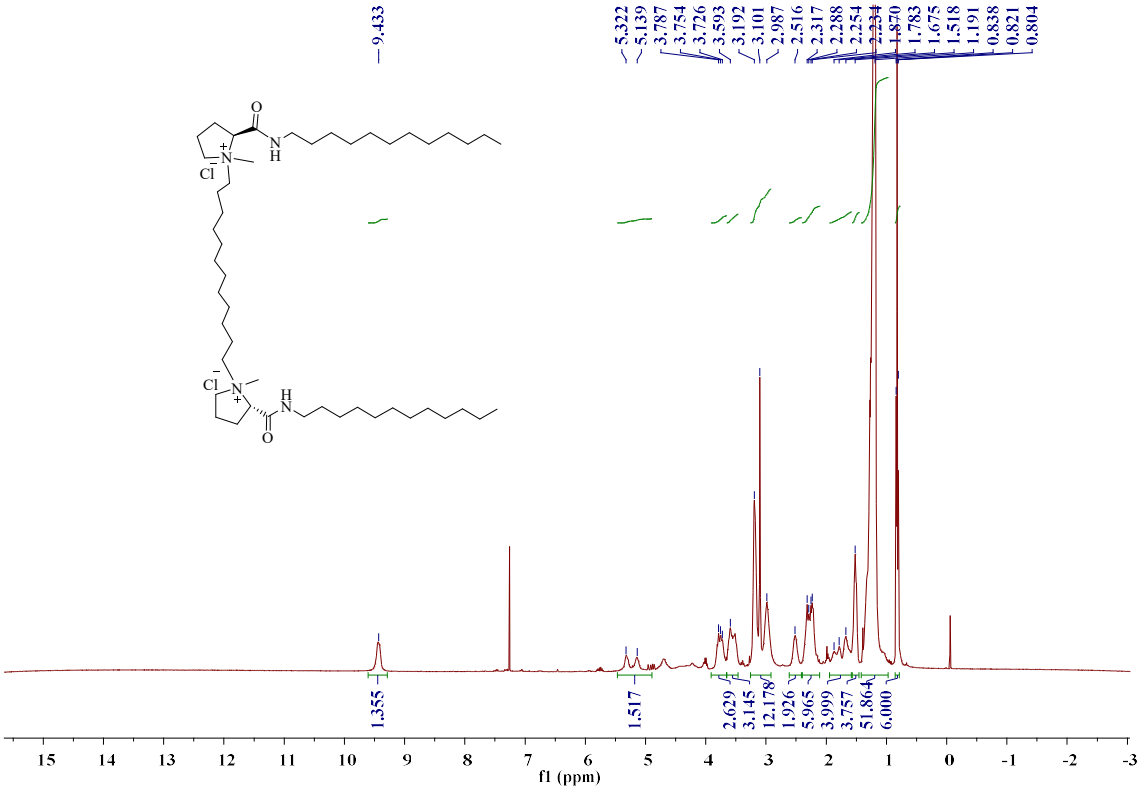

^{1}H NMR Spectrum of **Lipid Pro-1,10**

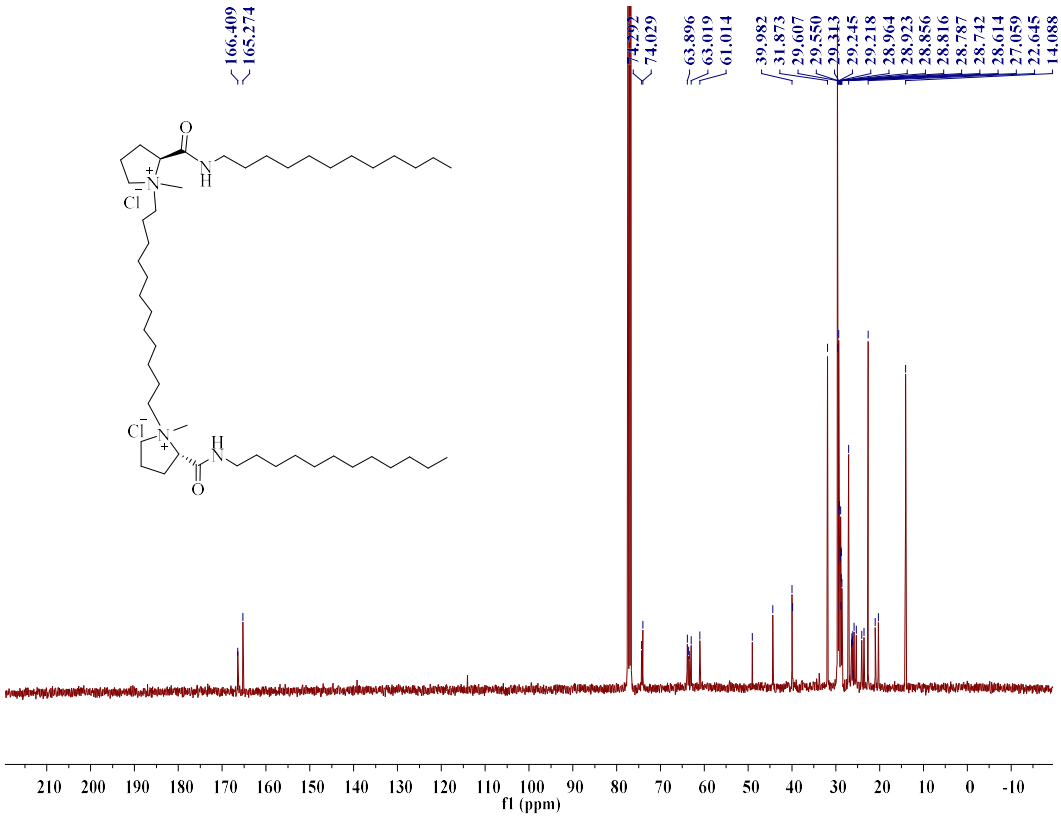

^{13}C NMR Spectrum of **Lipid Pro-1,12**

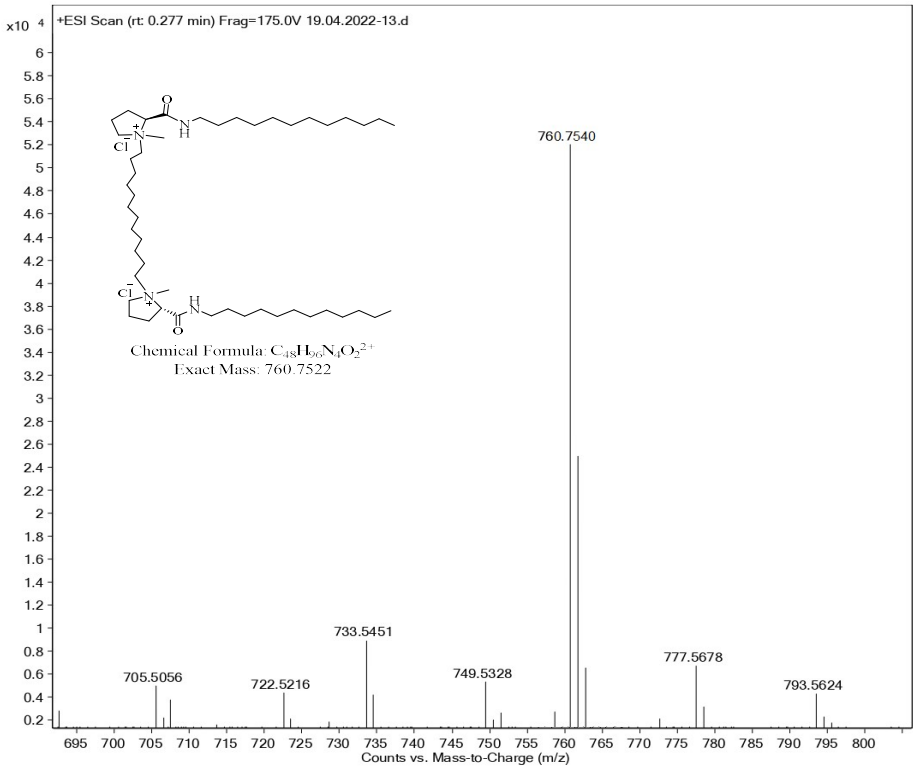

ESI-HRMS Spectrum of **Lipid Pro-1,12**

CHAPTER VI

Summary and Conclusions

In the present research study, alpha-tocopherol, cholesterol based cationic lipids and amino acid based gemini cationic lipids were successfully synthesized to develop safe and efficient liposomal formulations. Their applications in nucleic acid delivery and gene editing were also discussed.

Chapter I describes the introduction of gene delivery methods, classification of cationic lipids and gene editing techniques. Among the all counter parts of the lipid, head group has drawn lot of attention in many recent studies due to its close proximity towards the negative dipole of nucleic acid and significant role in self-assembly of bilayered membranes. Delivery and expression of therapeutic gene in gene therapy is a major challenge as it includes two barriers, i.e., uptake of gene into cells and endosomal escape.

In chapter II, we have used four different aromatic/hydrophobic amino acids namely glycine (G), proline (P), phenylalanine (F) and tryptophan (W) as head groups to study their influence on endosomal escape for the enhanced transfection efficacy. A detailed structure activity study of these lipids on transfection potentials with both circular pDNA as well as linear mRNA in multiple cultured cells using commercial transfecting reagents, LF 3000 and LFMM with respect to their physicochemical properties was discussed. These results revealed that, two aromatic hydrophobic head group containing lipids TTF and TTW exhibited better transfection than TTG and TTP in all the cell lines studied. Chloroquine treatment experiment revealed that, TTW cationic lipid alone showed no change in the transfection efficiency with and without chloroquine treatment which clearly indicated that, endosomal escape played major role for TTW in enhancing the transfection efficiency. The horizon of these cationic lipids mainly TTW for delivering genome-editing tools as a toolset was also mentioned in the chapter 2. From these results, we have observed that, TTW was found to be effective in gene delivery and gene editing.

In chapter III, the synthesis, characterization and transfection potentials of these tocopheryl ammonium based lipids were discussed. A detailed structure activity study of these lipids on transfection potentials with respect to their physicochemical properties was discussed. The endocytic pathway inhibitor assay proved that, AC- Toc, MC-Toc, DC-Toc and TC-Toc were involved in specifically clathrin-mediated endocytosis whereas control lipid DC-chol internalization occurs through both macropinocytosis and clathrin

mediated endocytosis. From these results we have observed that, by changing the hydrophobic moiety can influence the specificity of lipoplexes internalization pathway.

The synthesis, characterization of two di-peptide cationic amphiphiles with varying the hydrophobic moieties such as alpha-tocopherol and cholesterol using glycine and lysine were discussed in chapter IV. In this chapter, the synthesized liposomes TGK and CGK for delivering genome-editing tools having CRISPR/Cas9 encoded with pDNA was discussed. Among the synthesized two cationic lipids TGK was found to be efficient for nucleic acid delivery.

The gemini cationic lipids are the well-known class of non-viral lipid based systems for inducing better transfection profiles than a simple one due to their dimeric lipid nature and low cellular toxicities. In chapter V, structure activity study of these lipids on transfection potentials with respect to their physicochemical properties was discussed. All synthesized gemini cationic lipids from pro 1,2 to pro 1,12 exhibited higher transfection efficiency with pDNA compared with control lipid pro Cl was mentioned in chapter 5.

Future scope of the work

Aromatic hydrophobic R group containing amino acids are safe, economic and actually more efficient in nucleic acids delivery and for genome-editing applications. These findings can be further explored in the genome-editing approach for treating genetic disorders.

APPENDICES

List of Publications

1) ***Hithavani Rapaka****, Shireesha Manturthi, Porkizhi Arjunan, Vigneshwaran Venkatesan, Saravanabhavan Thangavel, Srujan Marepally, Srilakshmi V Patri* "Influence of hydrophobicity in hydrophilic region of cationic lipids on enhancing nucleic acid delivery and gene editing. **ACS Applied Bio Materials 2022**.
2) ***Hithavani Rapaka****, Shireesha Manturthi, Mallikarjun Gosangi, Brijesh Lohchania, Srujan Marepally, Srilakshmi V Patri* "Effect of Methylation in the Hydrophilic Domain of Tocopheryl Ammonium Based Lipids on their Nucleic Acid Delivery Properties". **ACS OMEGA 2022 (Accepted) DOI: 10.1021/acsomega.1c06889**
3) Gosangi, M.; **Rapaka, H**.; Ravula, V.; Patri, S. v. Evolution of New "Bolaliposomes" Using Novel α-Tocopheryl Succinate Based Cationic Lipid and 1,12-Disubstituted Dodecane-Based Bolaamphiphile for Efficient Gene Delivery. ***Bioconjugate Chemistry*** **2017**, *28* (7).

   https://doi.org/10.1021/acs.bioconjchem.7b00283.
4) Gosangi, M.; **Rapaka, H**.; Mujahid, T. Y.; Patri, S. v. Novel 1,2,3-Triazolium-Based Dicationic Amphiphiles Synthesized Using Click-Chemistry Approach for Efficient Plasmid Delivery. ***MedChemComm*** **2017**, *8* (5). https://doi.org/10.1039/c6md00699j.
5) Gosangi, M.; Ravula, V.; **Rapaka, H**.; Patri, S. v. α-Tocopherol-Anchored Gemini Lipids with Delocalizable Cationic Head Groups: The Effect of Spacer Length on DNA Compaction and Transfection Properties. ***Organic and Biomolecular Chemistry*** **2021**, *19* (20), 4565–4576.

   https://doi.org/10.1039/d1ob00475a.

Manuscripts under preparation

1) ***Hithavani Rapaka****, et al."*Influence of hydrophobic tail on Amino acid based dipeptide cationic lipids for efficient Gene delivery"
2) ***Hithavani Rapaka*** *et al.* "Proline head group based gemini like cationic lipids: The effect of spacer length on transfection properties"

BRIEF BIOGRAPHY OF THE AUTHOR

Mrs. Rapaka Hithavani was born in Parkal, Hanmakonda district of Telangana State, India. She has completed her secondary school education from her father's school *Vidyalaya High School*, Parkal. She has completed her Intermediate and B.Sc. in SR Educational Institutions, Warangal. After completion of her M.Sc. (Organic Chemistry) from National Institute Technology Warangal, she has joined for the Ph.D., programme in July 2013 under the guidance of Dr. P. V. Srilakshmi (Professor) Department of Chemistry, National Institute of Technology Warangal with the financial assistance from the NITW.